Regulation of inducible Nitric Oxide synthase in adipocytes and Perivascular adipose tissue by the Sphingolipid system

Ibrahim Aljaezi

BSc, MSc

Thesis submitted in fulfilment of the requirements for the degree of Doctor of Philosophy

2024

School of Cardiovascular and Metabolic Health,

College of Medical, Veterinary and Life Sciences

University of Glasgow

Abstract

Obesity is a major risk factor for cardiovascular disease, often characterized by chronic inflammation that can disrupt normal metabolic processes. One key factor in this inflammatory response is the upregulation of inducible nitric oxide synthase (iNOS) and nitric oxide (NO) production. The induction of iNOS in adipocytes and adipose tissue leads to increased production of NO which, in turn, contributes to the regulation of adipose tissue function and also influences lipid metabolism, insulin sensitivity, and the modulation of vascular function.

Perivascular adipose tissue (PVAT) surrounds blood vessels and has an anti-contractile effect, helping to maintain vascular homeostasis via release of a variety of bioactive molecules. In obesity-induced inflammation, some studies have demonstrated that inflammation within the PVAT can compensate or have an adaptive role to preserve endothelial dysfunction function; via upregulating iNOS protein and increasing NO production. Sphingolipid system, encompassing a complex network of bioactive lipids like ceramides, sphingosine, and sphingosine-1-phosphate (S1P), regulates various cellular processes in adipose tissue. Although research has revealed that the sphingolipid system promotes inflammation in adipose tissue, it remains unclear how this system regulates iNOS expression and function. In response, this thesis has characterised the role of the sphingolipid system in iNOS-derived nitric oxide production in adipose tissue and addressed how this influences PVAT-mediated anticontractile activity under inflammatory conditions. The aims were achieved by using a 3T3-L1 adipocyte cell line as well as thoracic aortic PVAT from mouse and rat to study vascular function. Interleukin-1β (IL-1β) or macrophage conditioned media were used in this study to induce iNOS expression and NO production.

In this thesis, Chapters 3 and 4 focus on the potential role of the sphingolipid system on IL-1β-induced iNOS expression and NO production in 3T3-L1 adipocytes. Initially, it was found that stimulation of 3T3-L1 adipocyte with IL-1β increases sphingosine Kinase 1 (SphK1) expression and that S1P-produced by SphKs enzymes activates various proinflammatory pathways including the phosphoinositide 3-kinase/ protein kinase B pathway (PI3K/Akt), mitogen-activated protein kinase MAPK kinase (MEK)/extracellular signal-regulated kinase pathway (MEK-ERK), Jun

N-terminal kinase pathway (JNK), but apparently had no effect on the nuclear factor kappa B pathway (NF-KB). In addition, exogenous S1P augmented-IL-1ß stimulated iNOS expression and NO production in 3T3-L1 adipocytes which was suggested to be through the Akt and MAPKs pathways (MEK-ERK pathway and JNK pathway). Chapter 4 investigated more fully how distinct SphKs isoforms and S1PRs modulate iNOS regulation in adipocytes stimulated with IL-1ß. The iNOS expression and NO production stimulated by IL-1 ß was inhibited by pre-treatment with a SphK1 inhibitor (PF543) but not a SphK2 inhibitor (ROME). Moreover, it was demonstrated that $S1PR_2$ inhibition with JTE 013 strongly suppressed IL-1ß-induced iNOS expression and NO production in 3T3-L1 adipocytes. This effect was accompanied by inhibition of MAPK and PI3K/Akt signalling, suppressing phosphorylation of ERK1/2, P38, JNK and Akt. Inhibition of ABCA1 with glybenclamide suppressed the additive effect of S1P on iNOS expression and NO production in stimulated adipocytes. Collectively, by targeting SphKs/S1P/S1PRs axis pathway, Chapter 3 and 4 provided evidence that SphK1/S1P/$S1PR_2$/ MAPKs and PI3K/Akt axis is required for IL-1ß induced iNOS expression and NO production in adipocytes.

In addition, chapter 4 has shown that conditioned medium from activated RAW 264.7 macrophages stimulated iNOS expression and NO production in 3T3-L1 adipocyte; however, prior inhibition of SphK1/$S1PR_2$ axis attenuated this. Similarly, inhibiting $S1PR_2$ in adipocytes prior to stimulation with conditioned medium diminishes iNOS expression and NO production.

In chapter five, it was found that S1P or S1P agonists did not modulate vascular tone in mouse thoracic aorta. Also, IL-1ß did not affect the anticontractile effect of PVAT in mouse experiments and pre-treatment with S1P exerted no effect. However, in rat aorta, it was confirmed that S1P induced a vasorelaxant effect. IL-1ß was found to enhance the relaxant effect of PVAT in rat aorta, which was most likely mediated by iNOS upregulation, increased NO production, and potassium channel activation in the vascular smooth muscle cells. Moreover, IL-1ß upregulated SphK1 in rat aortic PVAT; however, inhibiting SphK1/$S1PR_2$ axis did not reverse the hyporeactivty induced by IL-1ß. Collectively, IL-1ß induces a hyporeactive effect in rat aortic vessels independent of the sphingolipid axis pathway.

In summary, the results of this study imply that IL-1β induces an increase in SphK1 expression in 3T3-L1 adipocytes. The increased SphK1 induced by IL-1β appears to increase S1P production from adipocytes which could contribute to IL-1β-mediated iNOS regulation through activating $S1PR_2$. However, in the functional studies on rat aortic vessels with intact PVAT, it is likely that IL-1β-mediated hyporeactivity via iNOS upregulation was independent of the SphK1/S1P/$S1PR_2$ axis.

Table of Contents

List of Tables

List of Figures

Acknowledgement

Looking back at this PhD journey, there are many people at University of Glasgow whose help over the past 3 years has been invaluable and greatly appreciated. I want to convey my sincere appreciation and admiration to all those who contributed to this extraordinary journey.

Throughout my Ph.D. journey, I was fortunate to be supervised by Prof Simon Kennedy, and Dr Kenneth Watterson. Their expertise, guidance and insights have been instrumental in shaping the success of my research. Your contagious encouragement and optimism always kept me going. You have trusted in my decisions, guided me, supported me and were always available. I always knew that you believed in me and wanted the best for me. Thank you!

I would like to extend my thanks to colleagues past and present from Kennedy and Salt groups for helping me with just about everything. In addition, I would like to thank Dr Ian Salt who kindly allowed me to access to instruments and reagents and Dr Carmody for their generous provision of the RAW cells utilized in this thesis. Thanks, should also go to the laboratory technicians: John McAbney for all his help and teaching me the primary scientific technique utilized in this work, wire myography. I would also like to acknowledge Najran University and Saudi cultural bureau in London, Government of Saudi Arabia for their support and funding of this project.

Finally, I would especially like to thank my family. Words cannot adequately express the depth of my gratitude and appreciation to my parents as well as my brothers and sisters who consistently and unconditionally supported me during my work. I would like to dedicate this work to my father Amer Aljaezi, my mother Salha Alshadidi: I will forever be grateful for your loving kindness and compassion which began long before my birth and continues unabated.

Author's Declaration

I hereby declare that this thesis has been written solely by me unless otherwise stated. It is completely of my own composition and has not in whole or in part been submitted for any other degree. This work was carried out in the laboratory of Professor Simon Kennedy, School of Cardiovascular and Metabolic Health, College of Medical, Veterinary and Life Sciences, University of Glasgow, Glasgow, United Kingdom.

Ibrahim Amer A Aljaezi

June 2024

Abbreviations

3KDHR	**3-ketodihydrosphingosine reductase**
ABC	**ATP-binding cassette**
ACh	**Acetylcholine**
ATF	**Activating transcription factor**
BAT	**Brown adipose tissue**
BCA	**Bicinchoninic acid**
BH4	**Tetrahydrobiopterin**
Ca^{2+}	**Calcium ions**
cAMP	**Cyclic adenosine 3′,5′ -monophosphate**
CCL5	**Chemokine (C-C motif) ligand 5**
CerS	**Ceramide synthases**
cGMP	**Cyclic guanosine monophosphate**
C.M	**Conditioned medium**
CREB	**cAMP response element binding protein**
CVS	**Cardiovascular system**
DAG	**Diacylglycerol**
DES	**Dihydroceramide desaturase**
DIO	**Diet induced obesity**
DHS	**L-threodihydrosphingosine**
DMEM	**Dulbecco's modified eagles' medium**
DMS	**N,N-dimethylsphingosine**
DMSO	**Dimethyl sulfoxide**
DTT	**Dithiothreitol**
EAT	**Epididymal adipose tissue**
ECs	**Endothelial cells**
EGF	**Epidermal growth factor**
eNOS	**Endothelial nitric oxide synthase**
EWAT	**Epidydimal white adipose tissue**
ERK 1/2	**Extracellular signal-regulated kinase 1/2**
FAD	**Flavin adenine dinucleotide**
FCS	**Foetal calf serum**
FHL2	**Half LIM domain 2**
FMN	**Flavin mononucleotide**
GAPDH	**Glycerol 3-phosphate dehydrogenase 1**
GDNF	**Glial line-derived neurotrophic factor**
H_2O_2	**Superoxide**
H_2S	**Hydrogen sulfide**
HFD	**High fat diet**

Hoxc	**Homeobox C**
Hsp90	**Heat shock protein 90**
HUVECs	**Human umbilical vein endothelial cells**
IBMX	**3-isobutyl-1-methylxanthine**
IL-1ß	**Interleukin-1ß**
IL-6	**Interleukin-6**
IL-1R1	**IL-1 receptor**
IMM	**Inner membrane of the mitochondria**
iNOS	**Inducible nitric oxide synthase**
IP3	**Inositol trisphosphate**
IRAK	**Interleukin-1 receptor-associated kinase**
IWAT	**Inguinal white adipose tissue**
JNK	**Jun N-terminal kinase**
KPSS	**High potassium physiological salt solution**
LMO2	**LIM-domain-only protein 2**
LPS	**Lipopolysaccharide**
MAPK	**Mitogen-activated protein kinases**
MCP-1	**Monocyte chemoattractant protein-1**
MyD88	**Myeloid differentiation primary response 88**
NAPDH:	**Nicotinamide adenine dinucleotide phosphate**
NCS	**Newborn calf serum**
NF-KB	**Nuclear factor kappa B**
NGF	**Nerve-growth factor**
NO	**Nitric oxide**
NOA 280i	**Sievers Nitric Oxide Analyzer 280i**
NOS	**Nitric oxide synthase**
nNOS	**Neural nitric oxide synthase**
PBS	**Phosphate buffered saline**
PE	**Phenylephrine**
PECAM-1	**Platelet endothelial cell adhesion molecule 1**
PI3Ks	**Phosphatidylinositol 3-kinases**
PIP2	**Phosphatidylinositol 4,5-bisphosphate**
PKC	**Protein kinase C**
PLC	**Phospholipase C**
PPARγ	**Peroxisome proliferator-activated receptor γ**
PSS	**Physiological salt solution**
PVAT	**Perivascular adipose tissue**
RISC	**RNA interference silencing complex**
S1P	**Sphingosine 1 Phosphate**
S1PR	**Sphingosine 1 Phosphate receptor**
S1PP	**S1P phosphatases**

SAT	**Subcutaneous adipose tissue**
SDS-PAGE	**SDS-polyacrylamide gel electrophoresis**
SKIP	**Sphingosine kinase 1 interacting protein 1**
SOCE	**Store-operated calcium channels**
SPR	**Serine palmitoyltransferase**
SphK	**Sphingosine Kinase**
Spms2	**Spinster homolog 2**
TBS	**Tris-buffered saline**
TBST	**Tris-buffered saline - Tween 20**
TLR4	**Toll-like receptor 4**
TMS	**N,N,N-trimethylsphingosine**
TNF-α	**Tumour necrosis factor alpha**
TRAF2	**TNF receptor- associated factor 2**
TRAF6	**Tumour necrosis factor receptor-associated factor 6**
UCP-1	**Uncoupling protein 1**
VSMC	**Vascular smooth muscle cell**

Conference abstracts.

1. **Ibrahim Aljaezi**; Yazeed Alshuweishi; Kenneth Watterson; Simon Kennedy (2022) Involvement of sphingosine kinase 1/sphingosine-1-phosphate in inducible nitric oxide synthase expression and NO production by IL-1ß treated 3T3-L1 adipocytes. British Pharmacology Society Meeting, September (2022), Liverpool.

2. **Ibrahim Aljaezi**; Kenneth Watterson; Simon Kennedy; (2023) Interleukin-1ß (IL-1ß) regulates the anticontractile effect of perivascular adipose tissue in isolated rat aorta via the induction of Inducible nitric oxide synthase (iNOS). Scottish Cardiovascular Forum, February (2023), Aberdeen.

3. **Ibrahim Aljaezi**; Kenneth Watterson; Simon Kennedy; (2023) Interleukin-1ß (IL-1ß) regulates the anticontractile effect of perivascular adipose tissue in isolated rat aorta via the induction of Inducible nitric oxide synthase (iNOS). 19th World Congress of Basic & Clinical Pharmacology, July (2023), Glasgow.

4. **Ibrahim Aljaezi**; Kenneth Watterson; Simon Kennedy; (2024) Sphingosine kinase 1/sphingosine-1-phosphate receptor 2 axis modulates macrophage-mediated inducible nitric oxide synthase expression and nitric oxide production in adipocytes. Scottish Cardiovascular Forum, February (2024), Dundee.

Chapter 1 - Introduction

1.1 Cardiovascular disease

Cardiovascular disease comprises a group of diseases that affect the heart and/or blood vessels and includes cerebrovascular disease, coronary heart disease and peripheral arterial disease. According to data published by World Health Organisation (WHO) in 2021, cardiovascular disease caused around 32% of deaths globally in 2019 and 85% of these deaths were due to heart attack and stroke. About 695,000 people in the US died from heart disease in 2021, accounting for about one in every five deaths (Tsao et al, 2023). In addition, around seven million people in the UK are suffering from cardiovascular diseases, and they are considered the leading cause of death in the UK. The most common underlying causes of cardiovascular disease are hypertension, smoking, high cholesterol, diabetes and obesity (Robinson, 2021).

According to WHO Organization (2000), obesity is defined as abnormal or excessive fat accumulation in adipose tissue to the stage that health may be affected. The prevalence of obesity has increased in the majority of countries since the 1980s, and is now considered to be a global epidemic which accounts for over 2.8 million deaths annually (Boutari & Mantzoros, 2022). Obesity itself is one of the important risk factors for CVD and is strongly linked with the incidence of other cardiovascular risk factors including hypertension, insulin resistance, type 2 diabetes (T2D) and hyperlipidaemia (Boutari & Mantzoros, 2022; Powell-Wiley et al, 2021). A key feature in obese patients is chronic inflammation in adipose tissue depots and this is thought to play an important role in many cardiovascular diseases (Lowe, 2001). Among the numerous factors implicated in inflammation and its link to cardiovascular diseases, a number of researchers have focused on sphingolipid-derived mediators such as sphingosine 1-phosphate (S1P) and ceramide (Ouyang et al, 2020; Zhang et al, 2016).

1.2 Cardiovascular system

The cardiovascular system (CVS) is the principal circulatory system in the body that consists of the heart, blood vessels, and blood. The CVS has multiple functions in the body, which are concerned with the transportation of oxygen, nutrients, water, electrolytes, and hormones to all parts of the body. Besides that, the CVS

removes CO_2 and metabolic waste products from all cells and tissues of the body and returns them to the excretory organs such as the lungs and kidneys. In addition, the CVS is considered as a thermoregulatory system and also a part of the immune system infrastructure (Aaronson et al, 2020).

The blood is composed of plasma and blood cells, including erythrocytes, white blood cells, and platelets. The heart is a muscular organ that is responsible for pumping blood to all parts of the body while the blood vessels which transport the blood are divided into arteries, veins, and capillaries; and each of these vessels has a distinctive function in the body.

1.3 Structure of blood vessels

In all vessels apart from the capillaries, the arterial wall is made up of three concentric layers: the tunica intima, the tunica media, and the tunica adventitia/externa. The tunica intima consists of a single layer of endothelial cells (EC) on the basement membrane which is responsible for regulating substance exchange between the bloodstream and surrounding tissue. The tunica media is the middle layer smooth muscle which is responsible for regulating the vascular tone and the distribution of blood flow throughout the body. The tunica adventitia is the outermost layer which is composed of adventitia compacta, a layer of fibroblasts and perivascular adipose tissue (PVAT) (Figure 1-1).

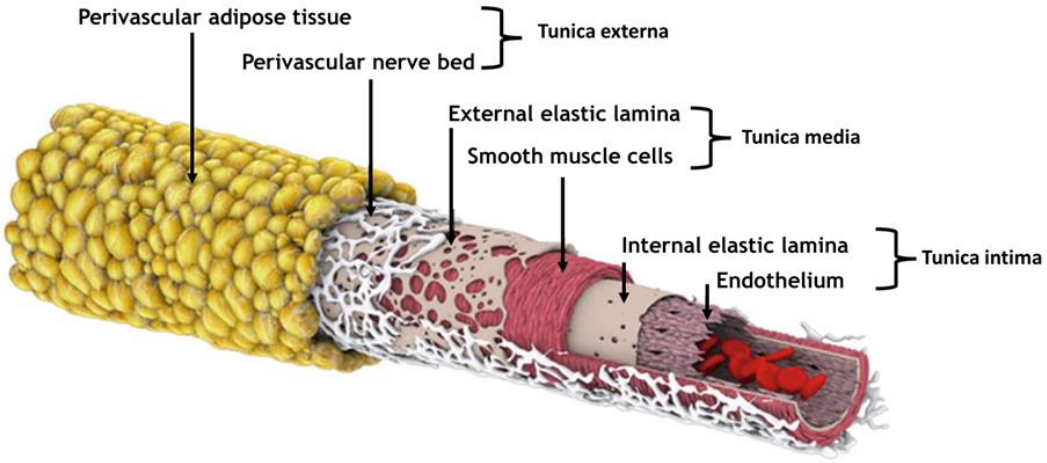

Figure 1-1 Structure of blood vessels.

The artery wall made up of three main layers; tunic externa composed of PVAT; tunica media composed of SMC; and tunica intima composed of EC, adapted from (Daly, 2019).

1.3.1 Endothelium layer

The endothelium layer is a single layer of cells that lines the inside of blood vessels, separating the vascular wall from circulating blood. The endothelium performs a variety of vital roles that assist cardiovascular health in general and vascular homeostasis. ECs play a central role in various physiological processes, including forming a structural barrier between the blood vessels and surrounding tissue, inflammation and immune response, blood clotting and anticoagulation, metabolic functions, angiogenesis and vascular tone regulation (Krüger-Genge et al, 2019). It produces and releases numerous molecules, including nitric oxide (NO), which have vasodilatory effects to help in blood flow regulation and blood pressure, maintaining adequate perfusion to different organs and tissues (Deanfield et al, 2007).

1.3.2 Vascular smooth muscle cells

Vascular smooth muscle cells (VSMCs) are a fundamental component of the blood vessel wall and play a key role in regulating blood vessel tone, diameter, and overall vascular dynamics. They control blood vessel tone and diameter via controlling vascular contraction and relaxation. In response to a variety of stimuli, including hormones like angiotensin II and neurotransmitters like noradrenaline, VSMCs actively contract. The decrease in blood vessel diameter caused by this vasoconstrictive influence raises blood pressure and vascular resistance. Conversely, VSMCs can relax in response to signals that promote vasodilation, for example, NO released by ECs diffuses to VSMCs and induces relaxation by increasing levels of cyclic guanosine monophosphate (cGMP) (Walford & Loscalzo, 2003; Wilson, 2011). Furthermore, VSMCs contribute to vascular regulation by modulating ion channels and membrane potential. Calcium channels are crucial for the regulation of intracellular calcium levels, a key determinant of VSMC contraction. Opening of voltage-gated calcium channels allows the influx of calcium ions (Ca^{2+}), leading to muscle contraction. Potassium channels are also present on VSMCs and activation of K^+ channels allow the efflux of K^+ ions, hyperpolarizing the cell, which then leads to the closure of voltage-gated calcium channels. As a result, intracellular calcium concentration is reduced and the decrease in calcium levels causes relaxation of the smooth muscle cells. Moreover,

VSMCs are involved in helping repair vascular injury under pathological conditions by changing phenotype from a contractile to a proliferative, migratory phenotype as well as a myofibroblast like phenotype (Chen et al, 2023b).

1.3.3 Perivascular adipose tissue

PVAT is a connective tissue that is located adjacent to veins and arteries. PVAT not only provides a support structure but is also recognised as an active tissue that modulates vascular tone. PVAT is mainly composed of adipocytes, but it also contains other cell types, including immune cells, fibroblasts, and endothelial cells (Nosalski & Guzik, 2017). PVAT is considered one of the most significant parts of the cardiovascular system. It has a paracrine signalling activity that regulates vasculature function, and was subsequently named by Cheng as: "the sixth man of the cardiovascular system" (Cheng et al, 2018). PVAT secretes a number of biologically active substances that regulate vascular function (Szasz et al, 2013), including adiponectin, leptin, cytokines, reactive oxygen species (superoxide, H_2O_2), hydrogen sulfide (H_2S), and nitric oxide (NO) (Almabrouk et al, 2014).

NO is one of a number of significant vasoactive substances released by PVAT to modulate vascular function either by endothelium-dependent or -independent pathways. NO can be produced by three isoforms of NO synthase (NOS): calcium-dependent endothelial cell NOS (eNOS), neuronal type NOS (nNOS), and an inducible type NOS (iNOS), which is generally calcium-independent (Förstermann & Sessa, 2012). Many studies have documented the role of NO in mediating the vasorelaxant influence of PVAT (Greenstein et al, 2009; Lynch et al, 2013; Xia et al, 2016).

PVAT is made up of two main types of fat tissue: white adipose tissue (WAT) and brown adipose tissue (BAT), depending on where it is located in the body. For example, PVAT of rodent mesenteric arteries is composed of WAT, while surrounding the aorta it is a mixture of WAT and BAT (Cinti, 2011; Fitzgibbons et al, 2011).

WAT is predominantly made up of large adipocytes with a single lipid droplet and significantly fewer mitochondria. These white adipocytes can be identified by

their expression of a number of markers include leptin, homeobox C8 (Hoxc8) and homeobox C9 (Hoxc9) (Ussar et al, 2014). It represents the most common type of adipose tissue, which is found in several distinct depots, including mesenteric, omental, retroperitoneal, gonadal, pericardial and many perivascular depots, and is primarily involved in energy storage. WAT takes up circulating free fatty acids and stores them as triglycerides during periods of excess energy (Cinti, 2011; Zwick et al, 2018). These triglycerides can then be mobilised to provide an essential supply of fuel when the body requires more energy. As well as lipid storage, WAT is a crucial endocrine organ involved in secreting numerous active biological proteins and other factors termed adipokines. These include adiponectin, resistin, lipocalin, tumour necrosis factor alpha (TNF-α), interleukin-6 (IL-6), interleukin-1β (IL-1β), interleukin-8 (IL-8), and interleukin-18 (IL-18). These adipokines are a significant player in insulin resistance, insulin sensitivity and inflammation (Funcke & Scherer, 2019).

Brown adipose tissue (BAT), in contrast to white adipose tissue (WAT), has a significant capacity for oxidation and functions mainly as a site of energy expenditure through a mechanism called non-shivering thermogenesis. BAT is located in many different sites over the body, including neck, supraclavicular, perirenal, mediastinal, cervical, axillary, and perirenal regions and also surrounds some blood vessels such as thoracic aorta. There are more mitochondria and lipid vacuoles in the adipocytes of BAT compared to WAT. The thermogenic activity of brown adipocytes is attributed to the presence of a distinctive marker protein termed uncoupling protein 1 (UCP-1) (Cannon & Nedergaard, 2004; Sakers et al, 2022). The role of UCP-1, which is found in the inner membrane of the mitochondria (IMM) of brown adipocytes, is to enhance IMM conductance for H^+ ions in order to dissipate the mitochondrial H^+ gradient and transform substrate oxidation energy into heat (Fedorenko et al, 2012). BAT are also thought to be capable of releasing cytokines such as IL-6 and TNF-α under inflammatory conditions, but to a lesser extent compared to WAT (Peek et al, 2020; Villarroya et al, 2018).

Recently a new type of adipose tissue was discovered named beige or brite adipocytes (brown like adipocytes). These adipocytes seem to have a mixed character between white and brown adipocytes. Beige adipocytes are found within

white adipose tissue (Chait & Den Hartigh, 2020) but there are conflicting views about the origins of these adipocytes; with some suggesting that beige adipocytes originate from progenitor smooth muscle-like pericytes present within WAT (Long et al, 2014). However, others suggest that beige adipocytes are generated via a process called browning; involving the conversion of white adipocytes into beige adipocytes (Harms & Seale, 2013). Beige adipocytes or brite adipocytes contribute to energy expenditure and thermogenesis, hence playing a crucial role in the regulation of systemic metabolism and body weight (Chait & Den Hartigh, 2020). The important beige cell markers include UCP-1, CD137, Tmem26, Tbx1, and other molecules (Ussar et al, 2014).

1.4 Obesity-dependent Inflammation of PVAT

The low-grade inflammation associated with obesity is one of several mechanisms that contribute to hypertension development. Macrophage infiltration into the adipose tissue is a key process in triggering the development of obesity-associated inflammation of adipose tissue. According to research, macrophages constitute only 5–10% of lean adipose tissue, however, in adipose tissue of obese subjects, up to 50% of cells are macrophages (Weisberg et al, 2003). Although the mechanisms of macrophage infiltration into adipose tissue is still unclear, many factors and events have been identified that lead to recruitment of macrophages and the development of inflammation in adipose tissue.

It was shown that Toll-like receptor 4 (TLR-4) is involved in macrophage recruitment into adipose tissue of obese patients and mice (Catalan et al, 2012; Saberi et al, 2009). After recruitment, macrophages are polarized from M2 (alternatively activated) into M1 (classically activated) which is dependent on the pro inflammatory secretory products of the adipocytes (Zeyda & Stulnig, 2007). The activated adipose tissue macrophage is the main cause of expression of proinflammatory mediators such as TNF-α and iNOS (Weisberg et al, 2003).

It is currently known that adipokines, or the secretions of adipose tissue, account for at least 600 different substances that can affect metabolism through endocrine, paracrine, and autocrine processes (Blüher, 2012). In obesity, adipose tissue has been recognised to secrete several proinflammatory mediators and

cytokines which have been linked to many cardiovascular diseases, including hypertension (Hu et al, 2021; Silvani et al, 2009), atherosclerosis (Quesada et al, 2018), diabetes and insulin resistance (Zatterale et al, 2020). For example, compared to lean adipose tissue, obese tissue has been shown to have a higher level of many proinflammatory cytokines, including TNF-α, IL-6, and IL-1ß.

1.4.1 IL-1β

IL-1ß is a proinflammatory cytokine which is primarily produced by macrophages and monocytes; however, in the context of adipose tissue, it can also be produced by adipocytes (Bing, 2015; Renovato-Martins et al, 2020).

IL-1ß has been shown to be a crucial player in hypertension development; causing vascular smooth muscle and extracellular matrix remodelling via a number of inflammatory pathways (Melton & Qiu, 2021). Moreover, IL-1ß plays a significant role in adipocyte-macrophage interaction, leading to adipose tissue dysfunction (Bing, 2015; Gao et al, 2014). Infiltration and activation of macrophages within the PVAT contributes to hypertension and it has been observed that IL-1 receptor antagonism decreases blood pressure in obese patients (Urwyler et al, 2020). A number of studies have reported that upregulation of IL-1ß in adipose tissue is associated with insulin resistance. For example, it has been observed that IL-1ß expression is elevated in the serum and WAT of obese patients and that positively correlated with both insulin resistance and body mass index (Moschen et al, 2011). In addition, another study has confirmed that IL-1ß is upregulated in adipose tissue of obese patients and obese mouse models and that the cytokine induces insulin resistance by affecting glucose transport in human and mouse adipocytes (Lagathu et al, 2006). Furthermore, IL-1ß was able to negatively affect insulin signalling in adipocytes and participates in the development of insulin resistance in these cells (Gao et al, 2014; Jager et al, 2007). In agreement with this, it was demonstrated by Handa and co-workers that insulin resistance was prevented in 3T3-L1 cells treated with IL-1ß by using an anti-IL-1ß monoclonal antibody (Handa et al, 2013).

1.4.1.1 IL-1β receptors subtypes

IL-1ß binds to the type I IL-1 receptor (IL-1R1), which is ubiquitously expressed. This interaction leads to the recruitment of a shared co-receptor, IL-1RAcP (IL-

1R3), by binding to the composite surface of the cytokine and the primary receptor complex. The IL-1R3 is the coreceptor for forming a trimeric signalling complex with IL-1β. In the resting state, IL-1R1 and IL-1R3 are present on the cell membrane. Once IL-1β binds to IL-1R1, a structural and conformational change occurs that allows IL-1R3 to bind to IL-1R1, facilitating the formation of active signalling complex. The binding of IL-1β to its receptors leads to the initiation of a multi-functional signalling complex, which triggers a cascade of inflammatory responses. This process is essential for the biological activities of IL-1β, allowing this cytokine to play a role in innate immunity (Fields et al, 2019; Kaneko et al, 2019).

1.4.1.2 IL-1β-dependent Inflammatory Signalling

IL-1β mediates inflammatory responses by stimulating and activating different signalling pathways: mitogen-activated protein kinases (MAPKs), canonical nuclear factor kappa B (NF-KB), and phosphatidylinositol 3-kinases (PI3Ks) PI3K/Akt (Jager et al, 2007; Nisar et al, 2021; Weber et al, 2010). These pathways have been recognised to regulate many inflammatory processes and enzymes such as COX-2 and iNOS, as summarised in Figure 1-2.

Mitogen-Activated Protein Kinases (MAPKs)

IL-1β activates the MAPKs pathway through a series of intracellular signalling events. In this process IL-1β binds to IL-1R1, initiating a cascade of events that eventually lead to MAPKs activation. One of the intracellular signalling processes initiated by the activated IL-1 receptor is via a protein known as Myeloid Differentiation Primary Response 88 (MyD88). MyD88 is recruited leading to activation of a series of protein kinases, including Interleukin-1 Receptor-Associated Kinase (IRAK) and Tumour Necrosis Factor Receptor-Associated Factor 6 (TRAF6). Following this, MAPK kinases such as the MEK family which includes MEK3/6, MEK4/7, and MEK1/2 are phosphorylated and they in turn phosphorylate and activate other MAPKs including extracellular signal-regulated kinase 1/2 (ERK1/2), Jun N-terminal kinase (JNK), and p38 (Kyriakis & Avruch, 2012; Muslin, 2008; Rose et al, 2010). Once these proteins (ERK1/2, JNK, and p38) are activated, they translocate into the nucleus and phosphorylate transcription factors like c-

Jun, c-fos and ATF-2, leading to the regulation of many inflammatory genes (Plotnikov et al, 2011).

Canonical Nuclear factor-κB (NF-κB) pathway

NF-KB is one of several crucial proinflammatory signalling pathways regulated by IL-1β. Under basal conditions, NF-KB, typically in the form of the p50-p65 heterodimer, is localised in the cytoplasm where it is coupled to IκBα. Once IL-1β binds to its receptor, it initiates a cascade involving MyD88, IRAK, and TRAF6. This leads to the activation of IKK complex, which consists of IKKα, IKKβ, and NEMO (NF-KB essential modulator, also known as IKKγ). The activation of IKKβ, leads to phosphorylation of IκB family proteins including IKβα. Once phosphorylated, IKβα is degraded which then leads to free NF-KB heterodimer p50-p65 being translocated into the nucleus where it initiates transcription of target genes including proinflammatory genes (Weber et al, 2010).

Phosphoinositide 3-kinase/ protein kinase B (PI3K)/Akt

PI3K/Akt is another pathway which has been reported to be activated by IL-1β via a series of signalling events. Following receptor activation by IL-1β and TRAF6 and IRAK activation, an upstream kinase (PI3K) is activated, which, in turn, activates Akt (protein kinase B) (Bavelloni et al, 1999; Chang et al, 2019; Martin & Wesche, 2002; Neumann et al, 2002). PI3K/Akt activation has been reported to regulate different inflammatory mediators and enzymes.

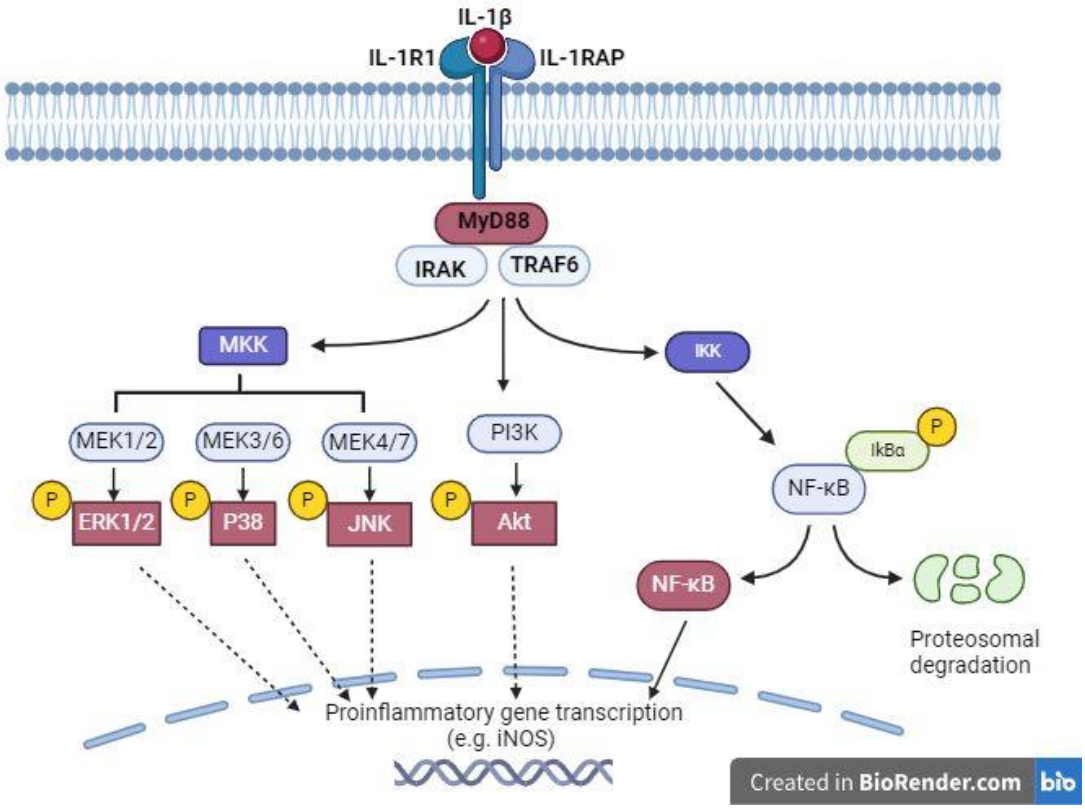

Figure 1-2 IL-1β signalling pathways.

Proinflammatory singling pathways activated in responses to IL-1R activation by IL-1β. These pathways including MAPKs, PI3K/Akt and NF-KB activated, ultimately lead to proinflammatory enzyme expression.

1.4.2 IL-1β-mediated Regulation of Inducible Nitric Oxide Synthase

iNOS is a 131 kDa mammalian protein composed of 1,153 amino acids organised into two main domains: an N-terminal oxygenase segment and a C-terminal reductase domain which includes a binding subdomain which binds flavin mononucleotide (FMN). This enzyme is responsible for the synthesis of NO from L-arginine in mammalian tissues. In addition to FMN, production of NO via iNOS requires other cofactors including nicotinamide adenine dinucleotide phosphate (NADPH), flavin adenine dinucleotide (FAD), heme, and (6R)-5,6,7,8-tetrahydrobiopterin (BH4) to catalyse the conversion of L-arginine to L-citrulline and NO (Figure 1-3). This process is mediated by calmodulin (CaM), which binds in a hinge region between the oxygenase and reductase domains stabilising the structure and facilitating the function of the enzymatic complex. It is expressed in response to various pro inflammatory stimuli (TNF-α, IL-1ß, interferon gamma) and microbial products (lipopolysaccharide-LPS) in various cells including monocytes, smooth muscle cells, macrophages, mast cells, endothelial cells, and

adipocytes. The expression of iNOS in these cells leads to generation of a high level of NO production compared to other isoforms (Engeli et al, 2004; Zamora et al, 2000).

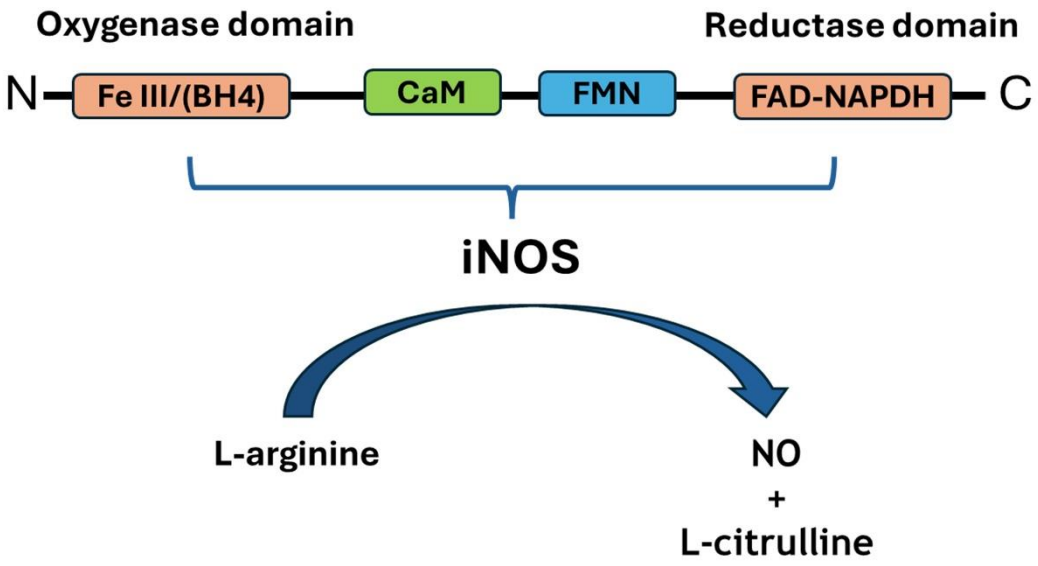

Figure 1-3 Structure and functional domains of iNOS enzyme.

The iNOS converts L-arginine into nitric oxide (NO) and L-citrulline, requiring a number of cofactors including: oxygen, reduced nicotinamide adenine dinucleotide (NADPH), tetrahydrobiopterin (BH4), flavin mononucleotide (FMN) and flavin adenine dinucleotide (FAD).

The expression of iNOS in adipose tissue and adipocytes is often upregulated in conditions associated with inflammation such as obesity and metabolic dysfunction (Araujo et al, 2018; Becerril et al, 2018). iNOS is typically induced when pro-inflammatory cytokines bind to receptors on the cell surface and activate different kinases including MAPKs, NF-KB and Akt, leading to the phosphorylation of various intracellular proteins and subsequent activation of specific transcriptional factors such as protein-1 (AP-1), activating transcription factor (ATF)-2, cAMP Response Element Binding Protein (CREB), Hypoxia-Inducible Factor (HIF), specificity protein 1 (Sp1), NF-KB and Signal Transducer and Activator of Transcription 1 (STAT1). The end result is induction of iNOS gene expression (Kleinert et al, 2004; Whitmarsh & Davis, 1996).

1.4.3 iNOS and lipid metabolism (lipolysis)

Lipolysis is a catabolic process which occurs during times of nutrient scarcity or increased physical activity. In this process, triglycerides (TAG) stored in fat cells (adipocytes) are broken down into free fatty acids and glycerol to be used by various tissues in the body (Ahmadian et al, 2010; Edwards & Mohiuddin, 2020). The control of lipolysis has been linked to iNOS expression in adipocytes, and inflammatory stimuli appear to be important. A study has demonstrated that iNOS inhibition augments cytokine-induced lipolysis in adipocytes (Penfornis & Marette, 2005). A human study has also shown that inhibition of NO release by subcutaneous adipose tissue results in the induction of lipolysis (Andersson et al, 1999). In addition, targeted disruption of the iNOS gene in obese mice has been shown to improve metabolic profile; suggesting an important link between iNOS and lipolysis (Becerril et al, 2018).

1.4.4 iNOS in obesity and insulin resistance

Elevated expression of iNOS was observed in adipose tissue of diabetic mice and obese humans (Engeli et al, 2004; Fujimoto et al, 2005; Jayarathne et al, 2018; Soskić et al, 2011) as well as obese rats (Jayarathne et al, 2018). Numerous studies have identified a potential link between iNOS expression and insulin resistance. iNOS knockout mice were shown to be protected from HFD-induced insulin resistance in adipocytes (Dallaire et al, 2008; Vilela et al, 2022). It was reported that inhibition of iNOS in mice fed with high fat diet (HFD) reduced the development of obesity-related insulin resistance (Tsuchiya et al, 2007). A further study has observed that iNOS expression and NO production inhibits insulin signalling and glucose uptake in 3T3-L1 adipocytes cocultured with macrophages (Fite et al, 2015). In addition, iNOS expression was proposed to be involved in palmitate-induced mitochondrial dysfunction and decreased adiponectin synthesis, which is associated with insulin resistance in 3T3-L1 adipocytes (Jeon et al, 2012).

1.5 Obesity-dependent PVAT Inflammation in Cardiovascular disease

Under physiological conditions, PVAT produces vasoactive substances which have anticontractile effects and this has been demonstrated in multiple vascular beds including rat aortic rings (Dubrovska et al, 2004; Löhn et al, 2002), human subcutaneous vessels (Greenstein et al, 2009), mouse gracilis artery (Saxton et al, 2022), and mouse thoracic aorta (Almabrouk et al, 2017). In contrast, PVAT has been shown to lose this effect in hypertension (Galvez-Prieto et al, 2008; Gálvez-Prieto et al, 2012), diabetes (Meijer et al, 2013), and obesity or high-far feeding (Almabrouk et al, 2018; Greenstein et al, 2009). The diminution in PVAT's anti-contractile effect in such diseases is attributed to adipokine imbalance (Szasz et al, 2013).

Considering the correlation between obesity and increased PVAT, it might be anticipated that PVAT should have a more pronounced anticontractile effect due to increased release of relaxing substances. However, current knowledge indicates that obesity causes changes to PVAT's structure and function, including changes in adipokine secretion, inflammation, and oxidative stress, resulting in diminished anticontractile effect. In obesity, PVAT tends to release more procontractile factors, such as superoxide and angiotensin while the release of anti-contractile factors including nitric oxide and hydrogen sulfide decreases (Sowka & Dobrzyn, 2021). The loss of anticontractile effect has been reported in many studies. For example, it was reported that the anti-contractile effect of PVAT is diminished in offspring of HFD-fed rats, which was due to a reduction in PVAT-derived NO bioavailability (Zaborska et al, 2016). In aorta isolated from mice fed with HFD, similar findings were observed, where PVAT lost its anti-contractile effect due to endothelial nitric oxide synthase (eNOS) dysfunction in PVAT (Xia et al, 2016). Almabrouk et al also demonstrated that the anticontractile effect of PVAT seems to be lost in mice fed a HFD via reduction of adiponectin secretion by the PVAT (Almabrouk et al, 2018).

Interestingly, these alterations in PVAT function in obesity and related conditions was reported to initiate a compensatory mechanism to preserve vascular function in a number of studies. Leptin is one adipokine that can be upregulated and

released by adipose tissue (Sowka & Dobrzyn, 2021). Early studies have shown that obese mice lacking leptin showed marked vascular dysfunction compared to wild type mice and that leptin promotes endothelial cells to release NO (Winters et al, 2000). Following studies reported that PVAT preserves vascular function of mesenteric artery isolated from HFD mice at an early period of feeding via leptin-indued NO overproduction (Gil-Ortega et al, 2010) while a more recent study showed that PVAT has an adaptive mechanism to restore vascular function via NO production in obese atherosclerotic rat model (Nakladal et al, 2022).

1.5.1 Mechanism of anti-contractility effect of PVAT

The modulatory effect of PVAT on VSMC tone was initially demonstrated by Soltis and Cassis in 1991, where they found that the presence of PVAT dramatically reduced norepinephrine-induced aortic ring contraction (Soltis & Cassis, 1991). Since this early study, many efforts have been made to understand the mechanisms by which PVAT induces vascular relaxation. It has been demonstrated that PVAT has an anticontractile effect on various different contractile agents, suggesting that PVAT releases transferable vasorelaxant substances or factors (Löhn et al, 2002). Since then, numerous studies have validated and confirmed the anticontractile effect of PVAT and shown that PVAT releases vasoactive substances causing vasodilation either via endothelium dependent or independent pathways.

1.5.1.1 Endothelium dependent mechanism

It was demonstrated that PVAT of rat thoracic aorta decreases the contractile responses to phenylephrine (PE) (Gao et al, 2007). In this study it was observed that transferring bathing solution of PVAT-intact rat aorta enhances the relaxant effect in endothelium intact vessels, however, in endothelium denuded vessels, the relaxant effect was diminished. These findings indicate that the endothelium layer was required for the full PVAT anticontractile effect to be observed. The activation of calcium-dependent K^+ channels in VSMC was suggested to be one the mechanisms by which this action was mediated via NO produced by endothelium (Gao et al, 2007). Moreover, it was also reported that adiponectin released from PVAT activates AdipoR1 on ECs to induce vasodilation in mouse mesenteric artery (Lynch et al, 2013). Furthermore, other vasoactive substances including omentin

and leptin released from PVAT have been reported to induce vasodilation via an endothelium-dependent pathway (Ahmed et al, 2023; Yamawaki et al, 2010). These adipokines seem to mediate their relaxant effect by stimulating eNOS activation in endothelium to promote the production of NO, which eventually leads to vasodilation (Ahmed et al, 2023).

1.5.1.2 Endothelium independent mechanism

On other hand, PVAT has been reported to alter vascular tone independently of endothelium such as in the rat aorta. In this study, it was suggested that H_2O_2 was produced by PVAT and subsequently led to activation of soluble guanylyl cyclase (sGC) in smooth muscle cells (Gao et al, 2007). Similarly, Fang and colleagues showed that inhibiting the K_{ATP} channel prevented the anticontractile action of endogenous H_2S from PVAT (Fang et al, 2009). Moreover, adiponectin has been reported to augment the relaxant effect of small mesenteric artery PVAT. In this study, it was suggested that adiponectin released from PVAT enhanced the relaxant effect of the vessel via modulating large-conductance Ca^{2+}-activated K^+ channels (BKCa) (Lynch et al, 2013). Furthermore, PVAT has been shown to decrease the contraction response to PE in rat mesenteric arteries, and this effect was attributed to voltage dependent, delayed-rectifier K (Kv) channel hyperpolarization in VSMC (Verlohren et al, 2004).

1.5.2 iNOS-derived NO and hyporeactivity induced by PVAT

The expression of iNOS in PVAT has been shown to modulate vascular function by enhancing the PVAT anticontractile effect. Several studies have demonstrated that iNOS-derived NO from PVAT may cause vasorelaxant effects. Administration of LPS to rats has been shown to lower contraction of aortic rings with intact PVAT. It has been suggested that the hyporeactivity is likely due to iNOS activation in PVAT (Hai-Mei et al, 2013). Moreover, an in vivo study has reported that PVAT of septic rat aorta decreases the contraction to PE (Awata et al, 2019). In the same study it was found that inhibition of iNOS with 7-nitroimadazole and 1400W reverses the hyporeactivity induced by PVAT in the aorta. Reis Costa and co-workers have shown that high-carbohydrate diet (HC-diet) enhances the anticontractile effect of PVAT in male Balb/c mice and that inhibition of iNOS with 1400W reestablished the contractile response induced by PE in the HC group (Reis

Costa et al, 2021). This study also reported that iNOS was much higher expressed in PVAT of HC-diet mice compared to the control group. Recently, it was reported that PVAT of thoracic aorta isolated from aged pre-atherosclerotic apolipoprotein E-deficient rats (ApoE$^{-/-}$ animals) fed with HFD improves vascular relaxation and enhances endothelial function via NO release (Nakladal et al, 2022). It was also shown that iNOS protein is highly expressed in the thoracic aorta PVAT of ApoE$^{-/-}$ animals, suggesting its role in NO production. Furthermore, an enhanced anticontractile effect of PVAT was seen in thoracic aorta of HFD-fed rats (Araujo et al, 2018). These findings suggest that the anticontractile effect is due to iNOS expression. In support of this suggestion, it was also found in this study that training the HFD group with aerobic exercise ameliorates the anti-contractile function of PVAT, which was associated with a significant decrease in the iNOS expression in the PVAT of thoracic aorta (Araujo et al, 2018).

1.6 Sphingolipid System

Sphingolipids are a class of cellular lipids which are emerging players in contributing to metabolic syndromes, such as obesity and type 2 diabetes (T2D). The sphingolipid system exerts its function in the body via different bioactive metabolites, including ceramide, sphingosine, sphingomyelin and sphingosine-1-phosphate (S1P). S1P and ceramide are bioactive metabolites that have been implicated in modulating inflammatory responses within adipose tissue via secretion of pro-inflammatory cytokines and chemokines from adipocytes and immune cells within adipose tissue, hence exacerbating inflammation (Fang et al, 2019; Kang et al, 2013).

1.6.1 Sphingosine 1 Phosphate

Sphingosine 1 phosphate is a metabolic product of sphingosine which was discovered in 1990 as a cell growth modulator (Olivera & Spiegel, 1993). S1P is produced by various types of cells, including erythrocytes, platelets, endothelial cells and also adipocytes (Ito et al, 2013; Mendelson et al, 2014; Thuy et al, 2014). S1P is responsible for various fundamental cellular functions and plays a significant role in physiology and pathophysiology of the cardiovascular system (Thuy et al, 2014).

1.6.1.1 Sphingosine-1-phosphate synthesis and degradation

S1P is formed through multiple steps; starting with ceramide production from sphingomyelin by the action of an enzyme called sphingomyelinase. Initially, ceramide is produced in three ways including de novo, metabolism of sphingomyelin and conversion of sphingosine by ceramide synthase as shown in figure 1-4. De novo production of ceramide takes place in the endoplasmic reticulum, starting with serine and palmitoyl-CoA condensation through serine palmitoyltransferase (SPT) to produce 3-ketodihydro-sphingosine. Following this step, 3-ketodihydrosphingosine reductase (3KDHR) reduces the 3-ketodihydro-sphingosine to form dihydrosphingosine. Ceramide synthases (CerS) acetylate dihydrosphingosine to generate dihydroceramides and then desaturation of dihydroceramides by the action of dihydroceramide desaturase (DES) produces ceramide (Pulkoski-Gross et al, 2015; Pyne & Pyne, 2000). Then, the ceramidase enzyme produces sphingosine from ceramide. Subsequently, phosphorylation of sphingosine by two sphingosine kinases produces S1P (Gandy & Obeid, 2013; Mendelson et al, 2014). S1P, in turn, is metabolized by S1P lyase (SPL) to phosphoethanolamine and hexadecanal. Alternatively, SIP can be dephosphorylated to sphingosine by the action of S1P phosphatases (S1PP) (Pulkoski-Gross et al, 2015; Pyne & Pyne, 2000). S1P exerts its functional roles through intracellular mechanisms, functioning as an intracellular second messenger within cellular compartments (Spiegel & Milstien, 2003). Alternatively, S1P can undergo export from the cellular interior to the extracellular milieu via specific transporters (Thuy et al, 2014), which will be discussed in more detail in (section 1.6.1.5).

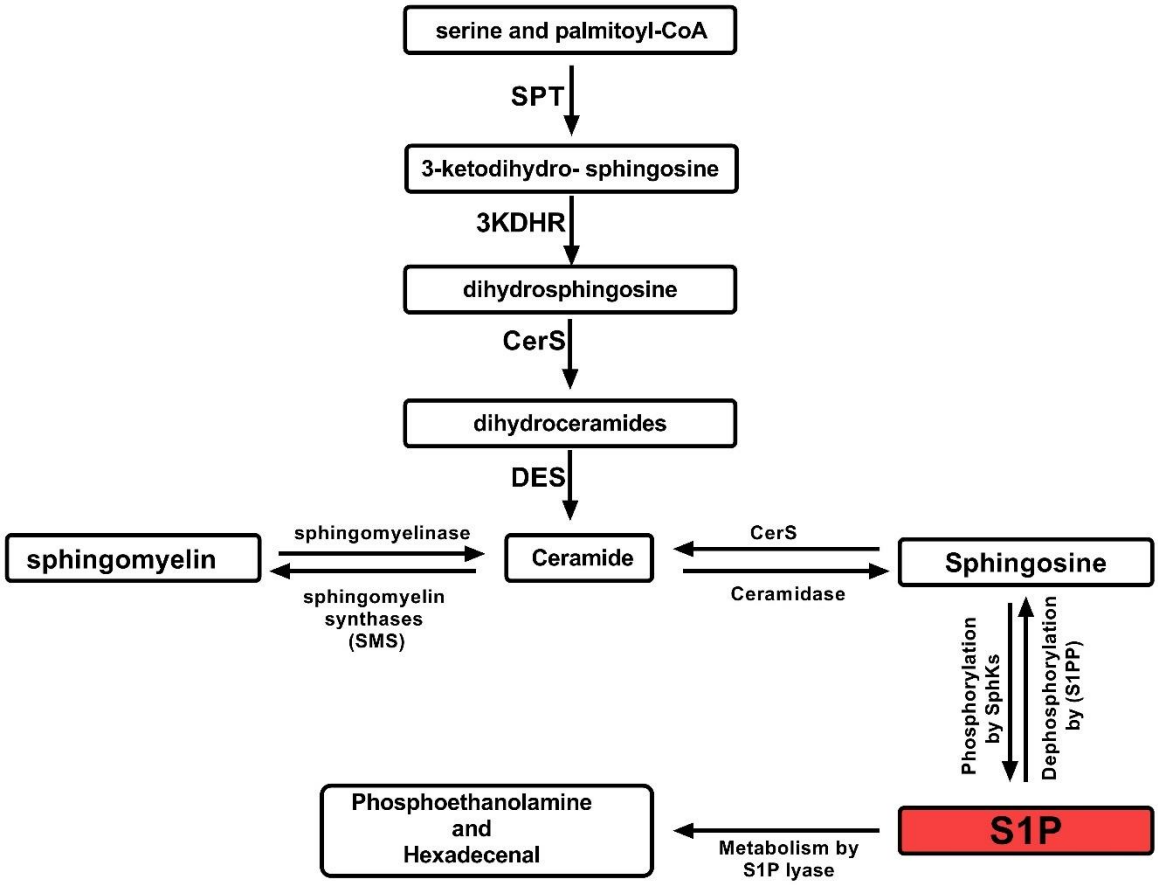

Figure 1-4 Schematic diagram of sphingosine-1-phosphate synthesis and metabolism.

Ceramide is mainly produced in three ways including: metabolism of sphingomyelin by sphingomyelinase; or by a de novo pathway starting from palmitoyl-CoA and serine via serine palmitoyltransferase (SPT), 3-ketodihydrosphingosine reductase (3KDHR), Ceramide synthases (CerS), and dihydroceramide desaturase (DES). Sphingosine can be converted to ceramide by CerS, or to Sphingosine 1 Phosphate by (S1P) Sphingosine kinase. S1P metabilsed S1P lyase (S1PL) to phosphoethanolamine and hexadecanal.

1.6.1.2 S1P in circulation

S1P concentration has a variable range within plasma and the tissues. In the plasma, S1P is found in its highest concentration, at a range between 0.1 and 1.2 μM, and the main source of plasma S1P is platelets (Venkataraman et al, 2008). In addition, platelets have a high level of S1P due to the lack of S1P lyase expression (Yatomi et al, 1995). However, tissues have a lower concentration of S1P which ranges between 0.5 and 75 pmol/mg (Venkataraman et al, 2008). Interestingly, the concentration gradient of S1P is affected by sphingosine kinase 1 (SphK1) activity. Venkataraman and co-workers indicate that the expression of SphK1 contributes to the S1P level in the plasma, emphasising the crucial role of SphK1 in determining tissue and circulating levels of S1P (Venkataraman et al, 2006).

Also, the concentration of S1P is altered under pathological conditions where, for example the severity of coronary artery stenosis in patients is associated with a high level of serum S1P (Deutschman et al, 2003), and serum S1P is also increased in patients with myocardial infarction (Polzin et al, 2017; Sattler et al, 2010). Adipose tissue is another contributor to plasma S1P, where it has been seen that obese mice (Wang et al, 2014) and obese humans (Ito et al, 2013) have higher levels of serum S1P compared to healthy mice and humans.

1.6.1.3 S1P transporter

S1P transporters are integral membrane proteins responsible for facilitating the translocation of S1P across cellular membranes. S1P is exported via specific transporters, and a number of S1P transporters have been identified as significant players in the physiological and pathological roles of S1P, including spinster homolog 2 (Spns2) transporter and ATP-binding cassette (ABC) transporters.

S1P release by Spns2 transporter

Spns2, belonging to the major facilitator superfamily (MFS) of non-ATP-dependent organic ion transporters and is a compact membrane protein of 58 kDa primarily located within the cell membrane (Chen et al, 2023a). Spns2 was the first identified mammalian S1P transporter and is the primary transporter facilitating the release of cellular S1P, as proven in a number of studies (Fukuhara et al, 2012; Nijnik et al, 2012). Kawahara and colleagues have reported that overexpression of Spns2 in zebrafish resulted in augmentation of S1P production (Kawahara et al, 2009). Several groups have then observed that the overexpression of Spns2 in mammalian cells and human embryonic kidney (HEK) 293 cells (Chen et al, 2023a; Nagahashi et al, 2013) increases the secretion of S1P. Conversely, Spns2 down-regulation resulted in a decrease in the release of S1P from HEK 293 cells (Nagahashi et al, 2013) and this was also seen in vascular endothelial cells of mice lacking Spns2 (Hisano et al, 2012). Investigations on Spns2-knockout mice have revealed that S1P levels in plasma and whole blood were markedly diminished by approximately 25–30% in these animals compared to wild-type (Nagahashi et al, 2013).

S1P release by ABC transporter

ABC transporters, including ABCA1 and ABCC1, are widely expressed in a number of cells and tissues, and play a fundamental role in transporting a diverse range of substrates across cell membranes (Theodoulou & Kerr, 2015). S1P has been recognised to be exported via ABC transporters in a number of studies. Several groups have reported that the suppression of ABC transporters with si-RNA including ABCA1 in astrocytes (Sato et al, 2007), and ABCC1 in mast cells (Mitra et al, 2006) resulted in a decrease in S1P production from these cells. In addition, it has been experimentally verified that the inhibition of ABCA1 using a non-selective inhibitor (glibenclamide), resulted in a decrease in S1P release induced by apoA in astrocytes (Sato et al, 2007) and HUVECs (Liu et al, 2016). Furthermore, the release of S1P induced by thrombin in rat platelets has been demonstrated to be inhibited by an ABCA inhibitor (glyburide). Consistent with these findings, in adipocytes the ABCA1 inhibitor glibenclamide decreased S1P in the media of adipocytes exposed to hypoxia (Ito et al, 2013). However, other studies have reported that S1P levels are not significantly affected by overexpression of ABCA1 and ABCC1 in Chinese hamster ovary (CHO) cells (Hisano et al, 2011) nor by the knock-out of ABCA1, ABCC1 and ABCA7 in mouse models (Lee et al, 2007).

S1P transport in the blood stream

It is known that S1P is mainly synthesised by blood cells including erythrocytes, activated platelets, neutrophils and monocytes which release it into plasma (Yatomi et al, 1995). In the blood, S1P is transported via binding to different proteins; albumin (30-40% of S1P) and lipoproteins, including HDL (50% of S1P), and LDL and VLDL (10% of S1P). S1P binds to HDL particularly via apolipoprotein M (ApoM) which functions as a chaperone for S1P, and controls the level of S1P within the bloodstream (Jozefczuk et al, 2020).

1.6.1.4 Sphingosine-1 phosphate receptors

The S1P receptors are a family of G-protein coupled receptors ($S1PR_1$, $S1PR_2$, $S1PR_3$, $S1PR_4$, and $S1PR_5$) and each one consists of approximately 400 amino acids (O'Sullivan & Dev, 2013). S1P receptors share common characteristics, including seven transmembrane α-helices that traverse the lipid bilayer, forming a polar

internal tunnel. The C terminus and three intracellular loops are exposed to the interior, while the N terminus and three extracellular loops are exposed to the exterior (Pulkoski-Gross et al, 2015; Spiegel & Milstien, 2003). The distribution of $S1PR_{1-5}$ is different among cells. Of these receptors, $S1PR_1$, $S1PR_2$, and $S1PR_3$ are most widely distributed in the cardiovascular tissues, and each one of these receptors has a different pattern of distribution in the main cell types of the CVS (Cannavo et al, 2017) and adipose cells, while $S1PR_4$ is mainly expressed in lymphoid tissues and $S1PR_5$ in the nervous system. Upon activation of the S1PRs by S1P, G-protein subunits, including (G_i, G_q, and $G_{12/13}$) are activated and released to regulate a wide range of downstream effector pathways (Jun et al, 2006; Li et al, 2016; Mastrandrea, 2013; O'Sullivan & Dev, 2013; Spiegel & Milstien, 2003). Each S1PR is coupled to specific G proteins, which mediate a different function (Figure 1-5).

$S1PR_1$: $S1PR_1$ was the first member of EDG family of GPCRs identified in 1990 in human umbilical vein endothelial cells (HUVEC) (Hla & Maciag, 1990; Yoh et al, 2002). $S1PR_1$ is widely expressed in ECs, VSMCs, fibroblasts and epithelial cells as well as adipocytes (Goetzl et al, 2004; Karuppuchamy et al, 2017; Mastrandrea, 2013). $S1PR_1$ activation mediates a wide range of cellular responses via coupling to specific heterotrimeric G-proteins and small GTPases. $S1PR_1$ mainly couples to G_i protein which causes adenylate cyclase suppression and subsequently leads to a decrease in the production of second messenger cyclic adenosine 3′,5′ - monophosphate (cAMP) and the activation of Ras, PI3K/Akt, and MAPKs family pathway (ERKs) (Gonda et al, 1999; Okamoto et al, 1998; Yoh et al, 2002). $S1PR_1$ signalling has been shown to induce the activation of Rac, a small GTPase in the Rho family. Furthermore, it was seen that $S1PR_1$ triggers phospholipase C (PLC) activation and Ca^{2+} mobilisation through Gi (Kluk & Hla, 2002; Okamoto et al, 1998). Taken together, $S1PR_1$ modulates a number of downstream cascades including, ERK1/2, PI3K/Akt and adenylyl cyclase via Gi and GTPases Rho and Rac signalling.

$S1PR_2$: $S1PR_2$ was initially identified as a GPCR in a rat aortic cDNA library, aiming to investigate a new signalling system in the vasculature (Okazaki et al, 1993; Yoh et al, 2002). S1P has been reported to have a high affinity for $S1PR_2$ (Gonda et al, 1999). $S1PR_2$ is expressed in various tissues and cell types, including lung, heart,

stomach, brain, thymus, kidney, adrenal glands, spleen and adipose tissue (Ishii et al, 2001; Mastrandrea, 2013). Unlike $S1PR_1$, $S1PR_2$ couples to multiple heterotrimeric G proteins including G_i, G_q and $G_{12/13}$, enabling it to influence multiple downstream pathways. The activation of $S1PR_2$ stimulates the PLC signalling pathway via the activation of a G protein, specifically G_q. PLC, in turn, cleaves phosphatidylinositol 4,5-bisphosphate (PIP_2) into inositol trisphosphate (IP3) and diacylglycerol (DAG). The resulting IP3 functions as a secondary messenger, enhancing the release of calcium ions (Ca^{2+}) from intracellular stores such as the endoplasmic reticulum. The subsequent increase in cytosolic Ca^{2+} levels play an important role in mediating various cellular responses, including cell migration, contraction, and other signalling events associated with the physiological and pathological effects of $S1PR_2$ activation (Cannavo et al, 2017). Moreover, $S1PR_2$ has been reported to regulate the adenylyl cyclase pathway via the activation of inhibitory G proteins, particularly G_i. The MAPKs family pathways (ERK-1/-2, JNK and p38), PI3K/Akt pathway, and NF-KB pathway (Aarthi et al, 2011; Gonda et al, 1999; Yu, 2021) represent additional G_i -dependent downstream signalling pathways associated with $S1PR_2$ activation. Furthermore, $S1PR_2$ can activate Rho and/or Rho kinase via coupling to G_q and $G_{12/13}$ (Skoura & Hla, 2009).

$S1PR_3$: $S1PR_3$ was initially identified from a human genomic library during an investigation of human cannabinoid receptors, and the amino acid sequence of $S1PR_3$ exhibits approximately 50% similarity to $S1PR_1$ and $S1RP_2$. $S1PR_3$ is similar to $S1PR_2$ in that it is widely expressed in various tissues and cell types, including organs lung, heart, stomach brain, thymus, kidney, adrenal glands, spleen and adipose tissue (Kluk & Hla, 2002). Like $S1PR_2$, $S1PR_3$ couples to multiple G proteins, including G_i, $G_{12/13}$, and G_q to eventually regulate several signalling pathways such as PLC/IP3/Ca^{2+}, MAPKs family pathways (ERKs), adenylyl cyclase, and small GTPases Rho and Rac (Kluk & Hla, 2002; Li et al, 2021; Siehler & Manning, 2002).

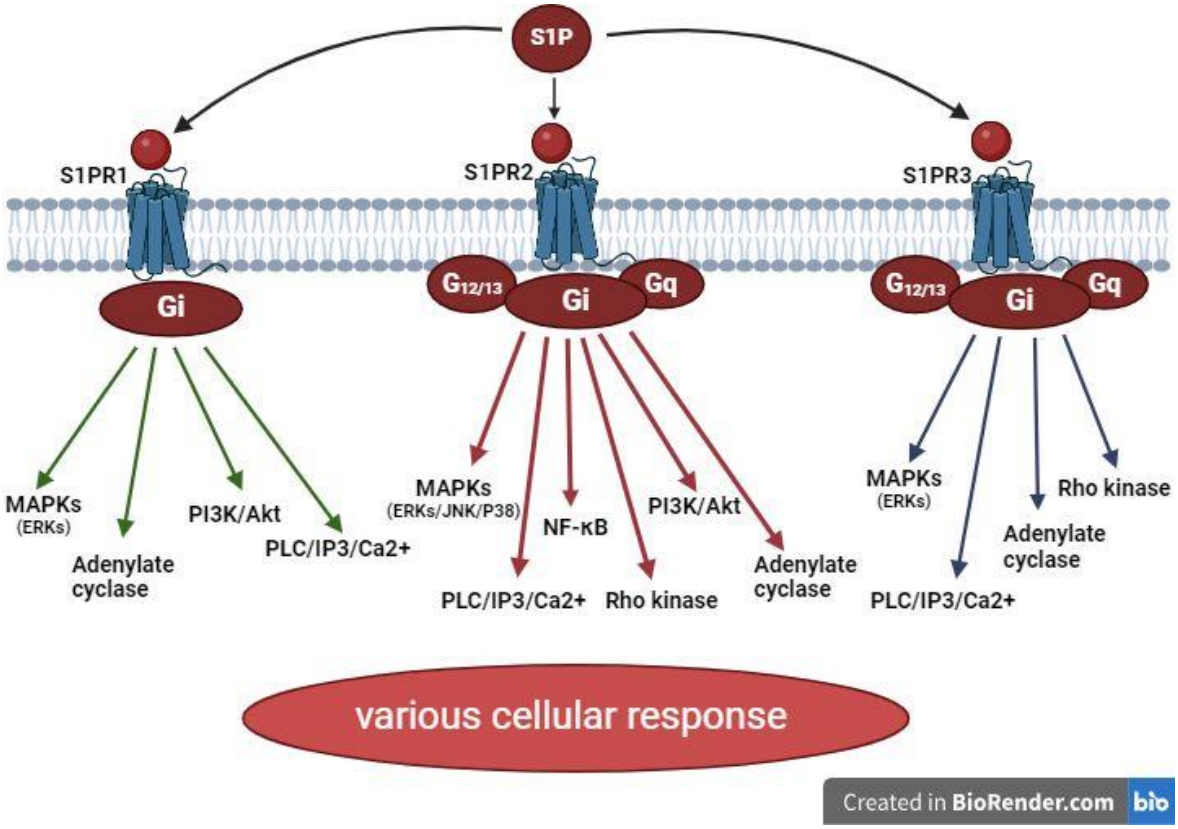

Figure 1-5 The S1P-S1PRs signalling.

This figure illustrates the signalling pathways activated by sphingosine-1-phosphate receptors (S1PRs), including S1PR1, S1PR2, and S1PR3. Each receptor activates its downstream signalling to regulates a diverse cell response. Abbreviations: Sphingosine 1 Phosphate (S1P), Sphingosine 1 Phosphate receptor (S1PR), Mitogen-Activated Protein Kinases (MAPKs), Nuclear factor-KB (NF-KB), Phosphoinositide 3-kinase/ protein kinase B (PI3K)/Akt, Phospholipase C (PLC), inositol trisphosphate (IP3).

Sphingosine 1 Phosphate agonists and antagonists

S1P receptors bind specifically to the endogenous ligands, S1P and dihydro-S1P (Contos et al, 2000). However, A number of selective small molecule S1PR agonists have been chemically synthesised and widely used in experimental studies including SEW2871 as a selective $S1PR_1$ agonist (Pan et al, 2006), CYM 5478 as a potent and selective $S1PR_2$ agonist (Herr et al, 2016) and CYM5541 which selectively binds to $S1PR_3$ receptor (Jo et al, 2012). Regarding S1PRs antagonists, $S1PR_1$ can be blocked by a selective antagonist called W146 (Sanna et al, 2006), $S1PR_2$ is antagonised by the highly selective compound JTE 013 (Osada et al, 2002; Parrill et al, 2004) and $S1PR_3$ can be blocked by a selective antagonist called BML-241 (CAY10444) (Salomone & Waeber, 2011). Fingolimod (FTY720) was the first S1PRs modulator identified and approved for multiple sclerosis (MS) treatment.

FTY720 is a prodrug which is phosphorylated by sphingosine kinases, particularly SphK2 to produce phospho-FTY720 which can bind to and activate all S1PRs except $S1PR_2$, causing internalization and degradation of the receptors (Brinkmann et al, 2010). Siponimod is a second generation of S1PRs modulators that is highly selective for $S1PR_1$ and $S1PR_5$, acting as a potent functional antagonist of $S1PR_1$ and $S1PR_5$ and recently approved by FDA in 2019 for the treatment of MS (Coyle et al, 2024).

1.6.1.5 Sphingosine 1 Phosphate intracellular signalling pathways

In addition to receptor-dependent signalling, S1P can also elicit its function intracellularly where it acts as a second messenger, including causing increased intracellular calcium levels (Birchwood et al, 2001) and cell survival (Zhang et al, 1991). In addition, S1P has been shown to regulate the function of a number of intracellular proteins. For example, TNF receptor- associated factor 2 (TRAF2) is a member of the TNF receptor associated protein family (TRAF), which is required for TNF receptor-mediated inflammation via NF-KB and MAPKs pathways. Intracellular S1P has been reported to bind to TRAF2 in order to activate NF-KB pathway (Alvarez et al, 2010). Moreover, prohibitin 2 (PHB2), is a conserved protein that regulates mitochondrial function, and it has been confirmed that intracellular S1P produced by SphK2 in mitochondria interacts with PHB2 to maintain mitochondria function (Strub et al, 2011). Another example is protein kinase C delta (PKCδ) which belongs to the protein kinase C family, and is proven to interact with the nuclear NF-KB pathway. It was also suggested that S1P produced by SphK1 interacts with PKCδ to activate the NF-KB pathway in macrophages (Puneet et al, 2010). It has also been documented that intracellular S1P activates the transcription factor peroxisome proliferator-activated receptor (PPAR)γ to regulate vascular development in vivo and in vitro (Parham et al, 2015).

1.7 Sphingosine Kinases

Sphingosine kinase is an enzyme involved in the generation of S1P. Two isoforms or variants of SphKs have been identified (SphK1 and SphK2) and there are important differences between the two; for example, SphK1 is generated from a gene located on chromosome 17 while SphK2 is generated from a gene on chromosome 19 (Cannavo et al, 2017). Structurally, the SphK isoforms are highly

similar with one subtle differences; both of these isoforms have a C-terminal region (CTR) and N-terminal region (NTR), in addition, they have an ATP-binding site and sphingosine recognition site. However, SphK2 has two additional regions at the N-terminal end and at the central region which make a difference in the amino acid length of around 250 residues (Jozefczuk et al, 2020). All human tissues express both SphK isoforms; SphK1 is highly expressed in heart, spleen, lung and leukocytes, whereases SphK2 is highly expressed in the liver. Three variants of SphK1 have been identified in human: SphK1a, SphK1b at 51 kDa, and SphK1c with molecular weight between 42.5 kDa and 51 kDa. For SphK2, two isoforms have been recognised in humans named SphK2a and SphK2b (Venkataraman et al, 2006). Several alternatively spliced variants of both SphK isoforms, differing at their N termini, have been identified in rats and mice (Alemany et al, 2007). In terms of SphKs localisation, Cannavo and his colleagues discuss in their review article that SphK1 is located mainly in the cytoplasm and can be translocated to the plasma membrane, whereas SphK2 is located at the endoplasmic reticulum and can also be associated with the mitochondria (Cannavo et al, 2017).

1.7.1 Sphingosine Kinase 1 regulation

Research over several decades has provided a plethora of knowledge about how SphK1 is regulated at transcriptional, post-transcriptional, and post-translational levels (Figure 1-6).

Transcription factor Sp1 is known to regulate SphK1 expression, and it has been reported that nerve-growth factor (NGF) upregulates Sp1 leading to increased SphK1 expression in PC12 cells, a rat pheochromocytoma cell line (Sobue et al, 2005). In glioblastoma cells, transcription factor AP-1 was shown to be responsible for SphK1 transcriptional induction in response to IL-1β (Paugh et al, 2009). Moreover, it has been demonstrated that the overexpression of SphK1 in human neuroblastoma cells in response to glial line-derived neurotrophic factor (GDNF) is dependent on the Sp1 and AP-2 transcription factor binding sites in the SphK1 promoter (Murakami et al, 2007). Other studies showed that HIF transcriptional factors could also regulate SphK1 gene expression, where it was reported that knockdown of HIF2α results in a decrease in SphK1 expression in U87MG glioma cells (Anelli et al, 2008). Several other different transcription factors have been

discovered that regulate SphK1 expression in different cells, including LIM-domain-only protein 2 (LMO2) (Matrone et al, 2017), and E2F transcription factor family members, E2F1 and E2F7 (Hazar-Rethinam et al, 2015).

Additionally, microRNAs have been identified as negative regulators of SphK1 expression at the translation level. miRNAs are short oligonucleotides, which degrade mRNAs by binding to RNA interference silencing complex (RISC) and target mRNA leading to either translation inhibition or increasing degradation of the targeted mRNA (Kim et al, 2009). For example, miR-124 overexpression has been reported to downregulate SphK1 by enhancing its degradation in ovarian cancer cells (Zhang et al, 2013). Another example is miR-506, which has been documented to interact with SphK1 in hepatocellular cancer cells causing SphK1 downregulation via a translation inhibition process (Lu et al, 2015). Recently, a number of miRNA have been identified which downregulate SphK1 translation, including miRNA-3677 in human osteosarcoma cells (Yao et al, 2020) and miRNA-6862 in neural cells (Xue et al, 2021).

The regulation of SphK1 can also be achieved by post-translation modification which either influences its localisation within the cells or promotes its activity. The cellular localisation of SphK1 is a crucial step in sphingolipid metabolism (Wattenberg et al, 2006). It is well known that SphK1 phosphorylation and cellular translocation into the plasma membrane is mediated via the phosphorylation of Ser225 site on SphK1 which causes S1P release and activation of S1PRs. For example, TNF-α, IL-1β and LPS have been reported to increase SphK1 activity by inducing its phosphorylation at Ser 225 in various cell types (Billich et al, 2005; Lee et al, 2019; Pitson et al, 2003). However, activity of SphK1 can also be regulated via mechanisms independent of Ser 225 phosphorylation. It has been reported in HEK-293 cells that SphK1 is translocated to the cell membrane by Gq protein in response to muscarinic receptor activation and bradykinin (Bruno et al, 2018; ter Braak et al, 2009). Others found that CIB1 protein-Ca^{2+} myristol switch protein-interacts with SphK1 to translocate it to the cell membrane in HeLa cells (Jarman et al, 2010).

Interaction with other proteins is another way of regulating SphK1 activity, which can either cause activation or inhibition. SphK1 activity is increased by the direct

interaction with other proteins including two Src family protein tyrosine kinases (PTKs). Fujita and colleagues have shown that SphK1 activity is increased as a result of the interaction with δ-Catenin/neural plakophilin-related armadillo repeat protein in primary rat embryonic hippocampal cells (Fujita et al, 2004). Moreover, Filamin A, known as an actin-cross-linking protein may also cause SphK1 activation in melanoma A7 cells, where it was shown that SphK1 activity is inhibited in cells lacking Filamine A (Maceyka et al, 2008). In addition, overexpression of TRAF2 has been documented to activate SphK1 in HEK 293T cells (Xia et al, 2002). Conversely, a number of studies have reported that several proteins can interact and inhibit the catalytic activity of SphK1. For instance, Sphingosine Kinase 1 Interacting Protein 1 (SKIP) was found to interact with SphK1 and attenuate its activity in HEK cells (Lacaná et al, 2002). Other proteins were identified which negatively regulate the activity of SphK1 by direct interaction, including platelet endothelial cell adhesion molecule 1 (PECAM-1) in HEK293 cells (Fukuda et al, 2004) and four-and-a-half LIM domain 2 (FHL2) in cardiomyocytes (Sun et al, 2006).

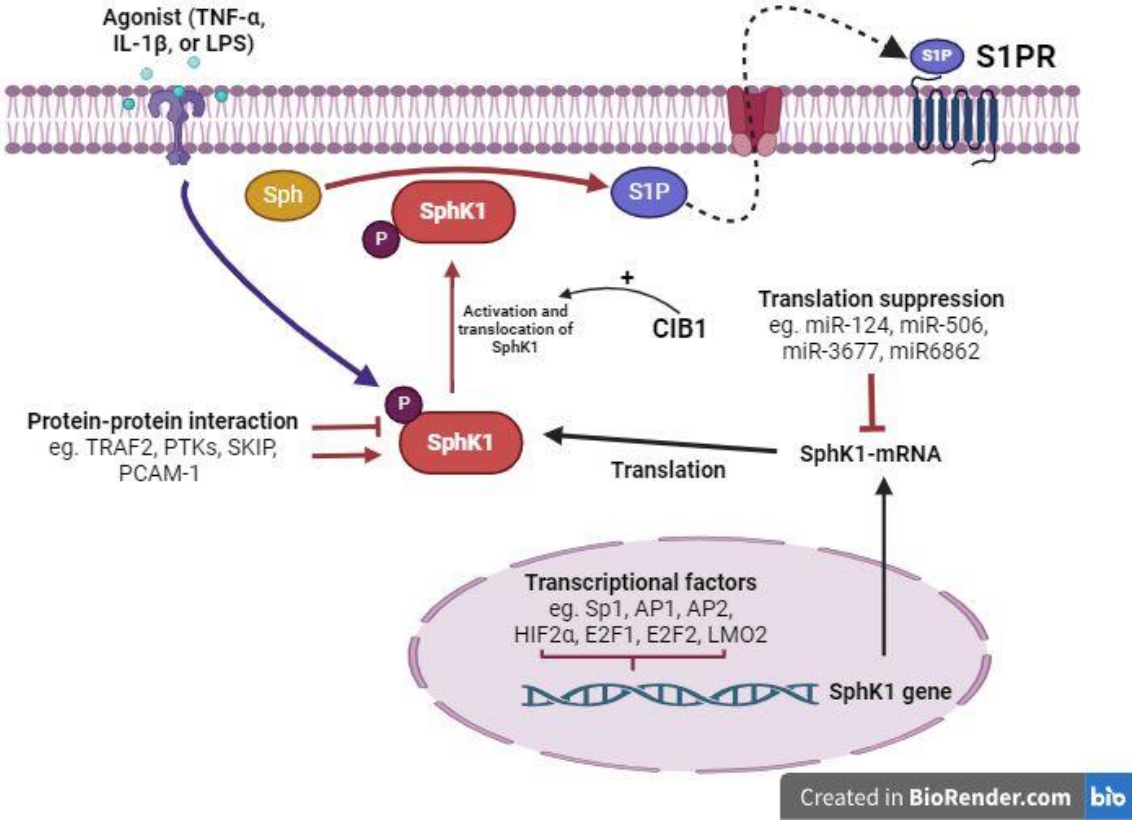

Figure 1-6 Schematic showing transcriptional, post-transcriptional, and post-translational mechanisms regulating SphK1 in cells.

Transcriptional regulation of SphK1 gene expression involves Sp1, AP1, AP2, HIF1a, E2F1, E2F2 and LM02. At the post-transcriptional level, noncoding RNAs, such as miR-124, miR-506, miR-3677 and miR6862 limit its translation. Post-translation regulation of SphK1 involves phosphorylation by stimuli such as IL-1β and TNF-α that can affect the subcellular localisation of SphK1; translocation is positively regulated by CIB1. Many protein-protein interactions with SphK1 have been shown to increase or decrease activity of SphK1. Localisation at the plasma membrane enables SphK1 to access its substrate Sphingosine (Sph) thereby leading to the production of S1P, which is then released via transporter to act on S1P receptors (S1PR).

1.7.2 Sphingosine Kinase 2 regulation

The regulation of SphK2 is less well studied compared to SphK1, however the catalytic activity of SphK2 increases in various cell lines in responses to number of stimuli including TNF-α and IL-1ß (Mastrandrea et al, 2005), LPS (Weigert et al, 2019; Yang et al, 2018), epidermal growth factor (EGF) (Hait et al, 2005) and hypoxia (Wacker et al, 2009). Similar to SphK1, SphK2 is subject to phosphorylation by different stimuli or ERK1/2, however, SphK2 is phosphorylated at two sites; Ser351 and Thr578 (Hait et al, 2007).

1.7.3 Sphingosine Kinases inhibitors

Over the last decades, extensive research has been undertaken to characterise and develop inhibitors of SphKs. L-threodihydrosphingosine (DHS), N,N-dimethylsphingosine (DMS), and N,N,N-trimethylsphingosine (TMS) were the first inhibitors identified targeting SphK1 and SphK2. However, these compounds inhibited other kinases including, protein kinase C (PKC), ceramide synthase (CerS), 3-phosphoinositide-dependent kinase and casein kinase II (Pitman & Pitson, 2010). A number of different non-lipidic small molecules, including SKI-I, SKI-II, SKI-III, and SKI-IV were then synthesised which exhibit high selectivity against SphK1 and SphK2. These compounds are the most widely used non-selective SphK inhibitors and they demonstrably reduce the amount of S1P in a number of cell types (French et al, 2003). Further studies were carried out to discover new compounds which are more selective for SphK1, including PF543, VPC96091, SK1-I (BML258) and compound 82 (Bu et al, 2021). PF543 is the most commonly used SphK1 inhibitor and shows a high selectivity for SphK1. It inhibits SphK1 via inducing proteasomal degradation of SphK1 which subsequently leads to lower S1P concentration (Byun et al, 2013). PF543 has been already used in a number of studies to investigate the physiological and pathological roles of SphK1 and these demonstrate its effect on S1P concentration in various cell types and animal models (Schnute et al, 2012; Yi et al, 2023). A number of selective SphK2 inhibitors have also been discovered such as (R)-FTY720-Ome (ROME), ABC294640, SG-12, K145, SKI-II and trans-12a (Neubauer & Pitson, 2013). ROME is a selective SphK2 competitive inhibitor and shows no inhibitory activity for SphK1 even at higher concentrations (Lim et al, 2011). It was reported that SphK2 inhibition with ROME decreased SphK2 expression and S1P concentration in LNCaP prostate cancer cells (Watson et al, 2013).

1.8 The role of Sphingosine Kinase/Sphingosine 1 Phosphate in vascular tone

Vascular tone is regulated by a range of circulating compounds which initiate vascular responses, either vasoconstriction or vasodilation. S1P is considered one of the crucial endogenous and vascular modulators that controls vascular function. The role of S1P in vascular tone was first reported in a study using rat isolated

mesenteric artery and intra-renal vessels, where it was shown that S1P induced vasocontraction and this effect was dependent on GPCR activation accompanied with increases in intracellular calcium (Bischoff et al, 2000). Subsequent research has further elucidated the distribution and specific role of S1PRs in vascular tone regulation. They contribute to inducing vasoconstriction or vasodilatation responses via several transduction pathways. The SphK/S1P system mediates vascular responses by either endothelium-dependent or endothelium-independent pathways. It is important to mention that the difference in response to these metabolites is dependent on vessel type, vascular bed, animal species, and receptor subtype expression (Michel et al, 2007).

Endothelial-dependent mechanism of S1P system

The S1P cascade mediates a divergent pathway in endothelial cells affecting endothelial integrity and vascular tone. Multiple studies have proven the crucial role of S1P in EC barrier integrity which is mediated by $S1PR_1$. For example, one study examined the involvement of S1P in enhancing integrity in human pulmonary artery ECs; they concluded that the involvement of S1P in the improvement of EC integrity was mediated by $S1PR_1$ (Singleton et al, 2005; Weigel et al, 2023). Similarly, another study published by Feistritzer and Riewald in 2005, identified the important role of $S1PR_1$ receptor in developing EC barrier integrity (Feistritzer & Riewald, 2005). These findings emphasise the significance of the S1P system in maintaining vascular integrity.

The ECs express surface $S1PR_1$ receptor highly compared with $S1PR_2$ and $S1PR_3$ subtypes (Wang et al, 2023). It has been demonstrated that S1P elicits vasorelaxation by eNOS downstream pathway (di Villa Bianca et al, 2006) and that this may be via $S1PR_1$ and $S1PR_3$ receptors on ECs (Igarashi & Michel, 2009). It has been shown that S1P can affect blood vessel tone by inducing vasodilation mediated by calcium sensitive and PI3 kinase cascade pathways, causing eNOS activation (Dantas et al, 2003; Liu et al, 2020). Previous work in our laboratory has shown that S1P causes an endothelium-dependent vasodilation response in rat aortic rings and coronary arteries through $S1PR_3$ receptor, and this response was achieved as a result of an increase of eNOS dependent NO formation (Alganga et al, 2019; Mair et al, 2010). In addition, $S1PR_3$ receptor is also implicated as a

mediator of vasodilation in mouse aorta in response to FTY720 (structural analogue of sphingosine-1-phosphate (S1P); and the vasodilation response was dependent on NO release via Akt-dependent eNOS phosphorylation (Tölle et al, 2005). Therefore, the S1P system likely to induce a vasodilation response in endothelium-intact beds, dependent on NO synthase. Intracellularly, S1P may modulate the eNOS expression in endothelial cells by the action of heat shock protein 90 (hsp90) (Roviezzo et al, 2006). Hsp90 is a regulatory protein that interacts with eNOS to maintain its enzymatic activity via facilitating the binding of cofactors and substrates necessary for NO production (Brouet et al, 2001).

Endothelium independent mechanism of S1P system

VSMCs express a different subtype of S1P receptors which initiate divergent intracellular signalling pathways (Coussin et al, 2002). The VSMCs express mainly $S1PR_2$ receptor and lower levels of $S1PR_1$ and $S1PR_3$ receptor (Alewijnse et al, 2004). VSMC contraction is initiated by the activation of specific receptors, leading to an increase in intracellular Ca^{2+} concentration through K^+ channel depolarization. This increase in Ca^{2+} activates MLCK, which ultimately leads to smooth muscle contraction. Also, contraction can be induced through a Ca^{2+}-sensitization pathway; mediated by activation of $G_{12/13}$ and RhoA cascade which ultimately leads to Rho-kinase cascade activation. VSMC modulates the vasoconstriction as a result of Rho kinase activation and intracellular calcium increases which are mediated by $S1PR_1$ receptor activation (Hemmings, 2006; Hemmings et al, 2006). Similarly, another study examined the receptor expression and which signalling pathway was causing vasoconstriction in response to S1P in VSMCs of rat cerebral artery and aorta. In the rat cerebral artery, vasoconstriction was mediated by Rho-kinase and increases in Ca^{2+} release from the sarcoplasmic reticulum which was mediated by $S1PR_2$ receptor and $S1PR_3$ receptor. However, in the aorta, the vasoconstriction was insignificant compared with the cerebral artery and this could be due to the low-level expression of $S1PR_2$ receptor and $S1PR_3$ receptor (Coussin et al, 2002). In addition, S1P could modulate vasoconstriction by activation of L-type Ca^{2+} channels and increasing intracellular Ca^{2+} concentrations (Bischoff et al, 2000). Other signal transduction pathways which modulate VSMCs constriction under the effect of S1P include phosphorylation of p38 MAPK and ERK1/2 (Hemmings, 2006). On the other hand,

intracellular S1P is also capable of inducing vasoconstriction by opening store-operated calcium channels (SOCE) which subsequently leads to the movement of calcium into the cells (El-Shewy et al, 2018). Generally, VSM is contracted in response to S1P via intracellular Ca^{2+} elevation, the influx of extracellular Ca^{2+}, or Rho- kinase pathway.

1.9 The role of Sphingosine Kinases/Sphingosine 1 Phosphates in adipose tissue function

1.9.1 Expression of SphKs and S1PRs in adipose tissue

SphK1 and SphK2 are expressed in cultured 3T3-L1 adipocytes and subcutaneous adipose tissue (SAT) (Hashimoto et al, 2009; Kitada et al, 2016), epididymal white adipose tissue (EWAT) (Kitada et al, 2016; Zhang et al, 2014) and BAT (Morishige et al, 2023). Similarly, $S1PR_{1-3}$ are expressed on 3T3-L1 adipocytes (Lee et al, 2017; Mastrandrea, 2013), differentiated rat white adipocytes (Jun et al, 2006), and in epididymal adipose tissue (EAT) and SAT (inguinal) (Chakrabarty et al, 2022). Furthermore, S1P concentration has been reported to positively correlate with obesity and to exhibit high levels in adipose tissue of obese humans and mice (Guitton et al, 2020; Samad et al, 2006).

1.9.2 Role of SphKs/S1P in adipogenesis and lipid metabolism

A plethora of studies have investigated the role of sphingolipid components including SphK1, SphK2, and S1PRs in the context of adipogenesis. SphK1 and SphK2 activation in 3T3-L1 adipocytes has been reported to increase over the period of adipogenesis which was accompanied by increases in S1P production (Hashimoto et al, 2009). In the same study, pharmacological and genetic inhibition of SphK1 significantly attenuated lipid droplet accumulation and adipogenic marker gene expression. Similarly, it has been shown that SphK1 and SphK2 increase during adipogenesis and SphK1 inhibition with SPHK-I2 led to a decrease in the accumulation of lipid droplets in mature adipocytes (Mastrandrea, 2013). Although SphK1 inhibition has been shown to attenuate adipogenesis, there are a number of reports showing that S1PRs activation also led to adipogenesis restriction. Treatment of 3T3-L1 preadipocytes with S1P inhibited differentiation and lipid accumulation accompanied by transcriptional factor downregulation

such as PPARγ, (C/EBPα) and adiponectin (Moon et al, 2014). In support of this, pharmacological or genetic inhibition of $S1PR_2$ led to increased adipogenesis, lipid accumulation and transcriptional factors, including PPARγ, (C/EBPα) and adiponectin in 3T3-L1 adipocytes (Jeong et al, 2015; Moon et al, 2015) while mice lacking S1P lyase had reduced adiposity compared to wild type (Bektas et al, 2010). Furthermore, it has been shown that silencing or antagonism of $S1PR_1$ led to promoted 3T3-F442A preadipocyte differentiation (Kitada et al, 2016).

1.9.3 Ceramide biosynthesis in adipose tissue inflammation

Ceramide levels have been reported to be elevated in adipose tissue of obese women (Kolak et al, 2007), adipose tissue of obese and diabetic patients (Candi et al, 2018; Chaurasia et al, 2016), and adipose tissue of HFD-fed mice (Turner et al, 2013). Targeting the biosynthesis of ceramide had a beneficial effect and promising results in inflamed adipose tissue. It was reported that HFD mice treated with SPT inhibitor myriocin had less weight gain and improved glucose tolerance and insulin sensitivity, compared to untreated HFD-mice (Yang et al, 2009). In the same study myriocin suppressed cytokine expression including monocyte chemoattractant protein-1 (MCP-1) in adipose tissue of HFD mice. In a similar study carried out by Turpin et al, it was shown that mice lacking CerS6 are protected from diet-induced obese (DIO) and expression of proinflammatory gene expression in WAT (Turpin et al, 2014). In mice lacking CerS5 challenged with HFD,it was reported that the mice were protected from HFD induced glucose intolerance and adipose tissue inflammation (Gosejacob et al, 2016).

1.9.4 Sphingosine kinases and S1P in adipose tissue inflammation

SphKs/S1P have been proposed to exert a proinflammatory role in different tissues and cell types. However, the role of the SphKs/S1P axis in regulating inflammation in adipocytes and adipose tissue remains to be fully elucidated. SphKs/S1P have a proinflammatory role and the system is upregulated in obese animal models and obese humans. For instance, it has been reported that SphK1, but not SphK2 is highly expressed in subcutaneous adipose tissue of obese mice compared to healthy mice (Hashimoto et al, 2009). Similar to this finding, Wang et al, reported that expression of SphK1 is increased in epididymal adipose tissue and mature

adipocytes isolated from HFD mice compared to mice on low fat diet (Wang et al, 2014). Moreover, S1P plasma levels are positively corelated with BMI in obese humans and diabetic mice in a number of studies (Ito et al, 2013; Nojiri et al, 2014). Another study demonstrated that S1P was increased in adipose tissue and plasma of DIO mice (Wang et al, 2014).

Other studies followed, providing further evidence that SphK1 promotes inflammation in adipose tissue and adipocytes. Deletion of SphK1 decreased proinflammatory cytokine expression including TNF-α, IL-6, and IL-1β in EAT of obese mice, whereas anti-inflammatory adipocytokines, including IL-10 and adiponectin were upregulated in obese mice lacking SphK1 (Wang et al, 2014). LPS was reported to increase proinflammatory cytokine expression, including CCL5, IL-6, pentraxin 3 (Ptx3) and TNF-α in SAT of lean Zucker rats, while rats treated with SphK1/2 or SphK1 inhibitors displayed a decrease in secretion of these proinflammatory cytokines in adipose tissue (Tous et al, 2014). In the same study, utilising 3T3-L1 adipocytes, the authors show that silencing SphK1 diminishes LPS-induced chemokine (C-C motif) ligand 5 (CCL5). Both in vitro and in vivo studies have reported that SphK1 promotes IL-6 production in adipocytes (Zhang et al, 2014). Recently, adipocyte-specific $SphK1^{-/-}$ mice were found to be protected from HFD-induced inflammatory cytokine expression in adipose tissue (Anderson et al, 2020). Furthermore, $SphK2^{-/-}$ mice were protected from HFD-induced leptin expression in EWAT and inguinal white adipose tissue (IWAT) which is a marker for obesity (Zhao & Lee, 2023). SphK1 was reported to be activated in M1 macrophages isolated from adipose tissue of DIO and ob/ob mice (Gabriel et al, 2017). Genetic or pharmacological inhibition of SphK1 were both shown to protect mice from HFD-induced M1 infiltration into adipose tissue (Wang et al, 2014). Similarly, studies utilising RAW 246.7 cells have reported an increase in SphK1 activity and S1P content in response to LPS treatment (Hammad et al, 2008; Wu et al, 2004).

Both SphK1 and SphK2 produce S1P, which has been linked to regulating the production of pro-inflammatory cytokines and to promote inflammation in adipose tissue. There are a number of lines of evidence demonstrating that S1P stimulates inflammation in adipocytes and adipose tissue. For example S1P promotes inflammation in 3T3-L1 adipocytes with increased inflammatory cytokine

secretion (Samad et al, 2006). In vivo studies have also shown that knockdown and pharmacological inhibition of $S1PR_2$ diminishes HFD-induced inflammation in mice (Asano et al, 2023; Kitada et al, 2016). However, $S1PR_1$ activation with SEW has also been reported to inhibit inflammation, causing lower expression of TNF-α and Cd11c in EAT of obese mice (Asano et al, 2023). A recent study carried out by Chakrabarty and coworkers reported that $S1PR_3$ expression is increased in adipose tissue (AT) of HFD mice, whereas mice which are $S1PR_3$-deficient ($S1PR_3^{-/-}$) exhibited a high inflammatory and macrophage infiltration profile in adipose tissue (Chakrabarty et al, 2022).

It is well known that immune cell infiltration and inflammation within the adipose tissue play an important role in insulin resistance and glucose intolerance. A number of in vitro and in vivo studies have reported that SphK1/S1P negatively regulates insulin resistance and lipolysis in adipose tissue, and this is linked to its impact on inflammatory mediators. For example, in a study carried out by Zhang et al, pharmacological or genetic inhibition of SphK1 promoted lipolysis dependent IL-6 upregulation in adipocytes (Zhang et al, 2014). Mice with $SphK1^{-/-}$ fed with HFD were shown to have enhanced insulin sensitivity and glucose tolerance which was attributed to the inhibition of inflammation in adipose tissue (Olefsky & Glass, 2010; Osborn & Olefsky, 2012; Wang et al, 2014). Moreover, the HFD-induced glucose intolerance and insulin resistance was reported to be diminished in $S1PR_2$ knockout mice. In agreement, HFD mice treated with $S1PR_2$ antagonist JTE-013 had improved insulin sensitivity (Kitada et al, 2016).

Overall, these few studies indicate that SphK1/S1P/$S1PR_2$ axis leans towards a pro-inflammatory influence in adipose tissue, particularly in the context of obesity, contributing to development of insulin of resistance and metabolic disorders such as type 2 diabetes. However further studies are necessary to fully understand the molecular mechanisms behind this.

1.10 Crosstalk between Sphingosine Kinases/ Sphingosine 1 Phosphate and iNOS regulation

Although iNOS has been documented to be either upregulated or downregulated by SphK1/S1P axis in different cell types and tissues under inflammatory condition

or disease (Li et al, 2020; Nayak et al, 2010; Wang et al, 2021), the SphK1/S1P/S1PRs axis and its potential role in iNOS regulation in 3T3-L1 adipocytes and adipose tissue remains to be investigated and will form the central focus of investigation in this project.

Pharmacological and genetic inhibition of SphK1 was reported to attenuate LPS-induced-iNOS expression and NO production in BV2 microglia. In the same study, treatment of BV2 microglia with S1P resulted in an increase in iNOS expression and NO production (Nayak et al, 2010). In 2017, Vasconcelos et al. demonstrated that DMS, an inhibitor of SphK1 was able to reduce iNOS gene expression in heart tissue of Trypanosoma cruzi-infected mice (Vasconcelos et al, 2017). Other studies followed, providing further evidence that $S1PR_2$ inhibition attenuates synthesis of protein or gene expression of iNOS in rat glomerular mesangial cell line (Gong et al, 2020), in the aorta of $ApoE^{-/-}$ animals (Ganbaatar et al, 2021), and iNOS expression and NO production in placenta tissue of the preeclampsia rat (Zhang et al, 2021). A recent study utilising a spinal cord injury (SCI) rat model demonstrated an increase in iNOS protein expression with a concomitant increase in SphK1 expression in spinal cord tissue, while conversely, SCI rats treated with PF543 showed a decrease in iNOS expression (Wang et al, 2021). In the same study, it was demonstrated that PF543 reduced the LPS-induced iNOS activation in HAPI microglial cell line and that exogenous S1P reversed the effect of SphK1 inhibition. On the other hand, a few studies have suggested that SphK1/S1P pathway activation had a negative effect on iNOS expression. For example, an early study carried out by Xin et al, using renal mesangial cells (Xin et al, 2004) demonstrated that S1P inhibits IL-1β-induced iNOS expression and NO production. Further studies have shown that S1P downregulates iNOS expression and NO production induced by IL-1β or LPS in rat VSMC (Machida et al, 2008), macrophages (Hughes et al, 2008) and chondrocytes (Stradner et al, 2008). A recent study using a mouse non-alcoholic fatty liver-ischaemia/reperfusion model (NAFL-I/R), found there was an elevation in iNOS expression in hepatocytes of mice lacking SphK1 (Li et al, 2020). In the same study, administration of S1P to (NAFL-I/R) diminished iNOS expression in hepatocytes isolated from the mice.

1.11 S1P and Perivascular adipose tissue

In addition to regulating vascular function, S1P is produced by adipose tissue and regulates many biological processes as discussed in section 1-9. However, the role of S1P in regulating PVAT-mediated anticontractile effects has not been investigated. Interestingly, some studies have proven that SphKs and its product S1P is upregulated in adipose tissue, including SAT and EWAT particularly in inflammatory conditions. These studies suggest that S1P could be exported from PVAT under inflammatory conditions to act in a paracrine or autocrine manner by binding to S1PRs either on PVAT cells to release of vasoactive substances from PVAT, or on vascular cells including endothelial cells and VSMCs to ultimately modulate vascular tone.

1.12 Hypothesis and Aim

Elevated levels of SphK1/S1P are strongly associated with proinflammatory cytokines, insulin resistance and Type 2 diabetes in obesity, and ablation of this system has been demonstrated to inhibit inflammation within adipose tissue. Although sphingolipids have been previously reported to promote inflammation via upregulation of the proinflammatory enzyme iNOS in a number of cells, an investigation into the role of the sphingolipid system on iNOS regulation in adipocytes and adipose tissue has yet to be undertaken. Thus, the principal research aim of this thesis was to investigate the role of the SphK/S1P system in iNOS regulation in 3T3-L1 adipocytes and PVAT subjected to a proinflammatory stimulus (IL-1ß) and how this system is involved in mediating the anticontractile effect of PVAT under inflammatory conditions. This was achieved through the following experimental aims:

The initial aim of this study was to investigate the expression of SphK1 in 3T3-L1 adipocytes and test whether exogenous S1P activates different proinflammatory pathways. Furthermore, to investigate the effect of a proinflammatory stimulus (IL-1ß) on SphKs expression and the effect of S1P on IL-1ß-mediated iNOS regulation in 3T3-L1 adipocytes.

The second aim was to fully address the specific role of both SphK isoforms (SphK1 and SphK2) and specific receptors ($S1PR_1$, $S1PR_2$, and $S1PR_3$) in iNOS regulation and the pathways involved in 3T3-L1 adipocytes. Moreover, the role of the sphingolipid system in paracrine signals between adipocytes and macrophages, particularly in iNOS regulation.

Finally, the effect of IL-1ß on PVAT-mediated hyporeactivity via iNOS regulation was investigated to assess its role in the anticontractile effect of PVAT.

Chapter 2 - Materials and Methods

2.1 Materials

2.1.1 Materials and chemicals

A list of materials and chemicals used in this thesis can be found in Table 2-1.

Table 2-1 Chemicals and suppliers

Supplier	Materials (Cat.No.)
Cayman Chemical, USA	CYM 5478 (29024) CAY10444 (CAY10005033)
Enzo Life Sciences (UK) Ltd	Thromboxane A2 mimetic, 9,11-dideoxy-11α,9α-epoxymethanoprostaglandin F2α (U46619)
Fisher Scientific UK Ltd, Loughborough, Leicestershire, UK	10 cm diameter dishes Bovine serum albumin (BSA)(PB1600-100) Corning tissue culture T75/T150 flasks High-Capacity cDNA Reverse Transcription (#4368814) NuPAGE™ LDS Sample Buffer (4X)(NP0007) Pierce™ BCA Protein Assay Kits (23277) Taqman® Universal Master Mix II (#4440040) Taqman® Fast Advance Master Mix (#4444557)
Invitrogen (GIBCO Life Technologies Ltd), Paisley, UK	Dulbecco's modified Eagles media (DMEM), high glucose Dulbecco's modified Eagles media (DMEM)+GlutaMAX Foetal calf serum (FCS) (USA origin) Foetal calf serum (FCS) (EU origin) Newborn calf serum (NCS) Phosphate buffered saline (PBS) Penicillin/streptomycin Trypsin
LI-COR, Biosciences, Lincoln, NE, USA	REVERT Total protein staining (926-11010)
New England Biolabs Inc, UK	Blue Prestained Protein Standard, Broad Range (11-250 kDa) (P7719S)
Qiagen Ltd, UK	RNeasy Mini Kit (74104) RNeasy Lipid tissue Mini Kit (74804)
Pall Corporation, UK	Transfer membrane, BioTrace™ NT, N/A, Nitrocellulose, Pore size: 0,2 µm, Rolls, 300×3000 (#66485)
R&D System	Recombinant mouse IL-1ß/IL-1F2 protein

Sigma-Aldrich Ltd, Gillingham, Dorset, UK	3-Isobutyl-1-methylxanthine (IBMX) (I5879) Acetylcholine (A6625) Dexamethasone Glybenclamide (G0639) Lipopolysaccharides from E.coli (L2630) Porcine Insulin (I5523) PF543 (PZ0234) Phenylephrine (P6126) ROME (857392O) Tween-20
Severn Biotech Ltd, Kidderminster, Hereford, UK	Acrylamide:Bisacrylamide (37.5:1; 30% (w/v) Acrylamide) (20-2100-10)
Tocris Bioscience, Bristol, UK	1400W dihydrochloride (1415) CYM5541 (4897) JTE 013 (2392) SEW2871 (2284) Sphingosine 1 Phosphate (1370) Troglitazone (3114) W146 (3602)
VWR International Ltd, Lutterworth, Leicestershire, UK	Falcon tissue culture 10 cm diameter dishes Falcon tissue culture 6/12 well plates

2.1.2 List of equipment and suppliers

A list of equipment used in this thesis can be found in Table 2-2.

Table 2-2 Equipment and supplier

Supplier	Equipment
ADInstruments, Oxford, UK	Chart™ 8 Pro software
Bio-Rad Laboratories Ltd, UK	Mini Trans-Blot Electrophoretic Transfer Cell+ Power pack
Danish Myo Technology, Aarhus, Denmark	Four-channel small vessel wire myograph
LI-COR Biotechnology, USA	Odyssey Sa Infrared Imaging System and Software
Thermo Scientific, Waltham, MA, USA	Nanodrop spectrophotometer

2.1.3 List of buffers and solutions

A list of buffers and solutions used in this thesis can be found in Table 2-3.

Table 2-3 Buffers and solutions

Name	Composition
High potassium physiological salt solution (KPSS)	62.5 mM KCl 1.2 mM $MgSO_4$, 24.9 mM $NaHCO_3$, 1.2 mM KH_2PO_4, 2.5 mM $CaCl_2$ and 11.1 mM Glucose
Physiological salt solution (PSS)	4.7 mM KCl, 1.2 mM $MgSO_4$, 24.9 mM $NaHCO_3$, 1.2 mM KH_2PO_4, 2.5 mM $CaCl_2$, 11.1 mM Glucose, and 119.0 mM NaCl
RIPA lysis buffer	25 mM Tris-HCl, pH 7.6 150 mM NaCl, 1% NP-40, 1% sodium deoxycholate, 0.1% SDS
Running buffer	25 mM Tris base, 190 mM glycine, 0.1% (w/v) SDS
Resolving gel solution	10% (v/v) acrylamide/0.33 % (v/v) bisacrylamide in 125 mM Tris-HCl (pH 8.8), 0.1 % (w/v) SDS, 0.1 % (w/v) APS, 0.05 % (v/v) TEMED
Stacking gel solution	250 mM Tris-HCl pH 6.8, 5 % (v/v) acrylamide, 0.1 % (w/v) SDS, 0.1 % (w/v) APS, 0.05 % (v/v) TEMED
Transfer buffer	25 mM Tris base, 192 mM glycine, 20% (v/v) ethanol
Tris-buffered saline (TBS)	20 mM Tris-HCl (pH 7.5), 137 mM NaCl
Tris-buffered saline - Tween 20 (TBST)	20 mM Tris-HCl pH (7.5), 137 mM NaCl, 0.1% (v/v) Tween 20
5 % blocking buffer	1g milk powder in 20ml TBST

2.1.4 Antibodies

A list of primary and secondary antibodies used in these experiments can be found in Table 2-4 and Table 2-5.

Table 2-4 Primary antibodies

Antibody	Source(Catalouge.N)	Species	Dilution
Akt	Cell Signalling Technology(#2920)	Mouse	1:1000
phospho-Akt (S473)	Cell Signalling Technology(#4058)	Rabbit	1:1000
ß-actin	Cell Signalling Technology(#4970)	Rabbit	1:1000
p44/42 MAPK (Erk1/2)	Cell Signalling Technology(#9102)	Rabbit	1:1000
Phospho-p44/42 MAPK (Erk1/2) (Thr202/Tyr204)	Cell Signalling Technology(#5726)	Mouse	1:1000
GAPDH	Invitrogen (PAI-988)	Rabbit	1:1000
iNOS	Cell Signalling Technology(#13120)	Mouse	1:1000
iNOS	Abcam (ab283655)	Rabbit	1:1000
IKBα phospho-S32	Cell Signalling Technology(#2859)	Rabbit	1:1000
IKBα	Cell Signalling Technology(#4814)	Mouse	1:1000
JNK	Cell Signalling Technology(#9252)	Rabbit	1:1000
Phospho- JNK (Thr183/Tyr185)	Cell Signalling Technology(#9255)	Mouse	1:1000
NFKB p65	Cell Signalling Technology(#6956)	Mouse	1:1000
Phospho-NFKB p65-S563	Cell Signalling Technology(#3033)	Rabbit	1:1000
p38 MAPK	Cell Signalling Technology(#9212)	Rabbit	1:1000
Phospho-p38 MAPK (Thr180/Tyr182)	Cell Signalling Technology(#9216)	Mouse	1:1000
SphK1	Santa Cruz (sc-365401)	Mouse	1:500
Phospho-SphK1 (Ser-225)	ECM Biosciences (#SP1641)	Rabbit	1:1000

All primary antibodies were prepared in TBST supplemented with 5% (w/v) BSA and were incubated overnight at 4°C.

Table 2-5 Secondary antibodies

Conjugate	Epitope	species	Dilution	Source(Catalouge.N)
IRDye® 800CW	Rabbit	Donkey	1:10000	LI-COR Biosciences, USA (# 926-32213)
IRDye® 680CW	Rabbit	Donkey	1:10000	LI-COR Biosciences, USA (# 926-68073)
IRDye® 800CW	Mouse	Donkey	1:10000	LI-COR Biosciences, USA (# 926-32212)

IRDye® 680CW	Mouse	Donkey	1:10000	LI-COR Biosciences, USA (# 925-68072)

All secondary antibodies were prepared in TBST supplemented with 5% (w/v) BSA and were incubated for 1 h with shaking at room temperature.

2.1.5 Animals

Male Sprague-Dawley (SD) rats were purchased from ENVIGO (UK). Male C57 BL6 mice were purchased from Harlan (UK). Mice and rats were housed in the Central Research Facility (CRF) at University of Glasgow and maintained on 12-hour cycles of light and dark and the room temperature was held at 21°C with free access to both food and water. All animal experiments were performed in accordance with the United Kingdom Home Office Legislation under the Animals (Scientific Procedure) Act 1986 (project licence PP1756142).

2.2 Methods

2.2.1 Cell culture and tissue procedures

2.2.1.1 Cell culture plastic ware

3T3-L1 preadipocytes were cultured in Corning T75 flasks, Falcon 10 cm diameter dishes, 6 well and 12 well plates. RAW cells were cultured in 10 cm diameter dishes and 6 well plates.

2.2.1.2 Recovery of cryopreserved cell stocks from liquid nitrogen

3T3-L1 pre-adipocytes originally purchased from (American Type Culture Collection, Manassas, VI, USA) were kindly provided by Dr Ian Salt (School of Molecular Bioscience, University of Glasgow). 3T3-L1 pre-adipocytes, a mouse fibroblast cell line were stored frozen in cryogenic vials in liquid nitrogen. The cells were removed from the liquid nitrogen when required and quickly thawed in a water bath at 37°C. The cells were then transferred to a T75 flask containing 10 ml of warmed media (Dulbecco's modified Eagles medium (DMEM) supplemented with 10% (v/v) newborn calf serum (NCS) and 1% (v/v) penicillin/streptomycin that had been equilibrated to 37°C in 10% (v/v) CO_2 and cultured overnight in an incubator at 37°C in a 10% (v/v) CO_2 atmosphere. The DMEM was then changed

the next day and replaced with fresh medium to remove the cryoprotective chemicals and debris dead cell.

2.2.1.3 Cell culture growth media and passaging 3T3-L1 cells

The murine 3T3-L1 pre-adipocyte cell line was grown at 37°C in a humidified atmosphere of 10% (v/v) CO_2 in T75 flasks in DMEM supplemented with 10% (v/v) NCS. Every two days, the media was replaced. When the confluency of 3T3-L1 cells in T75 flasks reached about 80%, the cells were routinely passaged. By aspiration, the cell growth medium was withdrawn, and the cells were washed in 5 ml of pre-warmed sterile PBS. The cells were then detached from the flasks using 3 ml of sterile trypsin-EDTA 0.05 % (v/v) added to each T75 flask and incubated at 37°C for one minute. The trypsin within the cell mixture was then neutralised by adding an appropriate volume of DMEM/NCS and the cell suspension was then divided as required. For experimental conditions, 3T3-L1 cells (passage 6-12) were grown in 6-well plates or Falcon 10 cm diameter dishes.

2.2.1.4 Preparation of 3T3-L1 for freezing

Culture medium was removed from T75 flasks, and the cells were then detached from the flasks using 3 ml of sterile trypsin-EDTA 0.05 % (v/v) added to each T75 flask. Flasks were then incubated at 37°C for one minute. After adding 7 ml of growing DMEM to each flask, cells were then collected in 15 ml universal tubes and pelleted by centrifugation (350 x g, 5 min). Culture medium was removed, and the pellets resuspended in a freezing media: foetal calf serum (FCS) containing 10% (v/v) dimethyl sulfoxide (DMSO). The re-suspended pellet was then transferred into polypropylene cryogenic vials. The cryogenic vials were then placed in a polycarbonate container for 24 hours at -80°C prior to transfer to liquid nitrogen for storage.

2.2.1.5 Preparation of 3T3-L1 preadipocyte differentiation medium

An adipogenic cocktail was prepared to differentiate 3T3-L1 preadipocytes into mature adipocytes. The differentiation medium consisted of DMEM supplemented with 10% (v/v) fetal calf serum (FCS), 0.5 mM 3-isobutyl-1-methylxanthine (IBMX),

0.25 mM dexamethasone, 1 µg/ml insulin, and 5 mM troglitazone which was filter-sterilized (50 µm) before use.

2.2.1.6 3T3-L1 preadipocyte differentiation protocol

3T3-L1 cells (passage 6-12) were maintained in DMEM containing 10% NCS and antibiotics (1% v/v penicillin-streptomycin). Two days post confluence, 3T3-L1 cells were incubated in culture media- DMEM supplemented with 10% (v/v) FCS, 0.5 mM IBMX, 0.25 µM dexamethasone, 1 µg/ml insulin and 5 µM troglitazone for 3 days. Then, the medium was changed to DMEM supplemented with 10% (v/v) FCS, 5 µM troglitazone and 1 µg/ml insulin for a further 3 days. At day 6, the medium was changed to DMEM supplemented with only 10% (v/v) FCS and 1% (v/v) penicillin-streptomycin and cells were used between day 8 and day 12. The successful differentiation of 3T3-L1 preadipocytes into mature adipocytes can be assessed in this study through morphological changes under the microscope, where mature adipocytes typically exhibit a round, lipid-filled morphology compared to the fibroblast-like appearance of preadipocytes.

2.2.1.7 Cell culture growth media and passaging RAW 264.7

RAW 264.7 cell line was a kind of gift from Dr Ruaidhri Carmody (School of Molecular Bioscience, University of Glasgow). RAW 264.7 cells were grown at 37°C in a humidified atmosphere of 5% CO_2 in 10 cm diameter dishes in DMEM + GlutaMAX supplemented with 10% (v/v) FCS, 1% (v/v) penicillin-streptomycin and 1% (v/v) L-Glutamine (200 mM). Every two days, the media was replaced. When the confluency of RAW 264.7 reached about 70-80%, the cells were routinely passaged. The cells were scraped gently from the dishes using a cell lifter to detach adherent cells into the medium. Cell suspension was collected into 50 ml tubes and diluted with an appropriate volume of DMEM/FCS and then divided as needed. For experimental conditions, RAW 264.7 cells were grown in 6-well plates or 10 cm diameter plates.

2.2.1.8 Preparation of RAW 264.7 macrophage conditioned media and 3T3-L1 co-culture.

RAW 264.7 were seeded in 10 cm diameter dishes or 6-well plates and grown to reach approximately 80% confluence. Then, the cells were stimulated with 100

ng/ml LPS for either long-term treatment (8 h or 24 h) or short-term treatment (5, 15, 30, 60, and 120 min). For some experiments, RAW 264.7 cells were preincubated with test substances (PF543-100nM and JTE 013-10μM) for 45 min and then were stimulated with 100 ng/ml LPS for 8 h. After that, conditioned medium (CM) was collected and kept at -80°C for further experiments. CM collected from macrophages was mixed with DMEM containing 10% FCS and 1% P/S in a ratio of 1:4 or 1:1 according to each study condition. The mixed medium was then filtered with a 0.2 μm filter to remove cell debris. 3T3-L1 adipocytes were then stimulated with filtered medium. In some experiments, adipocytes had been pre-treated with test compounds (Figure 2-1).

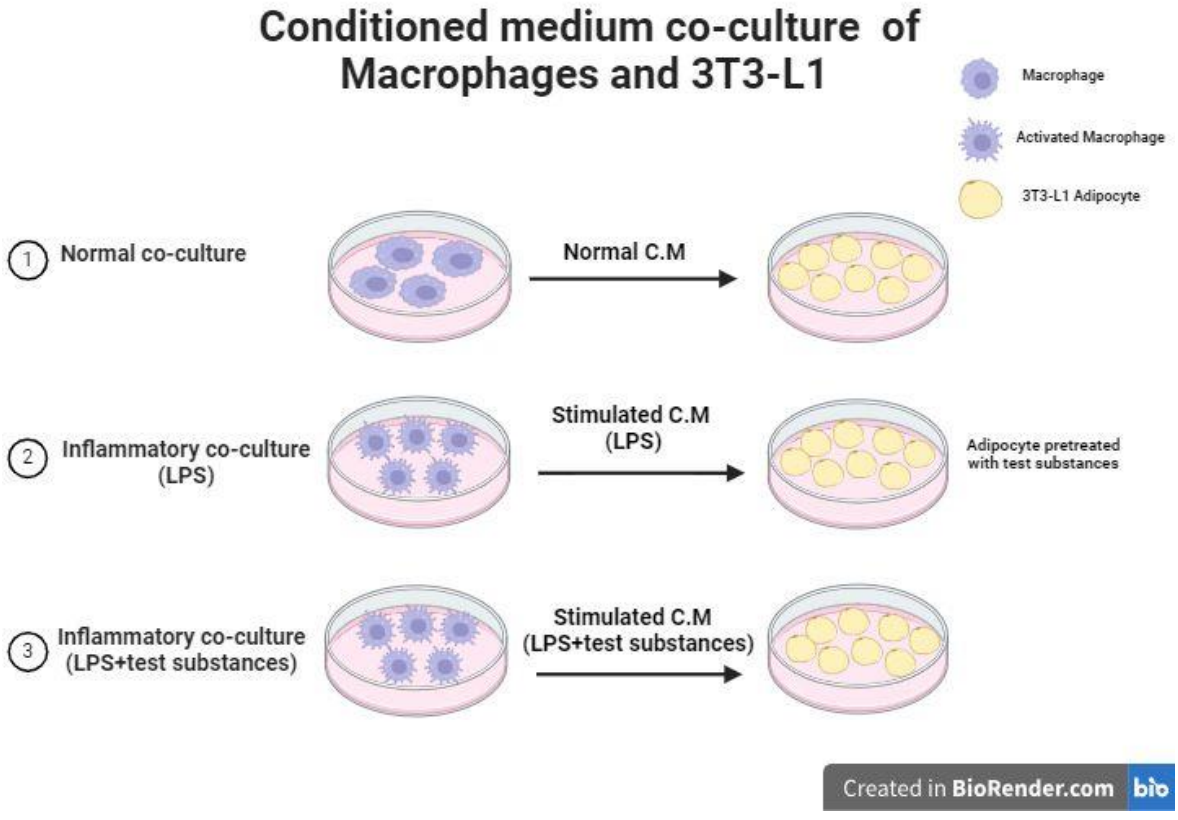

Figure 2-1 Conditioned medium (C.M) co-culture of macrophages (RAW cells) and 3T3-L1 adipocytes.

(1) C.M of normal macrophages collected and applied to 3T3-L1 adipocytes. (2) C.M of stimulated macrophages was collected and applied to 3T3-L1 adipocytes in the presence and absence of test substances ($S1PR_1$ antagonist W146 (10 μM), $S1PR_2$ antagonist JTE 013 (10 μM) or the $S1PR_3$ antagonist CAY10444 (10 μM)). (3) C.M of stimulated macrophages in the presence and absence of test substances (PF543-100nM and JTE 013-10μM) was collected and applied to 3T3-L1 adipocytes.

2.2.1.9 Preparation of 3T3-L1 cell lysates

Cells were grown in 6-well plates or 10 cm diameter dishes and differentiated as described above. At specific time points between day 8 and day 12, the medium was aspirated and replaced with 10% (v/v) FCS/DMEM supplemented with test substances (IL-ß, S1P, W146, CYM 5478, JTE 013, CAY, PF543, ROME) for specific time points at 37°C according to study design. For short-term treatment, cells were serum starved for 2 h in serum-free DMEM at 37°C before adding test substances (IL-1ß, S1P, and JTE 013) to the wells for various durations at 37°C. Then, at the end of the experiment, the media was removed and cells washed twice with cold PBS. 150 µl of ice-cold RIPA lysis buffer (25 mM Tris-HCl, pH 7.6 150 mM NaCl, 1% NP-40, 1% sodium deoxycholate, 0.1% SDS) with protease inhibitors and phosphatase inhibitors (ThermoFisher, UK) was added to each well. The cells were then scraped on ice and transferred to pre-cooled microcentrifuge tubes. The samples were briefly sonicated for 5 seconds and then centrifuged at maximum speed (17,000 x g, 10 min, 4°C). Finally, the supernatants were collected and stored at -20°C.

2.2.1.10 Preparation of RAW 264.7 macrophage lysates

RAW 264.7 macrophages cultured in 6-well plates were incubated in DMEM + GlutaMAX supplemented with 10% (v/v) FCS, 1% (v/v) penicillin-streptomycin and 1% (v/v) L-Glutamine (200 mM) supplemented with test substances (LPS 100 ng/ml) for various time points at 37°C. The media was removed, and cells washed with cold PBS. 150 µl of ice-cold RIPA lysis buffer was added to each well. After that, the cells were scraped on ice and transferred to pre-chilled microcentrifuge tubes and then centrifuged at maximum speed (17,000 x g, 10 min, 4°C). Finally, the supernatants were collected and stored at -20°C.

2.2.1.11 PVAT sample preparation

Thoracic aorta PVAT from male SD rats was dissected and weighed prior to immersion in 500 µl of PSS (118 mM NaCl, 4.7 mM KCl, 1.2 mM $MgSO_4$, 25 mM KH_2PO_4, 11 mM glucose and 2.5 mM $CaCl_2$), for 30 minutes at 37°C. Then, PVAT was stimulated with IL-1ß (10 ng/ml) for different time points with continuous oxygenation. In some experiments where the effect of S1P (10 µM) was being

assessed, S1P was added at the same time as the inflammatory stimulus. After that, PVAT was snap frozen and stored at-80°C. Conditioned media also was collected and snap frozen and stored at-80°C until it could be used for studying gene expression, protein expression and NO production.

2.2.1.12 Preparation of PVAT lysate

Thoracic PVAT was removed from storage at – 80 °C and transferred to new pre-chilled microcentrifuge tubes. 250 µl of ice-cold RIPA lysis buffer with protease inhibitors and phosphatase inhibitors (ThermoFisher, UK) was added to the tubes and the tissue homogenized using a battery-operated pestle motor mixer (Sigma-Aldrich, UK). The samples were briefly sonicated for 10 seconds and then centrifuged at maximum speed (17.000 x g, 10 min, 4°C). Finally, the supernatants were collected and stored at -20°C.

2.2.2 Gene analysis

2.2.2.1 RNA extraction from 3T3-L1 cells

Adipocytes grown in 6-well plates were incubated in DMEM supplemented with 10% (v/v) FCS in an incubator at 37°C, 10 % CO_2. Test treatments (IL-1β, PF543, ROME, W146, JTE 013, CAY) were added and incubated for various times in an incubator at 37°C, 10 % CO_2 according to each study design. The media was removed and washed twice with cold PBS. Total RNA from adipocytes was extracted as per the instructions given by the Qiagen RNeasy Mini kit. Briefly, all steps were performed at room temperature. 350 µl of RNeasy lysis buffer (RLT) was added to each well and collected with a cell scraper. Lysate was transferred to a RNeasy Mini spin column and homogenized by centrifugation at full speed (17,000 x g for 2 min). Each lysate was mixed gently by pipetting with an equal volume of 70% ethanol (v/v), transferred to a separate RNeasy mini column; and then centrifuged at full speed for 1 min. After discarding the flow through, columns were washed with 700 µl of wash buffer 1 (RW1) and centrifuged at full speed for 30 seconds. After discarding the flow through, 500 µl of wash buffer (RPE) was added to each column and centrifuged for 30 seconds. Columns were washed again with 500 µl of buffer RPE and centrifuged for 2 min then transferred to fresh, 2 ml collection tubes and centrifuged for 3 min at full speed. Finally, columns were transferred to new 1.5

ml collection tubes and RNA was eluted with 30 µl RNase-free water by centrifuging at full speed for 1 minute. The quality of the RNA was determined by a nano drop spectrophotometer at 260nm and 280nm absorbance. Acceptable readings for RNA quality were determined based on established criteria such as the A260/A280 ratio. The RNA samples were then stored at −80 °C.

2.2.2.2 RNA extraction from PVAT

Thoracic aorta (TA) PVAT from SD rats was dissected and immersed in PSS solution for 30 minutes at 37°C. Test substances (IL-1ß and S1P) were added and incubated for various times in myograph chamber with continuous oxygenation at 37°C according to each study design. Total RNA was isolated according to the RNeasy Lipid Tissue Mini Kit centrifugation protocol (Qiagen). Briefly, PVAT was transferred into 2 ml collection tubes containing two stainless steel beads (5 mm mean diameter). 1 ml of QIAzol lysis reagent was added and then tissue was homogenized using Tissue Lyser LT (Qiagen) for 5 min. Then, homogenates were left on the benchtop at room temperature (15–25°C) for 5 min. 200 µl chloroform was added and tubes shaken vigorously for 15 sec. After 2-3 minutes at room temperature, tubes containing the homogenates were centrifuged at 12,000 x g for 15 min at 4°C. After that, the sample separates into three phases: an upper, colourless, aqueous phase containing RNA; a white interphase; and a lower, red, organic phase. The upper, aqueous phase was transferred to a new tube with addition of an equal volume of 70% ethanol and then the tube was mixed thoroughly by vortexing. The sample was transferred to a RNeasy Mini spin column placed in a 2 ml collection tube and centrifuged for 15 sec at 8000 x g at room temperature.

Buffer RW1 (350 µl) was added to the RNeasy Mini spin column and centrifuged for 15 sec at 8000 x g to wash the membrane. DNase I solution was prepared and 80 µl was added directly to the RNeasy Mini spin column membrane, and then placed on the benchtop for 15 min. 350 µl of washing buffer RW1 was added to the RNeasy Mini spin column and centrifuged for 15 sec at 8000 x g. After discarding the flow through, 500 µl Buffer (RPE) was added and centrifuged for 15 sec at 8000 x g. Columns were washed again with 500 µl of buffer RPE and centrifuged for 2 min at 8000 x g. The RNeasy Mini spin column then was removed and placed in a new

2 ml collection tube to eliminate and dry any residual flowthrough and remove RPE buffer remaining on the outside of the spin column. The column was placed in a new 1.5 ml collection tube, and 30 µl of RNase-free water was added directly to the spin column membrane to elute the RNA. Centrifuging was performed for 1 min at 8000 x g. to obtain a high RNA concentration. The RNA concentration was determined using a NanoDrop™ 1000 spectrophotometer. The RNA samples were then stored at −80 °C.

2.2.2.3 cDNA generation by polymerase chain reaction (PCR)

1µg of RNA for each 20 µl reaction was used to synthesise the cDNA by High-capacity cDNA Reverse Transcription Kit (Applied Biosystems). Briefly, 1 µg of DNase I-treated RNA was diluted up to 10 µl with RNase-free H_2O, placed in a 0.5 ml PCR reaction tube and kept on ice. 2 µl of 10X Reverse Transcriptase buffer, 0.8 µl of 25X dNTP Mix (100 mM), 2 µl of 10X RT random primers, 1 µl of Multiscribe Reverse Transcriptase, and 4.2 µl of RNase-free dH_2O were added to each reaction tube, vortex-mixed and centrifuged for 15 s at 17.000 x g. Tubes were loaded into a thermal cycler and cDNA was generated with the following steps (step 1 – 25°C, 10 min; step 2 - 37°C, 120 min; step 3 – 85°C, 5 min; and step 4 – 4°C, until taken for storage). PCR products were kept at -80°C for long-term storage.

2.2.2.4 Quantitative real time-PCR (qPCR)

mRNA expression of chosen genes in adipocytes and PVAT was analysed using TaqMan probes and TaqMan Real-Time PCR Master Mix (Thermo Fisher Scientific). In a 384-well PCR plate, TaqMan probes (1µl per sample, as listed in Table 2-6), 2 µl cDNA, 2 µl of nuclease-free ddH_2O and 5 µl Taqman standard master mix solution was added per well. All samples were performed in triplicate. The PCR plate was then sealed using qPCR transparent plastic adhesive and centrifuged at 2000 x g for 5 min. Reactions were run on the QuantStudioTM 7 Flex Real-Time PCR System using a standard protocol (step 1 –95°C, 10 min, performed once; step 2 - 95°C, 15 s followed by 60°C, 1 min, repeated for 40 cycles; step 3 – 55°C, 80 cycles) and mRNA expression was analysed using QuantStudioTM Real- Time PCR Software. All data were normalised to levels of TATA box mRNA and relative quantification was calculated based on $^{\Delta\Delta}$Ct method (Rao et al, 2013).

Table 2-6 TaqMan probes

TaqMan probe name	Species	Assay ID
Nitric oxide synthase 2(Nos2)	Rat	Rn00561646_m1
Nitric oxide synthase 2(Nos2)	Mouse	Mm00440502_m1
Sphingosine kinase 1(SphK1)	Rat	Rn00682794_g1
Sphingosine kinase 1(SphK1)	Mouse	Mm00448841_g1
Sphingosine kinase 2(SphK2)	Mouse	Mm00445021_m1
TATA box binding protein (Tbp)	Rat	Rn01455646_m1
TATA box binding protein (Tbp)	Mouse	Mm01277042_m1

2.2.3 Protein analysis

2.2.3.1 Quantification of protein concentration

The Bicinchoninic acid (BCA) protein assay (ThermoFisher, UK) was used to determine the amount of protein in each sample of cell and tissue lysate based on a calibration curve made from a serial dilution of bovine serum albumin (BSA) (2 mg/ml) and H_2O. Lysate in duplicate (2µl) was added into each well and distilled water was then added to make it up to 10 µl. A working reagent (WR) was prepared by mixing BCA reagent A with BCA reagent B in a ratio of 50:1 (reagent A: B) (Pierce™ BCA Protein Assay Kit, Thermo Scientific™, UK). 200 µl of WR was then added to all samples and standards. A fluostar OPTIMA microplate reader was used to measure the absorbance at 595 nm after the plate was covered and incubated for 10 minutes at 37 °C.

2.2.3.2 Sample preparation

Protein samples were combined with 2 µl of 1mM Dithiothreitol (DTT) and 8 µl sample buffer- NuPAGE® LDS sample buffer [4X] to a final volume of 40 µl prior to protein loading. The samples were then heated for 5 minutes at 95°C.

2.2.3.3 Protein separation by SDS-PAGE

Proteins were separated by SDS-polyacrylamide gel electrophoresis (SDS–PAGE) according to their molecular weight. Different percentages of acrylamide gels (8%-10%) were prepared as a 1.5 mm thick vertical slab (Table 2-7).

Table 2-7 Resolving and stacking gel components for one gel.

Dilution components	Resolving gels		Stacking gel
%	8%	10%	5%
dH_2O	4.6 ml	4 ml	1.4 ml
30% acrylamide mix	2.7 ml	3.3 ml	0.33 ml
Resolving buffer-1.5 M Tris (pH 8.8) **Stacking buffer-1.0 M Tris (pH 6.8)**	2.5 ml	2.5 ml	0.25 ml
10% SDS	0.1 ml	0.1 ml	0.02 ml
10% ammonium persulphate	0.1 ml	0.1 ml	0.02 ml
TEMED	0.006 ml	0.004 ml	0.002 ml

After gels were prepared and polymerised, they were assembled in the Mini-PROTEAN® Tetra Vertical Electrophoresis Cell (Bio-Rad) and placed into a tank filled with SDS–PAGE running buffer (190 mM glycine, 25mM Tris base and 0.1 % (w/v) SDS). Then, equal amounts of lysate protein from the samples were loaded, along with blue pre-stained Protein Standard, Broad Range (11-250 kDa) in the first lane of each gel. Finally, gels were electrophoresed, using a Bio-Rad Mini-PROTEAN® Tetra Cell system- initially at 80 V for 20 min followed by 130 V until tracking dye had reached the bottom of the gel.

2.2.3.4 Western Blotting

Once the separation was completed, the protein samples were transferred to a nitrocellulose membrane for 135 minutes at 60 V using the Bio-Rad Mini-Transblot Cell transfer buffer containing 192 mM glycine, 25mM Tris base and 20% (v/v) ethanol. After the transfer was completed, the nitrocellulose membranes were incubated in 5% (w/v) dried skimmed milk powder (Marvel) diluted in Tris-buffered saline (TBS) for 1 h at room temperature with constant shaking. The membranes were then washed three times with TBS, each time for five minutes and then incubated overnight at 4 °C with the appropriate primary antibody (Table 2-4). Membranes were then washed in TBST (TBS + 0.1% Tween 20) and incubated for 1 h at room temperature with either anti-mouse secondary antibody or anti-rabbit secondary antibody (Table 2-5) diluted to 1:10000 in TBS-Tween (TBST) containing 5% (w/v) BSA and then washed with TBST three times.

2.2.3.5 Quantification of protein expression by LI-COR detection system

Membranes were visualized by Odyssey Sa infrared imaging system (LiCor Biosciences UK Ltd, Cambridge, U.K.). Then, for densitometric quantification of band intensity, Image Studio Lite (LI-COR) software was used.

2.2.3.6 Stripping of nitrocellulose membranes

Nitrocellulose membranes were incubated in stripping buffer (0.2 M NaOH) at room temperature for 5 min with continuous shaking. Then, membranes were washed three times with TBS, each time for five minutes.

2.2.4 Nitric oxide production assay

2.2.4.1 Preparation of PVAT conditioned media samples

Thoracic PVAT from SD rats was carefully dissected and weighed prior to being placed in Eppendorf tubes containing 500 µl of PSS solution. The PVAT samples were oxygenated in myograph chamber for 30 min at 37 °C. After that, PVAT was treated with test substances for specific time points with continuous oxygenation. PVAT was then collected, and 100 µl of CM from each sample was added to 200 µl

of methanol and centrifuged at 17,000 × g, 4°C for 20 min. The supernatants were then collected and stored at −20°C.

2.2.4.2 Preparation of 3T3-L1 cell condition media samples

Confluent adipocytes cultured in 6-well plates were preincubated for 45 min at 37°C with test substances in DMEM supplemented with 10% (v/v) FCS. The medium was then changed and cells reincubated with the same treatments in the presence and absence of IL-1β (10 ng/ml) or RAW 264.7 macrophage C.M. according to study design. 100 µl of medium from each well was then collected and 200 µl of methanol was added to each sample. The samples were centrifuged at 17,000 × g, 4°C for 20 min. The supernatants were then collected and stored at −20°C.

2.2.4.3 Detection of Nitric oxide

A Sievers Nitric Oxide Analyzer (NOA 280i) was used to measure NO concentration. The NO analyser determines NO levels in samples by measuring nitrite (NO_2^-), a product of the reaction between NO and dissolved oxygen. Iodide reacts with nitrite and converts it back to NO which reacts with O_2 to produce ozone (O_3), O_3 was detected by chemiluminescence, and the signal was converted to an electrical potential and displayed as mV by the NO analyser. A nitrite standard calibration curve was created by injecting 20 µl of serial dilutions of 100 µM, 50 µM, 10 µM, 1 µM, 500 nM, 100 nM, and 50 nM. Samples were injected at regular intervals to allow the output curve to return to baseline. The output in mV was then related to the amount of NO_2^- present in the sample using the NO_2- standard curve constructed on that day. Values of samples were corrected for NO_2- relative to the protein concentration or tissue weight.

2.2.5 Functional study (wire myography)

2.2.5.1 Vessel preparation and mounting for mouse studies

To prepare artery rings for functional studies, mice (25-35 g body weight) were killed by increasing the CO_2 concentration and then the heart and thoracic aorta was rapidly removed and placed into cold PSS solution. The thoracic aorta was dissected and cleaned of surrounding PVAT in some experiments while maintained in some segments. Arteries were cut into 1-2 mm rings under a binocular

microscope with fine dissecting scissors in order to perform aortic functional studies. The aortic rings were mounted on 40 µm wires in a four-channel wire myograph (Figure 2-2). Vessels were gassed with constant supply of 95% O_2, 5% CO_2 at 37°C in PSS buffer and equilibrated for 30 mins. The rings were stretched in a stepwise manner, in approximately 2mN steps with 5 minutes between each stretch until the optimal tension of 9.81 mN was reached.

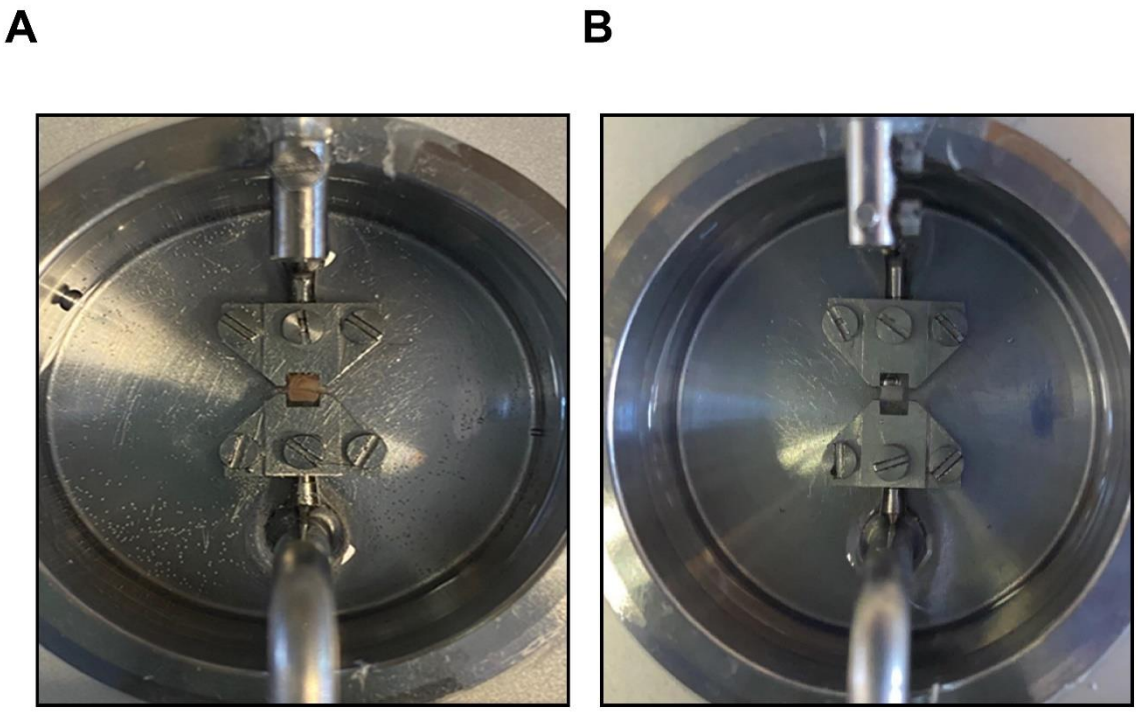

Figure 2-2 Representative images of mouse aortic rings mounted on a wire myograph.

Segments (1-2 mm) of mouse thoracic aorta with PVAT (A) and without PVAT (B) mounted on two wires with one connected to a force transducer and a computer to record the changes in tone of the vessel ring. The other wire was connected to an adjustable micrometer to adjust the tension on the vessel ring.

2.2.5.2 Testing the viability of the vessels for mouse studies

To investigate and check the viability of each ring after the dissection and mounting, two separate additions of high potassium physiological salt solution (KPSS, 62.5 mM) were added with washing three times between additions.

2.2.5.3 Endothelium check protocol for mouse studies

The rings were precontracted with phenylephrine (PE) (1×10^{-6} M) and acetylcholine (Ach) (1×10^{-6} M) was added in order to check the function of the

endothelium. In some experiments the rings were denuded of endothelium by gentle rubbing of the intimal surface with forceps. A relaxation to Ach < 20% was indicative of successful endothelial removal and relaxation to Ach > 50% was indicative of an intact endothelial layer (Figure 2-3).

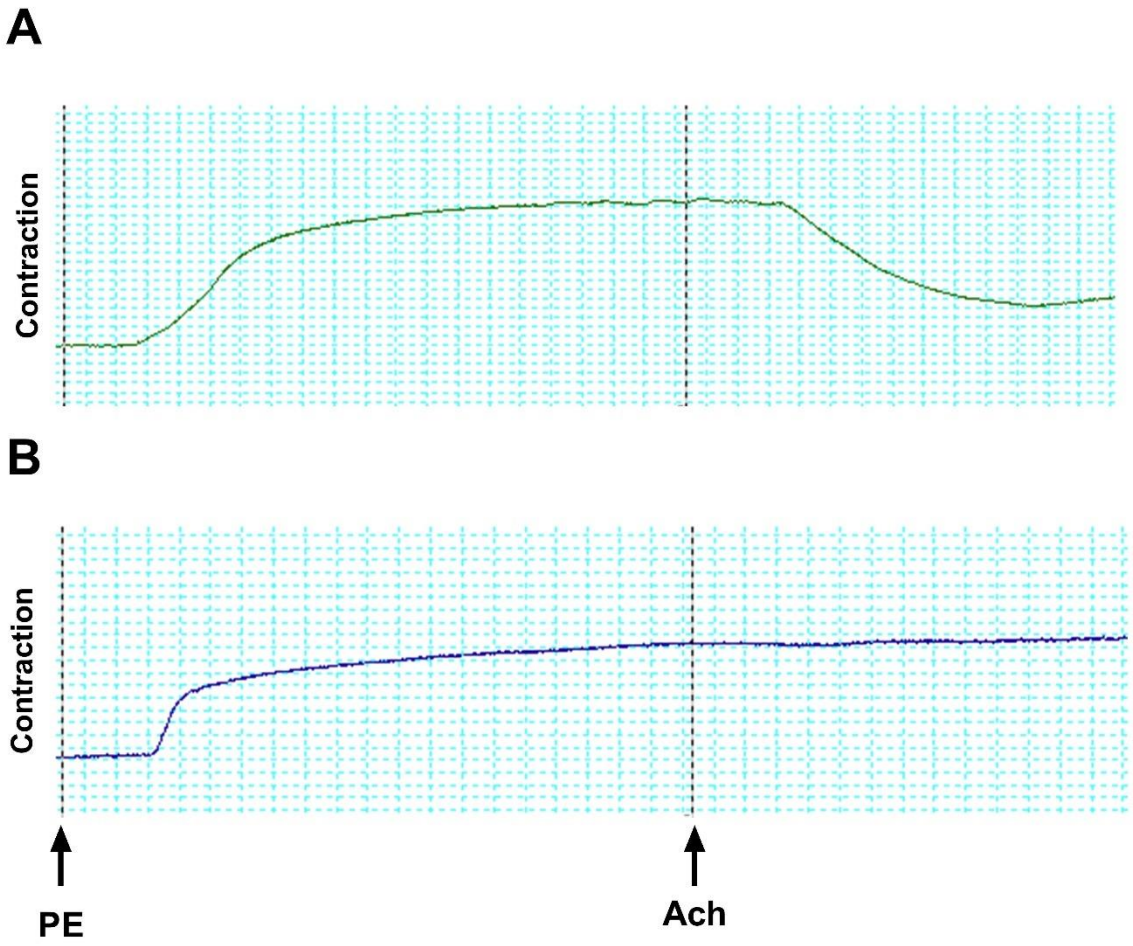

Figure 2-3 Representative image showing the contraction and relaxation recording in mouse thoracic aorta rings.

(A) Representative image of recording in endothelium-intact rings. (B) Representative image of recording in denuded rings.

2.2.5.4 Testing the anti-contractile effect of PVAT in mice studies

In order to investigate the specific role of PVAT on vascular reactivity, mouse thoracic rings with or without PVAT were mounted in a four-channel wire myograph. After the viability test and endothelium check were completed, rings were contracted with PE (1×10^{-6} M). Data were expressed as a percentage of KPSS contraction.

2.2.5.5 S1P agonists protocol for mice studies

The effect of S1P and S1P receptor agonists CYM5541, a selective $S1PR_3$ agonist and SEW2871, a selective $S1PR_1$ receptor agonist on vascular reactivity were assessed in PE (1×10^{-6} M) preconstricted rings. Cumulative concentration-response curves to S1P or S1P receptors agonists were constructed (1×10^{-9} M - 1×10^{-5} M) with addition at 5 mins intervals in the presence and absence of PVAT.

2.2.5.6 Inflammatory induction protocol for mouse studies

In order to investigate the specific role of PVAT on vascular reactivity under an inflammatory stimulus (IL-1ß 10 ng/ml), mouse thoracic rings with PVAT were mounted in the four-channel wire myograph. After the viability test and endothelium check were completed, rings were incubated with IL-1ß (10 ng/ml) for 2 hours. Concentration-response curves were then generated to PE (1nM-30µM). In some experiments where the effect of S1P was to be assessed, S1P (10µM) was added at the same time as the inflammatory stimulus.

2.2.5.7 Vessel preparation and mounting for rat studies.

To prepare arterial samples for functional studies, SD rats (180-350 g body weight) were killed by an increasing CO_2 concentration and then the heart and thoracic aorta was rapidly removed and placed into cold PSS solution. The thoracic aorta was dissected and cleaned of surrounding PVAT in some experiments while being maintained in some segments. Arteries were cut into 2-3 mm rings under a binocular microscope with fine dissecting scissors and were mounted on pins in a four-channel myograph (Figure 2-4). Vessels were gassed with constant supply of 95% O_2, 5% CO_2 at 37°C in PSS and equilibrated for 30 mins. The rings were stretched in a stepwise manner, in approximately 2mN steps with 5 minutes between each stretch until the optimal tension of 9.81 mN was reached.

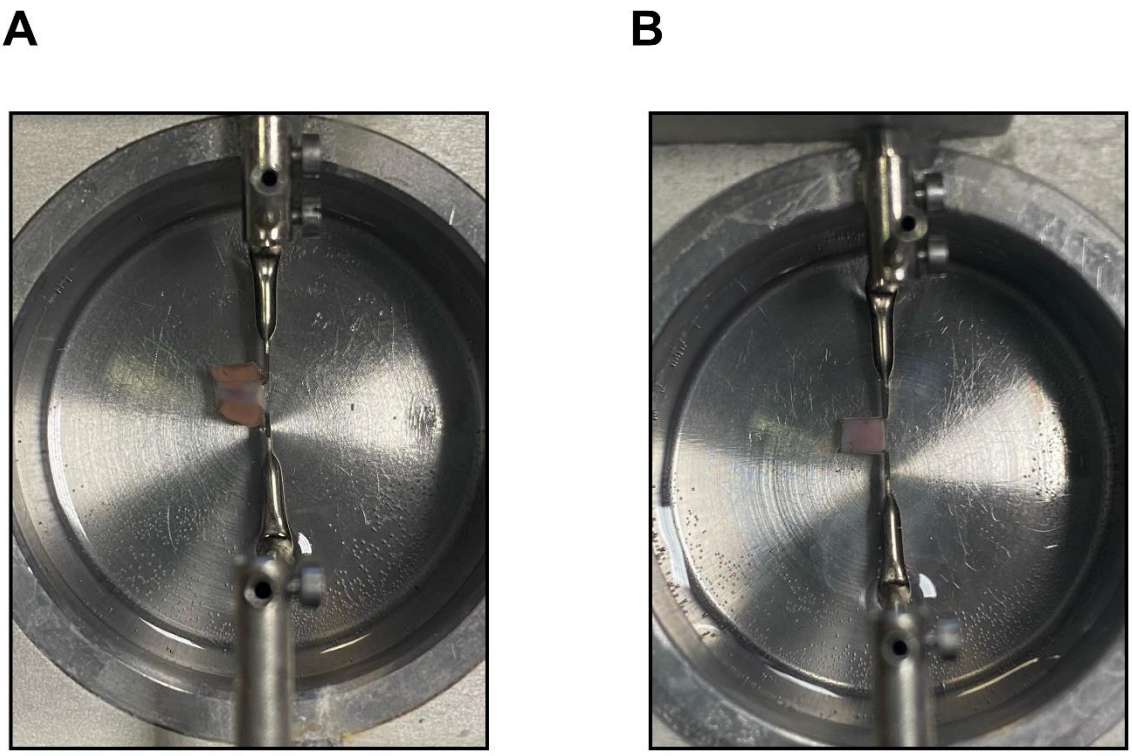

Figure 2-4 Representative images of rat aortic rings mounted on pins in a myograph.

Segments (2-3 mm) of rat thoracic aorta with PVAT (A) and without PVAT (B) mounted on two pins with one connected to a force transducer and a computer to record the changes in tone of the vessel ring. The other pin was connected to an adjustable micrometer to adjust the tension on the vessel ring.

2.2.5.8 Testing the viability of the vessels for rat studies

To investigate and check the viability of each ring after the dissection and mounting, two separate additions of (KPSS, 62.5mM) were added with washing three times between the two additions.

2.2.5.9 Endothelium check protocol for Rat studies

The rings were precontracted with U46619 (1×10^{-6} M) and Ach (1×10^{-6} M) was added in order to check the function of the endothelium. The rings were denuded of endothelium by gentle rubbing of the intimal surface with forceps and maintained in some segments. A relaxation to Ach < 20% was indicative of successful endothelial removal and relaxation to Ach > 50% was indicative of an intact endothelial layer (Figure 2-5).

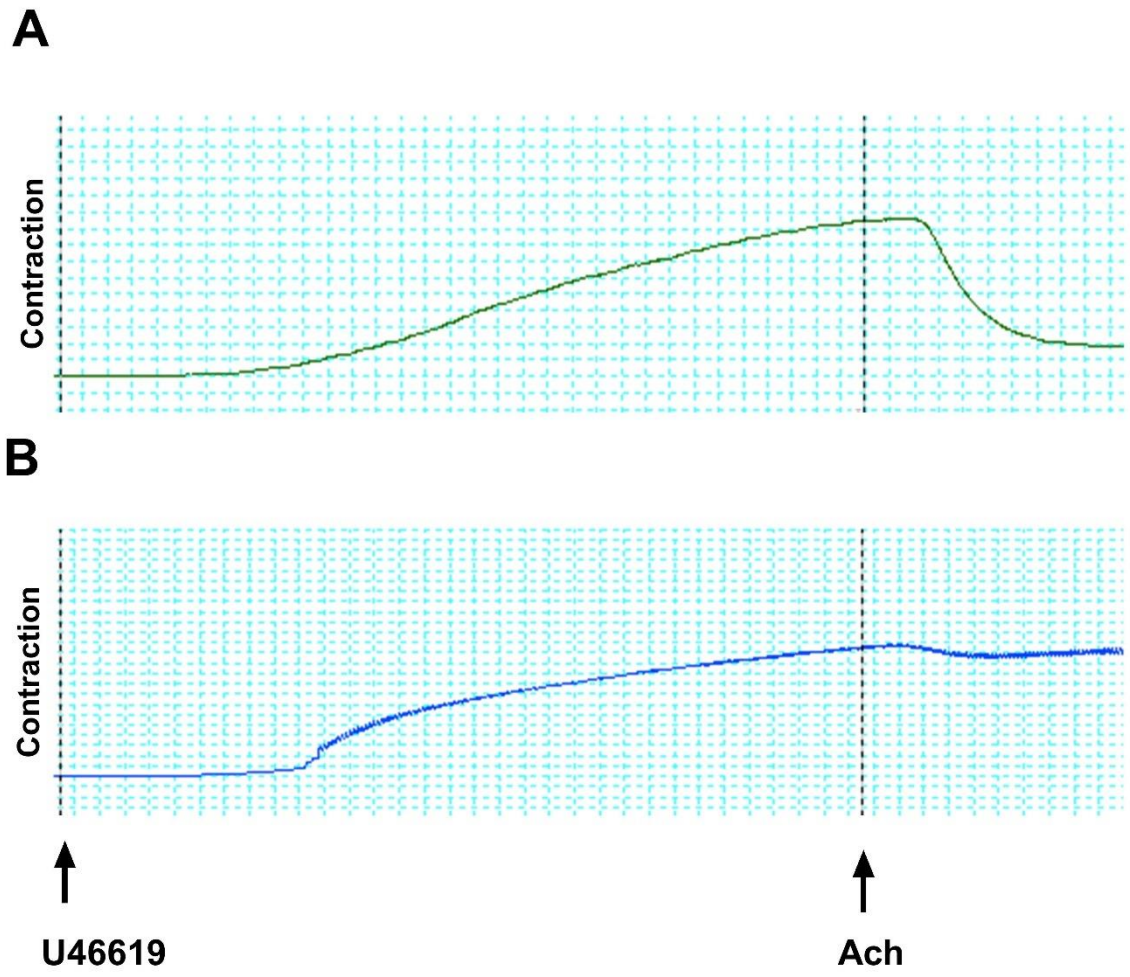

Figure 2-5 Representative image showing the contraction and relaxation recording in rat thoracic aorta rings.

Representative image of recording in intact-endothelium rings. (B) Representative image of recording in denuded-endothelium rings.

2.2.5.10 S1P agonist protocol for rat studies

To test whether S1P modulates vascular reactivity in rat, aortic rings were precontracted with U46619 (3×10^{-8} M). Once a plateau was achieved, a concentration response curve was generated by cumulative addition of S1P (1nM-3μM) at 5 min intervals in intact-endothelium rings without PVAT.

2.2.5.11 Testing the anti-contractile effect of PVAT in rat

In order to investigate the specific role of PVAT on vascular reactivity, rat thoracic rings with or without PVAT were mounted and endothelium checked.

Concentration-response curves were then generated to U46619 (1×10^{-9}-1×10^{-6} M) with data expressed as a percentage of KPSS contraction.

2.2.5.12 Inflammatory induction protocol in rat studies

In order to investigate the specific role of PVAT on vascular reactivity in the presence of an inflammatory stimulus (IL-1ß 10 ng/ml), rat thoracic rings with or without PVAT were mounted and checked for viability and the presence of an endothelium. They were then incubated with IL-1ß for 4 hours. Concentration-response curves were then generated to U46619 (1×10^{-9}-1×10^{-6} M). In some experiments where the effect of S1P (10 µM) was to be assessed, S1P was added at the same time as IL-1ß. Data were expressed as a percentage of KPSS contraction.

2.2.5.13 Effect of iNOS inhibition on vascular reactivity under inflammatory conditions

To test whether iNOS mediates the anticontractile effect of PVAT under inflammatory condition, the specific iNOS inhibitor 1400W (1×10^{-5} M) was added to the bath 10 min before concentration-response curves were generated to U46619 (1×10^{-9}-1×10^{-6} M). Data were expressed as a percentage of KPSS-induced contraction.

2.2.5.14 Effect of potassium channel inhibition on vascular reactivity under normal and inflammatory conditions

To test whether potassium channels are involved in the PVAT-mediated anticontractile effect under inflammatory conditions, the potassium channel blocker, tetraethylammonium (TEA, $5x10^{-6}$ M) was added to the bath 10 min before concentration-response curves were generated to U46619 (1×10^{-9}-1×10^{-6} M). Data were expressed as a percentage of KPSS-induced contraction.

2.2.5.15 Effect of SphK1/S1PR$_2$ inhibition on vascular reactivity under normal and inflammatory condition

To test whether SphK1/S1PR$_2$ mediates the PVAT-induced anticontractile effect under inflammatory conditions, SphK1 inhibitor (PF543; 100nM) or the S1PR$_2$ antagonist (JTE 013; 10µM) was added to the bath 30 min before adding the

inflammatory stimulus (IL-1β 10 ng/ml). Concentration-response curves were then generated to U46619 (1×10^{-9}-1×10^{-6} M). Data were expressed as a percentage of KPSS contraction.

2.2.6 Statistical analysis

All results are expressed as mean ± standard error mean (SEM) where *n* represents the number of experiments performed or number of animals used. Data were analysed with GraphPad Prism 8.0 software (California, U.S.A.) using Student's t-test when comparing two groups, or one or two-way ANOVA when comparing different groups followed by appropriate post-hoc tests. In all cases, a *P* value of less than 0.05 was considered statistically significant.

Chapter 3 – Investigating the potential role of S1P on IL-1β-dependent proinflammatory signalling and iNOS regulation in 3T3-L1 adipocytes

3.1 Introduction

Obesity is a major global health problem and an important risk factor for cardiovascular diseases such as hypertension, stroke, myocardial infarction and type 2 diabetes (Blüher, 2019). Obesity is described as the excessive accumulation of adipose tissue and cholesterol and is characterised by chronic inflammation in adipose tissue depots which may be an important link to many cardiovascular diseases (Reilly & Saltiel, 2017). It is well known that during development of obesity, the adipose tissue mass rises as a result of increases in adipocyte size (hypertrophy) and adipocyte number (hyperplasia). Within the adipose tissue, preadipocytes differentiate into mature adipocytes via a process named adipogenesis. This differentiation of adipocytes is controlled by expression of specific genes and transcription factors including peroxisome proliferator-activated receptor-γ (PPARγ) and CCAAT/enhancer-binding proteins (C/EBPs) which ultimately leads to differentiation of preadipocytes to mature adipocytes (Ahmad et al, 2020). Infiltration of macrophages and other immune cells is increased during adipose tissue hypertrophy, which is considered a major source of adipose-derived proinflammatory cytokines (Kawai et al, 2021). IL-1ß is a potent proinflammatory cytokine produced mainly by monocytes and macrophages and multiple studies implicate IL-1ß in the development of cardiovascular diseases such as heart failure, coronary artery disease and arrythmia (Gao et al, 2014; Szekely & Arbel, 2018).

In addition to production by inflammatory cells in inflamed adipose tissue, adipocytes and preadipocytes themselves can also produce IL-1ß (Coppack, 2001). Several studies have identified that IL-1ß is increased in obese subjects and correlated with diabetes and obesity-related insulin resistance (Spranger et al, 2003; Um et al, 2004; Xu et al, 2003). This cytokine binds to IL-1R1 and stimulates production of many other proinflammatory cytokines and enzymes via multiple proinflammatory pathways. NF-KB is the prominent pathway activated in response to IL-1ß. In cells NF-KB is complexed with IKBα located in the cytoplasm in an inactive state, once IL-1ß binds to IL-1R1, IKK is phosphorylated, which leads to IKBα degradation. Subsequently, NF-KB is released and translocated to the nucleus, where it binds to activate proinflammatory gene mediators (Yamazaki et al, 2009). In addition, the family of MAPK pathways, including p38, JNK, and

ERK1/2 are other pathways stimulated by IL-1β (Jager et al, 2007) and finally, phosphatidylinositol 3-kinases (PI3Ks) and Akt can also be activated to promote inflammation.

Inducible nitric oxide synthase (iNOS) is one of the proinflammatory enzymes expressed in adipose tissue and linked to many cardiovascular and metabolic diseases. Notably, it has been revealed that iNOS over-expression is crucial for the pathophysiology of obesity and associated with T2D incidence (Dallaire et al, 2008; Morris et al, 2002). iNOS is involved in host defence, is synthesised de novo in response to various inflammatory stimuli and has the ability to create high concentrations of NO over sustained periods of time. It has been shown that the NO produced by iNOS in adipose tissue interacts with reactive oxidants to cause nitrosative stress, which is a pivotal factor in adipocyte dysfunction and disorders related to obesity. Additionally, previous research demonstrated that HFD-induced adipose tissue inflammation and insulin resistance are prevented in iNOS-/- mice (Jang et al, 2016; Perreault & Marette, 2001; Ropelle et al, 2013). These results, among numerous others, have highlighted the importance of understanding the role of iNOS expression and function in adipose tissue as well as the molecular mechanism of iNOS up-regulation under inflammatory conditions in adipose tissue.

S1P is a bioactive lipid mediator that plays a crucial role in various pathological processes, including inflammation in the context of obesity. S1P is a metabolic product of sphingosine whose formation is catalysed by two isoforms of the enzyme sphingosine kinase (SphK1 and SphK2) (Cannavo et al, 2017). The S1P can be exported from cells and binds to S1P receptors to induce a multitude of cell responses. S1P receptors have common signalling characteristics and couple to G_i, G_q, and $G_{12/13}$ proteins. Furthermore, S1P activates NF-KB (Wollny et al, 2017), MAPKs Kinase, including ERK, p38 and JNK as well as Akt (Kluk & Hla, 2002). A variety of stimuli, including growth factors and inflammatory cytokines (TNF-α, IL-1β), can activate SphK1. When activated, phosphorylation of Ser225 in the R-loop causes SphK1 to translocate from the cytosol to the plasma membrane, where its substrate, sphingosine, is found. This causes the production and secretion of S1P. Additionally, SphK1 is likewise transcriptionally controlled by inflammatory stimuli. For example, it was discovered that SphK1 is elevated in glioblastoma by

the cytokine IL-1β via a JNK/c-Jun-dependent mechanism (Bonica et al, 2020; Paugh et al, 2009; Pitson et al, 2003). Another study has demonstrated that LPS upregulates SphK1 and increases its activity in rat adipose tissue and 3T3-L1 adipocytes (Tous et al, 2014). Similar to SphK1, SphK2 was reported to upregulated in response to inflammatory stimuli such as TNF-α and IL-1β in a rat insulinoma cell line (Mastrandrea et al, 2005).

There is a growing body of evidence suggesting that SphKs and S1P may play an important role in adipose tissue dysfunction. Therefore, the role of SphKs and S1P in adipose tissue inflammation has been thoroughly investigated over recent decades. For example, SphK1 and S1P expression are increased in diet-induced obesity (DIO) mice and Zucker Diabetic Fatty (ZDF) rats. Also, it has been shown that DIO lacking SphK1 show a decrease in proinflammatory cytokines and increased anti-inflammatory cytokines in EAT (Tous et al, 2014; Wang et al, 2014). Similarly, SphK1 has been reported to increase in SAT in HFD mice (Hashimoto et al, 2009). Moreover, plasma levels of S1P plasma are positively corelated with BMI in obese humans and diabetic mice (Ito et al, 2013; Nojiri et al, 2014). Furthermore, S1P has been reported to increase in the adipose tissue of obese humans compared to lean individuals and has also been shown to promote proinflammatory genes in 3T3-L1 adipocytes (Guitton et al, 2020; Samad et al, 2006). Collectively, these findings, along with many others, have convincingly illustrated that the SphKs/S1P system has a role in adipose tissue inflammation and is linked to many metabolic disorders.

Previous studies have indicated that the SphK1/S1P system is involved in the modulation of iNOS expression and NO production in various cell types under inflammatory stimuli (microglia, rat vascular smooth muscle cells, astrocytes and mesangial cells). Some studies have demonstrated the potential of inhibition of SphK1/S1P to reduce iNOS gene expression or NO production under inflammatory conditions (Nayak et al, 2010; Wang et al, 2021) implying a proinflammatory role of SphK1/S1P, while others indicate that S1P alleviates iNOS and NO production, suggesting an anti-inflammatory action (Machida et al, 2008; Xin et al, 2004). This dichotomy needs to be investigated further.

Although it is clear that the sphingolipid system can promote inflammation and is intimately linked to adipose tissue dysfunction, it is still unclear whether the sphingolipid system could represent a new therapeutic target for proinflammatory enzyme regulation, particularly iNOS in adipose tissue. To our knowledge, there have been no studies elucidating the involvement of SphKs/ S1P in IL-1β-mediated iNOS expression in 3T3-L1 adipocytes.

3.2 Aims

1. To investigate the expression of SphK1 in the process of 3T3-L1 preadipocyte adipogenesis and characterise the effect S1P has on proinflammatory pathways in 3T3-L1 adipocytes.

2. To investigate the effect of IL-1β on the protein and mRNA levels of SphKs in 3T3-L1 adipocytes.

3. To investigate the potential role of S1P on IL-1β-stimulated iNOS expression and related proinflammatory cascades in 3T3-L1 adipocytes.

3.3 Results

3.3.1 3T3-L1 preadipocytes differentiation confirmation

3T3-L1 cells were grown in 10cm-diameter dishes and differentiated two days post confluence by addition of adipogenic stimuli to the culture medium, as described in detail in the methodology section. Adipocyte differentiation was confirmed by the change in morphology and fat droplet accumulation in 3T3-L1 preadipocytes (A) to adipocyte cells (B) (Figure 3-1). Furthermore, this was confirmed by immunoblotting for PPARγ at specific time points: day 0, day 3, day 6, day 8 and day 12. The protein level of PPARγ rose significantly over the course of adipogeneses (Figure 3-1D).

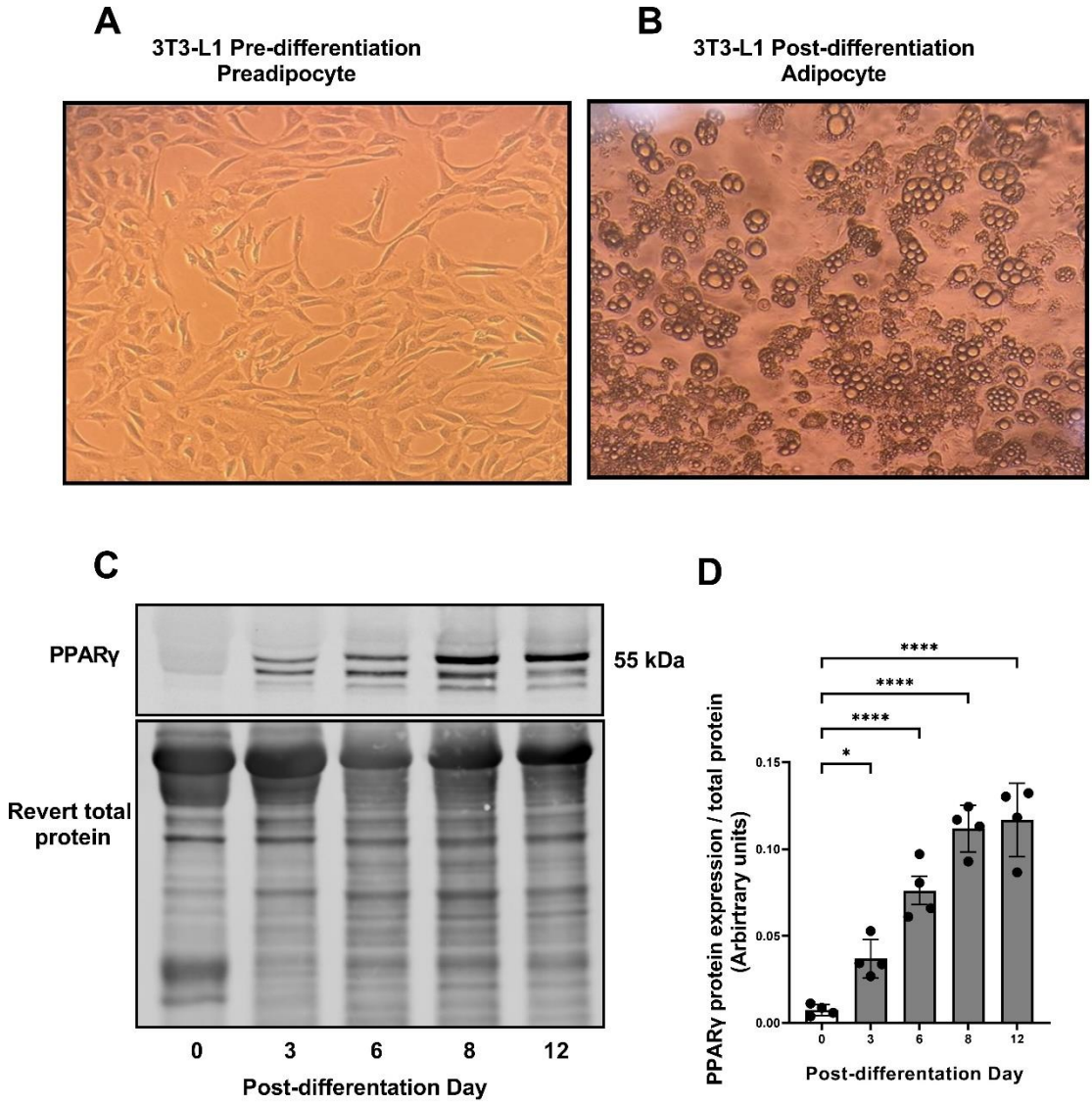

Figure 3-1 Cell morphology change and adipogenic marker PPARγ expression pre-and post-differentiation.

3T3-L1 fibroblasts were differentiated from preadipocytes to mature adipocytes as indicated in the methods. (A) Representative image of 3T3-L1 preadipocytes showing morphology before differentiation (at Day 0). (B) Representative image of 3T3-L1 mature adipocytes showing morphology after differentiation (at Day 8). (C-D) Representative image and graph for PPARγ (adipogenesis marker) protein expression at different time points (day 0, day 3, day 6, day 8, and day 12) during adipogenesis. Protein level of PPARγ was normalised to Revert total protein. The data represent samples from four different experiments expressed as the mean ± SEM. Statistical analysis was carried out using one-way ANOVA (with Dunnett's test). Asterisks indicate a p value of (*<0.05, **<0.0001).**

3.3.2 Sphk1 expression in adipocytes

The aim of this experiment was to confirm that SphK1 is expressed in an adipose tissue cell line and investigate its expression during differentiation of pre-adipocytes to adipocytes. SphK1 exists as several isoforms: SphK1a, SphK1b, and

SphK1c (Bonica et al, 2020). The anti-SphK1 antibody used in this study detected multiple bands between 34 kDa and 50 kDa. At specific time points: day 0, day 3, day 6, day 8, and day 12, protein was isolated and immunoblotting analysis was carried out to determine the SphK1 expression over the period of adipogenesis. The protein level of SphK1 rose dramatically in a time-dependent manner, with the maximum expression at day 8. SphK1 was significantly ($p^{***}<0.001$) increased at day 8, compared to day 0. Similarly, SphK1 was significantly ($p^{**}<0.01$) increased at day 8 compared to day 3. However, at later time points the level of SphK1 declined significantly ($p^{*}<0.05$) when comparing day 12 to day 8 (Figure 3-2).

It is well-established that 3T3-L1 preadipocytes undergo a proliferation phase before differentiation, during which they grow and divide. However, once they reach confluence and are induced to differentiate into adipocytes, they enter a growth-arrest phase. During adipogenesis, 3T3-L1 cells stop proliferating and begin to undergo morphological and biochemical changes characteristic of mature adipocytes (Fajas, 2003; Gregoire et al, 1998; Otto & Lane, 2005). The observed changes in SphK1 levels over the adipogenesis period (from day 1 to day 8, followed by a drop at day 12) occurred during the differentiation phase, when cell proliferation is suppressed due to contact inhibition and differentiation induction. Therefore, the increase in SphK1 expression is unlikely to be related to cellular proliferation. Instead, it likely reflects the role of SphK1 in adipocyte differentiation and function. By day 12, the reduction in SphK1 levels could be due to the cells reaching a more mature adipocyte state, where the regulatory mechanisms controlling SphK1 might undergo alterations.

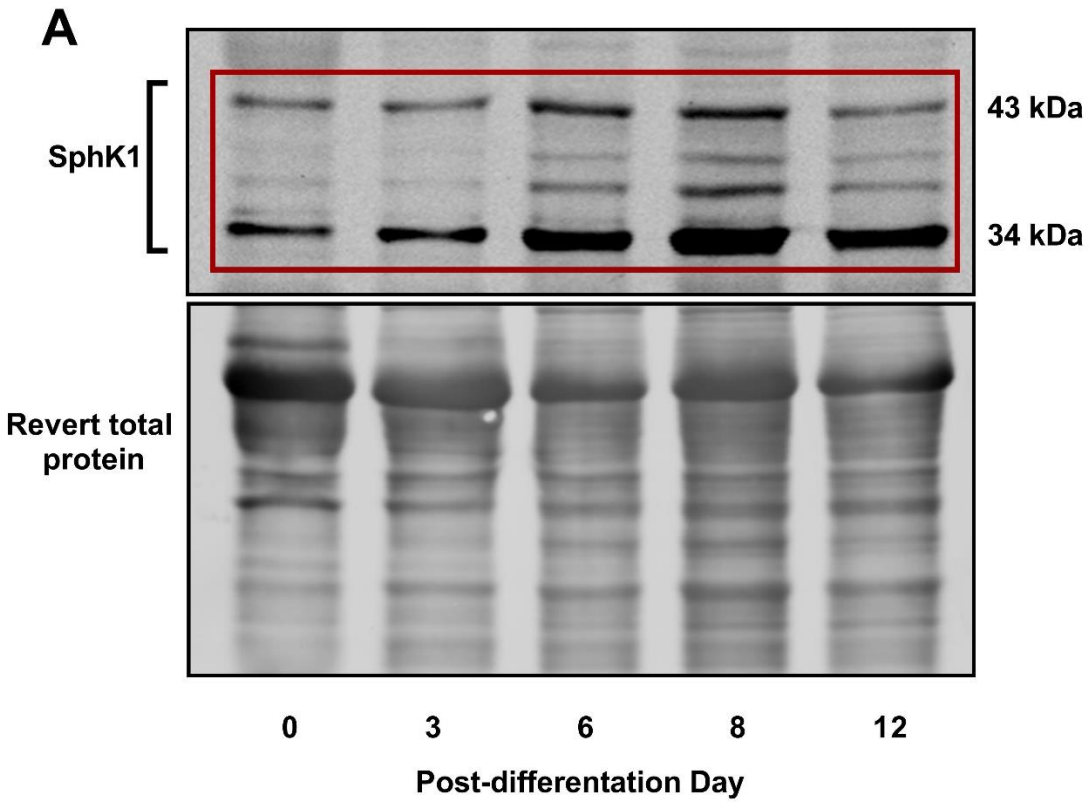

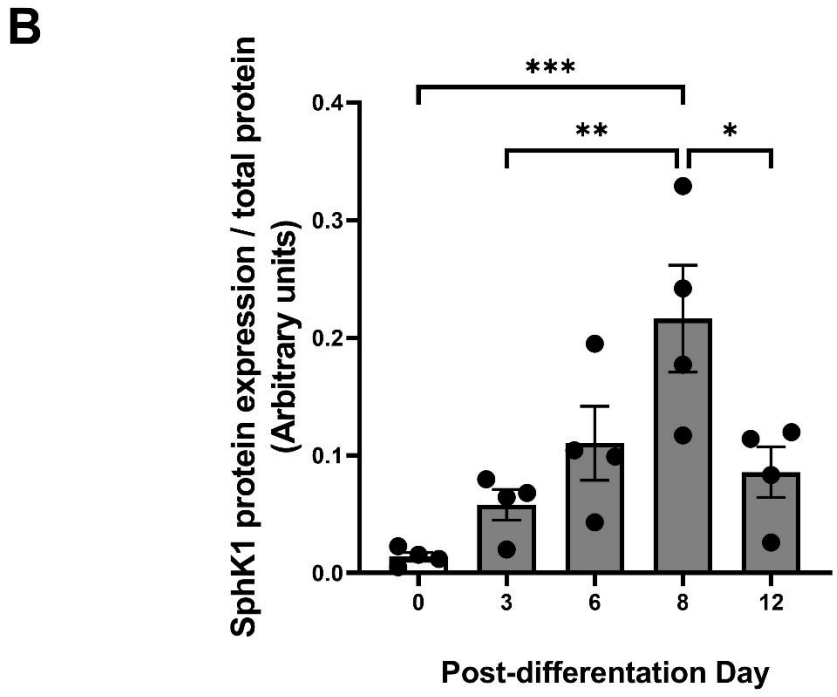

Figure 3-2 SphK1 expression over the period of adipogenesis.

3T3-L1 preadipocytes were differentiated to mature adipocytes as described in the methods. Cell lysates were prepared at different time points, (day 0, 3, 6, 8 and 12) and resolved by SDS-PAGE with the appropriate antibodies. (A and B) representative western blotting image and graph of SphK1 protein expression showing the change in SphK1 expression at indicated times over the period of adipogenesis. Protein level of SphK1 was normalised to Revert total protein. The data represent samples from four different experiments expressed as the mean ± SEM. Statistical analysis was carried out using one-way ANOVA (with Tukey's test). Asterisks indicate a p value of (*p<0.05, **p<0.01, *<0.001).**

3.3.3 Effect of Sphingosine 1 Phosphate on proinflammatory signalling pathways in 3T3-L1 adipocytes

3.3.3.1 The effect of S1P on Akt phosphorylation in 3T3-L1 adipocytes

Since SphK1 increased over the period of adipogenesis (up to day 8), it is of importance to characterise the effect of S1P, the product of SphK1 on adipocyte signalling. Many studies have shown that Akt has a crucial role in inflammatory response in adipocytes (Kugo et al, 2021) and so the effect of S1P on the PI3K/Akt pathway was studied by measuring Akt phosphorylation. 3T3-L1 adipocytes were incubated with S1P (10 μM) for 10 min, 20 min, 30 min, 60 min, and 120 min. After treatment, lysate was prepared, and p-Akt was detected by western blotting. S1P caused a significant (*$p<0.05$) increase in p-Akt at 10 min compared to untreated cells. Moreover, there was a small, though non-significant increase in p-Akt remaining at 20 min. Beyond that, p-Akt started to return to the basal level up to 120 min following S1P addition (Figure 3-3B).

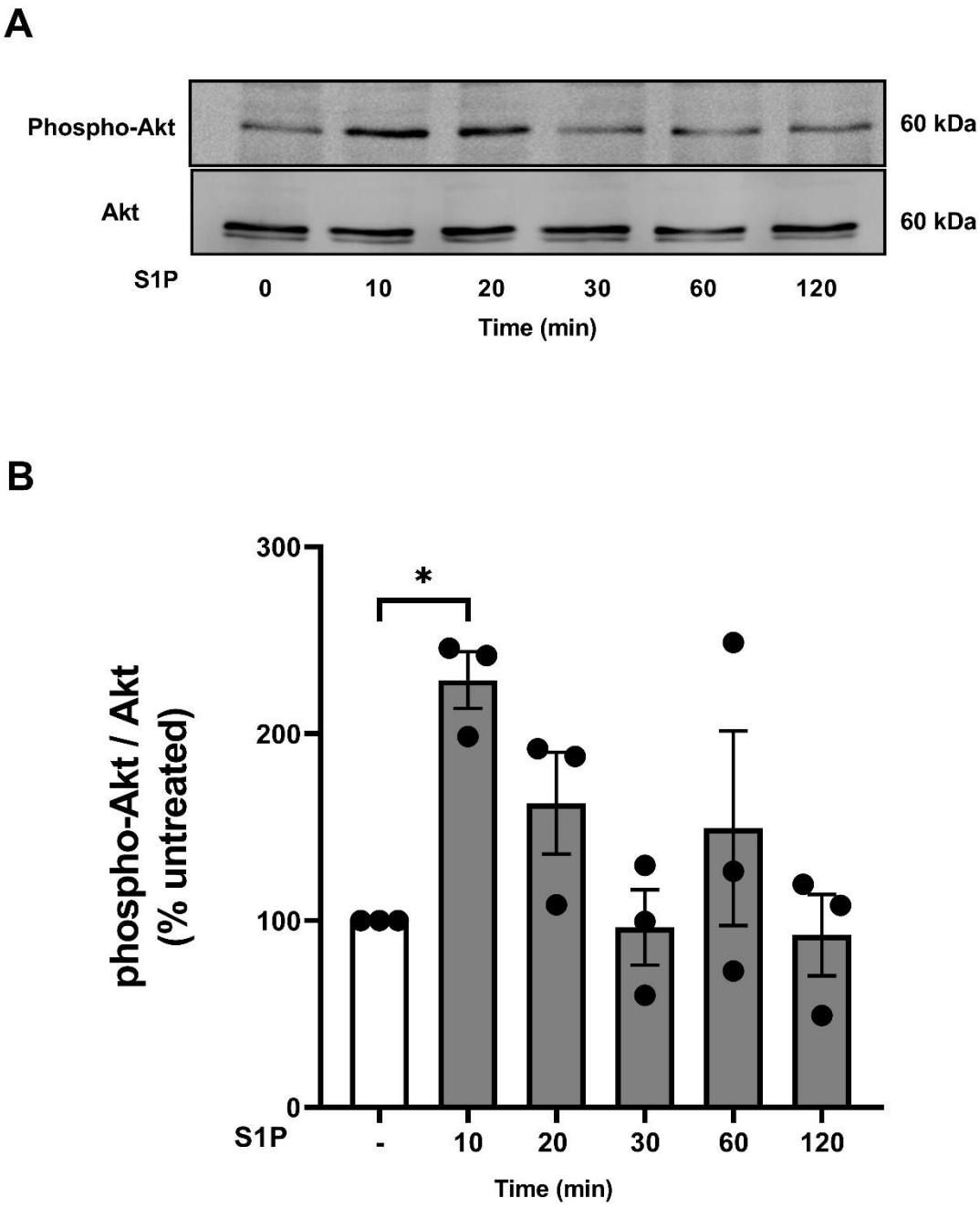

Figure 3-3 Effect of S1P on Akt phosphorylation in mature adipocytes.

3T3-L1 adipocytes were treated with S1P (10 μM) for different time periods. Cell lysates were prepared and resolved by SDS-PAGE with the appropriate antibodies. (A and B) representative western blotting image and graph of p-Akt protein expression showing the changes in Akt phosphorylation at 10 min, 20 min, 30 min, 60 min and 120 min. Protein level of p-Akt was normalised to the total level of Akt. The data represent samples from three different experiments expressed as the mean ± SEM of the % fold change relative to untreated. Statistical analysis was carried out using one-way ANOVA (with Dunnett's test). Asterisks indicate a p value of (*p<0.05).

3.3.3.2 The effect of S1P on MEK-ERK phosphorylation, P38 MAPK phosphorylation and JNK phosphorylation in 3T3-L1 adipocytes

MAPKs family pathways have been implicated in inflammatory responses in adipocytes (Nepali et al, 2015). Therefore, it was of importance to determine whether S1P influences this family of pathways. 3T3-L1 adipocytes were incubated with S1P (10 μM) for 10 min, 20 min, 30 min, 60 min and 120 min. After treatment, lysate was prepared, and p-MEK 1/2, p-ERK 1/2, p-P38, and p-JNK were detected by western blotting. S1P caused a significant (****$p<0.0001$) increase in p-MEK 1/2 and p-ERK 1/2 peaking at 10 min, compared to untreated cells. Thereafter, p-MEK 1/2 and p-ERK 1/2 levels started to return to the basal level at 20 min and there were no significant differences at any other time points (Figure 3-4).

However, treatment of adipocytes with S1P failed to induce P38 phosphorylation at any time point (Figure 3-5B) but did cause a significant (**$p<0.01$) increase in JNK phosphorylation peaking between 60 min and 120 min (Figure 3-5C).

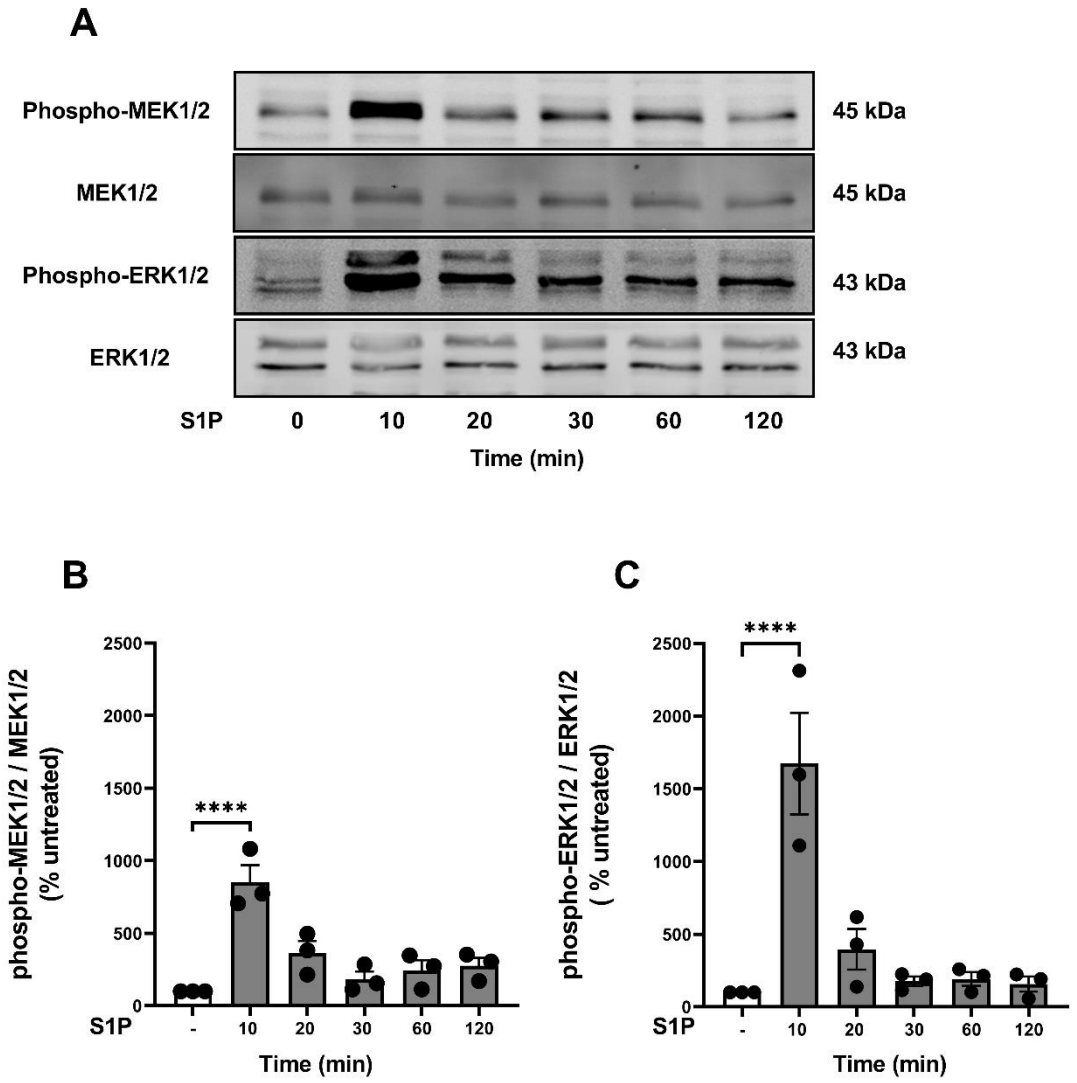

Figure 3-4 Effect of S1P on MEK-ERK pathways in mature adipocytes.

3T3-L1 adipocytes were treated with S1P (10 µM) for different time periods. Cell lysates were prepared at indicated time points and resolved by SDS-PAGE with the appropriate antibodies. (A) representative western blotting image of p-MEK 1/2 and p-ERK 1/2 protein expression showing the changes in the phosphorylation at 10 min, 20 min, 30 min, 60 min and 120 min. Phosphorylation of (B) MEK 1/2, (C) ERK 1/2 were normalised to total level of MEK 1/2 and ERK 1/2 respectively. The data represent samples from three different experiments expressed as the mean ± SEM of the % fold change relative to untreated. Statistical analysis was carried out using one-way ANOVA (with Dunnett's test). Asterisks indicate a p value of (**p<0.0001).**

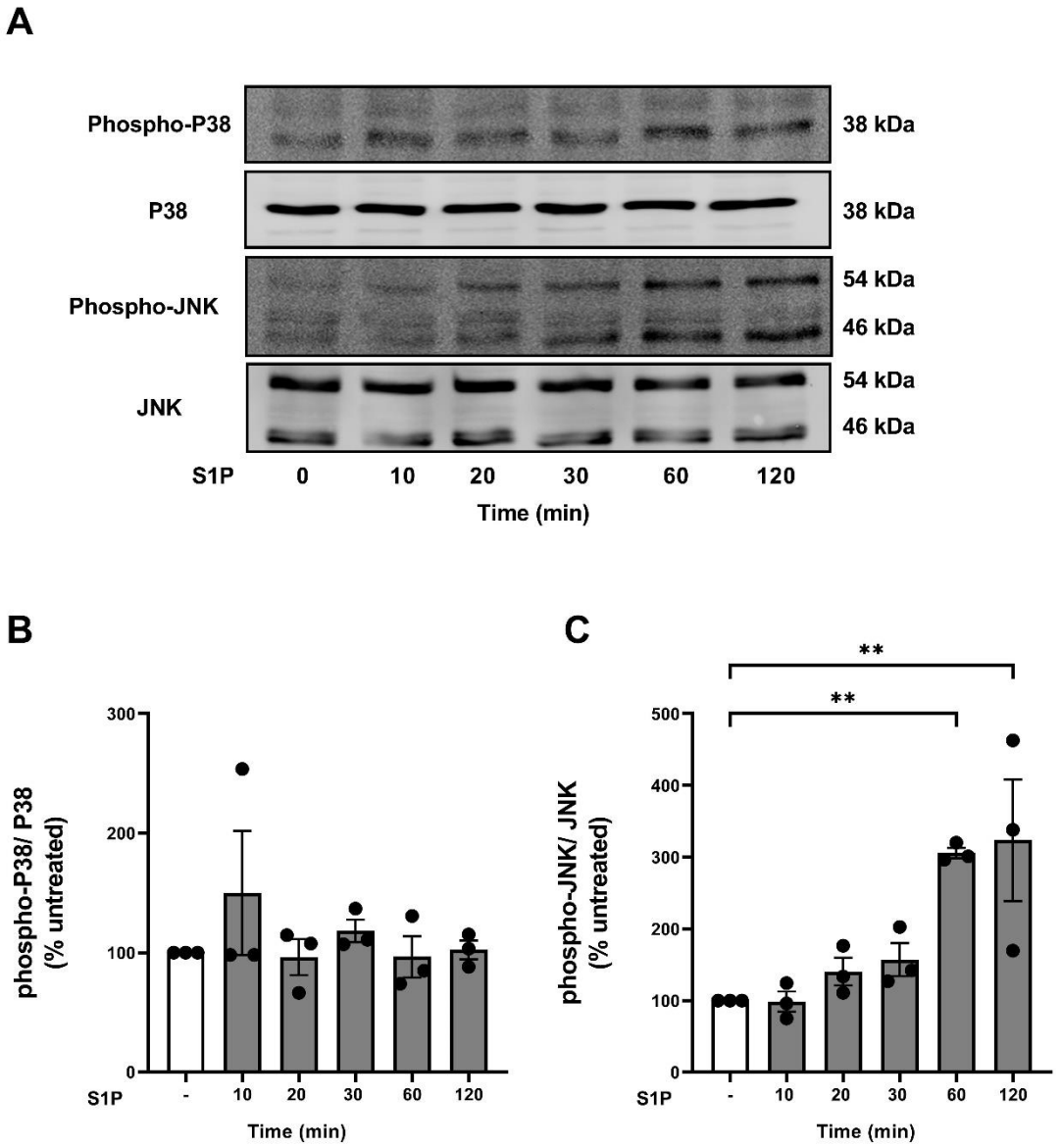

Figure 3-5 Effect of S1P on P38 and JNK pathways in mature adipocytes.

3T3-L1 adipocytes were treated with S1P (10 µM) for different time periods. Cell lysates were prepared at indicated time points and resolved by SDS-PAGE with the appropriate antibodies. (A) representative western blotting image of p-P38 and p-JNK protein expression showing the changes in the phosphorylation at 10 min, 20 min, 30 min, 60 min and 120 min. Phosphorylation of (B) P38 and (C) JNK were normalised to total level of P38 or JNK respectively. The data represent samples from three different experiments expressed as the mean ± SEM of the % fold change relative to untreated. Statistical analysis was carried out using one-way ANOVA (with Dunnett's test). Asterisks indicate a p value of (p<0.01).**

3.3.3.3 The effect of S1P on NF-KB signalling pathways in 3T3-L1 adipocytes

Previous studies have shown that S1P activates the NF-KB proinflammatory pathway in a number of cells (Cowart, 2016; Yaghobian et al, 2016). Therefore, p-NF-KB and p-IκBα were assessed in 3T3-L1 adipocytes treated with S1P (10 µM) for 10 min, 20 min, 30 min, 60 min, and 120 min. After treatment, lysate was

prepared, and p-NF-KB and p-IKBα were detected by western blotting. Treatment of 3T3-L1 adipocytes with S1P did not significantly affect NF-KB phosphorylation at any time point (Figure 3-6B). Similarly, p-IKBα was unaltered at any time point after S1P treatment (Figure 3-6C).

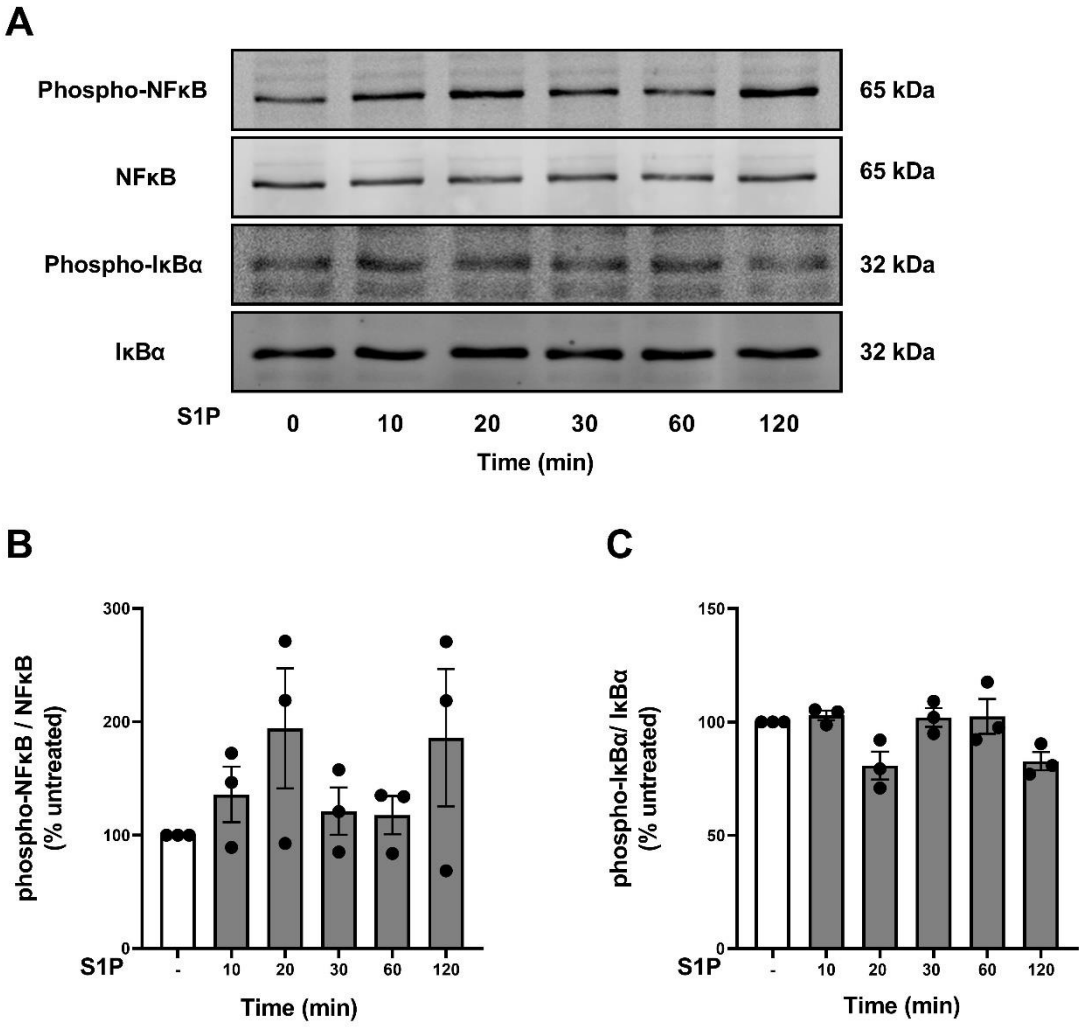

Figure 3-6 Effect of S1P on NF-KB pathway in 3T3-L1 adipocytes.

3T3-L1 adipocytes were treated with S1P (10 μM) for different time periods. Cell lysates were prepared at indicated time points and resolved by SDS-PAGE with the appropriate antibodies. (A) representative western blotting image of p-NF-KB and p-IKBα protein expression showing the changes in the phosphorylation at each time point. Phosphorylation of (B) NF-KB and (C) IKBα were normalised to total level of NF-KB or IKBα. The data represent samples from three different experiments expressed as the mean ± SEM of the % fold change relative to untreated. Statistical analysis was carried out using one-way ANOVA (with Dunnett's test).

3.3.4 The effect of IL-1β on SphK isoform expression in 3T3-L1 adipocytes

3.3.4.1 IL-1β upregulates mRNA expression of SphK1 and downregulates mRNA expression of SphK2

IL-1ß can induce an increase in SphK1 expression in a range of cell types, including glioblastoma cells (Paugh et al, 2009). Thus, I tested the effect of IL-1ß on mRNA levels of both isoforms of SphKs in 3T3-L1 adipocytes. 3T3-L1 adipocytes were stimulated with IL-1ß (10 ng/ml) for 0.5 h, 1 h, 2 h, 4 h, and 6 h. Treatment of 3T3-L1 adipocytes with IL-1ß (Figure 3-7A) caused a significant increase in Sphk1 mRNA expression after 4 h and 6 h (****p<0.0001 and ***p<0.001, respectively). A statistically significant (*p<0.05) reduction in Sphk2 mRNA expression was observed at 2 h in 3T3-L1 adipocytes treated with IL-1ß compared to untreated cells (Figure 3-7B).

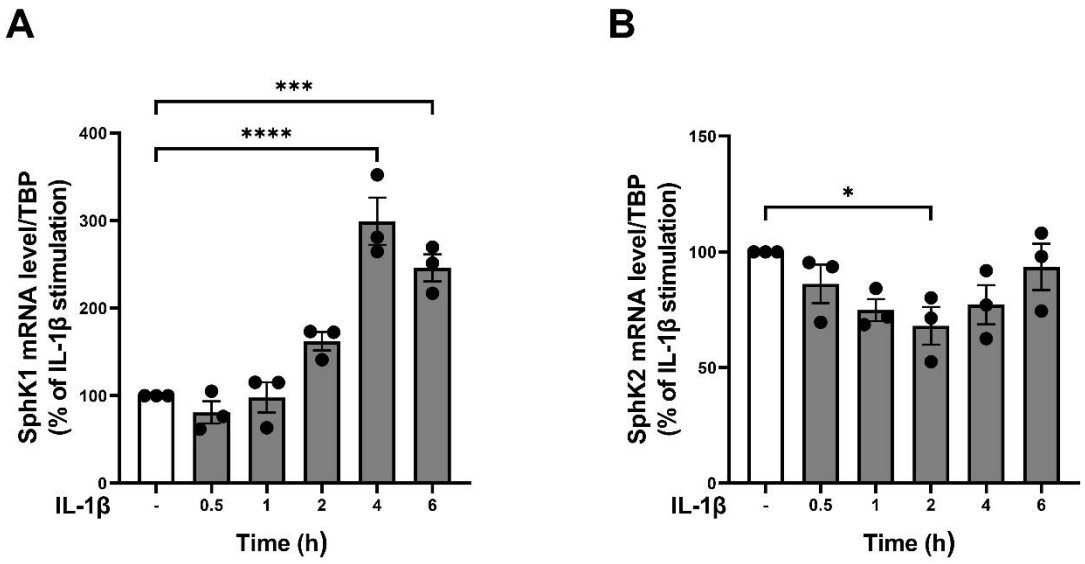

Figure 3-7 The effect of IL-1β on mRNA expression of SphK1 and SphK2 in 3T3-L1 adipocytes.

3T3-L1 adipocytes were stimulated with IL-1β (10 ng/ml) for the indicated time periods (shaded bars). RNA was isolated and quantified by qPCR. (A) qPCR analysis shows the changes in SphK1 mRNA at 0.5 h, 1 h, 2 h, 4 h and 6 h. (B) qPCR analysis shows the changes in SphK2 mRNA at 0.5 h, 1 h, 2 h, 4 h and 6 h. mRNA level of SphK1 and SphK2 was normalised to levels of TATA binding protein (TBP) mRNA levels. The data represent samples from three different experiments expressed as the mean ± SEM of the % fold change relative to untreated cells. Statistical analysis was carried out using one-way ANOVA (with Dunnett's test). Asterisks indicate a p value of (*p<0.05, ***p<0.001, ****p<0.0001).

3.3.5 IL-1β upregulates SphK1 protein expression but there is no significant difference in SphK1 phosphorylation

To confirm if IL-1β can also affect SphK1 expression and SphK1 phosphorylation, this was assessed in 3T3-L1 adipocytes treated with IL-1β (10 ng/ml) for various time points. Western blot analysis showed that IL-1β induced a significant increase in SphK1 expression after 4 h (*$p<0.05$), returning to basal levels of expression at 6 h post-treatment (Figure 3-8). This is consistent with gene level expression, which was also significantly increased at 4 h following IL-1β addition (Figure 3-7A). Moreover, IL-1β displayed a tendency to increase SphK1 phosphorylation at 60 min (Figure 3-9) in 3T3-L1 adipocytes, compared to the untreated level, although this did not reach statistical significance ($p = 0.09$).

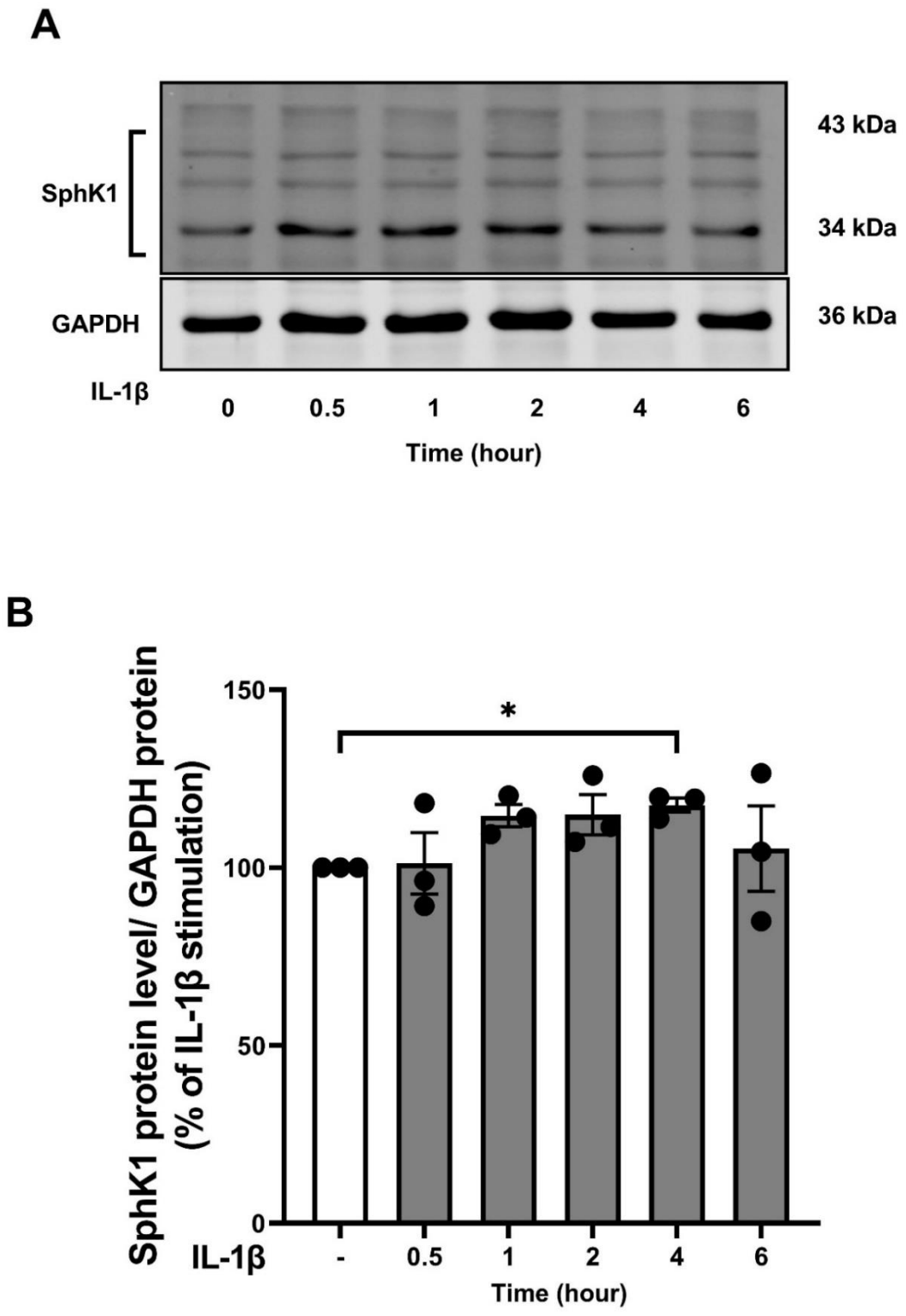

Figure 3-8 The effect of IL-1β on protein expression of SphK1 in 3T3-L1 adipocytes.

3T3-L1 adipocytes were stimulated with IL-1β (10 ng/ml) for the indicated time periods. Cell lysates were prepared at indicated time points and resolved by SDS-PAGE with the appropriate antibodies. (A and B) representative western blotting image and graph of SphK1 protein expression showing the changes in SphK1 expression at 0.5 h 1 h, 2 h, 4h and 6 h. Protein level of SphK1 was normalised to the level of GAPDH protein. The data represent samples from three different experiments expressed as the mean ± SEM of the % fold change relative to untreated. Statistical analysis was carried out using one-way ANOVA (with Dunnett's test). Asterisk indicates a p value of (*p<0.05).

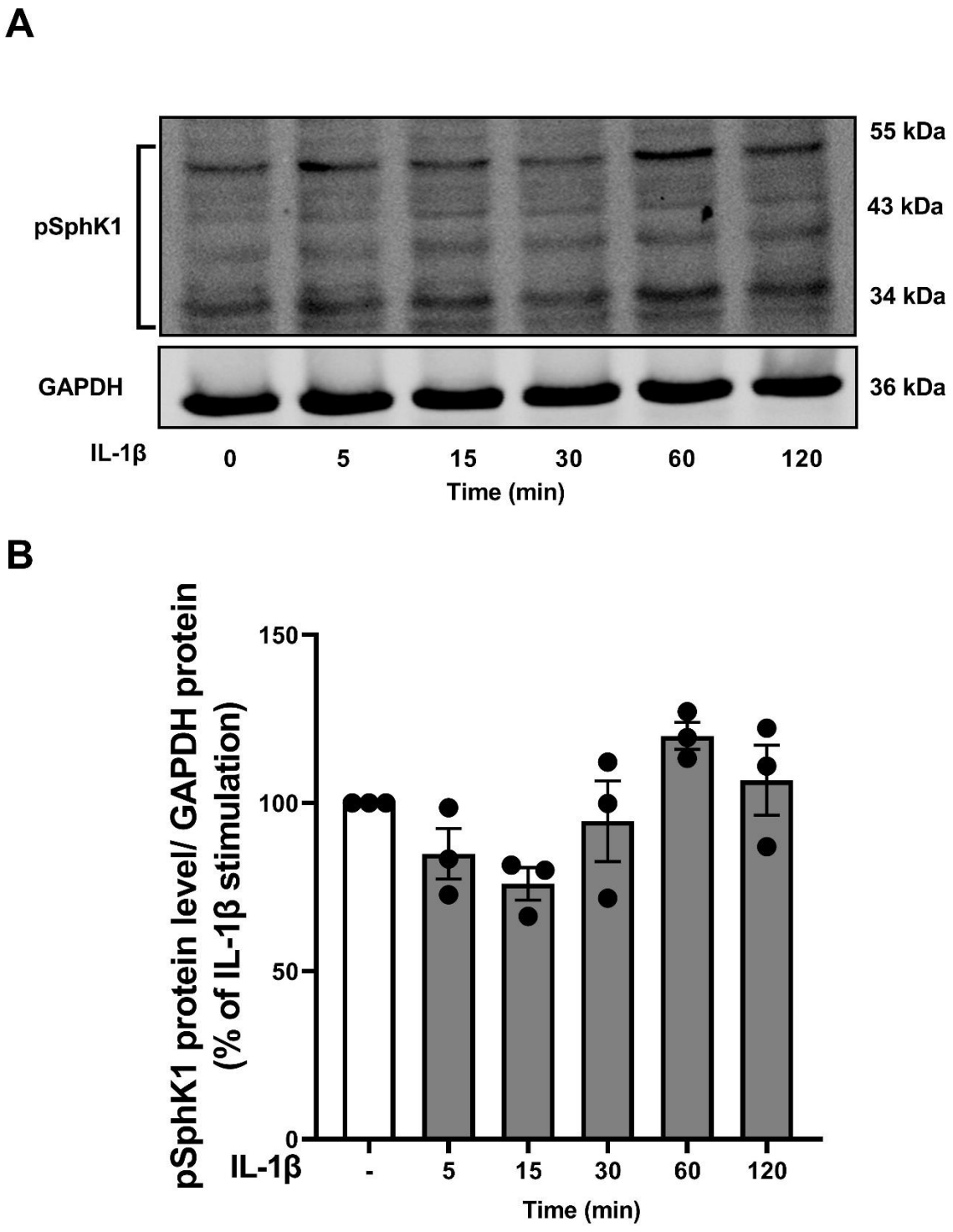

Figure 3-9 The effect of IL-1β on SphK1 phosphorylation in 3T3-L1 adipocytes.

3T3-L1 adipocytes were stimulated with IL-1β (10 ng/ml) for the indicated time periods. Cell lysates were prepared and resolved by SDS-PAGE with the appropriate antibodies. (A and B) representative western blotting image and graph of pSphK1 protein expression showing the changes in pSphK1 expression at 5 min, 15 min, 30 min, 60 min and 120 min. Protein level of pSphK1 was normalised to the level of GAPDH. The data represent samples from three different experiments expressed as the mean ± SEM of the % fold change relative to untreated. Statistical analysis was carried out using one-way ANOVA (with Dunnett's test).

3.3.6 IL-1β increases iNOS expression but has no effect on NO production in 3T3-L1 adipocytes after 6-hour stimulation

To establish if IL-1β induces iNOS expression and NO production in adipocytes, differentiated 3T3-L1 adipocytes were stimulated with IL-1β for 0.5 h, 1 h, 2 h, 4 h, and 6 h. IL-1β-induced iNOS protein expression was then determined by western blot analysis. Treatment of 3T3-L1 adipocytes with IL-1β (10 ng/ml; Figure 3-10B) caused a significant increase in iNOS compared to untreated cells after 4 h and 6 h (****$p<0.0001$). NO production, determined by nitrite/nitrate in the medium, was measured; however, it was found that IL-1β did not significantly alter NO production at 4 h or 6 h in 3T3-L1 adipocytes (Figure 3-10C).

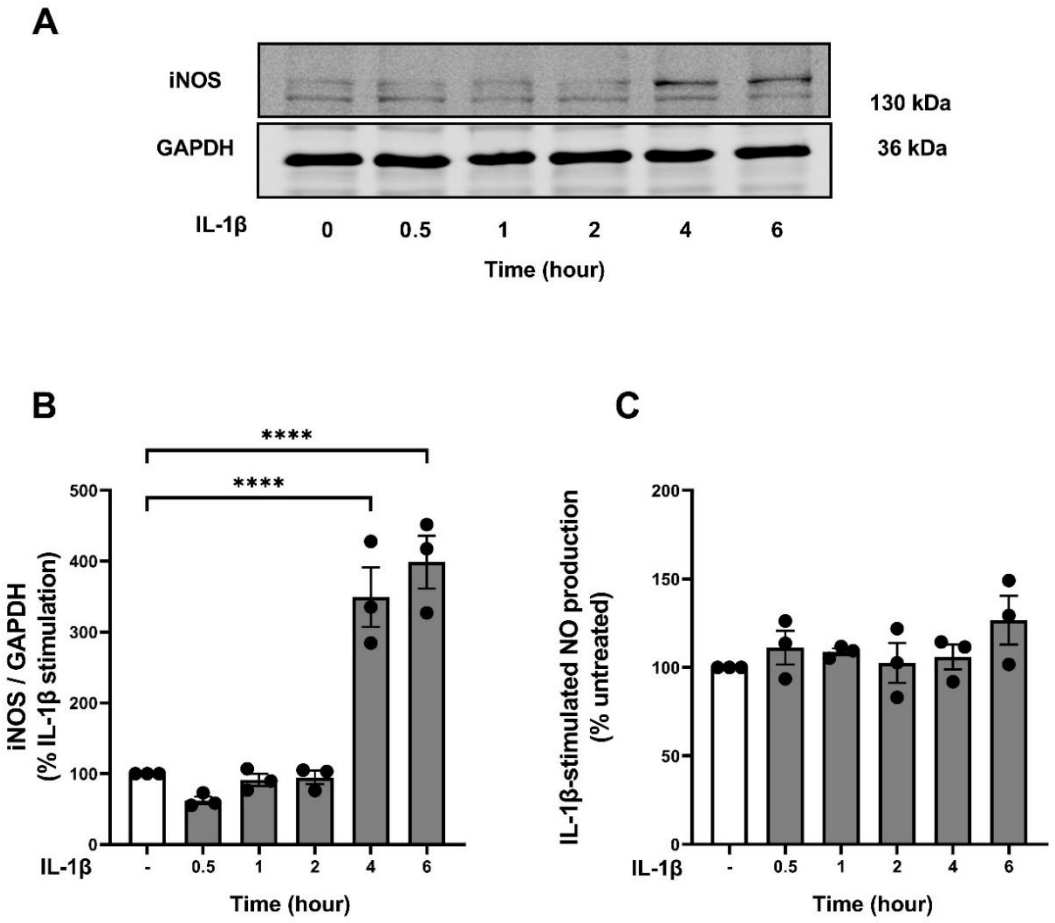

Figure 3-10 Effect of up to 6-hour stimulation with IL-1β on iNOS protein expression and NO production in 3T3-L1 adipocytes.

3T3-L1 adipocytes were stimulated with IL-1β (10 ng/ml) for time periods up to 6 hours. Cell lysates were prepared at indicated time points and resolved by SDS-PAGE with the appropriate antibodies. Media was collected and NO production was investigated by using a Sievers 280A NO Meter. (A and B) representative western blotting images and graph for the change in iNOS protein expression. Protein level of iNOS was normalised to the level of GAPDH. (C) IL-1β-stimulated NO production in 3T3-L1 adipocytes. The data represent samples from three different experiments expressed as the mean ± SEM of the fold change relative to untreated. Statistical analysis was carried out using one-way ANOVA (with Dunnett's test). Asterisks indicate a p value of (**p<0.0001).**

3.3.7 IL-1β increases iNOS expression and NO production in adipocytes after 24 hours incubation

Since NO production did not alter after 6-hours treatment, I decided to increase the incubation period with IL-1ß (10 ng/ml) to 24 h. 3T3-L1 adipocytes were then assessed for iNOS expression and NO production as previously. Treatment of 3T3-L1 adipocytes with IL-1ß (10 ng/ml) caused a significant increase in iNOS expression after 24 h (***p<0.001; Figure 3-11B). In contrast to earlier time points

NO production, determined by nitrite/nitrate in the medium, was also significantly (***p<0.001) increased (Figure 3-11C).

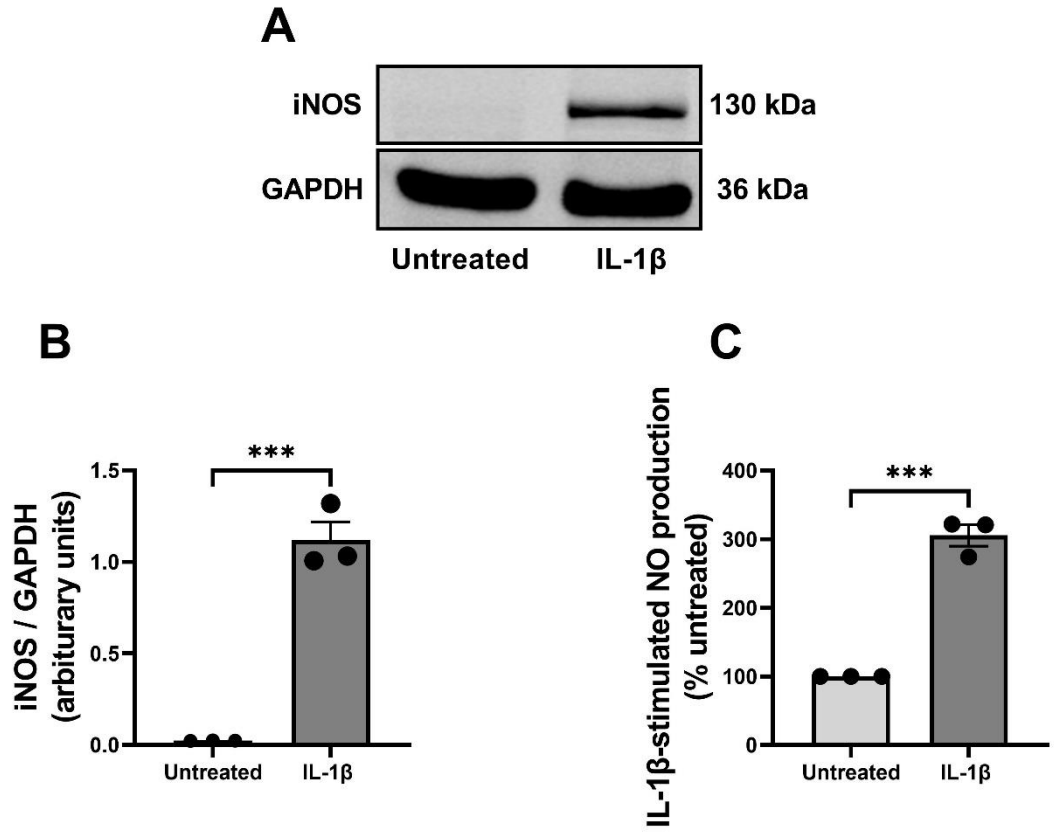

Figure 3-11 Effect of 24 hours stimulation with IL-1β on iNOS protein expression and NO production in mature adipocytes.

3T3-L1 adipocytes were stimulated with IL-1β (10 ng/ml) for 24 hours. Cell lysates were prepared and resolved by SDS-PAGE with the appropriate antibodies. Media was collected and NO production was investigated by using a Sievers 280A NO Meter. (A and B) representative western blotting images and graph for the change in iNOS protein expression. Protein level of iNOS was normalised to the level of GAPDH. (C) IL-1β-stimulated NO production in 3T3-L1 adipocytes. The data represent samples from three different experiments expressed as the mean ± SEM of the fold change relative to untreated. Statistical analysis was carried out using the Student's unpaired t-test. Asterisks indicate a p value of (*p<0.001).**

3.3.8 Exogenous S1P induces iNOS protein expression and NO production in IL-1β-stimulated 3T3-L1 adipocytes

As I had shown that IL-1ß upregulates SphK1 protein expression and mRNA levels in adipocytes, I now investigated whether S1P, the sphingolipid-product of the SphK1 enzyme, would affect iNOS expression and NO production in IL-1ß-stimulated adipocytes. 3T3-L1 adipocytes were stimulated with IL-1ß (10 ng/ml)

in the presence and absence of S1P (10 μM) for 24 hours. This concentration of S1P was chosen based on studies investigating adipocyte differentiation (Moon et al, 2014). After treatment, lysate was prepared, and iNOS expression was assessed by western blotting while NO production was determined by nitrite/nitrate in the medium. As shown in Figure 3-12 B and C, upon addition of S1P to IL-1β stimulated adipocytes, the protein expression of iNOS was significantly (***$p<0.001$) upregulated compared to cells treated with IL-1β alone. Similarly, the level of NO production, the product of iNOS, was significantly (**$p<0.01$) increased by co-treatment with S1P compared with cells treated with IL-1β alone. However, adipocytes treated with S1P alone did not show increased iNOS expression or NO production.

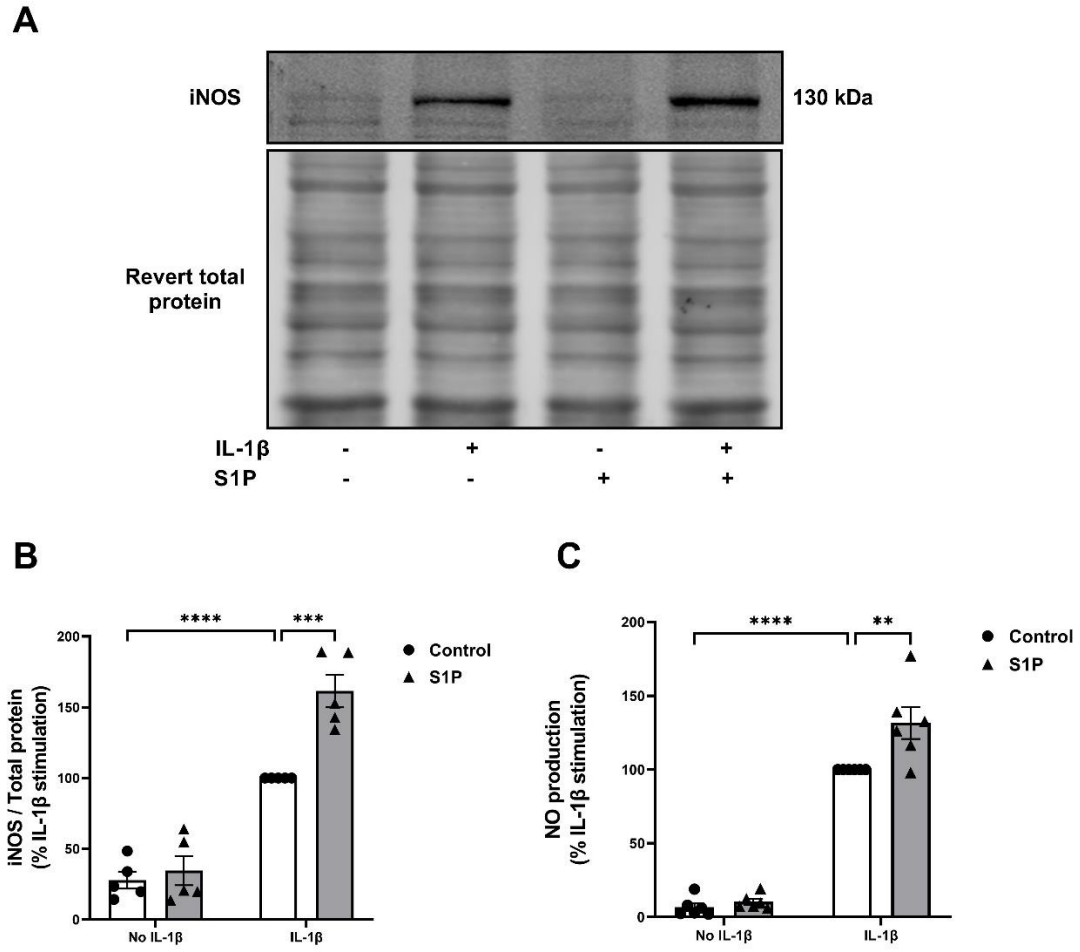

Figure 3-12 Effect of exogenous S1P on iNOS protein expression and NO production in stimulated 3T3-L1 adipocytes.

3T3-L1 adipocytes were stimulated with IL-1β (10 ng/ml) in the presence and absence of S1P (10 μM) for 24 hours. Cell lysates were prepared and resolved by SDS-PAGE with the appropriate antibodies. Media was collected and NO production was investigated by using a Sievers 280A NO meter. (A and B) representative western blotting images and graph for the change in iNOS protein expression. Protein level of iNOS was normalised to Revert total protein. (C) IL-1β stimulated NO production in 3T3-L1 adipocytes. The data represent samples from at least five different experiments expressed as the mean ± SEM % relative to IL-1β stimulation. Statistical analysis was carried out using two-way ANOVA (with Tukey's test). Asterisks indicate a p value of (p<0.01, ***p<0.001, ****p<0.0001).**

3.3.9 Effect of Sphingosine 1 Phosphate on IL-1β-stimulated proinflammatory signalling pathways

3.3.9.1 The effect of S1P on IL-1β-stimulated Akt phosphorylation in 3T3-L1 adipocytes

IL-1β has been shown to activate PI3K/Akt signalling cascade and has been implicated in iNOS regulation in multiple cell types. Also, this study has shown

that IL-1β upregulates SphK1 in 3T3-L1 adipocytes (Figure 3-8). Therefore, I speculated that IL-1β might increase S1P production to augment Akt phosphorylation, resulting in an additive effect. To determine whether S1P influences this inflammatory cascade, stimulated 3T3-L1 adipocytes were incubated with and without S1P. 3T3-L1 adipocytes were incubated with IL-1β for 15 min and 30 min following 20 min preincubation with S1P (10 μM). The extent of Akt phosphorylation was assessed as a measure of PI3K/Akt signalling cascade stimulation by western blotting.

Stimulation of 3T3-L1 adipocytes with IL-1β in the absence of S1P caused a significant (*$p < 0.05$) increase in Akt phosphorylation at 15 min compared to basal level (no addition of IL-1β), with a non-significant increase at 30 min. In the presence of S1P, there was a significant (***$p<0.001$ and **$p<0.01$, respectively) increase in IL-1β-stimulated Akt phosphorylation at both 15 min and 30 min compared to IL-1β treatment alone (Figure 3-13).

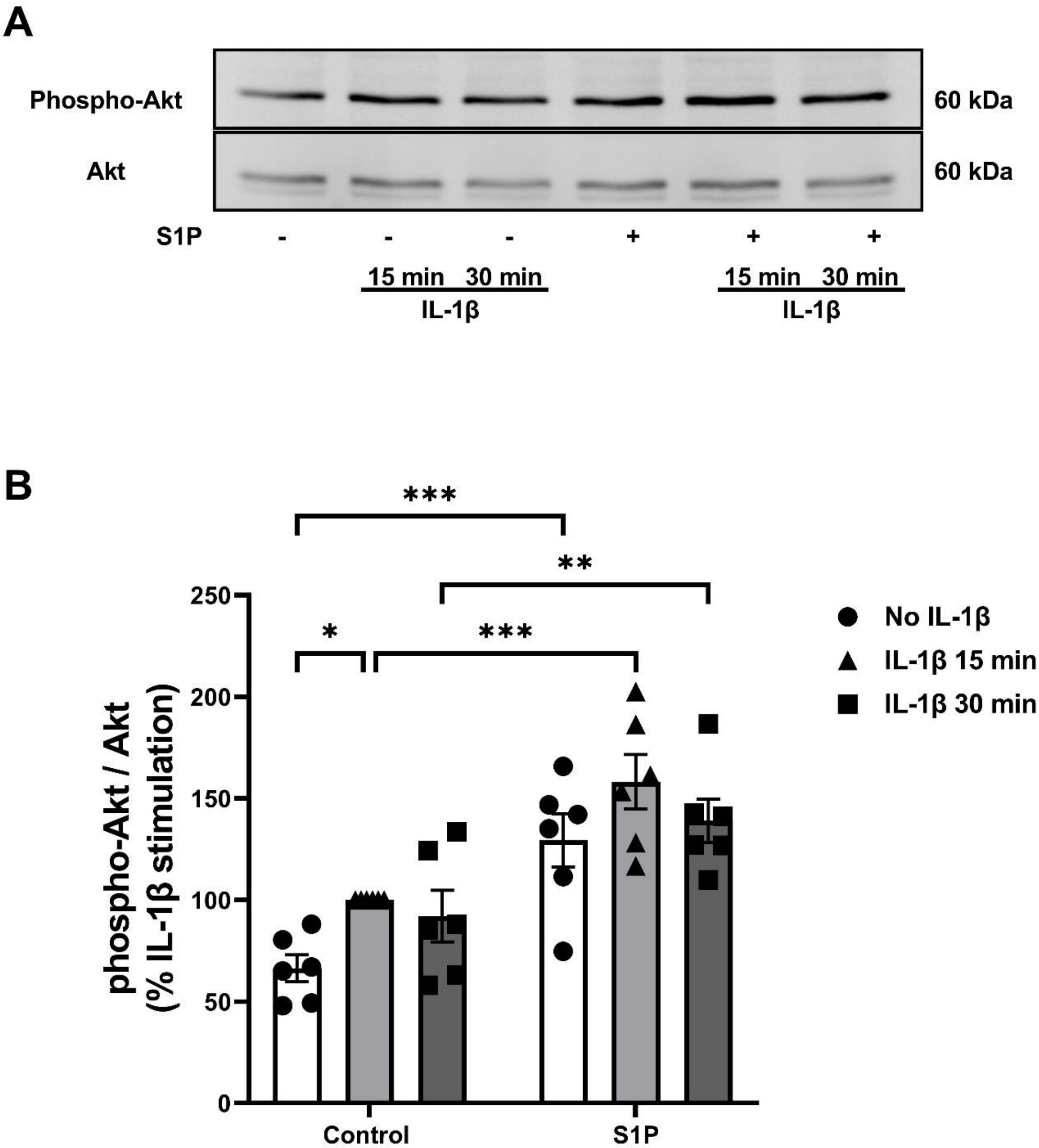

Figure 3-13 The effect of S1P on IL-1β-stimulated Akt phosphorylation in 3T3-L1 adipocytes.

3T3-L1 adipocytes were stimulated with IL-1β (10 ng/ml) for two time periods, 15 and 30 min following preincubation for 20 min in the presence or absence of S1P (10 µM). (A and B) representative western blotting image and graph of p-Akt protein expression showing the changes in Akt phosphorylation at 15 min and 30 min. Protein level of p-Akt was normalised to total level of Akt. The data represent samples from six different experiments expressed as the mean ± SEM % relative to IL-1β-stimulated phosphorylation. Statistical analysis was carried out using two-way ANOVA (with Fisher LSD test). Asterisks indicate a p value of (*p< 0.05, **p<0.01, ***p<0.001).

3.3.9.2 The effect of S1P on IL-1β-stimulated MAPKs phosphorylation in 3T3-L1 adipocytes

A second substantial pathway that has been linked to iNOS regulation by IL-1ß is MAPKs family pathway. Therefore, it was of interest to investigate whether S1P influences IL-1ß-stimulated MAPKs pathway. 3T3-L1 adipocytes were incubated with IL-1ß for 15 min and 30 min following 20 min preincubation with S1P (10 µM). The phosphorylation of MEK 1/2, ERK 1/2, P38, and JNK were assessed as a measure of stimulation by western blotting.

Stimulation of 3T3-L1 adipocytes with IL-1ß in the absence of S1P caused a gradual increase in p-MEK 1/2 which was significant (*$p<0.05$) at 30 min compared to basal level (no addition of IL-1ß). In the presence of S1P, MEK 1/2 phosphorylation increased significantly (**$p<0.01$) at both 15 min and 30 min, compared to IL-1ß treatment alone (Figure 3-14B). Furthermore, a significant increase in ERK 1/2 phosphorylation was observed at 15 min and 30 min compared to basal level (no addition of IL-1ß) in 3T3-L1 adipocytes stimulated with IL-1ß in the absence of S1P. In the presence of S1P, there was a significant (**$p<0.01$) increase in ERK 1/2 phosphorylation at 30 min compared to IL-1ß treatment alone (Figure 3-14C).

Stimulation of 3T3-L1 adipocytes with IL-1ß in the absence of S1P caused a significant (****$p<0.0001$ and **$p<0.01$, respectively) increase in P38 phosphorylation at 15 min and 30 min, compared to basal level (no addition of IL-1ß). S1P did not significantly impact P38 phosphorylation in stimulated adipocytes although there was a slight, though non-significant increase at 15 min compared to IL-1ß treatment alone (Figure 3-15B).

Stimulation of 3T3-L1 adipocytes with IL-1ß in the absence of S1P caused a significant increase in JNK phosphorylation at 15 min and 30 min (**$p<0.01$ and ****$p<0.0001$, respectively), compared to basal level (no addition of IL-1ß). In the presence of S1P, a significant (**$p<0.01$) increase in JNK phosphorylation was observed at 15 min and 30 min, compared to IL-1ß treatment alone (Figure 3-15C).

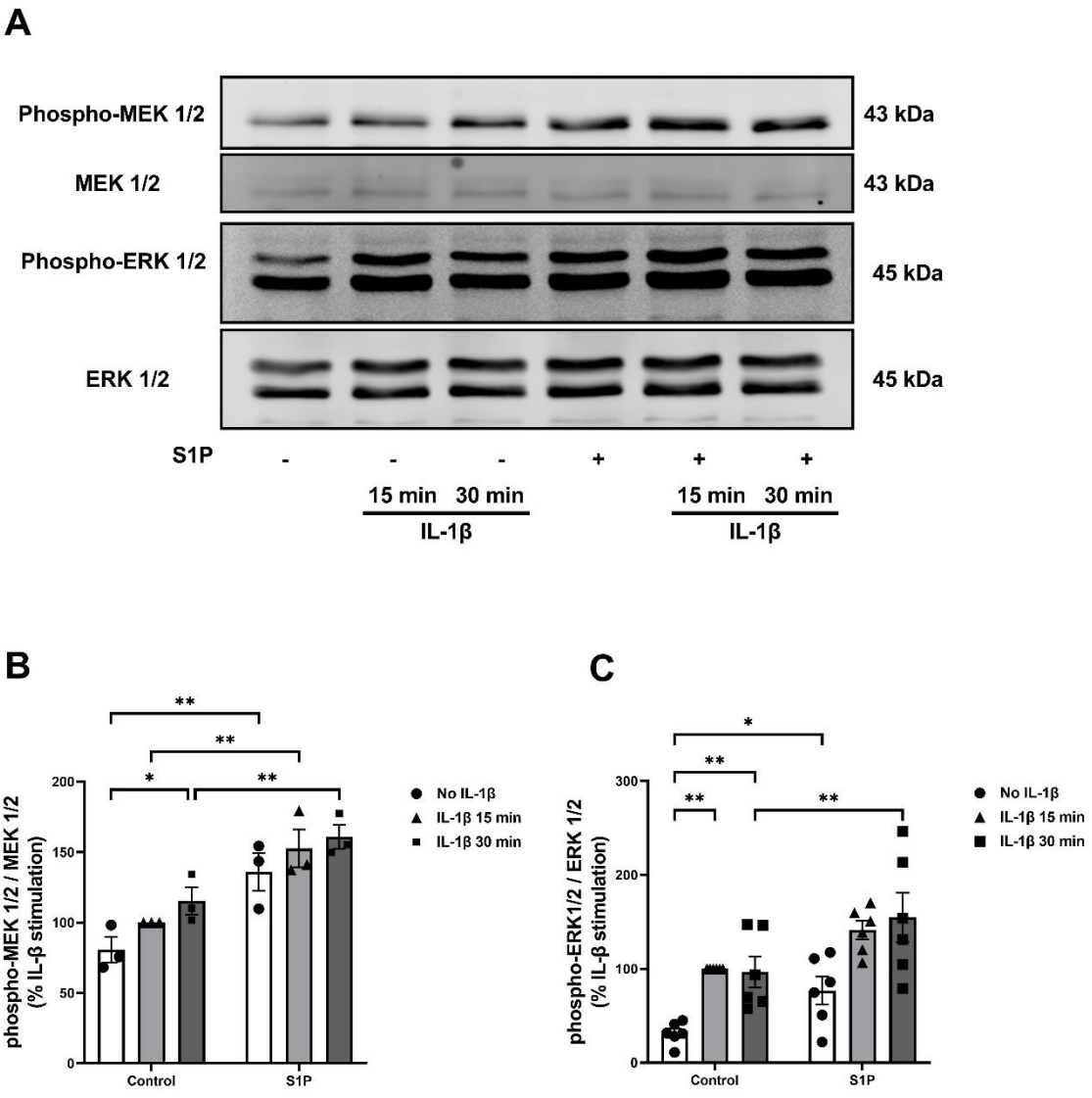

Figure 3-14 The effect of S1P on IL-1β activated MEK-ERK cascades in 3T3-L1 adipocytes.

3T3-L1 adipocytes were stimulated with IL-1β (10 ng/ml) for two time points: 15 and 30 min following preincubation for 20 min in the presence or absence of S1P (10 μM). Cell lysates were prepared and resolved by SDS-PAGE with the appropriate antibodies. (A) representative western blotting image of p-MEK1/2 and p-ERK 1/2 protein expression showing the changes in the phosphorylation at 15 min and 30 min. Phosphorylation of (B) MEK 1/2, (C) ERK 1/2 were normalised to total level of MEK 1/2 or ERK 1/2. The data represent samples from at least three different experiments expressed as the mean ± SEM % relative to IL-1β-stimulated phosphorylation. Statistical analysis was carried out using two-way ANOVA (with Fisher LSD test). Asterisks indicate a p value of (*p<0.05, **p<0.01).

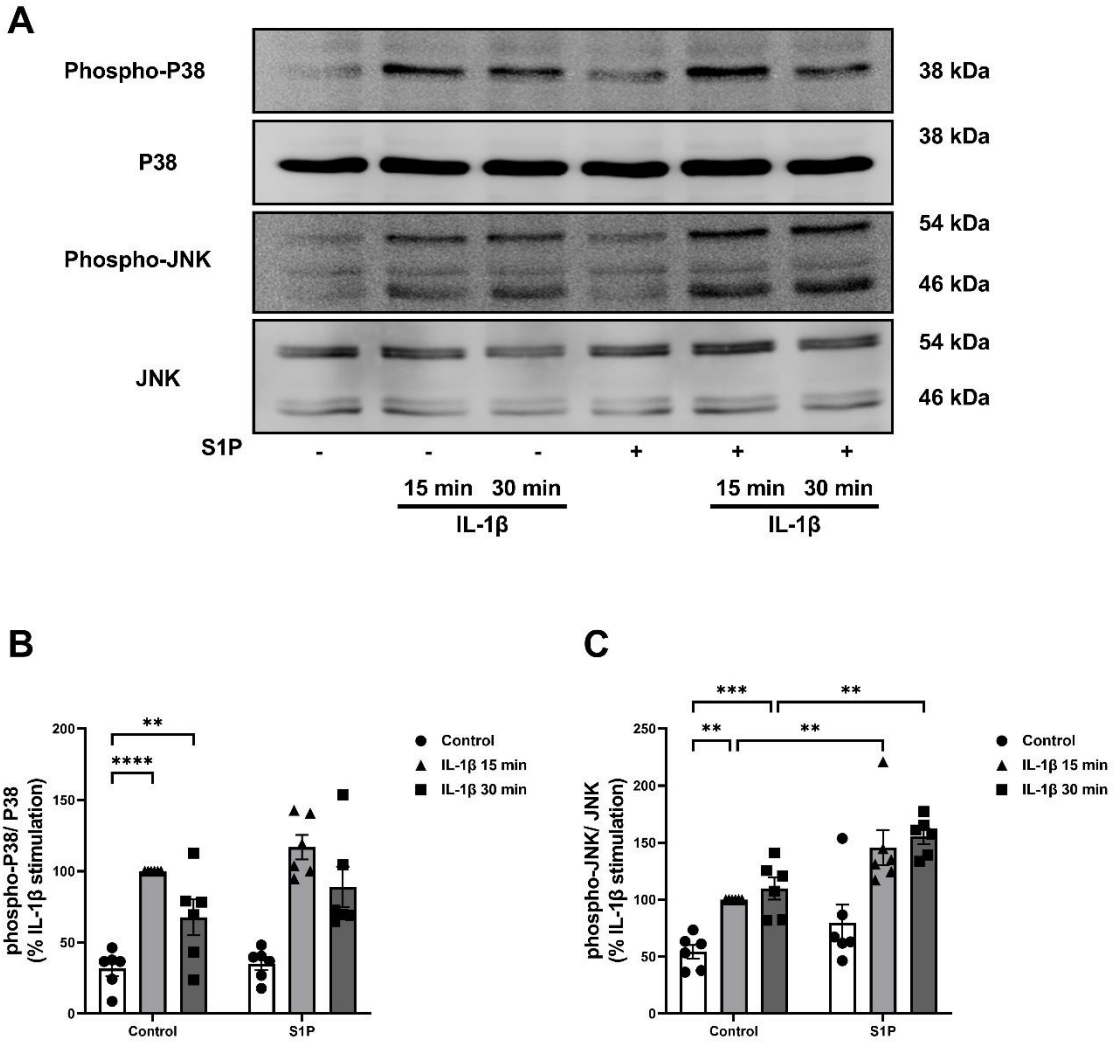

Figure 3-15 The effect of S1P on IL-1β activated P38 and JNK pathways in 3T3-L1 adipocytes.

3T3-L1 adipocytes were stimulated with IL-1β (10 ng/ml) for two time points: 15 and 30 min following preincubation for 20 min in the presence or absence of S1P (10 μM). Cell lysates were prepared and resolved by SDS-PAGE with the appropriate antibodies. (A) representative western blotting image of p-P38 and p-JNK protein expression showing the changes in the phosphorylation at 15 min and 30 min. Phosphorylation of (B) P38, (C) JNK were normalised to total level of P38 or JNK. The data represent samples from at least three different experiments expressed as the mean ± SEM % relative to IL-1β-stimulated phosphorylation. Statistical analysis was carried out using two-way ANOVA (with Fisher LSD test). Asterisks indicate a p value of (p<0.01, ***p<0.001, ****p<0.0001).**

3.3.10 The effect of S1P on IL-1β-stimulated NF-κB signalling pathways in 3T3-L1 adipocytes

Another pathway that may be linked to iNOS regulation by IL-1ß is the NF-KB pathway. Therefore, it was of interest to determine whether S1P influences IL-1ß-stimulated NF-KB pathway. The experimental protocol was as previously and the phosphorylation of NF-KB, IKBα and IKBα protein expression were assessed as a measure of stimulation by western blotting.

Stimulation of 3T3-L1 adipocytes with IL-1ß in the absence of S1P caused a significant increase in p-NF-KB at 15 min (****$p<0.0001$) and 30 min (***$p<0.001$), compared to basal level (no addition of IL-1ß). However, in the presence of S1P, NF-KB phosphorylation was not significantly different compared to that seen with IL-1ß treatment alone (Figure 3-16B). Similarly, IKßα phosphorylation increased significantly (****$p<0.0001$) in 3T3-L1 adipocytes stimulated with IL-1ß at 15 min in the absence of S1P. However, IKßα phosphorylation was similar in the presence of S1P, compared to IL-1ß treatment alone (Figure 3-16C), which is consistent with the lack of effect of S1P shown previously.

IKßα protein expression was observed to decline significantly (*$p<0.05$) at 15 min and 30 min following IL-1ß stimulation, compared to basal level (no addition of IL-1ß). However, S1P addition had no impact on IKßα protein (Figure 3-16D).

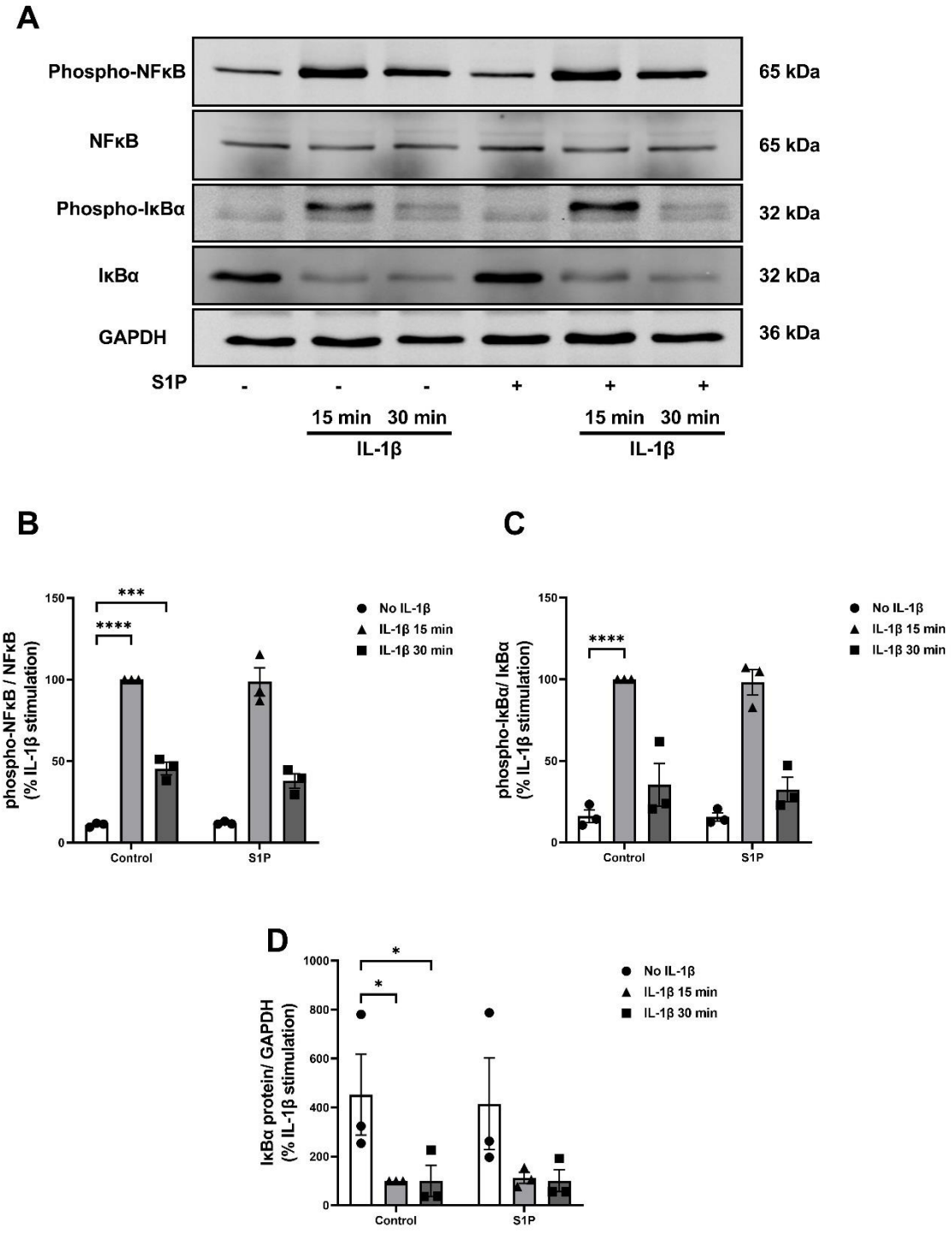

Figure 3-16 The effect of S1P on IL-1β stimulated NF-KB cascades.

3T3-L1 adipocytes were stimulated with IL-1ß (10 ng/ml) for two time points: 15 and 30 min following preincubation for 20 min in the presence or absence of S1P (10 μM). Cell lysates were prepared and resolved by SDS-PAGE with the appropriate antibodies. (A) representative western blotting image of p-NF-KB, p-IKBα and IKBα protein expression showing the changes in the phosphorylation at 15 min and 30 min. Phosphorylation of (B) NF-KB and (C) IKBα were normalised to total level of NF-KB and IKBα, respectively while IKBα protein was normalised to the level of GAPDH (D). The data represent samples from three different experiments expressed as the mean± SEM % relative to IL-1ß-stimulated phosphorylation. Statistical analysis was carried out using two-way ANOVA (with Fisher LSD test). Asterisks indicate a p value of (*p<0.05, ***p<0.001, ****p<0.0001).

3.4 Discussion

In this chapter, I investigated SphK1 expression in adipocytes and the effect of an inflammatory stimulus on this expression. I also studied the effect S1P has on proinflammatory pathways in 3T3-L1 adipocytes under control and inflammatory conditions. S1P was found to activate multiple proinflammatory signalling pathways in adipocytes including the PI3K/Akt pathway, MEK-ERK pathway and JNK pathway, but apparently had no effect on the NF-KB pathway. Also, I studied the effect of IL-1β on SphKs expression in 3T3-L1 adipocytes and the influence of S1P in IL-1β-mediated iNOS expression and NO production in 3T3-L1 adipocytes. The current work has identified that IL-1β increases Sphk1 expression, further supporting a role for Sphk1 and S1P in IL-1β-stimulated iNOS expression and NO production in 3T3-L1 adipocytes. Exogenous S1P augmented IL-1β- stimulated iNOS expression and NO production in 3T3-L1 adipocyte. The mechanisms by which S1P augments iNOS expression and NO production in stimulated 3T3-L1 adipocytes are likely to be through the Akt and MAPKs pathways (MEK-ERK pathway and JNK pathway), but independent of pathways via NF-KB.

In this study, I used a 3T3-L1 cell line, which is widely used for studying adipocyte function and related mechanisms. 3T3-L1 preadipocytes are differentiated into mature adipocytes upon addition of an adipogenic cocktail, as described in the methodology section. To validate that adipogenesis had occurred in response to the adipogenic cocktail, the morphology of cells and lipid accumulation was studied (Figure 3-1A and B). PPAR-γ protein expression was also used as a marker to validate adipogenesis and differentiation. It was found that PPAR-gamma rose gradually over the period of adipogenesis (Figure 3-1D).

Initially, I started by investigating and characterising the SphK1 expression over the period of adipogenesis. The protein level of SphK1 rose over the course of adipogenesis, studied by immunoblotting (Figure 3-2). These findings are in line with those published by (Hashimoto et al, 2009), who also found that SphK1 level rises during adipogenesis of 3T3-L1 preadipocytes, enhancing S1P content, and that SphK1 inhibitors reduce adipogenesis and lipid accumulation. Basal expression of SphK2 protein was not investigated in this study, as it was shown by Hashimoto et al (2009) that SphK2 is also increased with the same pattern as

SphK1. Elevation of SphK1 and SphK2 in adipocytes would be anticipated to increase S1P production from adipocytes. However, a few studies suggest that SphK1 and SphK2 have distinct roles in adipocyte function particularly in term of fat mass and lipid metabolism (Anderson et al, 2020; Ravichandran et al, 2019). Taken together, these findings suggest that SphKs/S1P could have an important role to play in adipocyte function.

It has been reported that S1P regulates multiple cellular processes in adipose tissue. Importantly, S1P has been shown to be involved in adipose tissue inflammation in 3T3-L1 adipocytes. The PI3K/Akt pathway, MAPKs family pathway, and NF-KB pathways are proinflammatory pathways implicated in many metabolic disorders in adipose tissue and proinflammatory processes within adipose tissue. Therefore, it was of interest to characterise the role of S1P on these proinflammatory pathways in 3T3-L1 adipocytes. PI3K/Akt is one of the pathways that has been studied widely in adipose tissue and linked to many inflammatory processes. For example, a recent study carried out by (Kugo et al, 2021) found that the PI3K/Akt pathway is involved in modulating many inflammatory species such as iNOS and ROS. Elevation of Akt phosphorylation has been reported in the inflamed adipose tissue of mice infected with tuberculosis. Also, in the same study, it was shown that Akt is required for macrophage infiltration and cytokine expression in adipocytes of infected mice (Martinez et al, 2019). There are conflicting reports regarding the effect of S1P on Akt activation. Some studies reported that S1P activates Akt in osteoblast-like cells (Matsuzaki et al, 2013), and hepatocytes (Osawa et al, 2011) while S1P has been reported to inhibit Akt activation in pancreatic ß cells (Japtok et al, 2015). In this study, the extent of Akt phosphorylation was used as a measure for PI3K/Akt activation. Figure 3-3 demonstrates that S1P activates Akt phosphorylation, peaking at 10 min in 3T3-L1 adipocytes. This is expected; PI3K/Akt is one of the downstream signalling pathways of S1P, and this is consistent with studies carried out on osteoblast cells and hepatocytes (Matsuzaki et al, 2013; Osawa et al, 2011), suggesting that S1P could contribute to the proinflammatory process in adipocytes via PI3K/Akt pathway.

The family of MAPKs are another set of proinflammatory pathways and have been shown to control many inflammatory processes in 3T3-L1 adipocytes. For example,

ERK1/2 has been reported to be required for expression of many inflammatory genes and also iNOS expression in adipocytes (Habibian et al, 2017). Moreover, ERK1/2 , JNK, and P38 have been implicated in adipocyte inflammation and particularly iNOS regulation (Nepali et al, 2015). Therefore, it was of interest to characterise the role of S1P on these pathways in 3T3-L1 adipocytes. My data showed that S1P strongly activates the MEK-ERK pathway (Figure 3-4). This is consistent with many studies showing that S1P activates ERK1/2 in zona glomerulosa cells (Brizuela et al, 2007), adipocytes (Kitada et al, 2016), and chondrosarcoma cells (Wang et al, 2019). In addition, S1P was shown to significantly activate JNK phosphorylation at 60 min and 120 min in 3T3-L1 adipocytes (Figure 3-5C). This result is consistent with previous observations where S1P activated JNK phosphorylation in adipocytes and bone marrow–derived monocyte/macrophages (BMMs) (Hou et al, 2021; Jun et al, 2006). Interestingly, although it is known that P38 phosphorylation is one of S1P's downstream signalling mechanisms, my findings (Figure 3-5B) contradicts some published studies which have reported that S1P activates P38 phosphorylation in rat white adipocytes (Jun et al, 2006) and BMMs (Hou et al, 2021). Consequently, it's probable that there are mechanisms particular to different cell types and/or the variations in incubation times, concentrations of S1P, or differences in receptor expression between cell types explain the discrepancy observed in this study.

NF-KB is one of the prominent inflammatory pathways that regulate multiple inflammatory processes within the adipose tissue. In addition, it has been reported that it regulates iNOS expression in 3T3-L1 adipocytes (Araki et al, 2007; Yang et al, 2002). Therefore, it was of importance to elucidate the effect of S1P on the NF-KB pathway in adipocytes. There is conflicting evidence in the literature regarding the effect of S1P on NF-KB pathways; S1P was reported to activate NF-KB in human embryonic kidney 293 (HEK 293) cells (Siehler et al, 2001), human kidney 2 cells (Yaghobian et al, 2016), and hepatocytes (Cowart, 2016), while S1P was reported to inhibit NF-KB pathway in vascular smooth muscle cells (Keul et al, 2019), human testis (Suomalainen et al, 2005) and macrophages (Hughes et al, 2008). The effect of S1P on the NF-KB pathway currently also remains poorly characterized in 3T3-L1 adipocyte. In our study, NF-KB activation was evaluated as the extent of NF-KB phosphorylation, IKBα phosphorylation along with IKBα protein degradation. Figure 3-6 demonstrates that S1P failed to activate any of

the NF-KB intermediates upstream. Our finding is consistent with a previous study in primary cultured rat intestinal smooth muscle cells where S1P failed to mediate NF-KB translocation (Gurgui et al, 2010). In this study, I did not investigate the translocation of proinflammatory transcription factor NF-KB to the nucleus; therefore, it is possible that more convincing data could be generated by investigating the effect of S1P on NF-KB nucleus translocation.

Several lines of evidence have shown that IL-1ß may upregulate SphK1 in a variety of cell lines. For instance, exposure of glioblastoma cells and astrocytes to IL-1ß upregulates SphK1 expression (Paugh et al, 2009). In the same study the SphK2 level was not altered. Moreover, Billich et al demonstrated that although IL-1ß increased SphK1 enzymatic activity with no effect on SphK2, the mRNA level of SphK1 was not altered in A549 lung carcinoma cells (Billich et al, 2005). However, in another study, the mRNA level of SphK1 was found to increase in human glioblastoma U373-MG cells treated with IL-1ß (Bryan et al, 2008). In addition, SphK1 mRNA level but not SphK2 mRNA level, was shown to be upregulated in isolated rat pancreatic islet cells exposed to IL-1ß (Mastrandrea et al, 2005). These findings imply that IL-1ß may regulate SphK1 either at the transcription or post-translation level. In the current study, it was found that treatment of 3T3-L1 adipocytes with IL-1ß for various time points led to a marked increase in SphK1 mRNA compared with untreated cells at 4h and 6h, whereas SphK2 was significantly downregulated at 2 h (Figure 3-7). Moreover, elevated SphK1 protein expression was also shown in 3T3-L1 adipocytes treated with IL-1ß for 4 h, which is consistent with the upregulation in the mRNA level (Figure 3-8). IL-1ß displayed a tendency to increase SphK1 phosphorylation at 60 min (Figure 3-9) in 3T3-L1 adipocytes, compared to the untreated level, although this did not reach statistical significance. To our knowledge, these data are the first to demonstrate the effect of IL-1ß on SphKs expression in 3T3-L1 adipocytes.

Considering the aforementioned findings and background, I hypothesized that IL-ß required the SphK1/S1P system to modulate iNOS expression and NO production in 3T3-L1 adipocytes. One paradigm could be that when IL-1ß activates SphK1, it is then re-located from the cytosol to the plasma membrane, where it is close to its substrate, sphingosine. Then, S1P is synthesised and exported through transporter proteins into the extracellular milieu where it acts as an agonist for

S1P receptors, inducing proinflammatory pathways that regulate iNOS expression and NO production.

A series of experiments was carried out to investigate the effect of IL-1β on iNOS expression and NO production in 3T3-L1 adipocytes. Previous studies have elucidated that IL-1β stimulates iNOS expression and NO production in rat vascular smooth muscle cells (Machida et al, 2008), rat aortic endothelial cells (Cortese-Krott et al, 2014), and 3T3-L1 preadipocytes (Park et al, 2021). Therefore, I decided to investigate the IL-1β effect has on iNOS expression and NO production in 3T3-L1 adipocytes. Treatment of 3T3-L1 adipocytes with IL-1β for up to 6 h, caused a significant increase in iNOS protein expression, while NO production was not altered consistently with iNOS expression (Figure 3-10). However, once I incubated 3T3-L1 adipocytes with IL-1β for 24h, iNOS protein expression markedly increased, and this did lead to a significant increase in NO production (Figure 3-11). Thus, in all subsequent experiments characterising iNOS expression and NO production, the IL-1β incubation time was kept at 24 h. As mentioned previously, S1P has been implicated in many proinflammatory processes within adipose tissue. Despite a variety of published studies investigating the role of S1P in adipose tissue dysfunction, the role of S1P in IL-1β-mediated iNOS expression and NO production in 3T3-L1 adipocytes has not been investigated so far. In the current study, since it is technically challenging to measure the S1P production from stimulated-adipocytes, I cotreated the cells with IL-1β and S1P to investigate iNOS expression and NO production. It was found that exogenous S1P significantly augments iNOS expression in IL-1β-stimulated 3T3-L1 adipocytes (Figure 3-12B). Consistent with iNOS protein expression, S1P markedly upregulated NO production by stimulated 3T3-L1 adipocytes (Figure 3-12C). This is consistent with other reports in macrophage polarization where co-treatment with S1P enhances iNOS expression under M1-polarization conditions (Müller et al, 2017). Another report has shown that S1P upregulates iNOS expression and NO production from murine HAPI microglial cell line (Wang et al, 2021). Also, S1P has been reported to upregulate many proinflammatory mediators, such as TNF-α and IL-6 in peripheral blood mononuclear cells and rat HAPI microglia cell line (Terlizzi et al, 2022; Wang et al, 2021) and IL-1β in osteoblasts (Hu et al, 2020), implying that S1P have an effect additive to that of IL-1β alone. In support of this, it was proven that S1P promotes increased levels of proinflammatory cytokines (TNF-α and IL-6) in 3T3-L1

adipocytes (Samad et al, 2006). Interestingly, however, S1P alone did not upregulate either iNOS expression or NO production in 3T3-L1 adipocytes, suggesting that the synergistic effect of S1P might be either via modulation of signalling pathway related to iNOS, causing an increase in iNOS protein expression and subsequently NO production, or promoting production of proinflammatory mediators, which subsequently have an additive effect to the IL-1β. Taken together, IL-1β is capable of activating SphK1, resulting in S1P production and ultimately S1P receptor activation, and this could be a new mechanism by which IL-1β is eliciting its effect indirectly in 3T3-L1 adipocytes. These data suggest a proinflammatory role of SphKs/S1P in adipose tissue, particularly through iNOS proinflammatory enzyme regulation in 3T3-L1 adipocytes and more widely, this process could be linked to many disorders associated with obesity. Although the role of S1P in iNOS regulation in adipose tissue has not previously been well studied, these data correlate with a study which confirmed that obese mice lacking SphK1 show a decrease in proinflammatory mediators in adipocytes, including TNF-α and IL-6 (Wang et al, 2014).

Since I confirmed that IL-1β upregulates SphK1, which I believe would lead to S1P production from 3T3-L1 adipocytes and further contribute to iNOS expression and NO production, it was of importance to investigate IL-1β-related mechanisms. The biological function of IL-1β is exerted by activating many signalling pathways, including a PI3K/Akt kinase and the three types of mitogen-activated protein (MAP) kinases (MEK-ERK1/2, JNK, and p38). Another prominent signalling pathway for inflammatory responses is NF-KB activation (Martin & Wesche, 2002). To examine the mechanisms responsible for the additive effect of S1P on IL-1β-mediated iNOS expression and NO production, 3T3-L1 adipocytes were incubated with S1P 20 min prior to IL-1β stimulation. It has been suggested that PI3K/Akt pathway regulates the expression of iNOS expression and NO production in 3T3-L1 adipocytes and other cells (Jang et al, 2004; Kleinert et al, 2010; Martin & Wesche, 2002; Nepali et al, 2015). I found that IL-1β significantly upregulated Akt phosphorylation, a PI3K downstream effector, while preincubation of adipocytes with S1P significantly amplified IL-1β-stimulated Akt phosphorylation (Figure 3-13), suggesting that this pathway might mediate the increased level of iNOS and NO production in stimulated adipocytes. These data support the few reports to date investigating the effect of S1P on cytokine-stimulated Akt pathway

activation. TNF-α stimulation of the Akt pathway was found to be reduced by inhibiting SphK1 in human hepatocytes (Osawa et al, 2001), and by SphK1 knockdown in human astrocytoma cells (Radeff-Huang et al, 2007). In A549 cells, a non-malignant lung epithelial cell line, overexpression of SphK1 boosted Akt phosphorylation, whereas SphK1 knockdown attenuated Akt phosphorylation (Zhu et al, 2015).

In addition, MAPKs family pathways are proven to regulate many proinflammatory processes within the adipose tissue. Furthermore, iNOS expression and NO production were linked to MAPKs pathways activation in 3T3-L1 adipocytes (Nepali et al, 2015). As shown in Figure 3-14, IL-1ß treatment alone resulted in an increase in MEK-ERK pathway phosphorylation at 15 min and 30 min. Activation of S1PRs with S1P significantly augmented IL-1ß-stimulated MEK-ERK phosphorylation. Similarly, IL-1ß has been shown to markedly upregulate P38 phosphorylation and JNK phosphorylation. Activation of S1PRs with S1P significantly augmented IL-1ß-stimulated JNK phosphorylation level, whereas P38 phosphorylation level was not significantly altered (Figure 3-15), implying that this pathway might mediate the increased level of iNOS and NO production in stimulated adipocytes. These data support the few reports to date investigating the effect of S1P on cytokine-stimulated MAPK pathway activation. LPS-stimulated ERK phosphorylation was found to be augmented by S1P in human endothelial cells and human aortic endothelial cells (Fernández-Pisonero et al, 2012). Similarly, another report has shown that P38 phosphorylation by LPS is augmented by S1P in microglia cells (Wang et al, 2021). It has also been reported that S1P-augmented IL-1ß stimulated ERK1/2 and P38 phosphorylation in mouse intestinal subepithelial myofibroblasts (Ohama et al, 2008).

The NF-KB pathway is one of the important pathways regulating iNOS expression and NO production in adipocytes (Kim et al, 2020). In the present study, I demonstrated that IL-1ß significantly upregulates NF-KB pathways by increasing NF-KB activation, IKBα phosphorylation, and IKBα degradation (Figure 3-16). This is not unexpected since IL-1ß is considered a potent activator of the NF-KB pathway. To our knowledge, the effect of S1P on IL-1ß activation in 3T3-L1 adipocytes has not previously been assessed. It is clear from Figure 3-16 that S1P has no additive effect on IL-1ß-stimulated NF-KB pathway. This finding is

consistent with our finding in Figure 3-6, where S1P alone has been shown to have no effect on this pathway, implying that the additive effect of S1P and IL-1β is most likely via an NF-KB-independent pathway. Conversely, S1P has been shown to upregulate iNOS expression in rat microglia cells (HAPI cells) stimulated with LPS which was dependent on the NF-KB pathway (Wang et al, 2021). As this contrary finding was in rat microglia cells, it is possible the effect of S1P on NF-KB is cell or tissue specific. Our finding is correlated with a study reported by Chandru and Boggaram, where they show that TNF-α causes an increase in proinflammatory IL-8 gene expression in lung epithelial cell via S1P which is independent of the NF-KB pathway (Chandru & Boggaram, 2007).

3.5 Conclusion

This study presents further evidence that the SphKs/S1P system is implicated in adipocyte function and involved in the adipocyte inflammatory response by regulating different proinflammatory signalling pathways, including PI3/Akt and MAPKs (MEK-ERK and JNK). Moreover, the data presented here demonstrate for the first time in adipocytes that IL-1β upregulates SphK1 expression. It is a reasonable assumption that the S1P produced by SphK1 enzyme could augment IL-1β-mediated iNOS expression and NO production in 3T3-L1 adipocytes. The underlying mechanisms by which S1P promotes IL-1β-mediated iNOS proinflammatory enzyme are likely via PI3K/Akt and MAPKs pathways and independent of NF-KB signalling pathway.

Chapter 4 - Investigating the involvement of SphK isoforms and S1PR subtypes in IL-1β-induced inducible nitric oxide synthase and Nitric Oxide production in 3T3-L1 adipocytes

4.1 Introduction

Two isoforms or variants of the enzyme sphingosine kinase (SphKs) have been identified (SphK1 and SphK2) that catalyse the generation of S1P from sphingosine (Cannavo et al, 2017). This can be exported from cells via transporters; ATP-binding cassette transporters (ABC) and the spinster 2 transporter (Spns2). S1P functions are largely mediated by five G protein-coupled receptors ($S1PR_1$, $S1PR_2$, $S1PR_3$, $S1PR_4$, and $S1PR_5$), which directly couple to a range of G protein subtypes (G_i, G_q, and $G_{12/13}$) (Li et al, 2016; O'Sullivan & Dev, 2013; Spiegel & Milstien, 2003). Activation of these subunits initiates a wide range of different downstream molecular signals including phosphoinositide-3 kinase (PI3K), extracellular signal-regulated kinase (ERK), c-Jun N-terminal kinase (JNK), p38 mitogen-activated kinase (MAPK) and nuclear kappa-B (NF-KB) (Kluk & Hla, 2002; Wang et al, 2023; Wollny et al, 2017). Of these receptors, $S1PR_1$, $S1PR_2$ and $S1PR_3$ were shown to be expressed and modulate a wide range of biological processes within the adipose tissue (Fang et al, 2019; Kluk & Hla, 2002).

It was demonstrated in the previous chapter that IL-1ß modulates SphKs expression in 3T3-L1 adipocytes, and I showed that exogenous S1P amplified IL-1ß-mediated iNOS expression and NO production in 3T3-L1 adipocytes. These findings are supported by data published previously on the SphKs/S1P/S1PR system, demonstrating that this signalling pathway contributes to adipose tissue dysfunction by promoting inflammation in adipose tissue (Fang et al, 2019; Wang et al, 2014). However, these data do not fully address the specific role of SphK isoforms (SphK1 and SphK2) and specific receptors ($S1PR_1$, $S1PR_2$, and $S1PR_3$) in iNOS proinflammatory enzyme regulation in 3T3-L1 adipocytes.

Overall, published data indicates that the SphKs/S1P/S1PRs pathway is implicated in many inflammatory processes within the adipose tissue. Indeed, it has been reported that genetic deletion and pharmacological inhibition of SphK1 in mice fed with HFD caused a decrease in many proinflammatory mediators, such as monocyte chemotactic protein-1 (MCP-1), TNF-α, and IL-6 (Wang et al, 2014). Similarly, pharmacological inhibition of SphK1 and SphK2 in Zucker diabetic fatty rats reduced LPS-stimulated chemokine (C-C motif) ligand 5 (CCL5), IL-6, and TNF-α in subcutaneous adipose tissue. In the same study, it was also shown that

cytokine production was diminished in 3T3-L1 adipocytes lacking SphK1 (Tous et al, 2014). Research over the past several decades has revealed that S1P is implicated in development of adipose tissue inflammation; however, limited data exist regarding which S1P receptor(s) is key in mediating adipose tissue inflammation. For instance, S1P has been shown to promote TNF-α and IL-6 in 3T3-L1 adipocytes (Samad et al, 2006). Knockdown and pharmacological inhibition of $S1PR_2$ has been shown to diminish HFD-induced inflammation in mice (Kitada et al, 2016). Consistent with this, another study carried out by the same group has shown that blocking $S1PR_2$ with JTE 013 decreased TNF-α in the adipose tissue of obese mice. In the same study, $S1PR_1$ activation has been shown to inhibit inflammation; suppressing TNF-α and M1 polarization in the adipose tissue of obese mice (Asano et al, 2023). Moreover, S1P has been shown to activate plasminogen activator inhibitor-1 (PAI-1) release from adipocytes, which is mediated by $S1PR_2$ (Lee et al, 2010). PAI-1 is an adipokine and is linked to adipose tissue inflammation (Ikeda et al, 2014). Furthermore, there is evidence that ABCA1 transporter is expressed in adipocytes, and it has been proven that ABCA1 inhibition with glibenclamide decreased S1P release from adipocytes under hypoxic conditions, confirming ABC transporter as an S1P transporter in adipocytes. These findings, along with many others, confirm the importance of investigating the role of SphK isoforms and the $S1PR_{1-3}$ axis in iNOS proinflammatory enzyme regulation in adipocytes.

The recruitment of macrophages is a crucial aspect of the inflammatory response associated with obesity. In obesity, adipocyte hypertrophy leads to the release of many proinflammatory mediators that attract immune cells, including macrophages. Once macrophages are recruited, they can polarize from M2 (alternatively activated) into M1 (classically activated). M1 macrophages are the predominant producer of proinflammatory mediators in adipose tissue. The complex inflammatory profile of inflamed adipose tissue arises from the secretion of a range of proinflammatory cytokines (IL-1β, IL-6, and TNF-α) produced by macrophages and adipocytes. Subsequently, low-grade inflammation is induced within the adipose tissue and when this persists it can lead to many metabolic disorders (Schaffler et al, 2006; Zeyda & Stulnig, 2007). An obesity-induced chronic, low-grade proinflammatory environment within the adipose tissue has been reported to have an effect on proinflammatory iNOS enzyme regulation in

adipose tissue (Dallaire et al, 2008). Moreover, it was found that SphK1 expression is increased in adipose tissue macrophages (Gabriel et al, 2017). Treatment of RAW 264.7 cells with LPS results in an increase in SphK1 activity and enhances S1P production (Hammad et al, 2008; Wu et al, 2004). It is proven that a paracrine interaction between macrophages and adipocytes mediates the inflammatory status in adipose tissue (Cai et al, 2022); therefore, it is important to elucidate the role of the sphingolipid system in mediating this paracrine signalling, especially in term of iNOS proinflammatory enzyme regulation in adipocytes.

While so far in this thesis, the data confirm that IL-1β modulates SphK expression and that applying exogenous S1P contributes to iNOS regulation in adipocytes, it is of importance to have a full understanding of IL-1β-mediated iNOS regulation via the sphingolipid system in adipocytes.

4.2 Aims

1. To determine the potential involvement of both isoforms of SphK, as well as the S1PRs, in regulation of iNOS expression and NO production in IL-1β-stimulated adipocytes.
2. To determine the effect of $S1PR_2$ inhibition on IL-1β-stimulated proinflammatory pathways in adipocytes and confirm the role of this pathway in iNOS regulation in adipocytes.
3. To investigate the role of the sphingolipid system in paracrine signals between adipocytes and macrophages, particularly in iNOS regulation.

4.3 Results

4.3.1 Inhibition of Sphk1 by PF543 reduces iNOS expression and NO Production in IL-1β-stimulated 3T3-L1 adipocytes

As I have shown that IL-1ß upregulates SphK1 expression and exogenous S1P augmented iNOS expression and NO production in stimulated adipocytes, I now investigated whether SphK1 enzyme inhibition would affect iNOS expression and NO production in stimulated adipocytes. 3T3-L1 adipocytes were preincubated with PF543 (100 nM) for 45 min prior to being stimulated with IL-1ß (10 ng/ml) for 24 hours. After treatment, lysate was prepared, and iNOS expression was assessed by western blotting while NO production was determined by the presence of nitrite/nitrate in the medium. RNA was isolated and quantified by qPCR.

Stimulation of 3T3-L1 adipocytes with IL-1ß in the absence of PF543 caused a significant (****$p<0.0001$) increase in iNOS expression and NO production. In the presence of PF543, iNOS expression and NO production were decreased significantly (*$p<0.05$, **$p<0.01$, respectively) compared to cells treated with IL-1ß alone. However, PF543 alone, in the absence of IL-1ß, had no effect on iNOS expression and NO production by adipocytes (Figure 4-1 B and C).

Moreover, stimulation of 3T3-L1 adipocytes with IL-1ß caused a significant (****$p<0.0001$) increase in iNOS mRNA expression. In the presence of PF543, there was a tendency towards a decrease in iNOS mRNA expression (Figure 4-1D) in IL-1ß stimulated 3T3-L1 adipocytes, compared to the cells treated with IL-1ß alone, although this did not reach statistical significance ($p =0.06$).

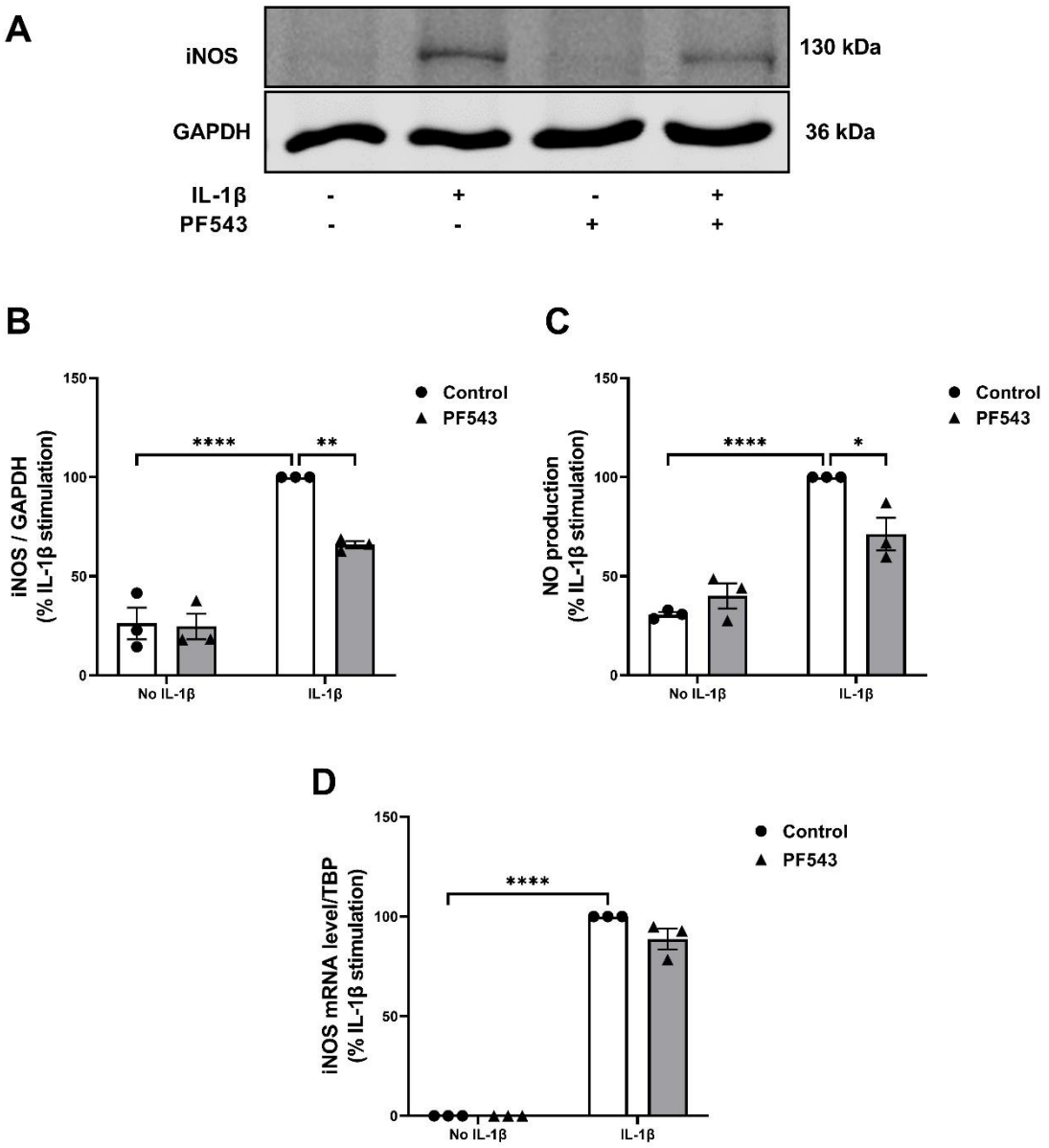

Figure 4-1 Effect of SphK1 inhibition on iNOS protein expression and NO production in stimulated in 3T3-L1 adipocytes.

3T3-L1 adipocytes were pretreated with SphK1 inhibitor PF543 (100 nM) for 45 min and then stimulated with IL-1β (10 ng/ml) for 24 hours. Cell lysates were prepared and resolved by SDS-PAGE with the appropriate antibodies. Media was collected and NO production was investigated by using a Sievers 280A NO Meter. RNA was isolated and quantified by qPCR. (A) representative western blotting images and (B) graph for the change in iNOS protein expression. Protein level of iNOS was normalised to level of GAPDH protein. (C) IL-1β-stimulated NO production in 3T3-L1 adipocytes. (D) qPCR analysis showing the changes in iNOS mRNA relative to levels of TATA binding protein (TBP) mRNA. The data represent samples from three different experiments expressed as the mean ± SEM of the % relative to IL-1β stimulation. Statistical analysis was carried out using two-way ANOVA (with Tukey's test). Asterisks indicate a p value of (*p<0 .05, **p<0.01, ****p<0.0001).

4.3.2 Inhibition of Sphk2 by ROME does not alter iNOS expression and NO production in IL-1β-stimulated 3T3-L1 adipocytes

Because SphK1 was required for iNOS expression and NO production in stimulated adipocytes (Figure 4-1), I next investigated whether SphK2 is also required. 3T3-L1 adipocytes were preincubated with ROME (10 μM) for 45 min prior to being stimulated with IL-1β (10 ng/ml) for 24 hours. After treatment, lysate was prepared, and iNOS expression was assessed by western blotting while NO production was determined by the presence of nitrite/nitrate in the medium. RNA was isolated and quantified by qPCR.

Stimulation of 3T3-L1 adipocytes with IL-1β in the absence of ROME caused a significant (**$p<0.01$) increase in iNOS expression and NO production. The IL-1β-stimulated increase in iNOS expression and NO production were not affected by the inhibition of SphK2 with ROME, although a high level of variation in iNOS expression was seen (Figure 4-2). Similarly, ROME alone had no effect on iNOS expression and NO production in stimulated adipocytes (Figure 4-2 B and C). Moreover, stimulation of 3T3-L1 adipocytes with IL-1β in the absence of ROME caused a significant (****$p<0.0001$) increase in iNOS mRNA expression but the presence of ROME did not alter the iNOS mRNA level (Figure 4-2D).

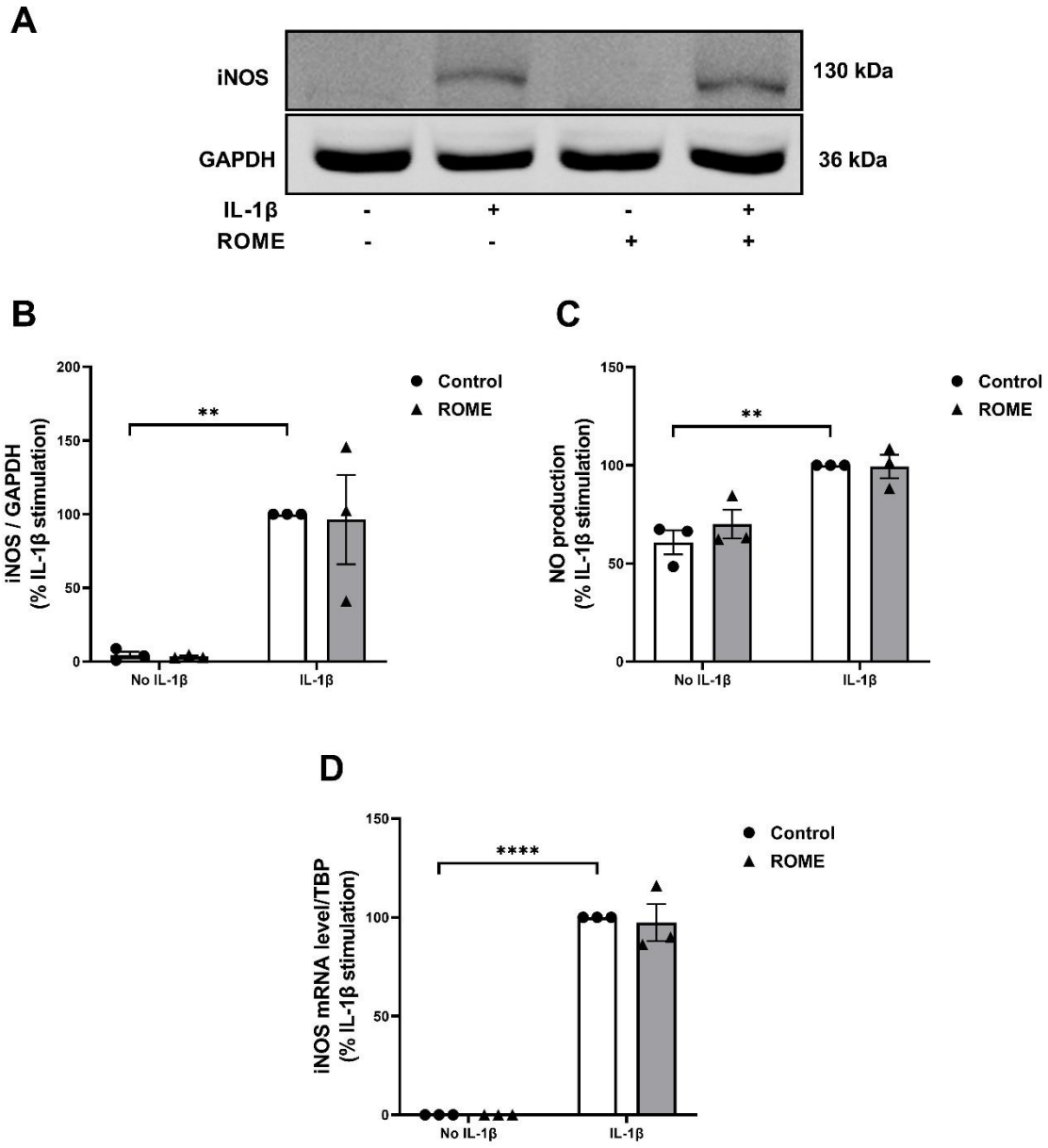

Figure 4-2 Effect of SphK2 inhibition on iNOS expression and NO production in stimulated 3T3-L1 adipocytes.

3T3-L1 adipocytes were pretreated with SphK2 inhibitor ROME (10 μM) for 45 min and were then stimulated with IL-1β (10 ng/ml) for 24 hours. Cell lysates were prepared and resolved by SDS-PAGE with the appropriate antibodies. Media was collected and NO production was investigated by using a Sievers 280A NO Meter. RNA was isolated and quantified by qPCR. (A) representative western blotting images and (B) graph for the change in iNOS protein expression. Protein level of iNOS was normalised to level of GAPDH protein. (C) IL-1β stimulated NO production in 3T3-L1 adipocytes. (D) qPCR analysis shows the changes in iNOS mRNA relative to levels of TATA binding protein (TBP) mRNA. The data represent samples from three different experiments expressed as the mean ± SEM of the % relative to IL-1β stimulation. Statistical analysis was carried out using two-way ANOVA (with Tukey's test). Asterisks indicate a p value of (p<0.01, ****p<0.0001).**

4.3.3 S1PR1-3 receptors are involved in iNOS expression in stimulated 3T3-L1 adipocytes

Upon confirmation that IL-1ß upregulates the protein and mRNA expression of SphK1 and that SphK1/S1P contributes to IL-ß-induced iNOS and NO production in adipocytes, I next examined the role of S1PRs in this process. 3T3-L1 adipocytes were pretreated with either the $S1PR_1$ antagonist W146 (10 µM), $S1PR_2$ antagonist JTE 013 (10 µM) or the $S1PR_3$ antagonist CAY10444 (10 µM) for 45 min. The cells were then stimulated with IL-1ß (10 ng/ml) for 24 hours. These concentrations of antagonists were chosen based on previous work (Kitada et al, 2016; Moon et al, 2015). After treatment, lysate was prepared, and iNOS expression was assessed by western blotting while NO production was determined by the presence of nitrite/nitrate in the medium. RNA was isolated and quantified by qPCR.

As shown in Figure 4-3B the protein expression of iNOS was significantly (*p<0 .05, ***p<0.001) suppressed by the pre-treatment with all three S1PR inhibitors in stimulated adipocytes compared to IL-1ß alone. Similarly, pre-treatment with S1PR inhibitors had a tendency to decrease iNOS mRNA level although it did not reach statistical significance due to the high degree of variability (Figure 4-3C).

However, the level of NO production, the product of iNOS, was significantly (****p<0.0001) reduced, but only by pre-treatment with the $S1PR_2$ inhibitor (JTE 013), suggesting a specific role for $S1PR_2$ (Figure 4-4).

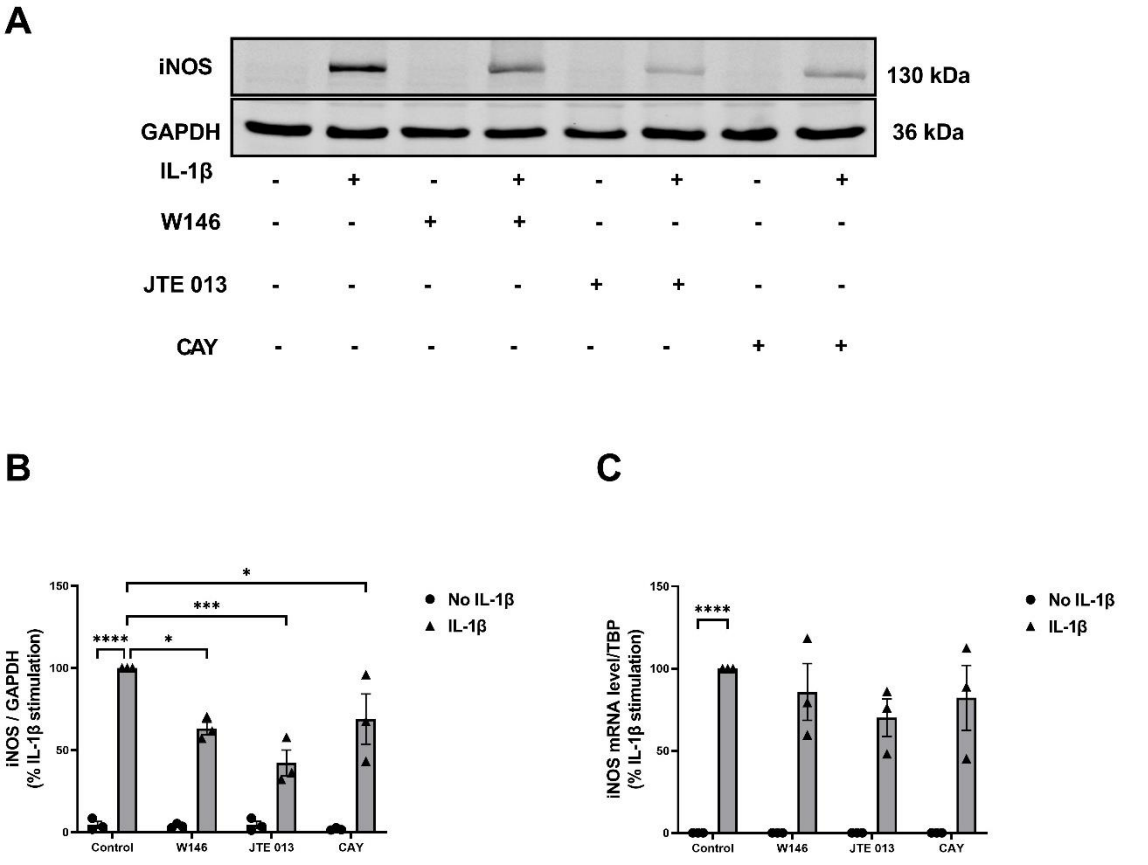

Figure 4-3 Effect of $S1PR_{1-3}$ antagonists on iNOS protein and mRNA expression in stimulated 3T3-L1 adipocytes.

3T3-L1 adipocytes were pretreated with the $S1PR_1$ antagonist W146 (10 μM), $S1PR_2$ antagonist JTE 013 (10 μM) or the $S1PR_3$ antagonist CAY10444 (10 μM) for 45 min then were stimulated with IL-1β (10 ng/ml) for 24 hours. Cell lysates were prepared and resolved by SDS-PAGE with the appropriate antibodies. RNA was isolated and quantified by qPCR. (A) representative western blotting images and (B) graph for the change in iNOS protein expression. Protein level of iNOS was normalised to the level of GAPDH protein. (C) qPCR analysis shows the changes in iNOS mRNA relative to levels of TATA binding protein (TBP) mRNA. The data represent samples from three different experiments expressed as the mean ± SEM of the % relative to IL-1β stimulation. Statistical analysis was carried out using two-way ANOVA (with Tukey's test). Asterisks indicate a p value of (*p<0.05, ***p<0.001, ****p<0.0001).

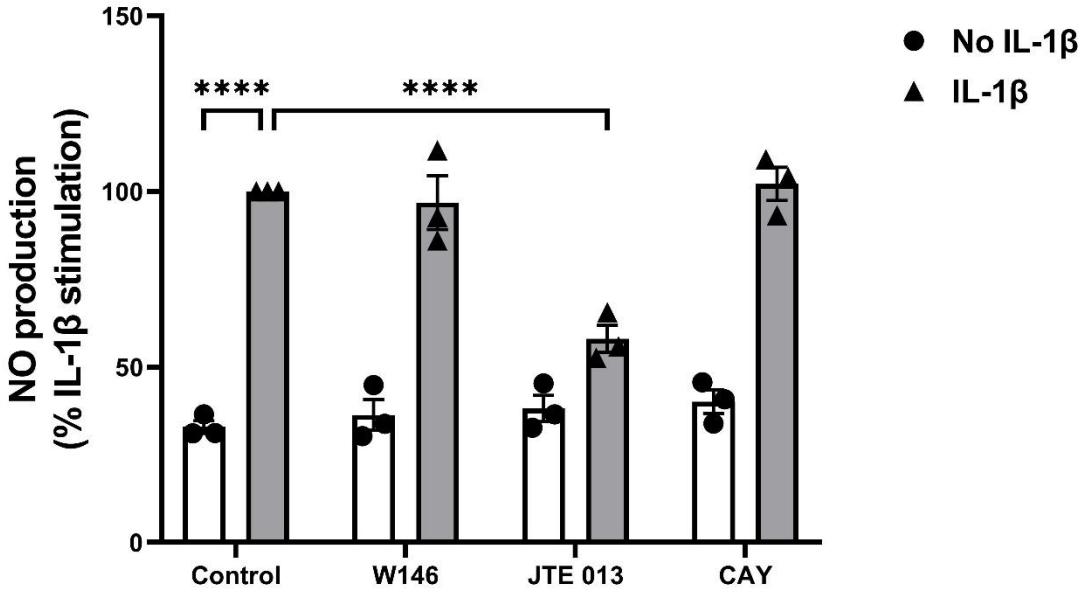

Figure 4-4 Effect of $S1PR_{1-3}$ antagonists on NO production in stimulated 3T3-L1 adipocytes.

3T3-L1 adipocytes were pretreated with the $S1PR_1$ antagonist W146 (10 μM), $S1PR_2$ antagonist JTE 013 (10 μM) or the $S1PR_3$ antagonist CAY10444 (10 μM) for 45 min then were stimulated with IL-1β (10 ng/ml) for 24 hours. Media was collected and NO production was investigated by using a Sievers 280A NO Meter. IL-1β stimulated NO production in 3T3-L1 adipocytes. The data represent samples from three different experiments expressed as the mean ± SEM of the % relative to IL-1β stimulation. Statistical analysis was carried out using two-way ANOVA (with Tukey's test). Asterisks indicate a p value of (**p<0.0001).**

4.3.4 $S1PR_2$ agonist CYM 5478 induces iNOS protein expression and NO production in stimulated 3T3-L1 adipocytes

As I have shown that $S1PR_2$ inhibition suppress iNOS protein expression and NO production in stimulated adipocytes, I now investigated whether $S1PR_2$ activation, would increase iNOS expression and NO production in stimulated adipocytes. 3T3-L1 adipocytes were stimulated with IL-1β (10 ng/ml) in the presence and absence of the $S1PR_2$ agonist CYM 5478 (10 μM) for 24 hours. After treatment, lysate was prepared, and iNOS expression was assessed by western blotting while NO production was determined by the presence of nitrite/nitrate in the medium.

As shown in Figure 4-5 B and C, upon addition of CYM 5478 to IL-1β stimulated adipocytes, the protein expression of iNOS was upregulated compared to cells treated with IL-1β alone, however this did not reach significance ($p=0.07$) due to a high degree of variability. Similarly, the level of NO production, the product of iNOS, was significantly ($*p<0.05$) increased by co-treatment with CYM 5478 compared with cells treated with IL-1β alone. However, adipocytes treated with CYM 5478 alone did not show increased iNOS expression or NO production.

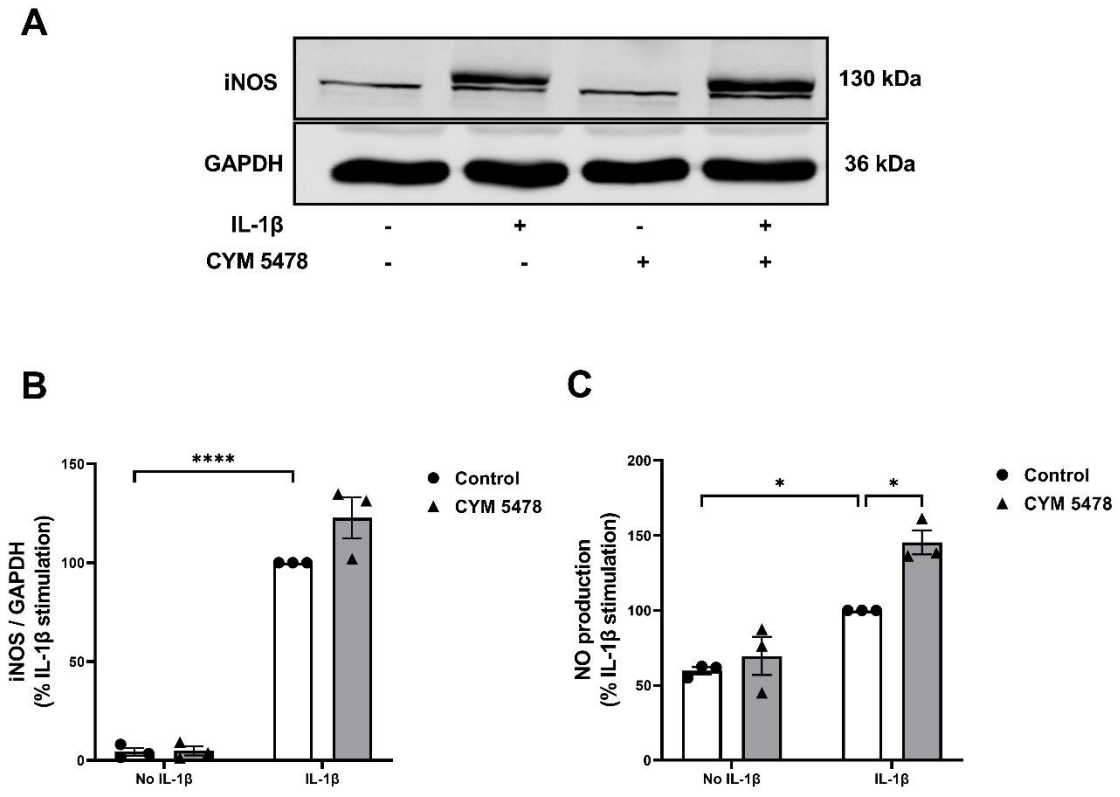

Figure 4-5 Effect of $S1PR_2$ agonist (CYM 5478) on iNOS protein expression and NO production in stimulated 3T3-L1 adipocytes.

3T3-L1 adipocytes were stimulated with IL-1β (10 ng/ml) in the presence or absence of CYM 5478 (10 μM) for 24 hours. Cell lysates were prepared and resolved by SDS-PAGE with the appropriate antibodies. Media was collected and NO production was investigated by using a Sievers 280A NO Meter. (A) representative western blotting images and (B) graph for the change in iNOS protein expression. Protein level of iNOS was normalised to level of GAPDH protein. (C) IL-1β stimulated NO production in 3T3-L1 adipocytes was increased by co-incubation with the $S1PR_2$ agonist. The data represent samples from three different experiments expressed as the mean ± SEM of the % relative to IL-1β stimulation. Statistical analysis was carried out using two-way ANOVA (with Tukey's test). Asterisks indicate a p value of (*p<0.05, ****p<0.0001).

4.3.5 Effect of $S1PR_2$ antagonism (JTE 013) on IL-1β stimulated proinflammatory signalling

4.3.5.1 $S1PR_2$ antagonist (JTE 013) significantly inhibits IL-1β-stimulated Akt phosphorylation in 3T3-L1 adipocytes

IL-1ß has been shown to activate the PI3K/Akt signalling cascade and has been implicated in iNOS regulation in multiple cell types. Also, $S1PR_2$ has been shown to upregulate the PI3K/Akt pathway in many cell types (Skoura & Hla, 2009). Therefore, I speculated that $S1PR_2$ inhibition by JTE 013 (10 μM) might inhibit IL-1ß-mediated Akt phosphorylation, resulting in an iNOS downregulation. This concentration was chosen based on previous work showing the role of JTE 013 on adipocyte differentiation in 3T3-L1 adipocytes (Kitada et al, 2016). To determine whether JTE 013 influences this inflammatory cascade, stimulated 3T3-L1 adipocytes were preincubated with and without JTE 013 (10 μM) for 24 h. 3T3-L1 adipocytes were then incubated with IL-1ß for 15 min and 30 min. The extent of Akt phosphorylation was assessed as a measure of PI3K/Akt signalling cascade stimulation by western blotting.

Stimulation of 3T3-L1 adipocytes with IL-1ß in the absence of JTE 013 caused a significant (*$p< 0.05$ and **$p<0.01$, respectively) increase in Akt phosphorylation at 15 min and 30 min compared to basal level (no addition of IL-1ß). In the presence of JTE 013, there was a significant (*$p<0.05$ and ***$p<0.001$ respectively) decrease in IL-1ß-stimulated Akt phosphorylation at both 15 min and 30 min compared to IL-1ß treatment alone (Figure 4-6).

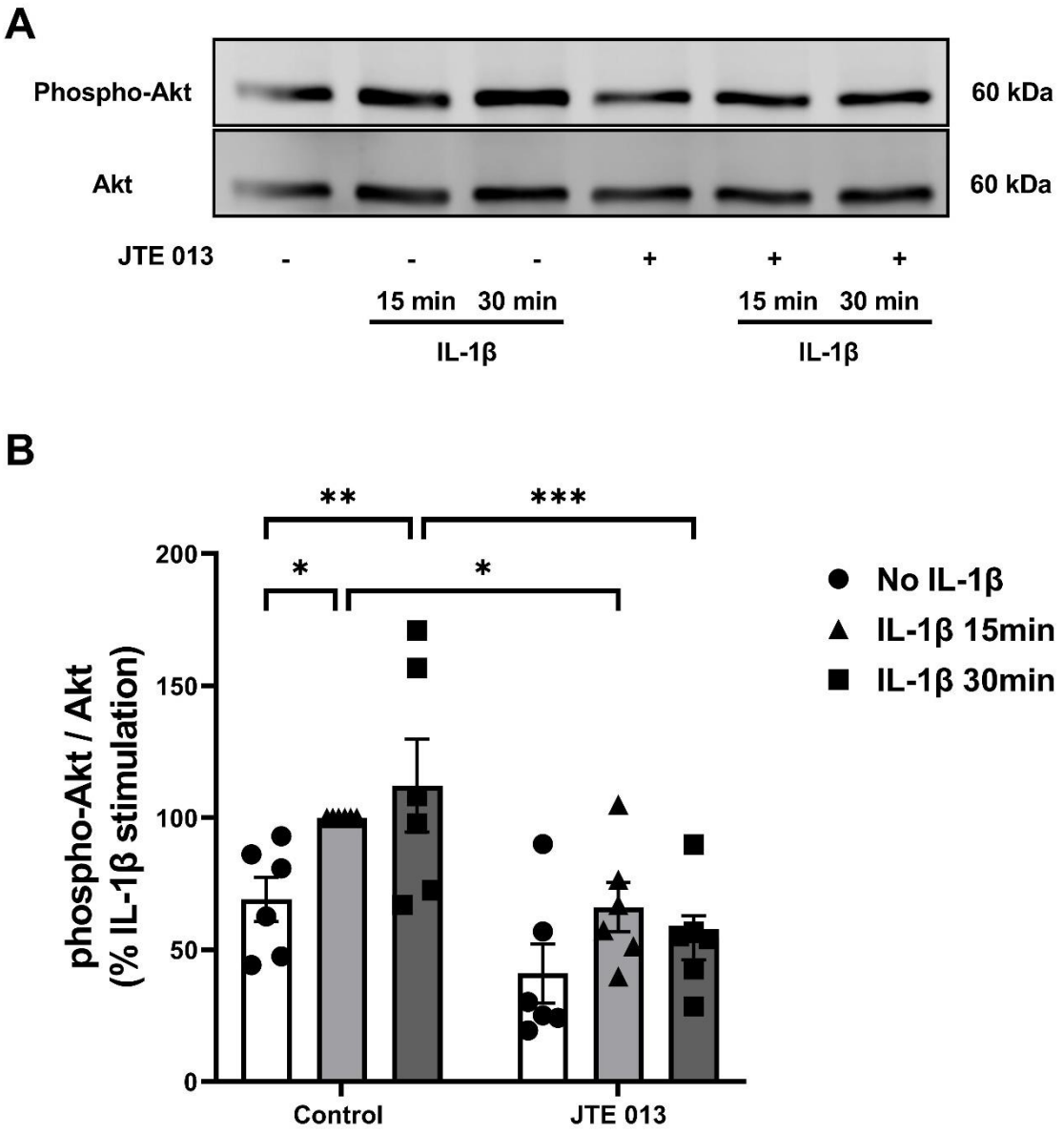

Figure 4-6 The effect of JTE 013 on IL-1β-stimulated Akt phosphorylation 3T3-L1 adipocytes.

3T3-L1 adipocytes were stimulated with IL-1β (10 ng/ml) for either 15 and 30 min following preincubation for 24 hours in the presence or absence of the $S1PR_2$ inhibitor JTE 013 (10 μM). Cell lysates were prepared and resolved by SDS-PAGE with the appropriate antibodies. (A) representative western blotting image and (B) graph of p-Akt protein expression showing the changes in Akt phosphorylation at 15 min and 30 min. Protein level of p-Akt was normalised to total level of Akt. The data represent samples from six different experiments expressed as the mean ± SEM or the % relative to IL-1β-stimulated phosphorylation. Statistical analysis was carried out using one-way ANOVA (with Fisher LSD test). Asterisks indicate a p value of (*p<0 .05, **p<0.01, ***p<0.001).

4.3.5.2 $S1PR_2$ antagonist (JTE 013) significantly inhibited IL-1β-stimulated MAPKs pathways phosphorylation 3T3-L1 adipocytes

A second pathway that has been linked to iNOS regulation by IL-1ß is MAPKs family pathway. Moreover, $S1PR_2$ has been shown to promote many inflammatory processes via MAPKs pathways (Blankenbach et al, 2016; Hou et al, 2021). Therefore, it was of interest to determine whether $S1PR_2$ inhibition influences IL-1ß-stimulated MAPKs pathway in 3T3-L1 adipocytes. 3T3-L1 adipocytes were incubated with IL-1ß for 15 min and 30 min following 24 h preincubation with JTE 013 (10 μM). The phosphorylation of MEK 1/2, ERK 1/2, P38, and JNK were assessed as a measure of stimulation by western blotting.

Stimulation of 3T3-L1 adipocytes with IL-1ß in the absence of JTE 013 caused an increase in p-MEK 1/2 which was significant (**$p<0.01$) at 15 and 30 min compared to basal level (no addition of IL-1ß). In the presence of JTE 013, MEK 1/2 phosphorylation decreased significantly (**$p<0.01$) at both 15 min and 30 min, compared to IL-1ß treatment alone (Figure 4-7B). Furthermore, a significant increase in ERK 1/2 phosphorylation was observed at 15 min and 30 min compared to basal level (no addition of IL-1ß) in 3T3-L1 adipocytes stimulated with IL-1ß in the absence of JTE 013. In the presence of JTE 013, there was a significant (*$p<0.05$) suppression in ERK 1/2 phosphorylation at both 15 min and 30 min compared to IL-1ß treatment alone (Figure 4-7C).

Stimulation of 3T3-L1 adipocytes with IL-1ß in the absence of JTE 013 caused a significant (****$p<0.0001$ and ****$p<0.0001$, respectively) increase in P38 phosphorylation at 15 min and 30 min, compared to basal level. In the presence of JTE 013, P38 phosphorylation decreased significantly (*$p<0.05$ and **$p<0.01$, respectively) at both 15 min and 30 min, compared to IL-1ß treatment alone (Figure 4-8B).

Stimulation of 3T3-L1 adipocytes with IL-1ß in the absence of JTE 013 caused a significant increase in JNK phosphorylation at 15 min and 30 min (****$p<0.0001$), compared to basal level. In the presence of JTE 013, a significant (*$p<0.05$) inhibition in JNK phosphorylation was observed at 15 min and 30 min, compared to IL-1ß treatment alone (Figure 4-8C).

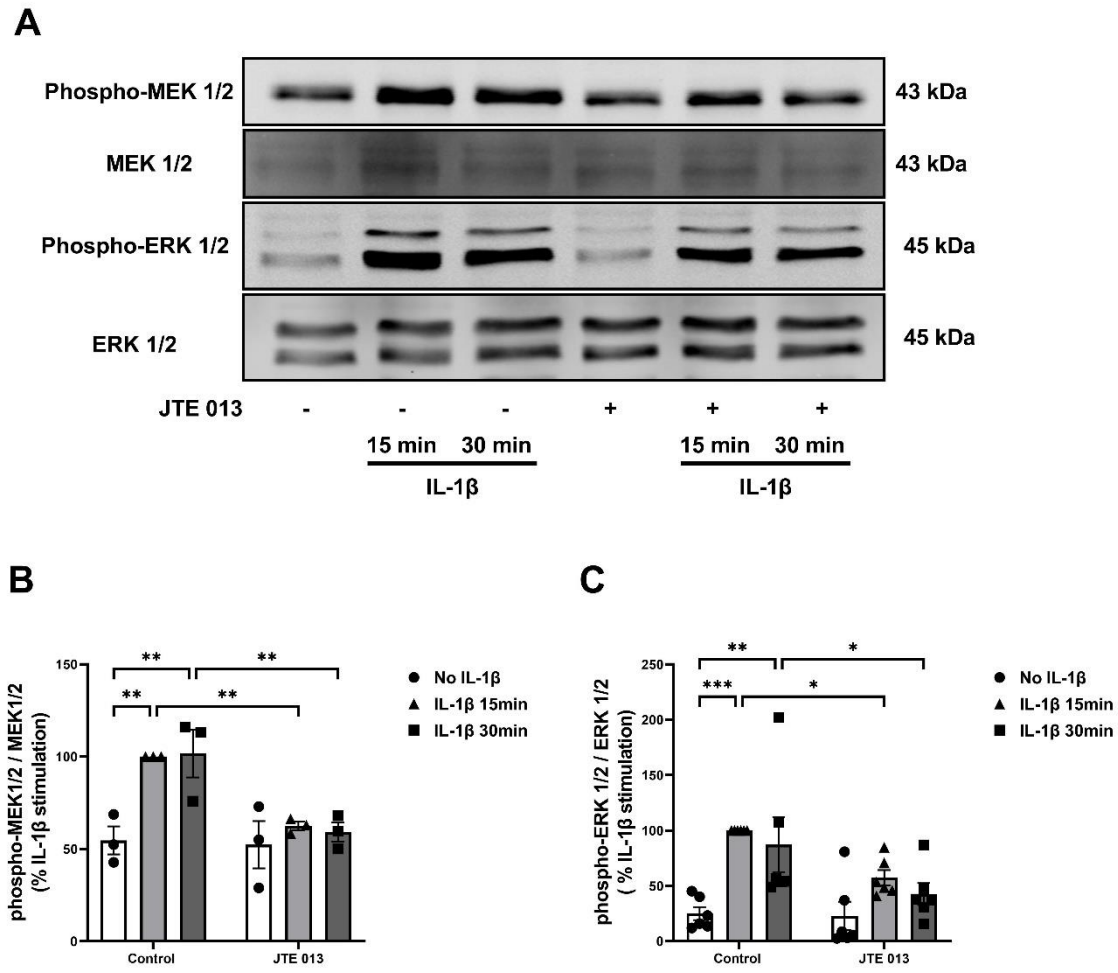

Figure 4-7 Effect of JTE 013 on IL-1β-stimulated MEK-ERK cascades in 3T3-L1 adipocytes.

3T3-L1 adipocytes were stimulated with IL-1β (10 ng/ml) for 15 and 30 min following preincubation for 24 hours in the presence or absence of $S1PR_2$ inhibitor JTE 013 (10 μM). Cell lysates were prepared and resolved by SDS-PAGE with the appropriate antibodies. (A) representative western blotting image of p-MEK 1/2 and p-ERK 1/2 protein expression showing the changes in the phosphorylation at 15 min and 30 min. Phosphorylation of (B) MEK 1/2 and (C) ERK 1/2 were normalised to total level of MEK 1/2 and ERK 1/2 respectively. The data represent samples from at least three different experiments expressed as the mean ± SEM of the % relative to IL-1β-stimulated phosphorylation. Statistical analysis was carried out using two-way ANOVA (with Fisher LSD test). Asterisks indicate a p value of (*p<0.05, **p<0.01, ***p<0.001).

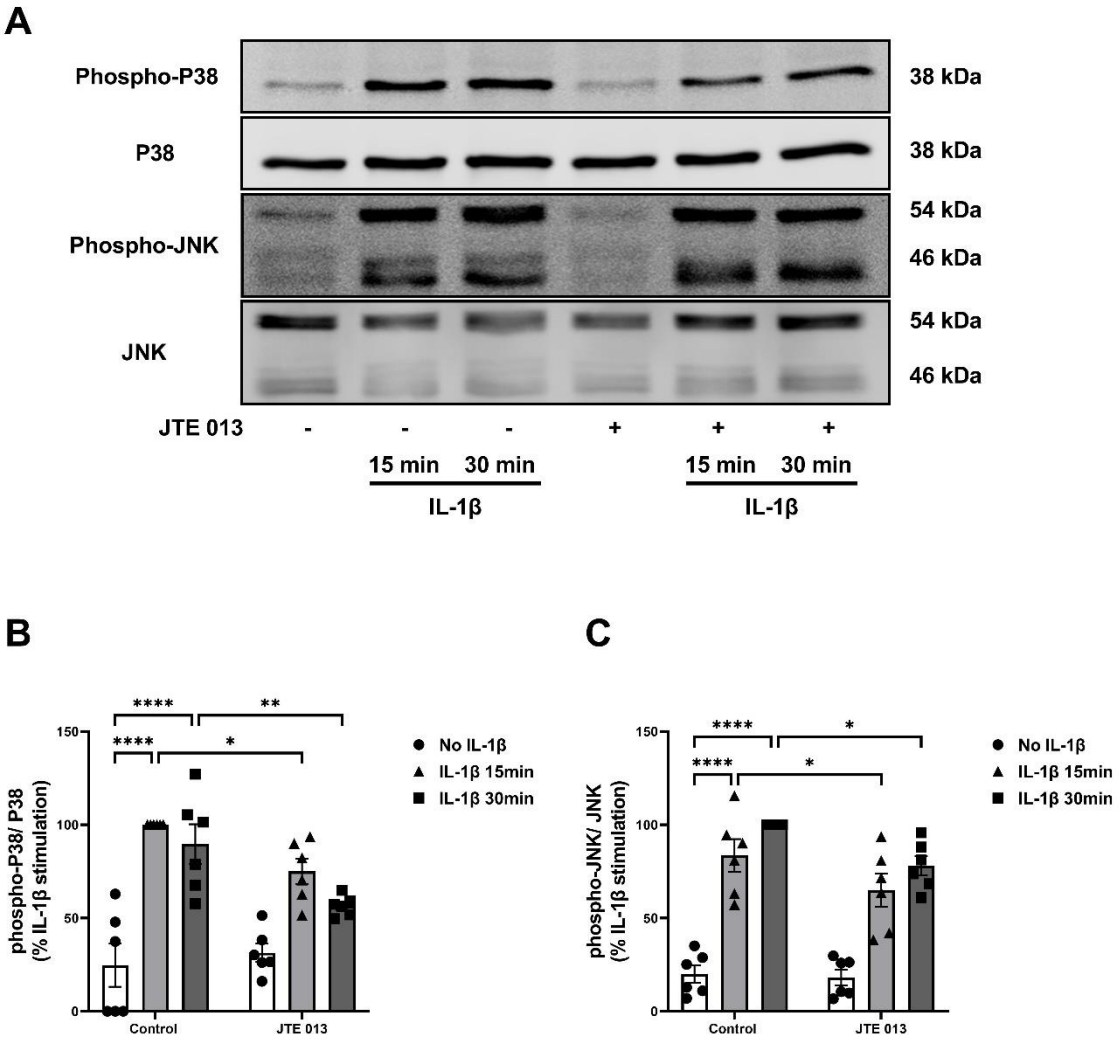

Figure 4-8 Effect of JTE 013 on IL-1β-stimulated P38 and JNK pathways in 3T3-L1 adipocytes.

3T3-L1 adipocytes were stimulated with IL-1β (10 ng/ml) for 15 and 30 min following preincubation for 24 hours in the presence or absence of $S1PR_2$ inhibitor JTE 013 (10 μM). Cell lysates were prepared and resolved by SDS-PAGE with the appropriate antibodies. (A) representative western blotting image of p-P38 and p-JNK protein expression showing the changes in the phosphorylation at 15 min and 30 min. Phosphorylation of (B) P38 and (C) JNK were normalised to total level of P38 or JNK respectively. The data represent samples from at least six different experiments expressed as the mean ± SEM of the % relative to IL-1β-stimulated phosphorylation. Statistical analysis was carried out using two-way ANOVA (with Fisher LSD test). Asterisks indicate a p value of (*p<0.05, **p<0.01, ****p<0.0001).

4.3.5.3 $S1PR_2$ antagonist (JTE 013) does not have any effect on IL-1β-stimulated IκβαIκβα and NF-KB phosphorylation

Another pathway that has been potentially linked to iNOS regulation by IL-1ß is the NF-KB pathway. Also, $S1PR_2$ has been shown to promote inflammation in many cell types via the NF-KB pathway (Yang et al, 2022). Therefore, it was of interest to determine whether $S1PR_2$ inhibition influences the IL-1ß-stimulated NF-KB pathway in 3T3-L1 adipocytes. 3T3-L1 adipocytes were incubated with IL-1ß for 15 min and 30 min following 24 h preincubation with JTE 013 (10 μM). The phosphorylation of NF-KB, IKBα and IKBα protein degradation were assessed as a measure of stimulation by western blotting.

Stimulation of 3T3-L1 adipocytes with IL-1ß in the absence of JTE 013 caused a significant increase in p-NF-KB at 15 min (****$p<0.0001$) and 30 min (****$p<0.0001$), compared to basal level (no addition of IL-1ß). However, in the presence of JTE 013, NF-KB phosphorylation was not significantly different compared to that seen with IL-1ß treatment alone (Figure 4-9B). Similarly, IKßα phosphorylation increased significantly in 3T3-L1 adipocytes stimulated with IL-1ß at 15 min and 30 min (****$p<0.0001$ and *$p<0.05$, respectively) in the absence of JTE 013. However, IKßα phosphorylation was similar in the presence of JTE 013, compared to IL-1ß treatment alone (Figure 4-9C).

IKßα protein expression was observed to decline significantly (***$p<0.001$ and ****$p<0.0001$, respectively) at 15 min and 30 min following IL-1ß stimulation, compared to basal level (no addition of IL-1ß). However, JTE 013 addition had no impact on IKßα protein level (Figure 4-9D).

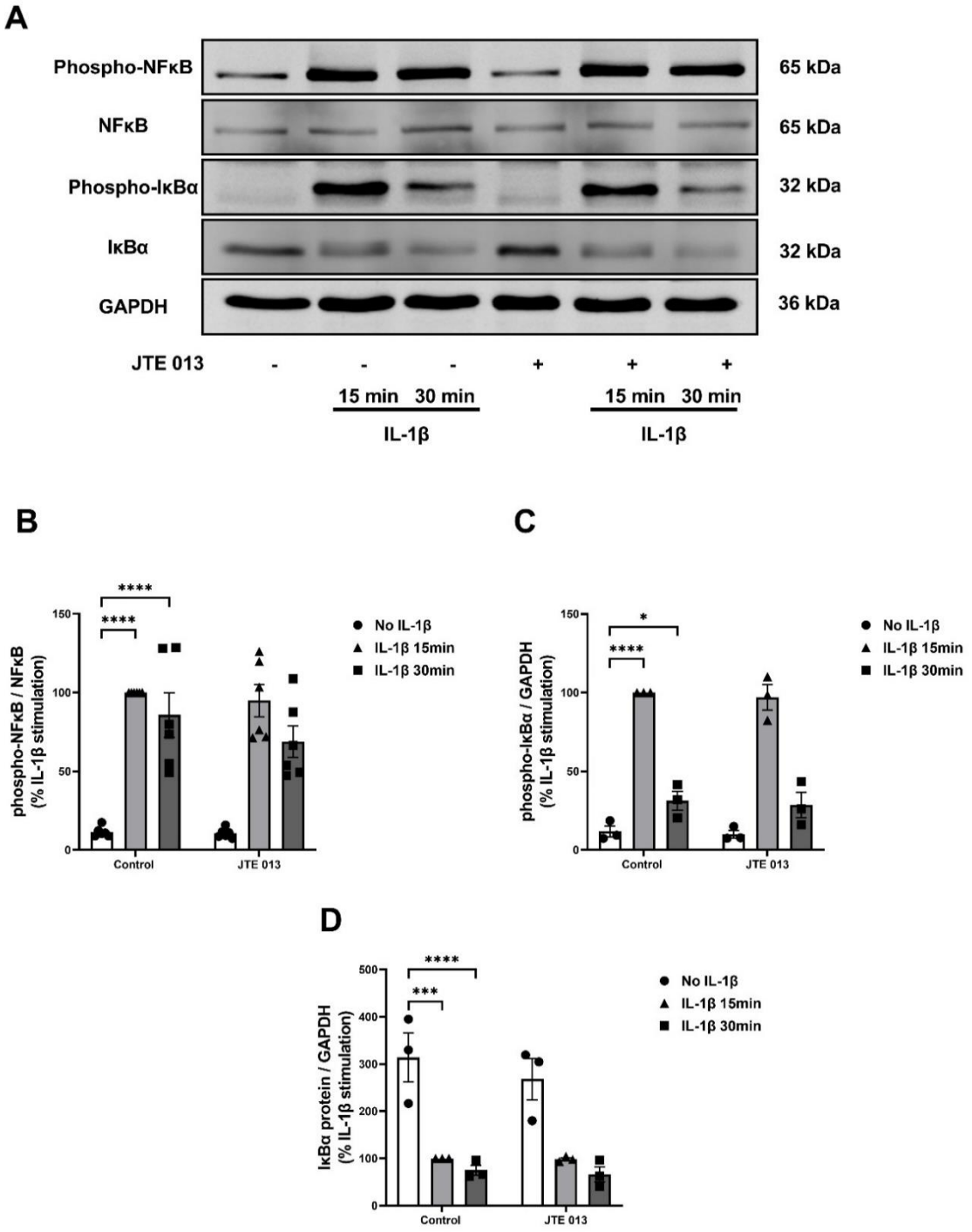

Figure 4-9 Effect of JTE 013 on IL-1β-stimulated NF-KB signalling pathways in 3T3-L1 adipocytes.

3T3-L1 adipocytes were stimulated with IL-1β (10 ng/ml) for 15 or 30 min following preincubation for 24 hours in the presence or absence of the $S1PR_2$ inhibitor JTE 013 (10 μM). Cell lysates were prepared and resolved by SDS-PAGE with the appropriate antibodies. (A) representative western blotting image of p-NF-KB, p-IKBα and IKBα protein expression showing the changes in the phosphorylation at 15 min and 30 min. Phosphorylation of (B) NF-KB, (C) IKBα and (D) IKBα protein were normalised to total level of NF-KB, IKBα, or GAPDH respectively. The data represent samples from three different experiments expressed as the mean ± SEM of the % relative to IL-1β-stimulated phosphorylation. Statistical analysis was carried out using Two-way ANOVA (with Fisher LSD test). Asterisks indicate a p value of (*p<0.05, ****p<0.0001).

4.3.6 Effect of MAPK inhibitors and a P13K/Akt inhibitor on IL-1β-stimulated iNOS expression and NO production in 3T3-L1 adipocytes

Previous studies have reported that MAPKs pathway and P13K/Akt are implicated in regulation of many proinflammatory mediators. Also, in this study, these pathways have been seen to be regulated by S1P/$S1PR_2$ in IL-1ß stimulated adipocytes. Given that, the S1P/$S1PR_2$ pathway could participate in IL-1ß-mediated iNOS regulation via MAPKs and P13K/Akt pathways. Therefore, specific MAPK inhibitors and a P13K/Akt inhibitor were used to confirm whether the anti-inflammatory effect of JTE 013 (an $S1PR_2$ inhibitor) on IL-1ß-mediated iNOS upregulation is mediated via MAPKs and P13K/Akt pathways in adipocytes. 3T3-L1 adipocytes were preincubated with PD98059 (MEK-ERK pathway inhibitor-50 µM), SP600125 (JNK pathway inhibitor-25 µM), SB202190 (P38 pathway inhibitor-25 µM) or LY294002 (P13K/Akt inhibitor-20 µM) for 45 min prior to being stimulated with IL-1ß (10 ng/ml) for 24 hours. After treatment, lysate was prepared, and iNOS expression was assessed by western blotting while NO production was determined by the presence of nitrite/nitrate in the medium.

As shown in Figure 4-10, stimulation of 3T3-L1 adipocytes with IL-1ß in the absence of MAPKs and PI3K/Akt inhibitors caused a significant (****$p<0.0001$) increase in iNOS expression and NO production. PD98059 (ERK 1/2 inhibitor), SP600125 (JNK inhibitor), and LY294002 (PI3K/Akt inhibitor) significantly suppressed iNOS expression and NO production in IL-1ß stimulated adipocytes. However, IL-1ß-induced iNOS expression and NO production was significantly (****$p<0.0001$) augmented by SB202190 (P38 inhibitor) pretreatment.

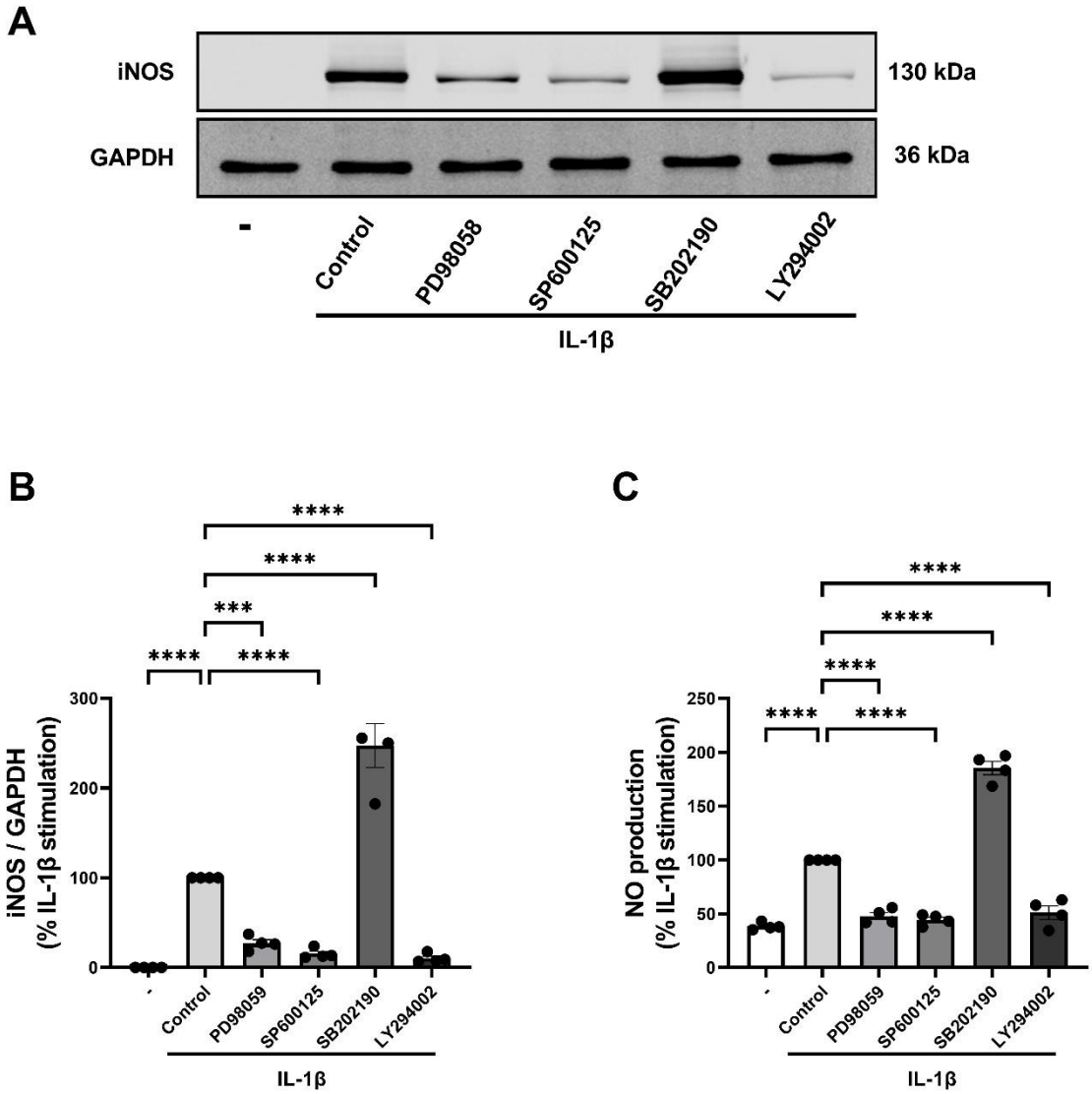

Figure 4-10 Effect of MAPKs inhibitors and a P13K/Akt inhibitor on IL-1β-stimulated iNOS expression and NO production in 3T3-L1 adipocytes.

3T3-L1 adipocytes were pretreated for 45 min with 50 μM PD98059 (ERK 1/2 inhibitor), 25 μM SP600125 (JNK inhibitor), 25 μM SB202190 (P38 inhibitor) or 20 μM LY294002 (PI3K/Akt inhibitor) and were then stimulated with IL-1β (10 ng/ml) for 24 hours. Cell lysates were prepared and resolved by SDS-PAGE with the appropriate antibodies. Media was collected and NO production was investigated using a Sievers 280A NO Meter. (A) representative western blotting images and (B) graph for the change in iNOS protein expression. Protein level of iNOS was normalised to level of GAPDH protein. (C) IL-1β-stimulated NO production in 3T3-L1 adipocytes. The data represent samples from three different experiments expressed as the mean ± SEM of the % relative to IL-1β stimulation. Statistical analysis was carried out using one-way ANOVA (with Bonferroni's test). Asterisks indicate a p value of (*p<0.001, ****p<0.0001).**

4.3.7 ATP-binding cassette transporter (ABCA1) inhibitor glybenclamide attenuates iNOS expression and NO production induced by IL-1β

Collectively, the findings from chapter 1 and 2 proposed that IL-1ß upregulates SphK1, resulting in S1P production inside adipocytes which is then exported outside via transporters. The additive effect of S1P and IL-1ß seems to be caused by activation of $S1PR_2$. ATP-binding cassette transporter (ABCA1) is one of many transporters that has been validated as being expressed in adipocytes. A recent study showed that ABCA1 functions as an S1P transporter in adipocytes (Ito et al, 2013). Therefore, I speculated that ABCA1 might transport S1P resulting from IL-1ß-mediated SphK1 activation outside the cell to allow S1PRs activation in adipocytes. To test this possibility, an ABCA1 inhibitor (glybenclamide) was used. 3T3-L1 adipocytes were stimulated with IL-1ß (10 ng/ml) and S1P (10 µM) in the presence and absence of glybenclamide (10 µM) for 24 hours. After treatment, lysate was prepared, and iNOS expression was assessed by western blotting while NO production was determined by the presence of nitrite/nitrate in the medium.

Incubation of 3T3-L1 adipocytes with IL-1ß in the absence of glybenclamide caused a significant increase, compared to the untreated cells, in both iNOS expression and NO production (****$p<0.0001$). A significant reduction (*$p<0.05$, ***$p<0.001$) was observed in iNOS expression and NO production in the presence of glybenclamide, compared to IL-1ß treatment alone.

Incubation of 3T3-L1 adipocytes with IL-1ß and S1P in the absence of glybenclamide caused a significant (*$p<0.05$, ***$p<0.001$, respectively) increase, in iNOS expression and NO production, compared to IL-1ß treatment alone. In the presence of glybenclamide, the additive effect of exogenous S1P was decreased and became non-significant although there was still a tendency towards an additive effect, suggesting that intracellular S1P resulting from IL-1ß-induced SphK1 activation is important for the additive effect of S1P on IL-1ß-mediated iNOS regulation (Figure 4-11).

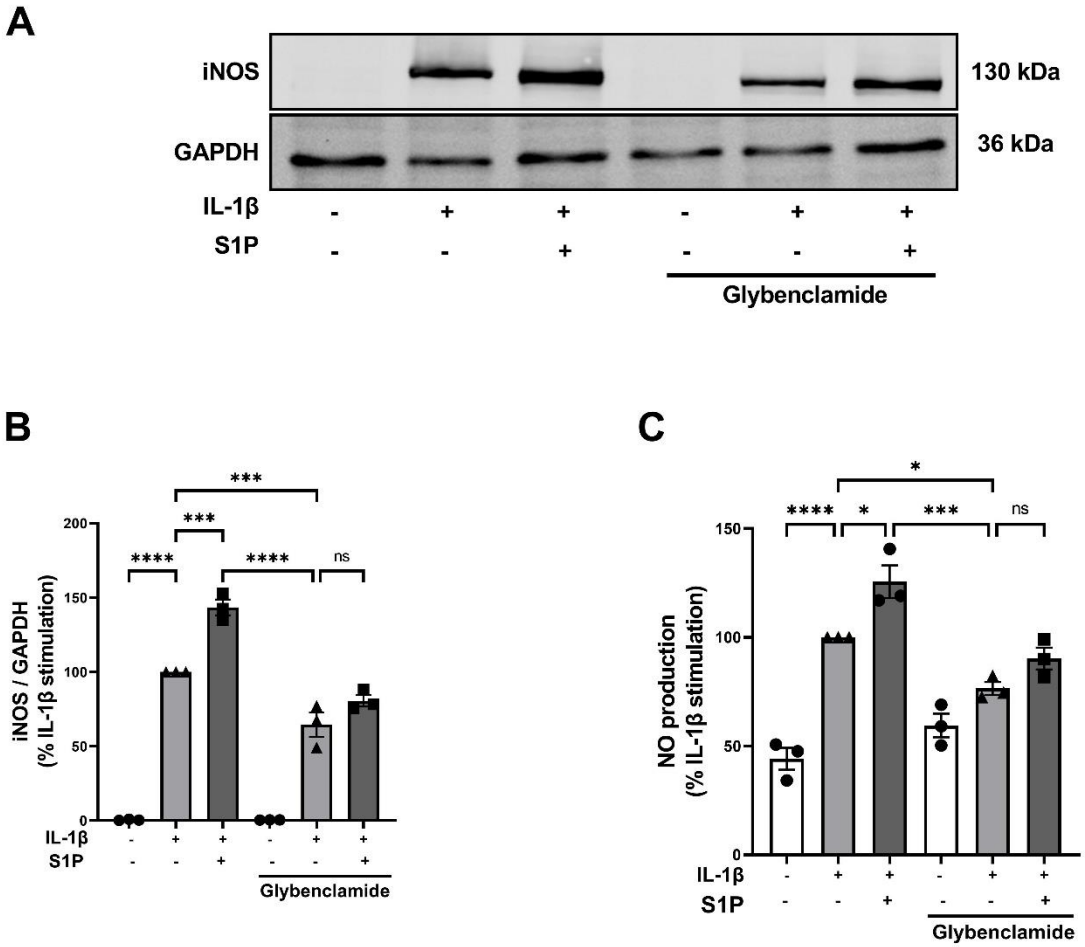

Figure 4-11 Effect of ATP-binding cassette transporter inhibitor -ABCA1 (glybenclamide) on iNOS protein expression and NO production in stimulated adipocytes.

3T3-L1 adipocytes were stimulated with IL-1β (10 ng/ml) alone or in combination with S1P (10 μM) in the presence and absence of glybenclamide (10 μM) for 24 hours. Cell lysates were prepared and resolved by SDS-PAGE with the appropriate antibodies. Media was collected and NO production was investigated by using a Sievers 280A NO Meter. (A) representative western blotting images and (B) graph for the change in iNOS protein expression. Protein level of iNOS was normalised to level of GAPDH protein. (C) IL-1β stimulated NO production in 3T3-L1 adipocytes. The data represent samples from three different experiments expressed as the mean ± SEM of the % relative to IL-1β stimulation. Statistical analysis was carried out using one-way ANOVA (with Tukey test). Asterisks indicate a p value of (*p<0.05, ***p<0.001, ****p<0.0001).

4.3.8 Conditioned media derived from activated macrophages upregulates iNOS expression and NO production in 3T3-L1 adipocytes

The complex inflammatory profile of inflamed adipose tissue arises from the interplay between adipocytes and macrophages. Since macrophages secrete a range of proinflammatory cytokines and other products, it was of interest to establish the effect of activated macrophages on iNOS regulation in 3T3-L1 adipocytes. Murine RAW 264.7 macrophages were activated with LPS (100 ng/ml) for either 8 or 24 hours, and conditioned medium was collected. 3T3-L1 adipocytes were then stimulated with the conditioned medium, diluted to 1:4 and 1:2 in DMEM for 24 hours. After treatment, lysate was prepared, and iNOS expression was assessed by western blotting while NO production was determined by nitrite/nitrate in the medium.

Stimulation of 3T3-L1 adipocytes with macrophage-conditioned medium activated with LPS for 8 hours caused a significant (*$p<0.05$) increase in iNOS expression at both dilutions compared to untreated cells. Moreover, conditioned medium activated with LPS for 24 hours also caused a significant (*$p<0.05$, ****$p<0.0001$) increase in iNOS expression at both dilutions relative to untreated cells (Figure 4-12B).

Similarly, NO production by the adipocytes showed a significant increase when the cells were treated conditioned media activated for either 8 or 24 hours (*$p<0.05$, **$p<0.01$, ***$p<0.001$; Figure 4-12C).

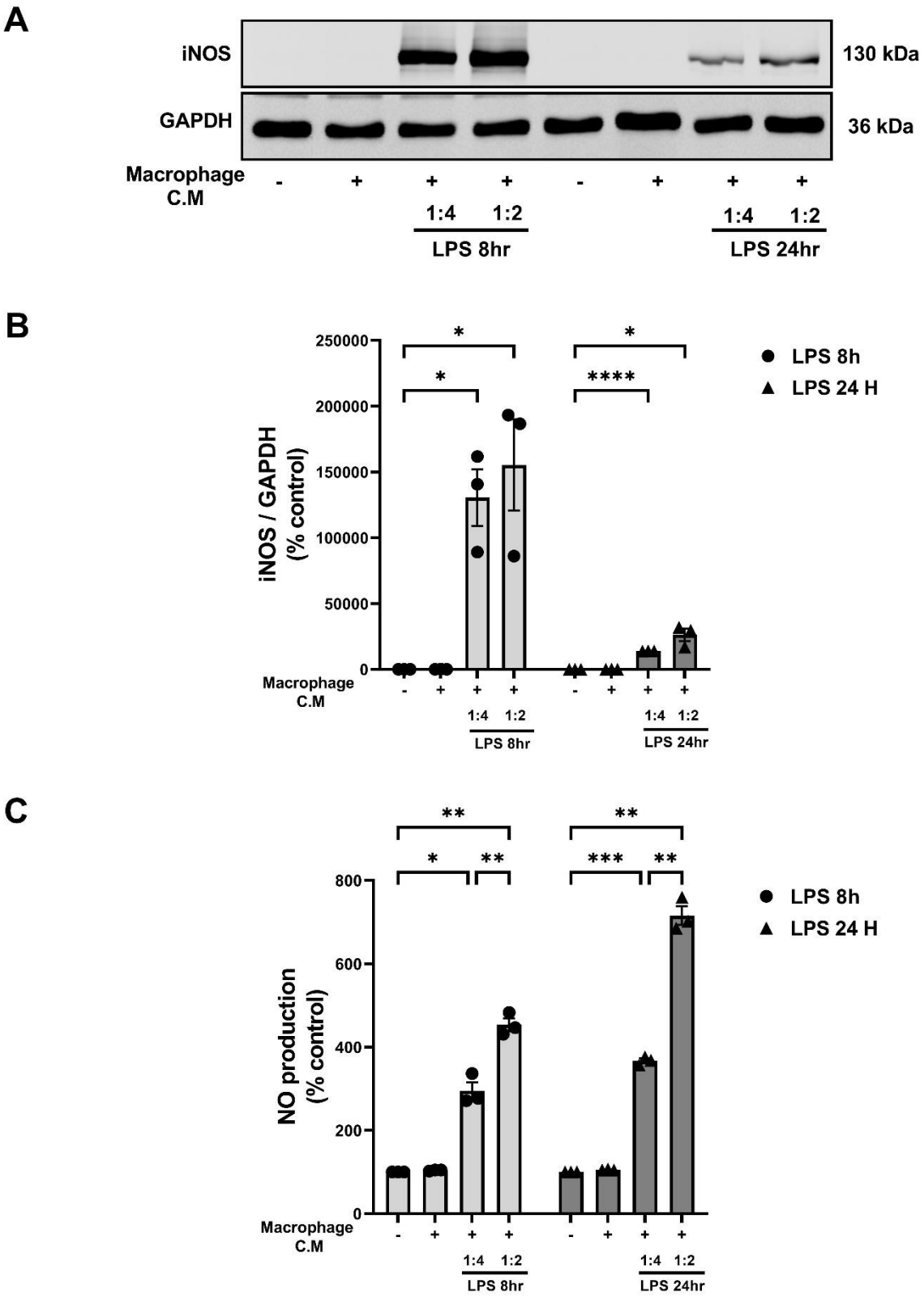

Figure 4-12 Effect of conditioned media derived from activated macrophages (RAW 267.4) on iNOS and NO production in 3T3-L1 adipocytes.

RAW 264.7 macrophages were activated with LPS (100 ng/ml) for 8 hours or 24 hours and conditioned medium collected and stored at -80°C. 3T3-L1 adipocytes were stimulated with conditioned medium diluted at 1:4 or 1:2 with DMEM for 24 h. Cell lysates were prepared at indicated time points and resolved by SDS-PAGE with the appropriate antibodies. Media was

collected and NO production was investigated by using a Sievers 280A NO Meter. (A) representative western blotting images and (B) graph for the change in iNOS protein expression. Protein level of iNOS was normalised to level of GAPDH protein. (C) NO production in 3T3-L1 adipocytes stimulated with RAW 264.7 conditioned media. The data represent samples from three different experiments expressed as the mean± SEM. Statistical analysis was carried out using two-way ANOVA (with LSD test). Asterisks indicate a p value of (*p<0.05, **p<0.01, ***p<0.001, ****p<0.0001).

4.3.9 LPS activates SphK1 phosphorylation in RAW 267.4 cell

SphK1 and its product S1P have been proposed to be activated in RAW 267.4 macrophages treated with LPS. To confirm this, RAW 267.4 macrophages were treated with 100 ng/ml LPS for 5 min, 15 min, 30 min, 60 min and 120 min. LPS-induced SphK1 phosphorylation was then determined by western blot analysis. Treatment of RAW 267.4 cells with LPS (Figure 4-13) caused a significant increase in SphK1 phosphorylation compared to untreated cells after 120 min (**p<0.01).

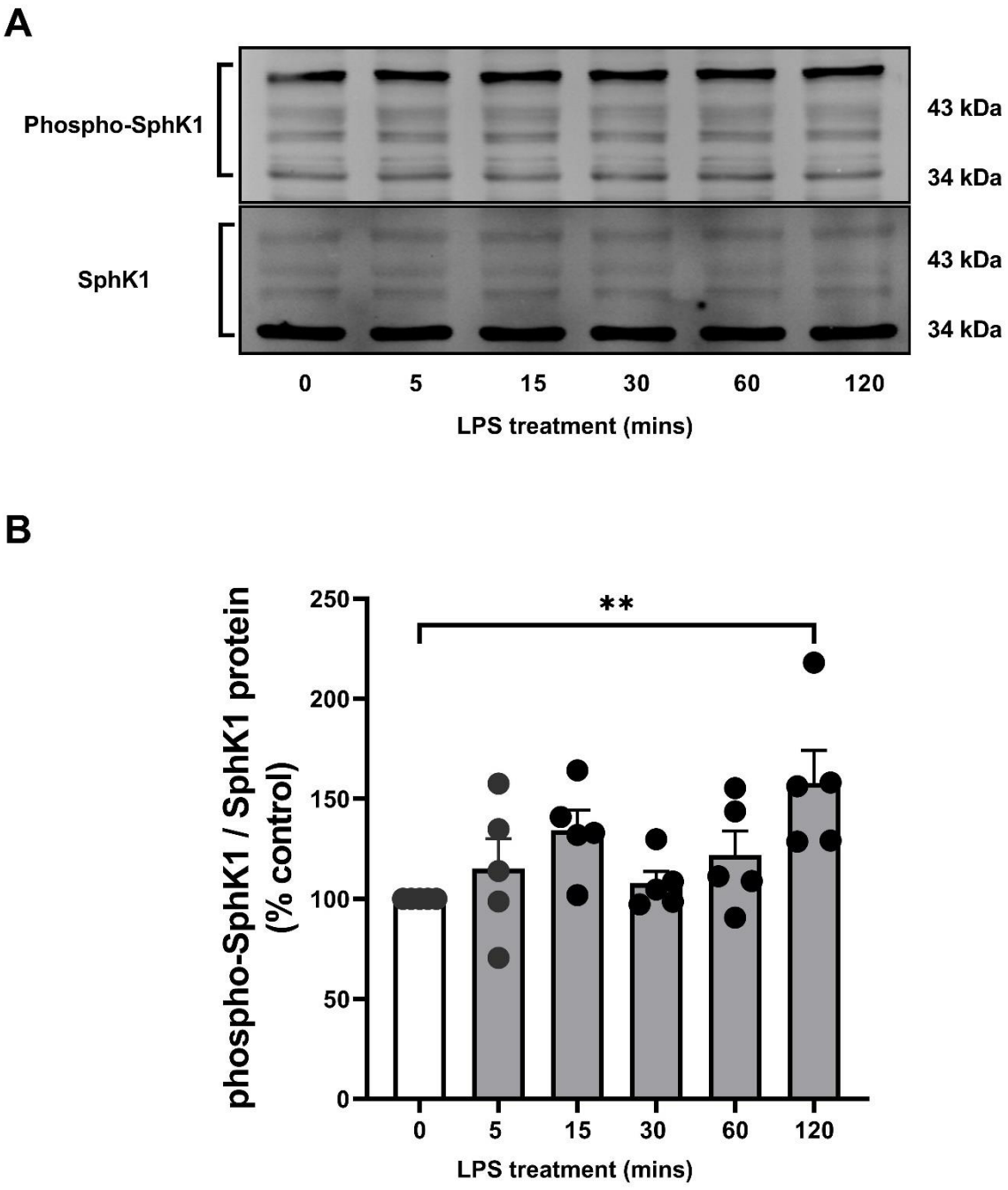

Figure 4-13 The effect of LPS on the SphK1 phosphorylation in RAW 267.4 cells.

RAW 267.4 cells were stimulated with LPS (100 ng/ml) for the indicated times. Cell lysates were prepared and resolved by SDS-PAGE with the appropriate antibodies. (A) representative western blotting image and (B) graph of pSphK1 protein expression showing the changes in pSphK1 expression at 5 min, 15 min, 30 min, 60 min and 120 min. Protein level of pSphK1 was normalised to level of SphK1. The data represent samples from five different experiments expressed as the mean ± SEM fold change relative to control (no LPS treatment). Statistical analysis was carried out using one-way ANOVA (with Dunnett's test). Asterisks indicate a p value of (p<0.01).**

4.3.10 SphK1 inhibition in LPS-activated macrophages decreases iNOS expression and NO production in 3T3-L1 adipocytes co-cultured with activated RAW 267.4 conditioned media

LPS upregulates pSphK1 in macrophages (Figure 4-13), suggesting that the cells would increase S1P production which could be involved in macrophage-mediated-iNOS regulation in adipocytes by activating S1PRs. To investigate the role of SphK1 in macrophage-mediated iNOS regulation in 3T3-L1 adipocytes, conditioned media was collected from activated macrophages in the presence and absence of the SphK1 inhibitor, PF543 (100 nM). 3T3-L1 adipocytes were then incubated for 24 hours in this conditioned media from macrophages to assess the effect on iNOS expression and NO production. After treatment, lysate was prepared, and iNOS expression was assessed by western blotting while NO production was determined by the presence of nitrite/nitrate in the medium.

As shown in Figure 4-14, incubation of 3T3-L1 adipocytes with macrophage conditioned media treated with LPS in the absence of PF543, caused a significant increase in iNOS expression and NO production (****$p<0.0001$). When treated with PF543, there was a significant reduction (*$p<0.05$) in iNOS expression and NO production compared to treatment with macrophage conditioned media activated with LPS alone.

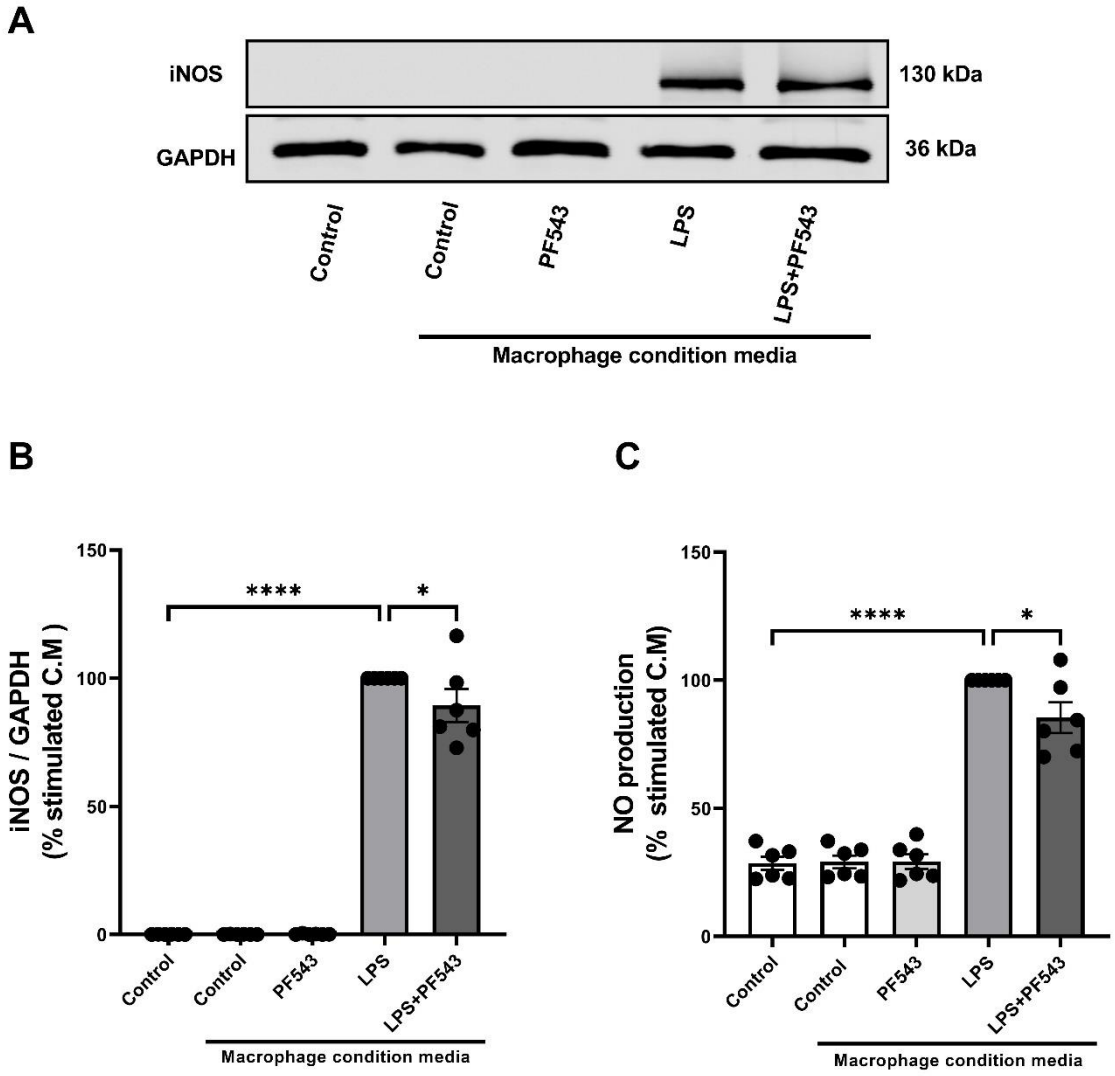

Figure 4-14 The effect of SphK1 inhibition in activated macrophages on iNOS expression and NO production in 3T3-L1 adipocytes co-cultured with activated RAW 267.4 conditioned media.

RAW 264.7 macrophages were pretreated with SphK1 inhibitor PF543 (100 nM) for 45 min and then were activated with LPS (100 ng/ml) for 8 hours in the presence and absence of PF543 (100 nM). Then, conditioned medium was collected and stored at -80 °C. 3T3-L1 adipocytes were stimulated with 1:4 dilution of the conditioned medium for 24 hours. Cell lysates were prepared and resolved by SDS-PAGE with the appropriate antibodies. Media was collected and NO production was investigated by using a Sievers 280A NO Meter. (A) representative western blotting images and (B) graph for the change in iNOS protein expression. Protein level of iNOS was normalised to level of GAPDH protein. (C) NO production in 3T3-L1 adipocytes stimulated with RAW 264.7 conditioned media. The data represent samples from six different experiments expressed as the mean ± SEM of the % relative to RAW 267-C.M stimulation. Statistical analysis was carried out using one-way ANOVA (with Bonferroni's test). Asterisks indicate a p value of (*p<0.05, ****p<0.0001).

4.3.11 $S1PR_2$ antagonism in activated macrophages reduces iNOS expression and NO production in 3T3-L1 adipocytes co-cultured with activated RAW 267.4 C.M

It has been established in this thesis that $S1PR_2$ mediates iNOS expression and NO production in 3T3-L1 adipocytes. However, the role of the $S1PR_2$ receptor in macrophages was unknown. To investigate this conditioned media was collected from activated macrophages in the presence and absence of an $S1PR_2$ inhibitor, JTE 013 (10 μM). 3T3-L1 adipocytes were then incubated for 24 hours in the conditioned media from macrophages to assess whether $S1PR_2$ inhibition could affect iNOS expression and NO production in 3T3-L1 adipocytes. After treatment, lysate was prepared, and iNOS expression was assessed by western blotting while NO production was determined by nitrite/nitrate in the medium.

Incubation of 3T3-L1 adipocytes with macrophage conditioned media treated with LPS in the absence of JTE 013, caused a significant increase in iNOS expression and NO production (****$p<0.0001$). When treated with JTE 013, there was a significant reduction (**$p<0.01$, ***$p<0.001$) in iNOS expression and NO production in 3T3-L1 adipocytes compared to macrophage conditioned media activated with LPS alone (Figure 4-15).

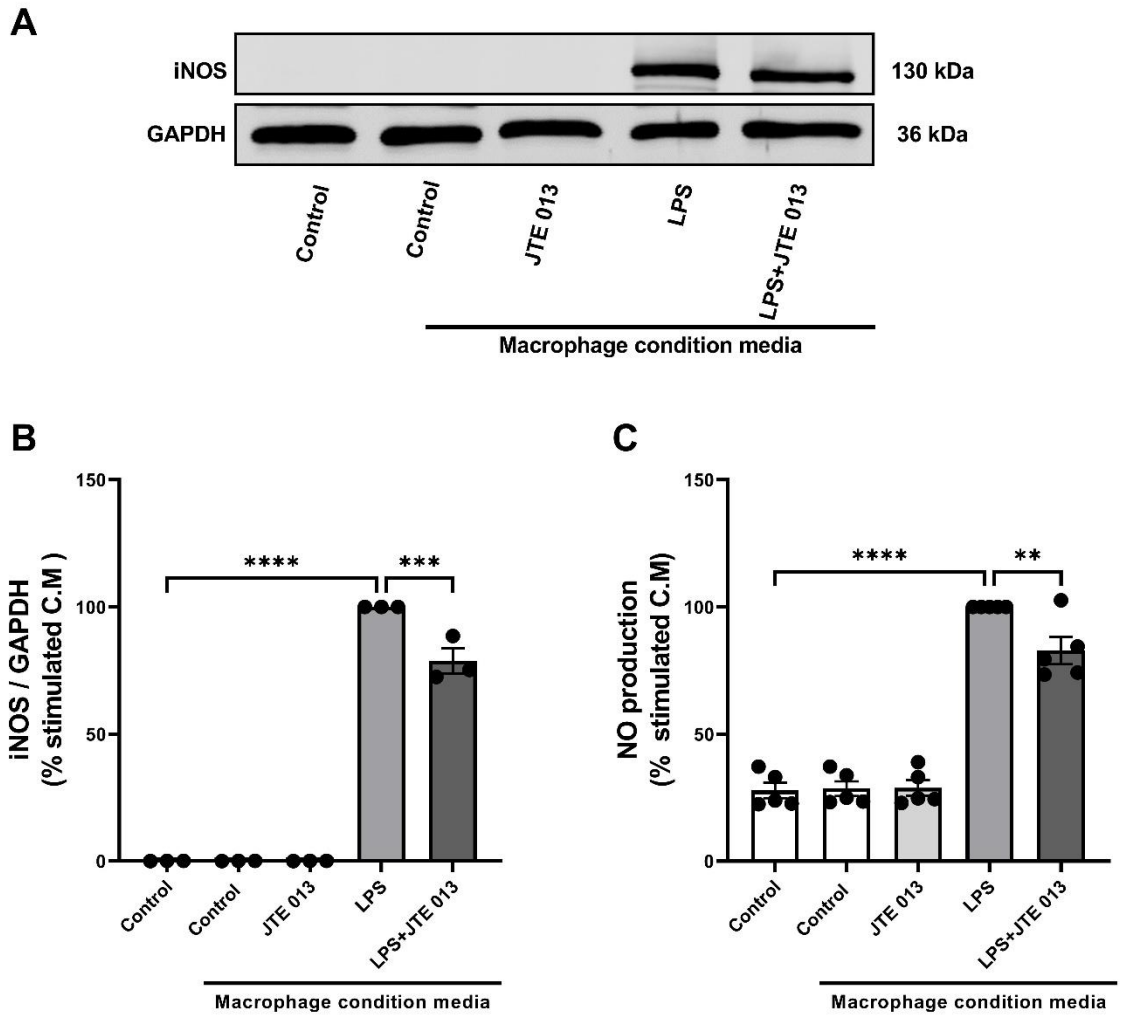

Figure 4-15 The effect of S1PR2 inhibition in activated macrophages on iNOS expression and NO production in 3T3-L1 adipocytes co-cultured with activated RAW 267.4 C.M.

RAW 264.7 macrophages were pretreated with JTE 013 (10 μM) and then were activated with LPS (100 ng/ml) for 8 hours in the presence and absence of JTE 013 (10 μM). Then, conditioned medium was collected and stored at -80ºC. 3T3-L1 adipocytes were stimulated with 1:4 dilution of the stimulated conditioned medium for 24 h. Cell lysates were prepared and resolved by SDS-PAGE with the appropriate antibodies. Media was collected and NO production was investigated by using a Sievers 280A NO Meter. (A) representative western blotting images and (B) graph for the change in iNOS protein expression. Protein level of iNOS was normalised to level of GAPDH protein. (C) NO production in 3T3-L1 adipocytes stimulated with RAW 264.7 conditioned media. The data represent samples from at least three different experiments expressed as the mean ± SEM of the % relative to RAW 267 C.M stimulation. Statistical analysis was carried out using one-way ANOVA (with Bonferroni's test). Asterisks indicate a p value of (p<0.01, ***p<0.001, ****p<0.0001).**

4.3.12 Effects of S1P receptors antagonism in 3T3-L1 adipocytes on iNOS expression and NO production following co-culture with activated RAW 267.4 C.M

To further investigate whether $S1PR_{1-3}$ inhibition in 3T3-L1 adipocytes would affect macrophage-mediated iNOS regulation, adipocytes were incubated with $S1PR_1$ antagonist W146 (10 μM), $S1PR_2$ antagonist JTE 013 (10 μM) or the $S1PR_3$ antagonist CAY10444 (10 μM) for 45 min prior to being stimulated with activated macrophage conditioned media for 24 hours. After treatment, lysate was prepared, and iNOS expression was assessed by western blotting while NO production was determined by nitrite/nitrate in the medium.

Incubation of 3T3-L1 adipocytes with condition media stimulated with LPS in the absence of W146 caused a significant (****$p<0.0001$) increase in iNOS expression and NO production. In the presence of W146, there was a significant decrease in iNOS expression, relative to adipocytes incubated with conditioned media alone while NO production was not affected (Figure 4-16 B and C).

Incubation of 3T3-L1 adipocytes with stimulated macrophage conditioned media in the absence of JTE 013 caused a significant (****$p<0.0001$) increase in iNOS expression and NO production, compared to untreated cells while in the presence of JTE 013, there was a significant decrease in iNOS expression and NO production (Figure 4-16 E and F).

Incubation of 3T3-L1 adipocytes with stimulated macrophage conditioned media in the absence of CAY caused a significant (****$p<0.0001$) increase in iNOS expression and NO production, compared to untreated cells and preincubation of 3T3-L1 adipocytes with CAY did not alter iNOS expression and NO production stimulated by macrophage conditioned media (Figure 4-16 H and I).

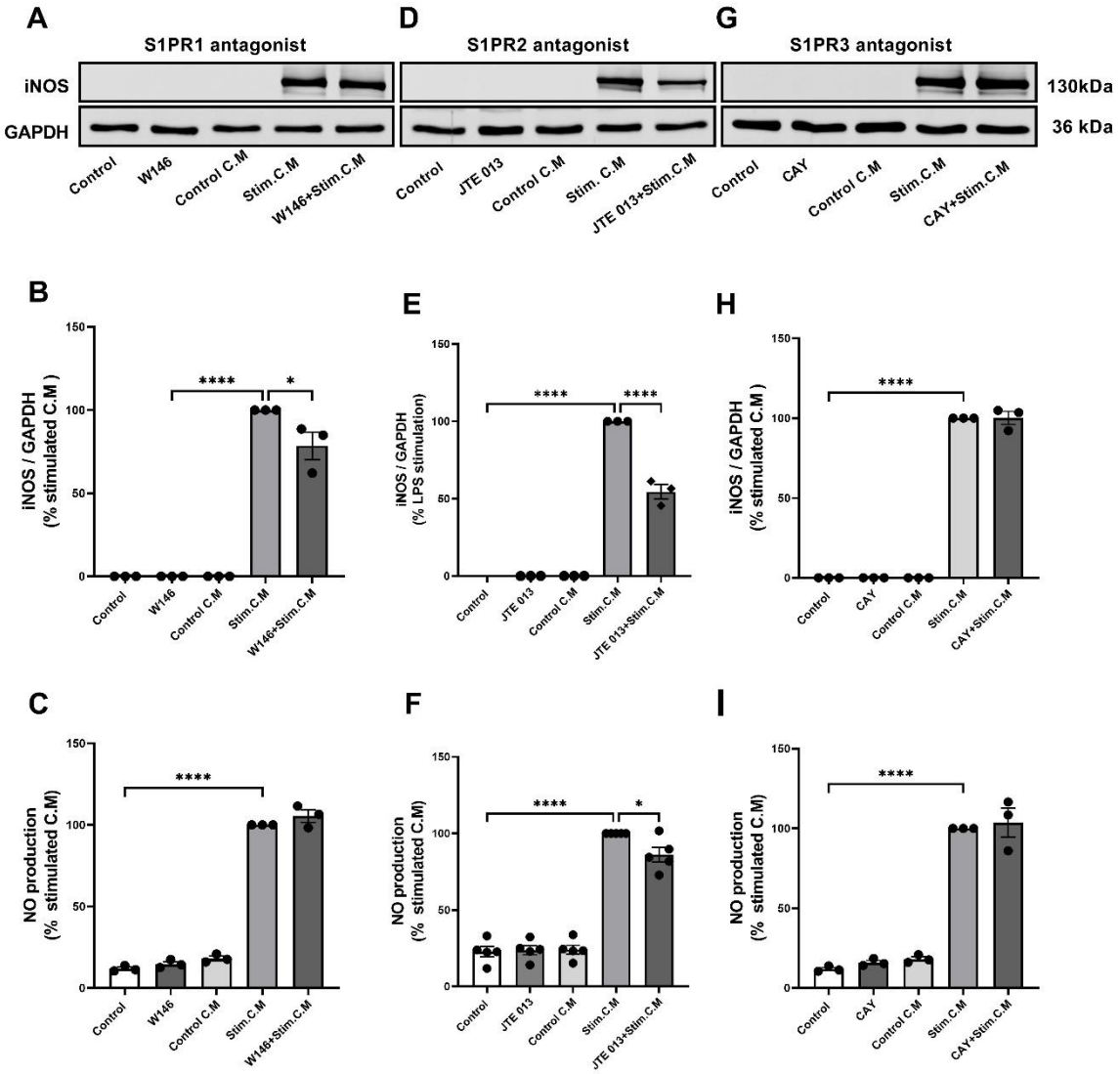

Figure 4-16 The effect of S1P receptor inhibition on iNOS expression and NO production in 3T3-L1 adipocytes co-cultured with activated RAW 267.4 C.M.

RAW 264.7 macrophages were activated with LPS (100 ng/ml) for 8 hours. Then, conditioned medium was collected and stored at -80°C. 3T3-L1 adipocytes were pretreated with $S1PR_1$ inhibitor W146 (10 µM), $S1PR_2$ inhibitor JTE 013 (10 µM) and $S1PR_3$ inhibitor CAY10444 (10 µM) then were stimulated with 1:4 dilution of stimulated conditioned medium in the presence and absence of the three inhibitors for 24h. Cell lysates were prepared and resolved by SDS-PAGE with the appropriate antibodies. Media was collected and NO production was investigated by using a Sievers 280A NO Meter. (A, D, and G) representative western blotting images and graphs (B, E and H) for the change in iNOS protein expression. Protein level of iNOS was normalised to level of GAPDH protein. (C, F, and I) NO production in 3T3-L1 adipocytes stimulated with RAW 264.7 conditioned media. The data represent samples from at least three different experiments expressed as the mean ± SEM of the % relative to RAW 267 C.M stimulation. Statistical analysis was carried out using one-way ANOVA (with Bonferroni's test). Asterisks indicate a p value of (*p<0.05, ****p<0.0001).

4.4 Discussion

In the previous chapter, it was found that IL-1β upregulates SphK1, which would then be expected to generate S1P which could contribute to IL-1β-mediated iNOS regulation in 3T3-L1 adipocytes. In support of this hypothesis, exogenous S1P was found to augment iNOS expression and NO production in 3T3-L1 adipocytes stimulated with IL-1β (Figure 3-12). Thus, in this chapter, it was important to investigate more fully how SphKs/S1PRs modulate iNOS regulation in adipocytes stimulated with the cytokine IL-1β as well as a more physiologically-relevant stimulus, namely macrophage-conditioned media. Use of conditioned media from macrophages would more accurately reflect the interplay between macrophages and adipocytes in the adipose tissue. The data presented in this chapter indicate that SphK1/$S1PR_2$ is the most likely axis modulating iNOS regulation and NO production via MAPKs and PI3K/Akt pathways. Furthermore, secretory products from activated macrophages upregulate iNOS expression and NO production in 3T3-L1 adipocytes, while activated macrophages treated with SphK1 inhibitor or an $S1PR_2$ antagonist have suppressed ability to upregulate iNOS expression and NO production in adipocytes. Furthermore, although antagonism of $S1PR_1$ receptor in 3T3-L1 adipocytes prior to stimulation with macrophage conditioned media decreased iNOS expression, it did not suppress NO production as was seen with the $S1PR_2$ antagonist.

A number of studies have reported that SphK isoforms are implicated in the regulation of many inflammatory processes (Tous et al, 2014; Wang et al, 2014). Elevated levels of SphK1 have been reported in the adipose tissue of obese mice (Hashimoto et al, 2009). In the current study, pre-treatment of 3T3-L1 adipocytes with a SphK1 inhibitor (PF543) significantly decreased IL-1β-mediated iNOS expression and NO production (Figure 4-1), suggesting SphK1 activity promotes iNOS regulation and then NO production in 3T3-L1 adipocytes. This result is consistent with previous observations which showed the involvement of SphK1 in iNOS regulation in microglial cells (Nayak et al, 2010) and in murine HAPI microglial cell line (Wang et al, 2021). My data is also supported by data from Trypanosoma cruzi-infected mice in which iNOS gene expression and proinflammatory mediators (IL-1β and TNF-α) were decreased in mice treated with SphK1 inhibitor DMS (Vasconcelos et al, 2017). In contrast, SphK2 inhibition

by ROME failed to inhibit IL-1β-mediated iNOS expression and NO production in 3T3-L1 adipocytes (Figure 4-2), implying it is not involved in iNOS regulation. In support of the differential role of SphK isoenzymes seen in this study, it has been reported that SphK1 promotes inflammation in mice with inflammatory arthritis, while SphK2 protects these mice by improving inflammatory arthritis (Lai et al, 2009). However, in my study, SphK2 inhibition by ROME did not show an additive effect to IL-1β-mediated iNOS expression, although IL-1β has been shown to downregulate SphK2 gene expression in the previous chapter which could account for the lack of effect of ROME. The ROME compound is one of the most selective and potent SphK2 inhibitors available (Pyne et al, 2020), however, it is possible to use other compounds to confirm whether SphK2 has a protective role in iNOS regulation. Moreover, it has been reported that SphK1 is the predominant isoform of SphK producing S1P into the circulation (Qi et al, 2021), which could also underlie why only SphK1 inhibition has a protective effect in modulating iNOS regulation in 3T3-L1 adipocytes. Measuring S1P production in adipocytes stimulated with IL-1β in the presence and absence of SphK isoenzymes may also further elucidate the distinct role of SphK isoenzymes. To our knowledge, these data are the first to demonstrate that IL-1β requires SphK1 but not SphK2 in order to regulate iNOS in 3T3-L1 adipocytes.

S1P exerts its biological effects by activating a wide range of S1PRs. $S1PR_{1-3}$ are expressed in adipose tissue and adipocytes (Jun et al, 2006; Mastrandrea, 2013). To address which specific receptor is involved in iNOS regulation, I used the selective $S1PR_1$ antagonist W146, $S1PR_2$ antagonist JTE 013, and $S1PR_3$ antagonist CAY10444. The findings imply that all three receptors have a role in the regulation of iNOS expression in stimulated adipocytes (Figure 4-3). However, only the $S1PR_2$ antagonist strongly suppressed NO production in stimulated adipocytes (Figure 4-4). These results implied that $S1PR_2$ activation with a specific agonist, CYM 5478 in stimulated 3T3-L1 adipocytes would have the opposite effect to JTE 013 and indeed, CYM 5478 augmented iNOS expression and NO production in IL-1β-stimulated 3T3-L1 adipocytes (Figure 4-5). It is clear that the effect of CYM 5478 is not as strong as the effect of JTE 013, which could be due to activation of $S1PR_2$ by CYM 5478 not being as effective as activation by endogenous S1P. Another possible reason is the difference between JTE 013 and CYM 5478 on their binding sites; JTE 013 is an antagonist which binds to orthosteric site on the receptor,

while CYM 5478 is agonist bind to allosteric sites (Chew et al, 2016; Satsu et al, 2013). Therefore, this discrepancy in binding sites might result in activating different G protein subunits to induce distinct downstream signalling pathway (Digby et al, 2010). Supporting this idea, the magnitude of CYM 5478 induced iNOS expression and NO production in stimulated adipocytes was similar to that induced by S1P, as seen in previous chapter. This suggests that the agonist binding to a distinct binding site might result in coupling to a different G protein subunit from antagonist. It also important to note that JTE 013 has broader inhibition of proinflammatory signalling in adipocytes as seen in this chapter, hence result in a stronger overall effect compared to the more targeted effects of an agonist CYM 5478. More investigations are needed to delineate the effect of CYM 5478 in proinflammatory signalling in 3T3-L1 adipocytes. These data are consistent with the many studies to date investigating the involvement of $S1PR_2$ in iNOS regulation. $S1PR_2$ inhibition has been reported to suppress iNOS protein expression in rat glomerular mesangial cell line (Gong et al, 2020), and NOX2 gene expression in the aorta of $ApoE^{-/-}$ animals (Ganbaatar et al, 2021). These data also support a recent study showing that there was a reduction in NOX2 gene expression in epididymal adipocytes of HFD mice deficient in $S1PR_2$ (Kitada et al, 2016). Also of relevance to the current study, $S1PR_2$ inhibition by JTE 013 was shown to decrease iNOS expression and NO production in placenta tissue of the preeclampsia rat (Zhang et al, 2021). Additionally, this is in agreement with Skoura et al. (2007), showing that $S1PR_2$ activation upregulates COX-2 in endothelial cells (Skoura et al, 2007), and also with previous work by Du et al. (2012), showing that JTE-013 reduces endothelium monolayer hyper-permeability caused by LPS and TNF-α (Du et al, 2012). To my knowledge, these data demonstrate for the first time that $S1PR_2$ inhibition suppresses iNOS expression and NO production in IL-1ß-stimulated adipocytes.

It is well known that S1PRs modulate a differential effect via several distinct and divergent pathways. Also, IL-1ß stimulates a wide range of pathways that are involved in iNOS regulation and NO production. Despite $S1PR_{1-3}$ receptors all being implicated in modulating iNOS expression in 3T3-L1 adipocytes, $S1PR_2$ appears to be the dominant receptor involved in iNOS expression and NO synthesis. This could be attributed to several factors. $S1PR_1$ and $S1PR_3$ have been reported to signal via G_i, whilst $S1PR_2$ has been found to couple with multiple Gα subunits, including G_i,

G_q, and $G_{12/13}$ (Bryan & Del Poeta, 2018). In addition, it is possible that $S1PR_2$ regulates post-translation modifications of iNOS that are required for its activity. For example, iNOS phosphorylation by protein kinase A (PKA), and protein kinase C (PKC) can increase NO production, and $S1PR_2$ could activate these pathways. $S1PR_2$ couples to $G_{12/13}$ subunits, activating RhoA/ROCK pathway (Aarthi et al, 2011), which is involved in iNOS activation (Glotfelty et al, 2023), while other S1P receptors activate alternate G protein subunits. Further comprehensive mechanistic studies will be necessary to elucidate how $S1PR_2$ cascades regulate iNOS and NO production versus $S1PR_1$ and $S1PR_3$.

$S1PR_2$ is one of the S1PRs implicated in many inflammatory processes within adipose tissue. $S1PR_2$ regulates various cellular signalling pathways, including PI3K/Akt, ERK, JNK, p38 MAPK, and NF-KB (Kluk & Hla, 2002; Wang et al, 2023; Yang et al, 2022). Moreover, it was discussed in Chapter 3 that these pathways are implicated in many inflammatory processes within adipose tissue. Here, I further investigated which of these downstream pathways are affected by $S1PR_2$ inhibition in IL-1ß-stimulated adipocytes. It was found that JTE 013 strongly downregulates iNOS expression and NO production in IL-1ß-stimulated adipocytes; therefore, it was important to characterise this effect further. IL-1ß was found to significantly upregulate Akt phosphorylation, a PI3K downstream effector, while preincubation of adipocytes with JTE 013 significantly suppressed IL-1ß-stimulated Akt phosphorylation (Figure 4-6), suggesting that JTE 013 was capable of modulating the PI3K/Akt pathway stimulated by IL-1ß, and, as a result, to decrease iNOS expression and NO production. These data support the few reports to date investigating the effect of $S1PR_2$ inhibition on proinflammatory cytokines via the PI3K/Akt pathway. It has been reported that $S1PR_2$ inhibition by JTE 013 downregulates COX-2 expression in human cholangiocellular carcinoma cell line via PI3K/Akt pathway suppression (Liu et al, 2015). Moreover, these data support the findings of Michaud and co-workers, who reported that chemoattractant-stimulated Akt phosphorylation in bone marrow-derived macrophages (BMDM) is decreased in cells lacking $S1PR_2$ (Michaud et al, 2010).

In addition, MAPK family pathways are proven to regulate many proinflammatory processes within adipose tissue. The phosphorylation of MAPK family pathways, including ERK1/2, JNK, and p38, are implicated in iNOS expression in 3T3-L1

adipocytes (Nepali et al, 2015). To further explore the mechanisms of JTE 013 in iNOS regulation in stimulated adipocytes, I assessed the IL-1ß-stimulated MAPKs phosphorylation in 3T3-L1 adipocytes treated with JTE 013. As shown in Figure 4-7, IL-1ß treatment alone resulted in an increase in MEK-ERK pathway phosphorylation at 15 min and 30 min. Inhibition of $S1PR_2$ with JTE 013 significantly suppressed IL-1ß-stimulated MEK-ERK phosphorylation. Similarly, IL-1ß has been shown to markedly upregulate P38 phosphorylation and JNK phosphorylation. Inhibition of $S1PR_2$ with JTE 013 significantly suppressed IL-1ß-stimulated JNK phosphorylation and P38 phosphorylation (Figure 4-8), implying that JTE 013 is able to suppress iNOS via suppressing these pathways in stimulated adipocytes. These data support a recent study by Hou et al. (2021), who reported that JTE 013 blunts NLRP3 inflammasome-driven inflammation in bone marrow-derived monocyte/macrophages (BMMs) via MAPKs (ERK1/2, JNK, and P38) pathways (Hou et al, 2021). It has been reported that $S1PR_2$ inhibition by JTE 013 downregulates COX-2 expression in human cholangiocellular carcinoma cell line via ERK1/2 pathway suppression (Liu et al, 2015), and JTE 013 suppresses LPS-induced inflammation in alveolar epithelial cells via JNK pathway inhibition (Liu et al, 2021). Moreover, these data support previous finding where JTE 013 has been shown to have a protective effect against oxidative stress-induced cerebrovascular endothelial barrier impairment via ERK1/2 and P38 suppression (Cao et al, 2019).

The NF-KB pathway is one of the important pathways regulating iNOS expression and NO production in adipocytes (Kim et al, 2020). To further explore the mechanisms of JTE 013 in iNOS regulation in stimulated adipocytes, I assessed the IL-1ß-stimulated NF-KB activation pathway in 3T3-L1 adipocytes treated with JTE 013. However, while IL-1ß significantly upregulated NF-KB pathways by increasing NF-KB activation, IKBα phosphorylation, and IKBα degradation (Figure 4-9), inhibition of $S1PR_2$ with JTE 013 did not attenuate the IL-1ß-stimulated NF-KB pathway activation. This could be explained if this mechanism was not one of the mechanisms by which JTE 013 inhibited iNOS expression in stimulated adipocytes. In contrast to our finding, it was reported that JTE 013 inhibits NF-KB activation in lipopolysaccharide LPS-induced rat glomerular mesangial cells (RMCs) (Gong et al, 2020). Also, it has been reported that knockdown of $S1PR_2$ or pharmacological inhibition by JTE 013 decreases the inflammatory response in acinar cells of

pancreatitis mouse models via the NF-KB pathway (Yang et al, 2022). The same study reported that JTE 013 suppresses NF-KB activation in RAW264.7 macrophages treated with taurocholic acid (TCA). Our finding is consistent with the data shown in chapter three, where S1P did not alter the NF-KB pathway, further supporting that S1P mediates upregulation of iNOS enzyme via NF-KB independent pathways.

A network of signalling molecules can induce iNOS expression and its product NO. The MAPKs and PI3K/Akt pathways play a significant role in the regulation of iNOS in many cells (Kugo et al, 2021; Nepali et al, 2015). My results showed the activation of ERK, JNK, P38, and Akt in stimulated adipocytes was suppressed by JTE 013 pretreatment. Therefore, to confirm whether the ability of JTE 013 to suppress IL-1β-stimulated iNOS expression and NO production was dependent upon PI3K/Akt and MAPKs pathway activation, pharmacological inhibitors of these pathways were utilised. Here I showed that the inhibitors of PI3K/Akt, ERK1/2, and JNK, but not the inhibitor targeting P38, suppressed iNOS expression and NO production in stimulated adipocytes (Figure 4-10). These results provide further strong evidence that the effect of JTE 013 on iNOS expression and NO production was mediated by the PI3K/Akt and MAPK pathways (ERK and JNK).

It was anticipated that inhibition of P38 phosphorylation might blunt the iNOS expression and NO production in response to IL-1β in adipocytes. However, P38 inhibition contradicts the anticipated anti-inflammatory paradigm and, as Figure 4-10 shows, inhibition of P38 by SB202190 significantly augmented IL-1β induced iNOS expression and NO production in adipocytes. In mouse J774 macrophages and human colon epithelial cells T-84, SB202190 has been demonstrated to have a concentration-dependent bidirectional effect on iNOS expression and NO generation (Lahti et al, 2002). Moreover, it has been shown that SB202190 might activate JNK phosphorylation, leading to transcription factor 2 activation (ATF-2), and increased AP-1 DNA binding in multiple cells lines (Muniyappa & Das, 2008). ATF-2 is a transcription factor which complexes with AP-1 DNA binding proteins to induce inflammatory gene expression, including the iNOS gene (Aktan, 2004). Therefore, the mechanism by which SB202190 augments iNOS regulation in stimulated adipocytes may be dose-dependent or via JNK phosphorylation;

however, further investigation is required to uncover the precise role of $S1PR_2$ in P38 pathway activation, particularly in iNOS regulation in adipocytes.

Numerous studies have shown that ATP-binding cassette transporter (ABC), including ABC transporter A1 (ABCA1), is widely implicated in transporting S1P out of many cells. For example, it has been demonstrated that ABCA1 inhibition by a non-selective inhibitor (glybenclamide) decreased S1P release induced by apoA in astrocytes (Sato et al, 2007), and HUVECs (Liu et al, 2016). Moreover, it has been shown that thrombin-induced S1P release from rat platelets is inhibited by another ABCA inhibitor (glyburide) (Kobayashi et al, 2006). ABCA1 is expressed in adipocytes, and it has also been shown that hypoxia increases S1P concentration in 3T3-L1 adipocyte conditioned media, while it was reduced by ABCA1 inhibition with glybenclamide under hypoxia conditions (Ito et al, 2013). Therefore, it was speculated that when SphK1 is activated in response to IL-1β it catalyses S1P from sphingosine, which is subsequently released through the ABCA1 transporter to modulate adipocyte function via S1PRs. In order to investigate whether the ABCA1 transporter has a role in the additive effect of S1P on IL-1β in upregulating iNOS expression and NO production, 3T3-L1 adipocytes were stimulated with IL-1β and S1P in the presence and absence of glybenclamide. The data show that S1P significantly augmented IL-1β-mediated iNOS expression and NO production in 3T3-L1 adipocytes and that in the presence of glybenclamide, the additive effect of S1P on iNOS expression and NO production was abolished (Figure 4-11). This finding might indicate that a significant part of intracellular S1P resulting from IL-1β participates in inducing iNOS expression and NO production from adipocytes. It is worth noting that the ABCA1 alone inhibitor significantly suppressed iNOS expression and NO production, which is consistent with a previous study where glybenclamide has been shown to inhibit iNOS expression in LPS-stimulated BV2 microglial cells (Xu et al, 2017). This experiment was an attempt to gain further insight into how ABCA1 transporter regulate iNOS expression, and the role it has in the additive effect of S1P in iNOS regulation in stimulated adipocytes. Therefore, further experiments could confirm the importance of S1P transporters either using pharmacological inhibition or by siRNA, and importantly, measuring S1P concentration released by the adipocytes.

It is well known that M1 activated macrophages are the primary source of most of the proinflammatory mediators within the adipose tissue. Moreover, it has been suggested that macrophage infiltration into adipose tissue plays a critical role in the regulation of many proinflammatory enzymes. It has been previously shown that adipose tissue macrophages are responsible for iNOS expression within the adipose tissue (Weisberg et al, 2003). Furthermore, SphK1 and its product S1P is expressed in adipose tissue macrophages and in activated RAW 264.7 cells (Hammad et al, 2008; Wang et al, 2014; Wu et al, 2004). A plethora of studies exist proposing a proinflammatory role of the sphingolipid lipid system in adipose tissue (Asano et al, 2023; Kitada et al, 2016; Wang et al, 2014). Therefore, another aim of this study was firstly to characterise the effect of conditioned medium (CM) from LPS-activated macrophages on the regulation of the iNOS in 3T3-L1 adipocytes and, secondly, to establish an in vitro model for the study of the sphingolipid system's role in paracrine signal-inducing iNOS regulation in adipocytes.

In this set of experiments, RAW 264.7 macrophage cells were treated with LPS to polarise macrophages towards the M1 phenotype and promote proinflammatory mediator secretion. Utilising an indirect co-culture technique, CM of activated macrophages was collected and applied to 3T3-L1 adipocytes to establish that iNOS is upregulated by activated macrophage CM. Figure 4-12 demonstrated that stimulation of adipocytes with 1:4 and 1:2 dilution of CM activated with LPS for 8 hours significantly upregulated iNOS expression and NO production. Similarly, CM activated with LPS for 24 hours stimulated iNOS expression and NO production in adipocytes (Figure 4-12). The phenotype of macrophages was not examined in this study; however, iNOS expression in adipocytes treated with activated macrophages is considered strong evidence that macrophages are differentiated into typical M1 macrophages under the stimulation of LPS. These data confirm and establish the paracrine role between macrophages and adipocytes in iNOS regulation within the adipose tissue.

According to the aforementioned findings and background, I hypothesised that SphK1 in macrophages is upregulated in response to LPS and the S1P produced is important in paracrine signalling between macrophages and adipocytes. Figure 4-13 demonstrated that LPS stimulates SphK1 phosphorylation in RAW 264.7 cells.

Having demonstrated the ability of LPS to activate SphK1 in macrophages, a potential role for SphK1 in activated macrophage-induced iNOS regulation in adipocytes was investigated. Interestingly, stimulation of 3T3-L1 adipocytes with activated macrophage conditioned media caused a significant increase in iNOS expression and NO production, which was significantly decreased when activated macrophages were treated with SphK1 inhibitor (Figure 4-14). This observation suggests that SphK1 activation results in increased S1P production from macrophages, and subsequently, S1P itself acts directly on S1P receptors to augment iNOS expression in adipocytes. In support of this finding, it has been demonstrated that LPS activates SphK1 in RAW 264.7 macrophages and increases S1P concentration in conditioned media (Hammad et al, 2008). To further confirm these findings, I examined which S1P receptors are involved by pretreating adipocytes with the selective $S1PR_1$ antagonist W146, $S1PR_2$ antagonist JTE 013, and S1PR3 antagonist CAY10444 prior to stimulating with CM of activated macrophages. It was found that $S1PR_1$ and $S1PR_2$ have a role in the regulation of iNOS expression in adipocytes stimulated with activated macrophages. However, only the $S1PR_2$ antagonist suppressed NO production in adipocytes (Figure 4-16). This correlates well with earlier finding in this study, where it was shown that exogenous S1P augments iNOS regulation via $S1PR_2$ in adipocytes stimulated with IL-1ß.

Recently a number of studies have demonstrated that $S1PR_2$ participates in inflammatory cell infiltration. For example, $S1PR_2$ inhibition by JTE 013 has been shown to decrease the inflammatory cell infiltration and goblet cell production in asthmatic mouse tissues (Liu et al, 2021), and also to decrease the inflammatory cell infiltration in placenta preeclampsia rats (Zhang et al, 2021). Another study has reported that HFD-induced macrophage polarization and recruitment to adipose tissue are ablated in mice lacking $S1PR_2$ (Kitada et al, 2016). Therefore, I hypothesised that inhibition of macrophage $S1PR_2$ with JTE 013 would limit the macrophage polarization or secretion of LPS-stimulated proinflammatory mediators, subsequently reducing iNOS upregulation in 3T3-L1 adipocytes exposed to activated macrophage conditioned media. Figure 4-15 demonstrated that stimulation of 3T3-L1 adipocytes with activated macrophage conditioned media causes a significant increase in iNOS expression and NO production, which was significantly decreased when activated macrophages were treated with $S1PR_2$

inhibitor (JTE 013). These data support previous findings where JTE 013 has been shown to decrease cytokine levels (IL-1ß) in the plasma of mice treated with LPS (Skoura et al, 2011), and provide further evidence in support of $S1PR_2$ as a key mediator in driving inflammatory crosstalk between immune cells and adipocytes in adipose tissue. Although $S1PR_2$ has been reported to affect macrophage polarization and cytokine release, the precise mechanism of JTE 013 on activated macrophage-induced iNOS regulation requires further studies. To my knowledge, no study has directly evaluated whether $S1PR_2$ in macrophages contributes to macrophage-induced-iNOS regulation in 3T3-L1 adipocytes.

Taken together, the findings from the third aim of this chapter support the proposition that the SphK1/S1P/$S1PR_2$ axis plays a pivotal role in mediating the interaction between macrophages and adipocytes, thereby influencing the regulation of iNOS within the adipose tissue microenvironment. It is conceivable that macrophages play a role in generating S1P, subsequently activating $S1PR_2$ receptors either on the surface of macrophages themselves or on neighbouring adipocytes, thereby contributing to iNOS regulation.

4.5 Conclusion

This chapter examined the role of SphK isoforms and S1PRs in iNOS regulation in stimulated 3T3-L1 adipocytes. Inhibition of SphK1 with PF543, but not SphK2 using ROME, decreased iNOS expression and NO production in stimulated adipocytes. $S1PR_2$ appears to be the dominant receptor mediating the iNOS expression and NO production in 3T3-L1 adipocytes via MAPKs (MEK-ERK and JNK) and PI3K/Akt pathway, without any observed effects on NF-KB signalling. Furthermore, the data shows that stimulation of 3T3-L1 adipocytes with activated macrophage conditioned media increased iNOS expression and NO production. Moreover, it was suggested that release of macrophage-derived S1P activates $S1PR_2$ receptors on either macrophages or adjacent adipocytes, eventually contributing to the iNOS regulation within the adipose tissue (Figure 4-17).

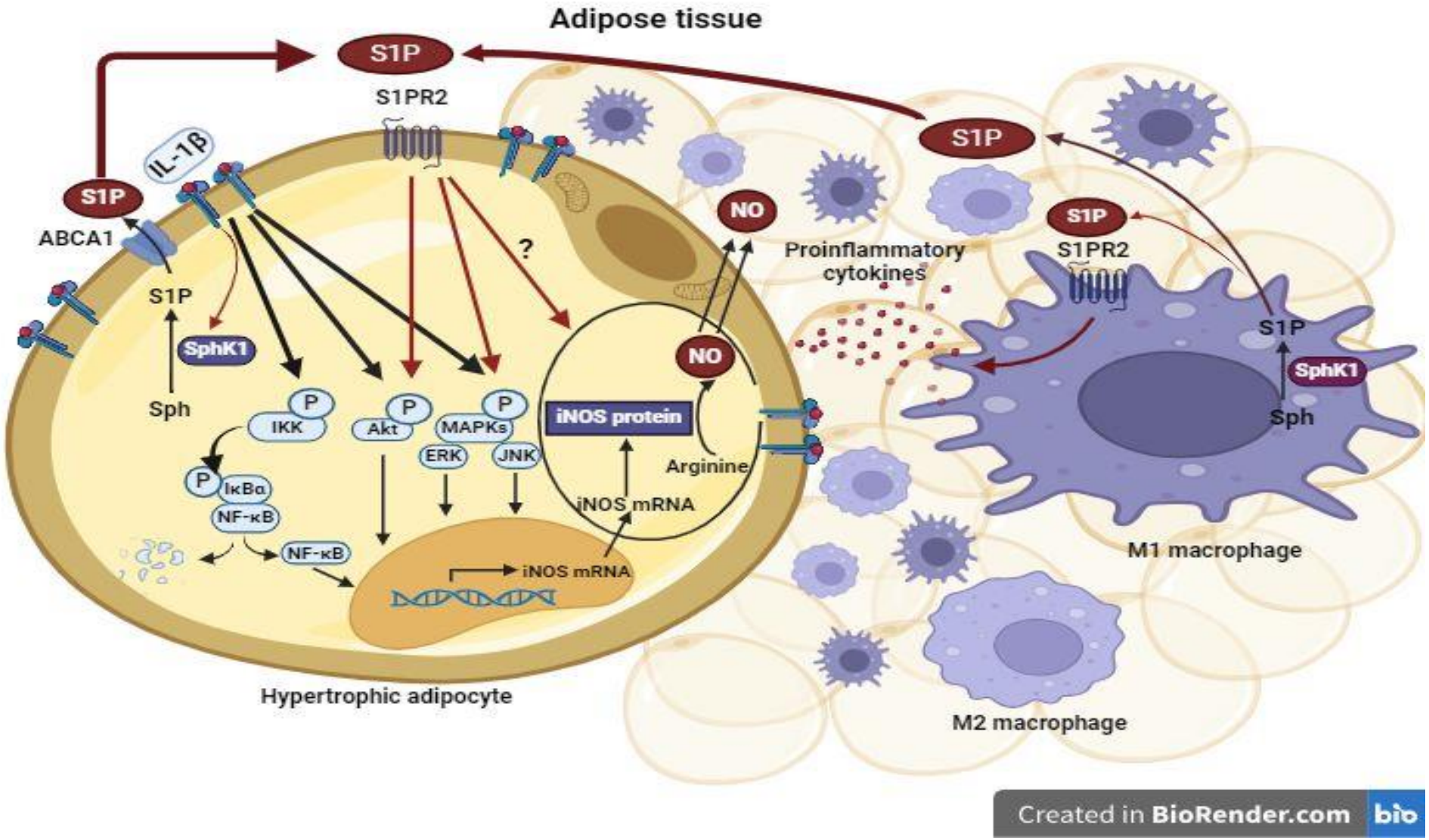

Figure 4-17 Schematic model of iNOS proinflammatory enzyme regulation by SphK1/S1P/S1PR$_2$ in adipose tissue

Chapter 5 - Characterising the role of SphK1/S1P/S1PR$_2$ in the anti-contractile effect of perivascular adipose tissue in mouse and rat aorta.

5.1 Introduction

In chapters 3 and 4, it was demonstrated that IL-1β promotes iNOS proinflammatory enzyme expression in 3T3-L1 adipocytes via the SphK1/S1P/ $S1PR_2$ axis pathway. Furthermore, the findings also support the proposition that the SphK1/S1P/$S1PR_2$ axis plays a pivotal role in mediating the interaction between macrophages and adipocytes, thereby influencing the regulation of iNOS within the adipose tissue microenvironment. Therefore, it was important to extend this investigation to perivascular adipose tissue (PVAT) to gain further insight how this system regulates iNOS in more complex and physiologically relevant environment, which more accurately reflects the in vivo conditions and potential interactions with vascular function.

PVAT is adipose tissue that surrounds blood vessels, and it has important paracrine effects that regulates the vasculature, by producing and releasing number of endogenous substances (Cheng et al, 2018; Szasz et al, 2012). NO is among the endogenous substances diffusing from PVAT causes relaxation via activation of the cyclic guanosine monophosphate (cGMP) pathway through activation of soluble guanylate cyclase in smooth muscle cells. PVAT-derived mediators may also interact with endothelium, stimulating endothelial cells to produce additional NO, further enhancing vasodilation (Szasz et al, 2013). In addition, PVAT-derived NO could activate potassium channels in endothelium and vascular smooth muscle cells as part of the vasodilator effect (Stanek et al, 2021).

NO can be produced by three isoforms of NO synthase (NOS): calcium-dependent endothelial cell NOS (eNOS), neuronal type NOS (nNOS), and an inducible type (iNOS), which is generally calcium-independent (Förstermann & Sessa, 2012). iNOS produces relatively high amounts of NO and its expression can be induced by a variety of cytokines including IL-1β, TNF-α, and LPS (Kleinert et al, 2004). IL-1β is a potent proinflammatory mediator produced by various cell types, including macrophages, preadipocytes and adipocytes (Coppack, 2001; Renovato-Martins et al, 2020). IL-1β activates various downstream signalling pathways upon binding to its receptor, inducing iNOS expression and subsequent nitric oxide production, contributing to inflammatory processes (Cortese-Krott et al, 2014; Park et al, 2021). The expression of iNOS has been implicated in many cardiovascular diseases

associated with inflammation, such as obesity, insulin resistance, diabetes, septic shock, heart failure, and atherosclerosis (Shah, 2000; Soskić et al, 2011). However, iNOS also has an important role in protecting against viral and bacterial infections, decreasing leukocyte adhesion, having anti-platelet activity, antioxidant activity, reducing vascular permeability, and improving cardiac diastolic function. On the other hand, iNOS expression has been associated with many harmful effects, such as reduced cardiac efficiency and inhibition of cardiac contractility (Shah, 2000).

The expression of iNOS protein in PVAT has been reported in many inflammatory diseases, such as septic shock (Hai-Mei et al, 2013; Kapur et al, 1999), atherosclerosis (Nakladal et al, 2022), and obesity (Araujo et al, 2018; Reis Costa et al, 2021). iNOS-derived NO released by PVAT has been reported to cause hypoactivity of surrounding vessels in multiple studies. For example, LPS upregulates iNOS expression in PVAT of rat thoracic aorta and was shown to cause hyporeactivity (Hai-Mei et al, 2013). Moreover, it was demonstrated that hyporeactivity induced by PVAT in septic mice was inhibited by an iNOS inhibitor (Awata et al, 2019). Similarly, a high-carbohydrate diet caused hypoactivity in mouse thoracic aorta with intact PVAT, and this was attenuated by iNOS inhibition (Reis Costa et al, 2021). However, the underling mechanism of iNOS regulation in PVAT is still under investigation.

S1P, the product of the enzyme Sphk1 binds to and activates S1P receptors in endothelial and vascular smooth muscle cells and this has a significant role in controlling vascular tone. Indeed, S1P has demonstrated a vasodilator effect in multiple studies by interacting with the $S1PR_1$ and $S1PR_3$ receptors in endothelial cells to activate endothelial nitric oxide synthase (eNOS) to produce and release NO (Igarashi & Michel, 2009). However, paradoxically, S1P can exert a vasoconstrictor effect via activation of several different S1P receptor subtypes including $S1PR_1$, $S1PR_2$ and the $S1PR_3$ receptor in VSMCs (Coussin et al, 2002). Furthermore, SphKs/S1P signalling has been implicated in adipose tissue function, and more importantly, to be activated under inflammatory conditions. Briefly, SphK1 and its product S1P are increased in obese mice and promote inflammation in epididymal adipose tissue (Tous et al, 2014; Wang et al, 2014). Similar findings were also shown in human inflamed subcutaneous adipose tissue in comparison to

less inflamed adipose tissue (Fayyaz et al, 2014). Although it is known that S1P can modulate vascular smooth muscle and endothelial function, it is still unknown whether the sphingolipid system can modulate the anti-contractile effect of PVAT under inflammatory condition. These findings, along with many others, highlight the importance of investigating the interaction between the sphingolipid system and the regulation of iNOS in PVAT, particularly in relation to vascular reactivity.

Several studies have examined the effect of IL-1β on vascular function via the iNOS-dependent pathway. For example, it was demonstrated that IL-1β suppresses contraction to PE in rat aortic rings, and this has been linked with the activation of iNOS (Soler et al, 2003; Yang et al, 2004). Moreover, another study has reported that IL-1β causes gradual relaxation in isolated rat superior mesenteric arteries via the iNOS-dependent pathway (Yuui et al, 2016). However, the direct effect of IL-1β on production of NO derived from iNOS in the PVAT has been poorly studied.

Considering the published data and the results presented in chapters 3 and 4, the hypothesis is that IL-1β will promote iNOS-derived NO production in PVAT to cause a vasorelaxant effect. This effect is anticipated to be mediated through the SphK1/S1P/$S1PR_2$ axis pathway, either by modulating iNOS activity within the adipose tissue or additionally by triggering the release of S1P from adipose tissue, thereby exerting a paracrine influence on vascular tone. Taken together, this chapter will investigate the role of the sphingolipid system in regulation of iNOS-derived NO from PVAT and how this affects its anticontractile function.

5.2 Aims

1. To investigate the effect of PVAT on contractile responses to PE in a mouse aortic ring and to test whether S1P agonists induce vascular relaxation in mouse aortic rings with and without PVAT.

2. To investigate the effect of IL-1β in the presence and absence of S1P on the anticontractile effect of PVAT in mouse aortic rings.

3. To investigate the effect of PVAT on contractile responses to U46619 and to test whether S1P agonists modulate vascular relaxation in rat aortic rings.

4. To investigate the effect of IL-1β on iNOS expression and NO production in in rat aortic rings containing PVAT and whether this accounts for its anticontractile effect.

5. To investigate the direct contribution of potassium channels to the IL-1β-augmented PVAT anticontractile effect in rat aortic rings.

6. To investigate the effect of IL-1β on SphK1 phosphorylation and gene expression in PVAT of the rat thoracic aorta and test whether the SphK1/S1P/$S1PR_2$ axis pathway is implicated in IL-1β-mediated hyporeactivity.

5.3 Results

5.3.1 PVAT decreases the contraction response in mouse thoracic aorta

It was demonstrated previously in our lab that PVAT of the mouse thoracic aorta attenuates the contraction to U46619 (Almabrouk et al, 2017). Therefore, to confirm the anticontractile effect of PVAT in this study, a contractile response to a different constrictor agent, PE (1×10^{-6} M) was tested in rings of mouse thoracic aorta with intact endothelium in the presence and absence of PVAT. The presence of PVAT significantly ($p<0.05$) inhibited contraction induced by PE (% of maximum KPSS-induced contraction 58.65 ± 25.34%) compared to rings without PVAT (98.32 ± 31.87%) in mouse thoracic aorta (Figure 5-1).

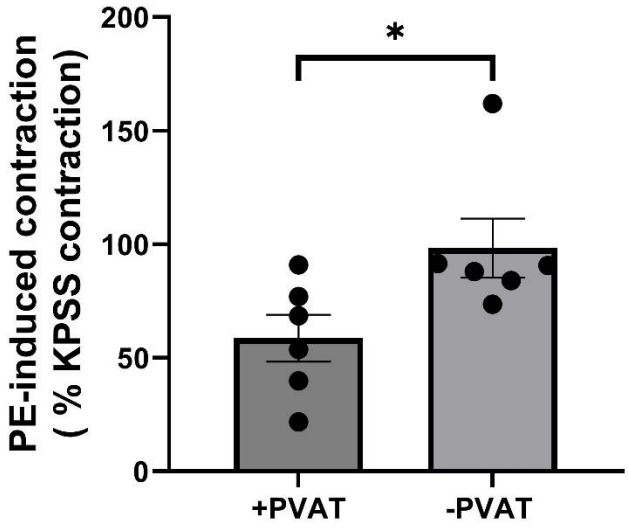

Figure 5-1 Effect of PVAT on vascular contraction in mouse thoracic aorta.

Contraction response to PE (1×10^{-6} M) in endothelium-intact thoracic aorta rings in the presence (n=6) and absence of PVAT (n=6). The data represent samples from six independent experiments expressed as the mean ± SEM % of KPSS-induced contraction. Statistical analysis was carried out using Student's unpaired t-test. Asterisks indicate a p value of (*p<0.05).

5.3.2 S1P and S1P agonists do not induce vasorelaxation in mouse aorta

To examine the effect of sphingolipids on vascular function in mouse aorta, S1P and S1P agonists were added to the mouse aorta in the presence or absence of PVAT. Addition of S1P (1nM-3μM) to endothelium-intact thoracic aorta did not induce a measurable relaxation in either rings with or without PVAT, the maximum relaxation was 11 ± 9% in rings with PVAT compared to 2.33 ± 1.53% in rings without PVAT (Figure 5-2A).

CYM5541, a $S1PR_3$ agonist was added to the mouse aorta in concentrations ranging from 1 nM to 10 μM in the presence and absence of PVAT. Addition of CYM5541 to endothelium-intact thoracic aorta did not induce a significant relaxation in either rings with or without PVAT; the maximum relaxation was 7.00 ± 12.28% in rings with PVAT, compared to 5.33 ± 0.57% in rings without (Figure 5-2B).

SEW2871, a $S1PR_1$ agonist was then tested at concentrations ranging from 1 nM to 10 μM in the presence and absence of PVAT, as shown in Figure 5-2C. Addition of SEW to endothelium-intact thoracic aorta did not induce any relaxation in either rings with or without PVAT; the maximum relaxation was 0.33 ± 1.52% in rings with PVAT, compared to 1.00 ± 1.73% in rings without PVAT.

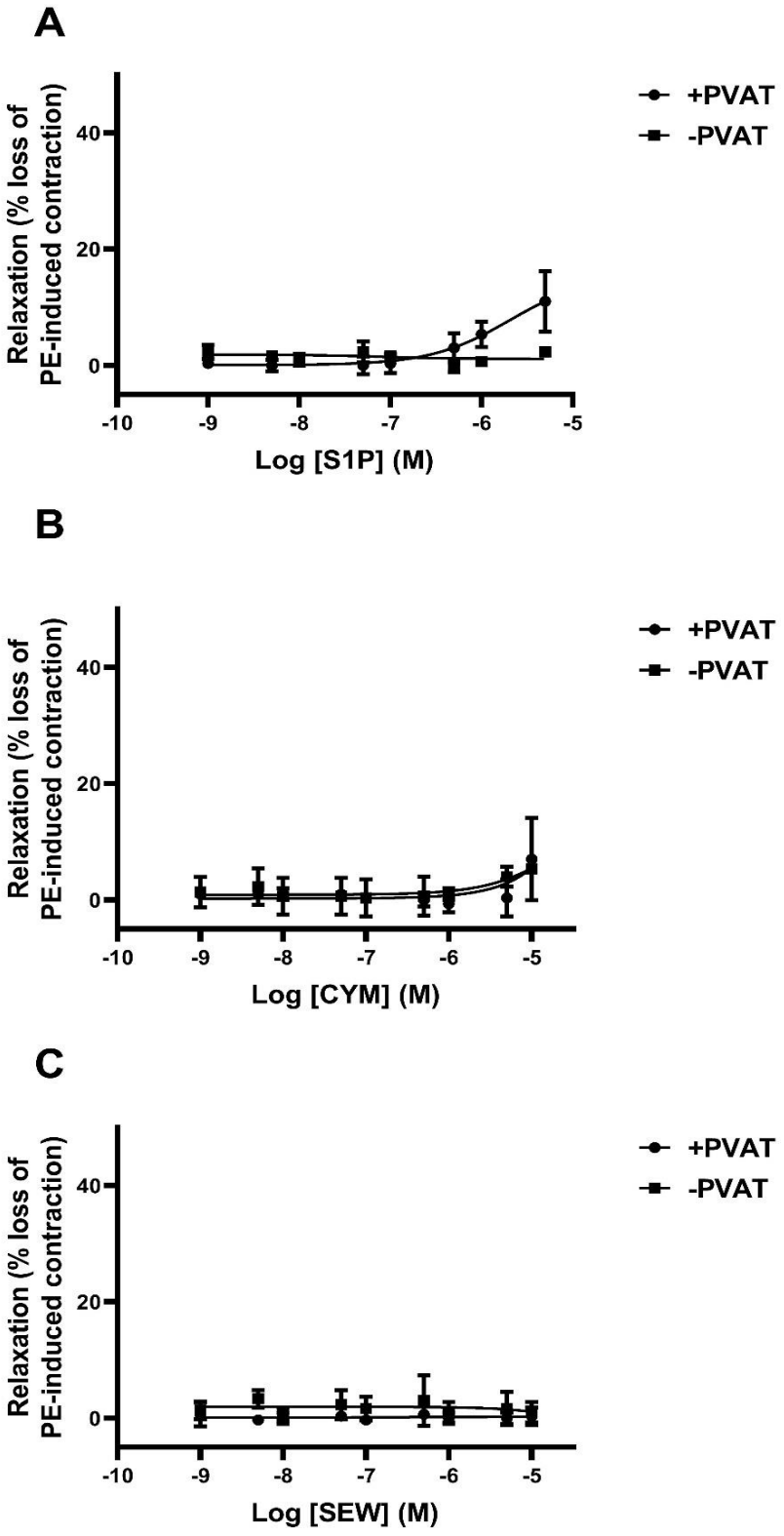

Figure 5-2 Effect of S1P and S1P agonists on vascular tone in phenylephrine-precontracted, endothelium-intact mouse thoracic aorta.

(A) Concentration–response curves to S1P (1nM-3μM) in rings with perivascular adipose tissue (PVAT) compared to aortic rings without PVAT (n=3). (B) Concentration–response curves to CYM5541 (1nM–10μM) in rings with and without PVAT (n=3). (C) Concentration–response curves to SEW2871 (1nM–10μM) in rings with and without PVAT (n=3). Statistical analysis was carried out using two-way ANOVA (with Bonferroni's test).

5.3.3 Effect of IL-1β on vascular activity in mouse thoracic aorta with PVAT

In order to determine whether IL-1ß alters the contractile response to PE, a series of experiments was carried out in endothelium-intact mouse thoracic aorta with intact PVAT under control and inflammatory conditions. Concentration response curves to PE (1nM-30μM) were constructed in rings in the presence and absence of IL-1ß (10 ng/ml). Addition of PE to intact thoracic aorta with PVAT in the presence or absence of IL-1ß resulted in a concentration-dependent contraction. Preincubation of rings with PVAT with IL-1ß for 2 hours did not significantly alter the contractile response to PE (% of maximum KPSS-induced contraction 100.10 ± 31.59%) compared with rings under control conditions (113.59 ± 43.53%) (Figure 5-3A).

Pre-treatment of rings with PVAT with S1P (10 μM) did not significantly alter the contraction induced by PE in intact mouse aorta with PVAT (% of maximum KPSS-induced maximum contraction, 113.98 ± 47.87%), compared to untreated rings (113.59 ± 43.59%) under normal conditions (Figure 5-3B). Similarly, under inflammatory conditions, pretreatment with S1P prior to being incubated with IL-1ß did not significantly affect the contraction induced by PE (% of maximum KPSS-induced contraction 112.33 ± 32.32%), compared to rings incubated with IL-1ß alone (% of maximum KPSS-induced contraction 100.10 ± 31.59%) (Figure 5-3C).

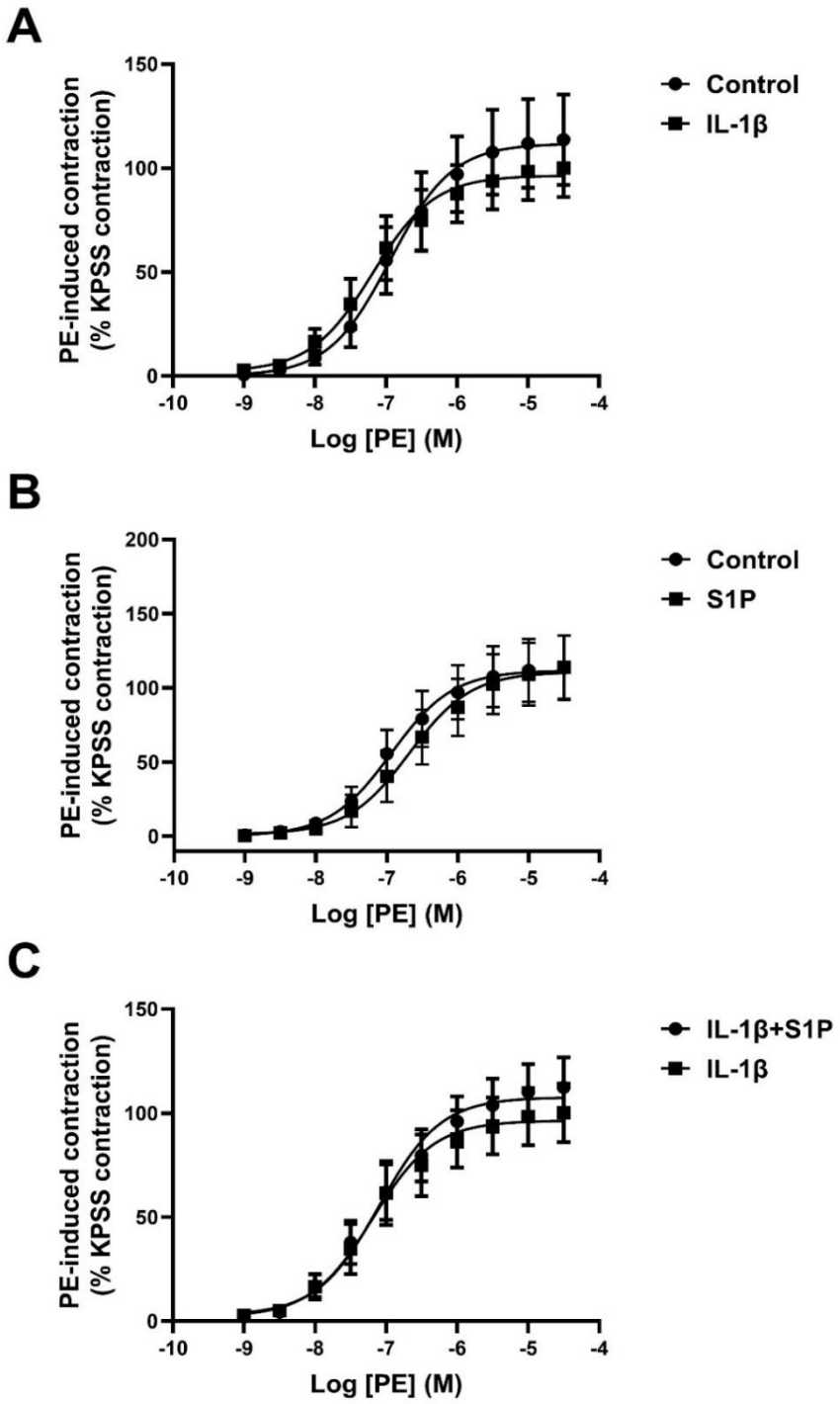

Figure 5-3 Effect of IL-1β on contractile response to PE (1nM-30μM) in mouse aortic rings.

Aortic rings were preincubated with either IL-1β (10 ng/ml) alone or IL-1β plus S1P (10 μM) for 2 hours before concentration response curves were constructed. (A) Concentration response curves for the contractile effect of PE (1nM-30μM) in endothelium-intact mouse aorta with PVAT in presence (n=5) and absence of IL-1β (n=4). (B) Concentration response curves for the contractile effect of PE (1nM-30μM) in endothelium-intact mouse aorta with PVAT in presence (n=5) and absence of S1P (n=4). (C) Concentration response curves for the contractile effect of PE (1nM-30μM) in endothelium-intact mouse aorta rings with PVAT preincubated with IL-1β alone (n=5) compared to rings preincubated with IL-1β plus S1P (n=5). Data are expressed as a percentage of maximum KPSS contraction for n arteries from different animals. Statistical analysis was carried out using two-way ANOVA (with Bonferroni's test).

5.3.4 S1P induces vascular relaxation in rat thoracic aorta

Since there was no observable effect of either S1P or selective S1P agonists on vascular activity in mouse aortic rings, a decision was taken to use rats since we previously confirmed in our lab that S1P induces a vasorelaxant effect in rat thoracic aorta (Alganga et al, 2019). To confirm that S1P has a relaxant effect on rat aorta, S1P was added to endothelium-intact thoracic aorta precontracted with U46619 (the contractile agent used by Alganga et al) in increasing concentrations (1nM–3μM). A relaxant effect to S1P was observed (maximal relaxion 30 ± 2.64%) which was significantly greater than the loss of contractile tone in time control rings (maximal relaxation 0.66 ± 1.15%; Figure 5-4).

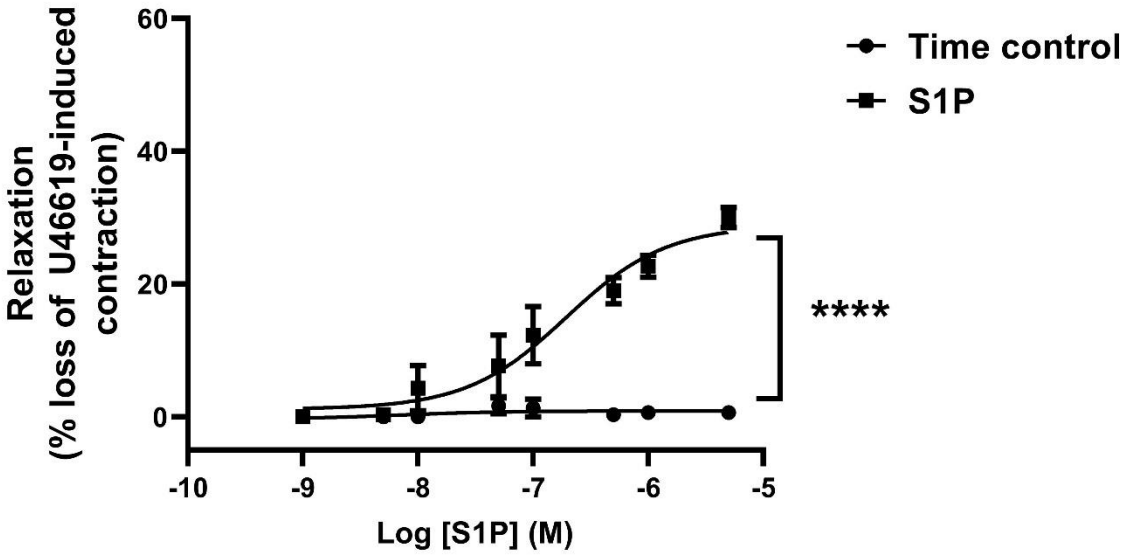

Figure 5-4 Effect of S1P on vascular tone in rat thoracic aorta.

Concentration–response curve to S1P (1nM–3μM) in U46619 pre-contracted endothelium-intact aortic rings compared to time control. Data are expressed as mean ± SEM for 3 arteries from different animals. Statistical analysis was carried out using two-way ANOVA (with Bonferroni's test). Asterisks (****) indicate a p value of <0.0001.

5.3.5 PVAT decreases the contractile response to U46619 in rat thoracic aorta

To test whether the presence of PVAT can alter contraction in rat aorta, a concentration response curve to U46619 (1×10^{-9}-1×10^{-6} M) was performed in endothelium-intact rat thoracic aorta in the presence and absence of PVAT. The

presence of PVAT significantly ($p<0.01$) decreased contraction induced by U46619 (% of maximum KPSS-induced contraction 104.80 ± 30.87%), compared to rings without PVAT (% of maximum KPSS-induced contraction 121.99 ± 9.33%; Figure 5-5).

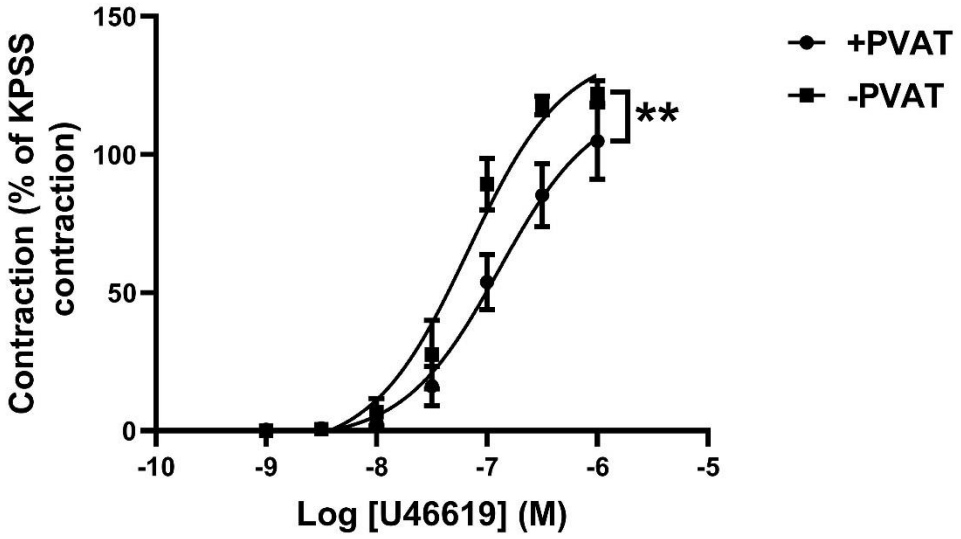

Figure 5-5 Effect of PVAT on contractile response to U46619 in rat aortic rings.

Concentration response curves to U46619 (1×10^{-9}-1×10^{-6} M) in endothelium-intact rat aorta in the presence (n=5) and absence (n=4) of PVAT. Data are expressed as a percentage of maximum KPSS contraction and shown as mean ± SEM for at least 4 arteries from different animals. Statistical analysis was carried out using two-way ANOVA (with Bonferroni's test). Asterisks indicate a p value of <0.01.

5.3.6 IL-1β induces iNOS and NO production in PVAT from rat thoracic aorta

To establish if IL-1β induces iNOS expression and NO production in PVAT from thoracic aorta, PVAT samples were stimulated with IL-1β for 1 h, 2 h, 4 h, 6 h and 8 h. IL-1β-induced iNOS protein expression was then determined by western blot analysis. IL-1β (10 ng/ml) started to cause a significant (*$p<0.05$, **$p<0.01$) increase in iNOS in PVAT at time points of 4 h and longer (Figure 5-6B). NO production, determined by nitrite/nitrate in the medium, was also measured and it was found that IL-1β started to increase NO production after 4 h, however, this only became significant after 6 h and 8 h in PVAT (Figure 5-6C).

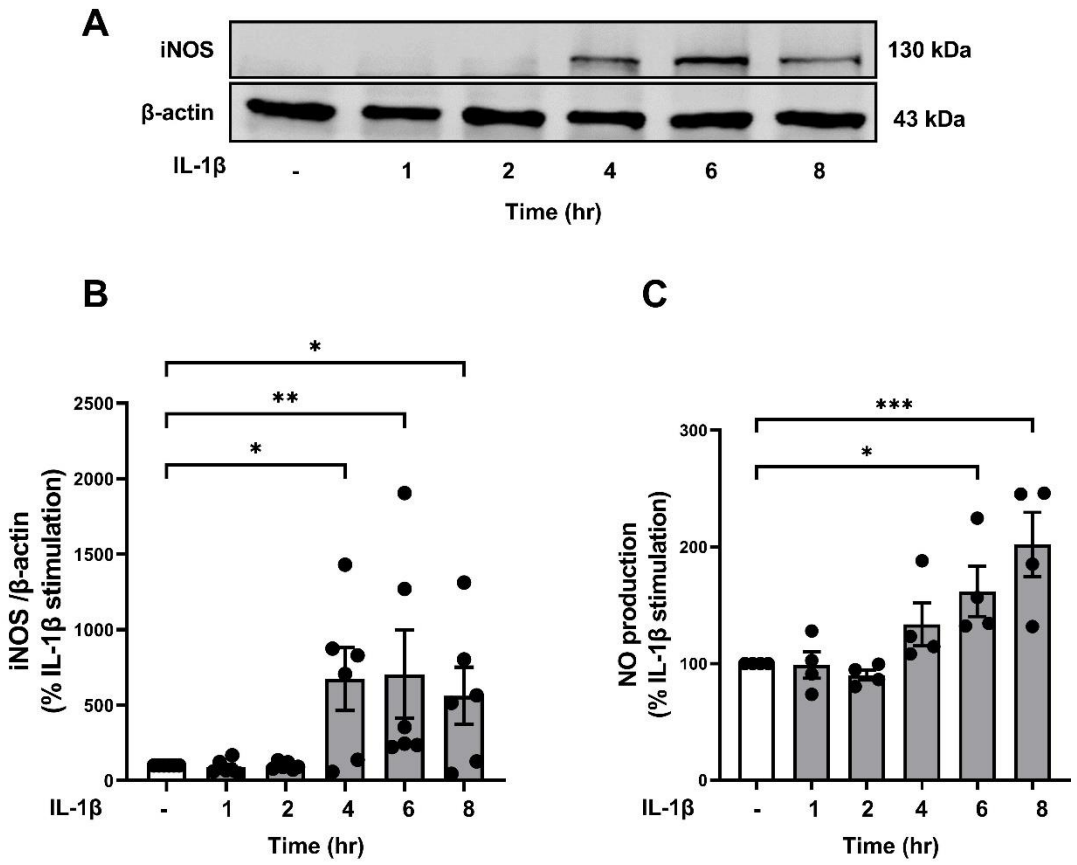

Figure 5-6 Effect of an inflammatory stimulus (IL-1β) on iNOS expression and NO production by PVAT from rat thoracic artery.

PVAT was stimulated with IL-1β (10 ng/ml) for various time points. PVAT lysates were prepared at indicated time points and resolved by SDS-PAGE with the appropriate antibodies. Media was collected and NO production was investigated by using a Sievers 280A NO Meter. (A and B) representative western blotting images and graph for the change in iNOS protein expression. Protein expression of iNOS was normalised to the expression of β-actin. (C) IL-1β stimulated NO production in PVAT. The data represent samples from at least four different experiments expressed as the mean ± SEM of the % fold change relative to control (untreated). Statistical analysis was carried out using one-way ANOVA (with Fisher LSD test). Asterisks indicate a p value of (*p<0.05, **p<0.01, ***p<0.001).

5.3.7 IL-1β decreases contraction to U46619 in rat aortic rings with and without PVAT

In order to determine whether IL-1β alters the contractile response to U46619, a number of experiments in vessels with and without PVAT under control and inflammatory conditions. Addition of U46619 ($1x10^{-9}$-$1x10^{-6}$ M) to endothelium-intact thoracic aorta without PVAT in the presence or absence of IL-1β resulted in a concentration-dependent contraction. Preincubation of vessels without PVAT with IL-1β (10 ng/ml) for 4 hours significantly attenuated the contractile response

to U46619 (% of maximum KPSS-induced contraction 110.29 ± 6.15%) compared with vessels under control conditions (% of maximum KPSS-induced contraction 121.99 ± 9.33) (Figure 5-7A).

Repeating these experiments in vessels with PVAT also resulted in a concentration-dependent contraction in response to U46619. However, preincubation of vessels with IL-1β (10 ng/ml) for 4 hours significantly attenuated the contractile response to U46619 (maximal contraction 83.39 ± 33.32%) compared with vessels under control conditions (maximal contraction 113.11 ± 28.90) (Figure 5-7B).

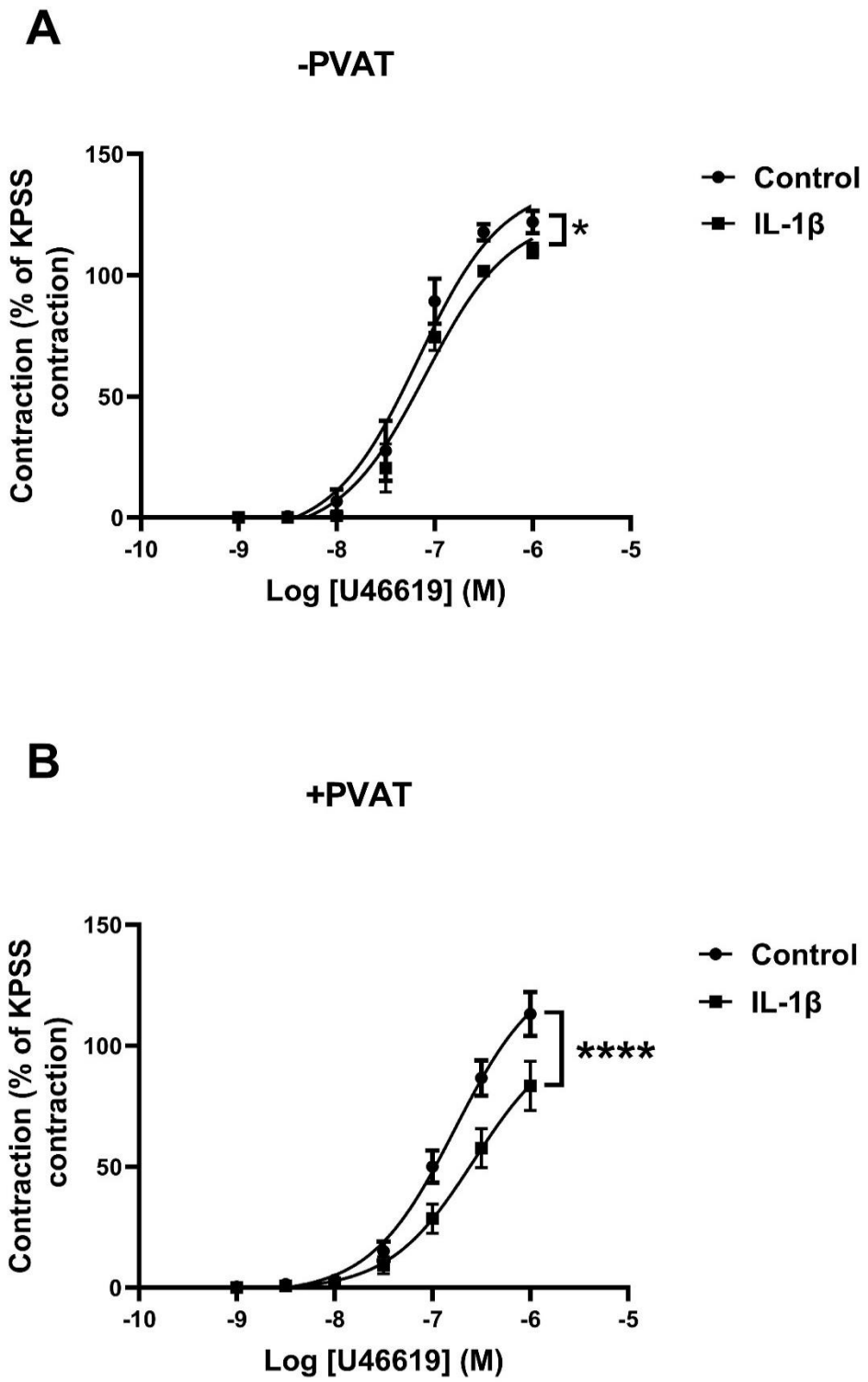

Figure 5-7 Effect of IL-1β on contractile response to U46619 in rat aortic rings with and without PVAT.

(A) Concentration response curves for the contractile effect of U46619 (1×10^{-9}-1×10^{-6} M) in endothelium-intact rat aorta without PVAT in presence (n=4) and absence (n=4) of IL-1β. (B) Concentration response curves for the contractile effect of U46619 (1×10^{-9}-1×10^{-6} M) in endothelium-intact rat aorta with PVAT in the presence (n=10) and absence of IL-1β (n=10). Data are expressed as a percentage of maximum KPSS contraction and shown as mean ± SEM for n arteries from different animals. Statistical analysis was carried out using two-way ANOVA (with Bonferroni's test). Asterisks indicate a p value of (*p<0.05, ****p<0.0001).

5.3.8 IL-1β upregulates iNOS mRNA and NO production in rings with PVAT

Since it was shown that IL-1ß augments the anticontractile effect of PVAT in rat thoracic aorta, experiments were performed to investigate whether IL-1ß would affect iNOS gene expression and NO production in rings with PVAT. After testing the effect of IL-1ß on vascular reactivity, the conditioned media bathing the ring and the rings themselves with attached PVAT were collected. RNA was isolated from rings with PVAT and quantified by qPCR. NO production was determined by nitrite/nitrate in the medium.

Rings with PVAT incubated with IL-1ß, demonstrated an increase in iNOS gene expression compared to rings under control condition (Figure 5-8A), since n=2 for these experiments, statistical analysis was not possible. Similarly, rings with PVAT incubated with IL-1ß, had a significant ($p<0.05$) increase in NO production compared to rings under control condition (Figure 5-8B).

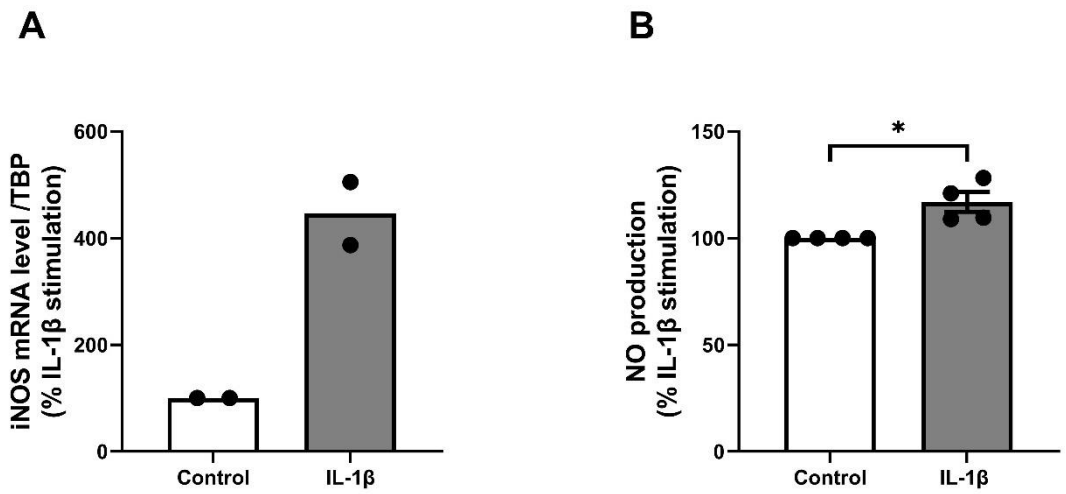

Figure 5-8 The effect of IL-1β on iNOS mRNA expression and NO production in aortic rings with PVAT.

RNA was isolated and quantified by qPCR. (A) qPCR analysis showing the changes in mRNA levels of iNOS following 4h of 10 ng/ml IL-1β treatment of aortic rings with intact PVAT relative to levels of TATA binding protein (TBP) mRNA. (B) Media from IL-1β-treated and untreated aortic rings with PVAT was collected, and NO production was investigated by using a Sievers 280A NO Meter. The data represent samples from two independent experiments for iNOS gene expression and four different experiments for NO production, expressed as the mean ± SEM of the % fold change relative to control (untreated). Statistical analysis was carried out using the Student's unpaired T-test. Asterisks indicate a p value of <0.05.

5.3.9 IL-1β does not affect contraction to U46619 in rat aortic rings with intact PVAT and denuded-endothelium

In order to determine whether the endothelium alters the contractile response to U46619 in rat aortic rings with PVAT under inflammatory conditions, a number of experiments were carried out in vessels with PVAT and either intact endothelium or mechanically removed endothelium. Addition of U46619 ($1x10^{-9}$-$1x10^{-6}$ M) produced a concentration-dependent contraction in all rings whether under control or inflammatory conditions. Figure 5-9A shows that the contractile response to U46619 in rings with intact PVAT was not significantly altered when the endothelium was removed (% of maximum KPSS-induced contraction 117.50 ± 26.25% vs. 113.11 ± 28.90%). The contractile response to U46619 was also not significantly altered in denuded rat thoracic aorta preincubated with IL-1β for 4 hours (% of maximum KPSS-induced contraction 112.95 ± 31.54%; Figure 5-9B) compared with denuded vessels under control conditions (% of maximum KPSS-induced contraction 117.79 ± 28.26%; Figure 5-9B).

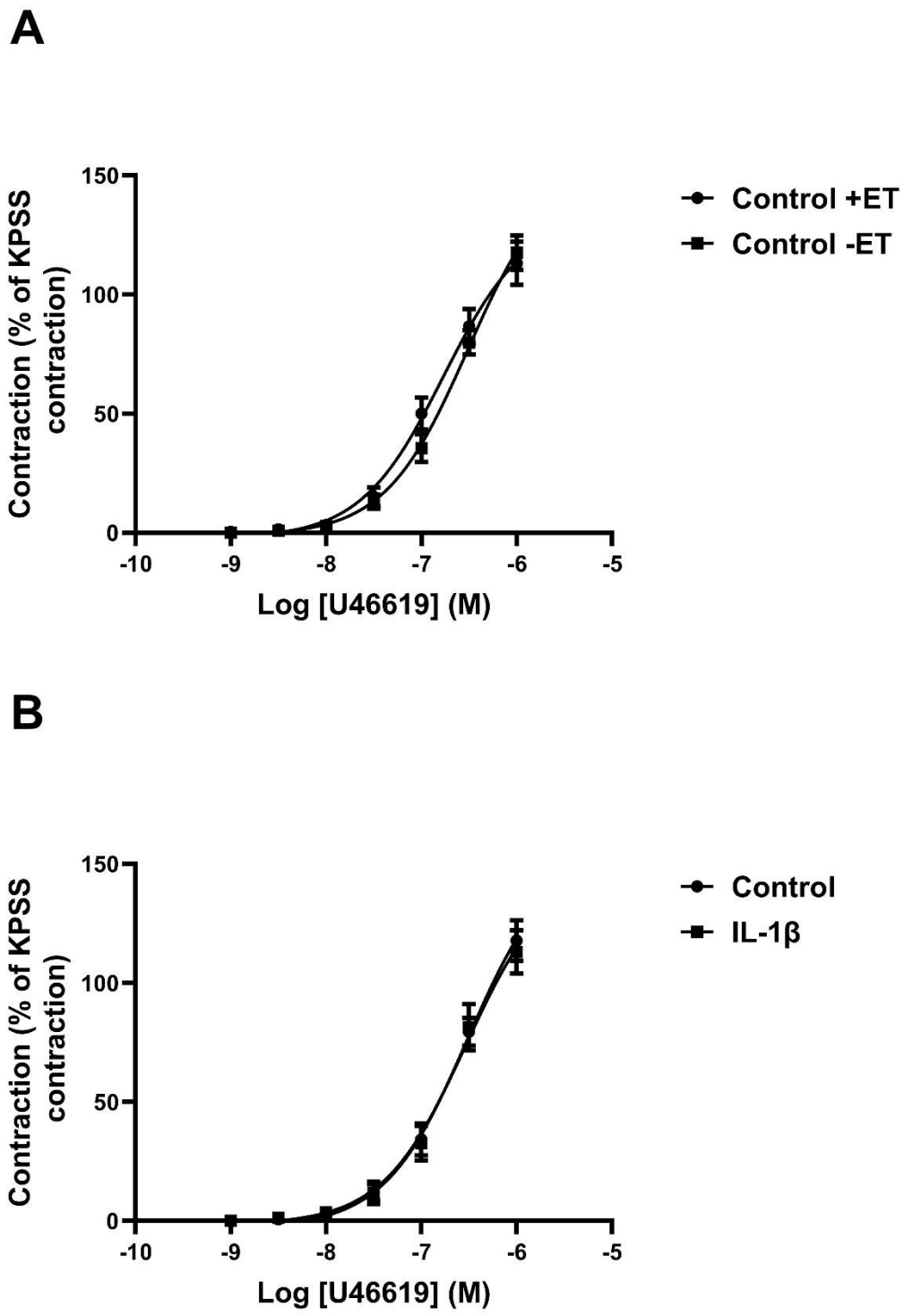

Figure 5-9 The effect of IL-1β on contraction to U46619 in rat aortic rings with intact PVAT.

Contractile responses to U46619 in rat aorta with PVAT in the presence and absence of endothelium under normal and inflammatory conditions (10 ng/ml IL-1β). (A) Concentration response curves for the contractile effect of U46619 (1×10^{-9}-1×10^{-6} M) in endothelium-intact rat aorta with PVAT (n=10) compared to rings with denuded-endothelium (n=13). (B) Concentration response curves for the contractile effect of U46619 (1×10^{-9}-1×10^{-6} M) in endothelium-denuded rat aorta under normal conditions (n=11) compared to inflammatory conditions (n=12). Data are expressed as a percentage of maximum KPSS contraction and shown as mean ± SEM for n arteries from different animals. Statistical analysis was carried out using two-way ANOVA (with Bonferroni's test).

5.3.10 1400W (iNOS inhibitor) attenuates the hypo-contractility induced by IL-1β in aortic rings with PVAT and either an intact or denuded-endothelium

In order to confirm whether IL-1ß-induced hypocontractililty is due to iNOS upregulation, a series of experiments was carried out to examine the response of endothelium-intact and denuded rat thoracic aorta with PVAT under inflammatory conditions (IL-1ß). Addition of U46619 ($1x10^{-9}$-$1x10^{-6}$ M) to rings in the presence and absence of endothelium resulted in a concentration-dependent contraction under inflammatory conditions. The selective iNOS inhibitor 1400W was added 10 min before generating dose response curves.

Pretreatment of endothelium-intact vessels with 1400W (10 μM) prior to generating dose response curves in rings preincubated with IL-1ß (10 ng/ml) for 4 hours significantly attenuated the hypo-contractile response to U46619 (% of maximum KPSS-induced contraction 134.84 ± 23.16%) compared with vessels incubated with IL-1ß alone (% of maximum KPSS-induced contraction 83.39 ± 32.33%) (Figure 5-10A).

Pretreatment of denuded vessels with 1400W (10 μM) also significantly attenuated the contractile response to U46619 (% of maximum KPSS-induced contraction 125.45 ± 28.77%) compared with vessels incubated with IL-1ß alone (% of maximum KPSS-induced contraction 103.99 ± 31.92%) (Figure 5-10B).

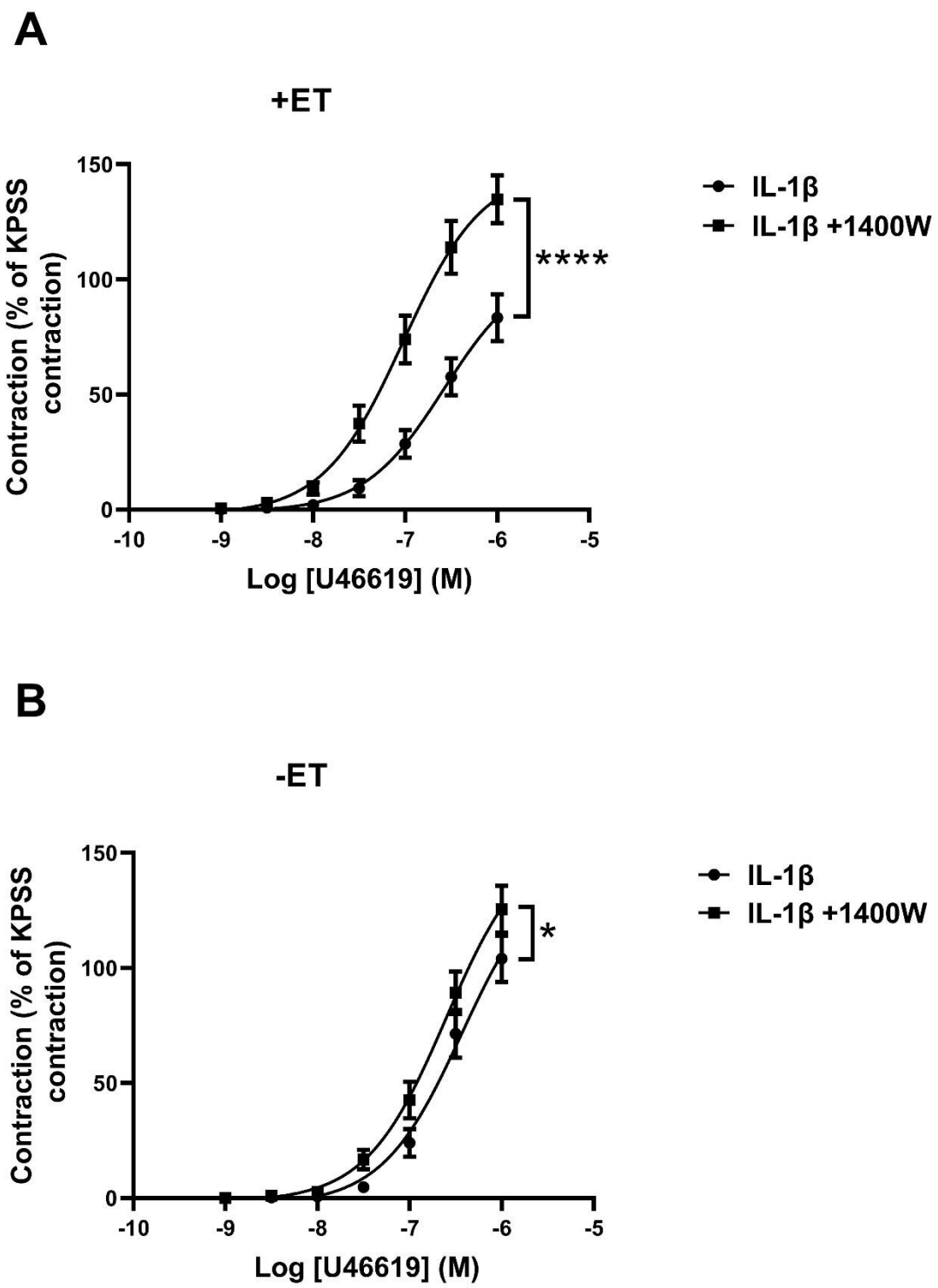

Figure 5-10 Contractile responses to U46619 in rat aorta with PVAT in presence and absence of iNOS inhibitor, 1400W ($1x10^{-5}$ M), under inflammatory conditions (10 ng/ml IL-1β).

(A) Concentration response curves to U46619 ($1×10^{-9}$-$1×10^{-6}$ M) in endothelium-intact rat aorta with PVAT in presence (n=10) and absence (n=5) of 1400W. (B) Concentration response curves to U46619 ($1×10^{-9}$-$1×10^{-6}$ M) in endothelium-denuded rat aorta with PVAT in presence (n=10) and absence (n=8) of 1400W. Data are expressed as a percentage of maximum KPSS contraction and shown as mean ± SEM for n arteries from different animals. Statistical analysis was carried out using two-way ANOVA (with Bonferroni's test). Asterisks indicate a p value of (*p<0.05, ****p<0.0001).

5.3.11 Role of potassium channels in IL-1β-mediated hypo-reactivity in rat aortic rings with PVAT

5.3.11.1 TEA attenuates the hypo-contractility to U46619 in aortic rings with PVAT induced by IL-1β

It has been demonstrated that potassium channels contribute to the anti-contractile effect of PVAT (Szasz et al, 2013). Therefore, it was important to elucidate whether potassium channels participate in IL-1ß-mediated hypo-reactivity in rat aortic rings with PVAT. Addition of U46619 ($1x10^{-9}$-$1x10^{-6}$ M) to an endothelium-intact thoracic aorta with PVAT in the presence and absence of a non-selective potassium channel blocker, tetraethylammonium (TEA) ($5x10^{-6}$ M) resulted in a concentration-dependent contraction under normal (control) and inflammatory (IL-1ß) conditions. TEA was added 10 min before generating the concentration response curve.

The contractile response in rat thoracic rings with PVAT to U46619 was similar in the presence (% of maximum KPSS-induced contraction 115.17 ± 30.60%) and absence (% of maximum KPSS-induced contraction 113.11 ± 28.90%) of TEA under control conditions (Figure 5-11A). Preincubation of endothelium-intact aortic rings with PVAT with TEA led to a significant (****$p<0.0001$) inhibition of IL-1ß-mediated hypo-reactivity (% of maximum KPSS-induced contraction 118.88 ± 27.82; Figure 5-11B) compared with IL-1ß alone (% of maximum KPSS-induced contraction 83.39.1 ± 33.32; Figure 5-11B).

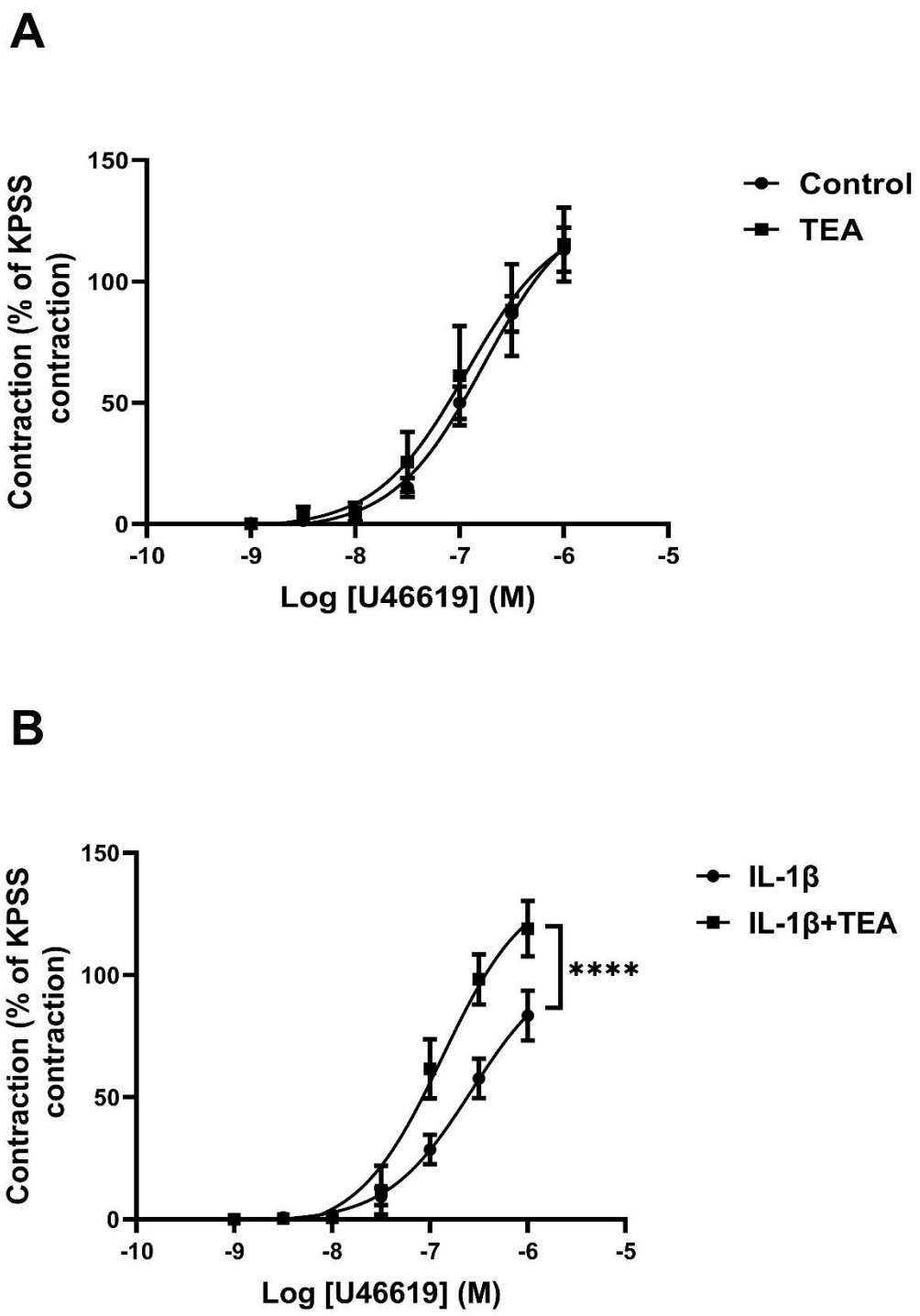

Figure 5-11 Contractile responses to U46619 in rat aorta with PVAT in presence and absence of the non-selective potassium channel blocker, tetraethylammonium ($5x10^{-6}$ M) under normal and inflammatory conditions (10 ng/ml IL-1β).

(A) Concentration response curves to U46619 ($1×10^{-9}$-$1×10^{-6}$ M) in endothelium-intact rat aorta with PVAT in presence (n=10) and absence (n=4) of TEA under normal conditions. (B) Concentration response curves for the contractile effect of U46619 (1×10-9-$1×10^{-6}$ M) in endothelium-intact rat aorta with PVAT in presence (n=10) and absence (n=6) of TEA under inflammatory conditions (10 ng/ml IL-1β). Data are expressed as a percentage of maximum KPSS contraction and shown as mean ± SEM for n arteries from different animals. Statistical analysis was carried out using two-way ANOVA (with Bonferroni's test). Asterisks indicate a p value of ****p<0.0001.

5.3.12 IL-1β activates SphK1 phosphorylation in aortic PVAT

To establish if IL-1β induces pSphK1 expression in PVAT from thoracic aorta, isolated PVAT was stimulated with IL-1β for 1 h, 2 h, 4 h, 6 h and 8 h. IL-1β-induced SphK1 protein phosphorylation was then determined by western blot analysis. Treatment of PVAT with IL-1β (10 ng/ml) (Figure 5-12) caused a significant increase in SphK1 phosphorylation compared to untreated PVAT at 4 h.

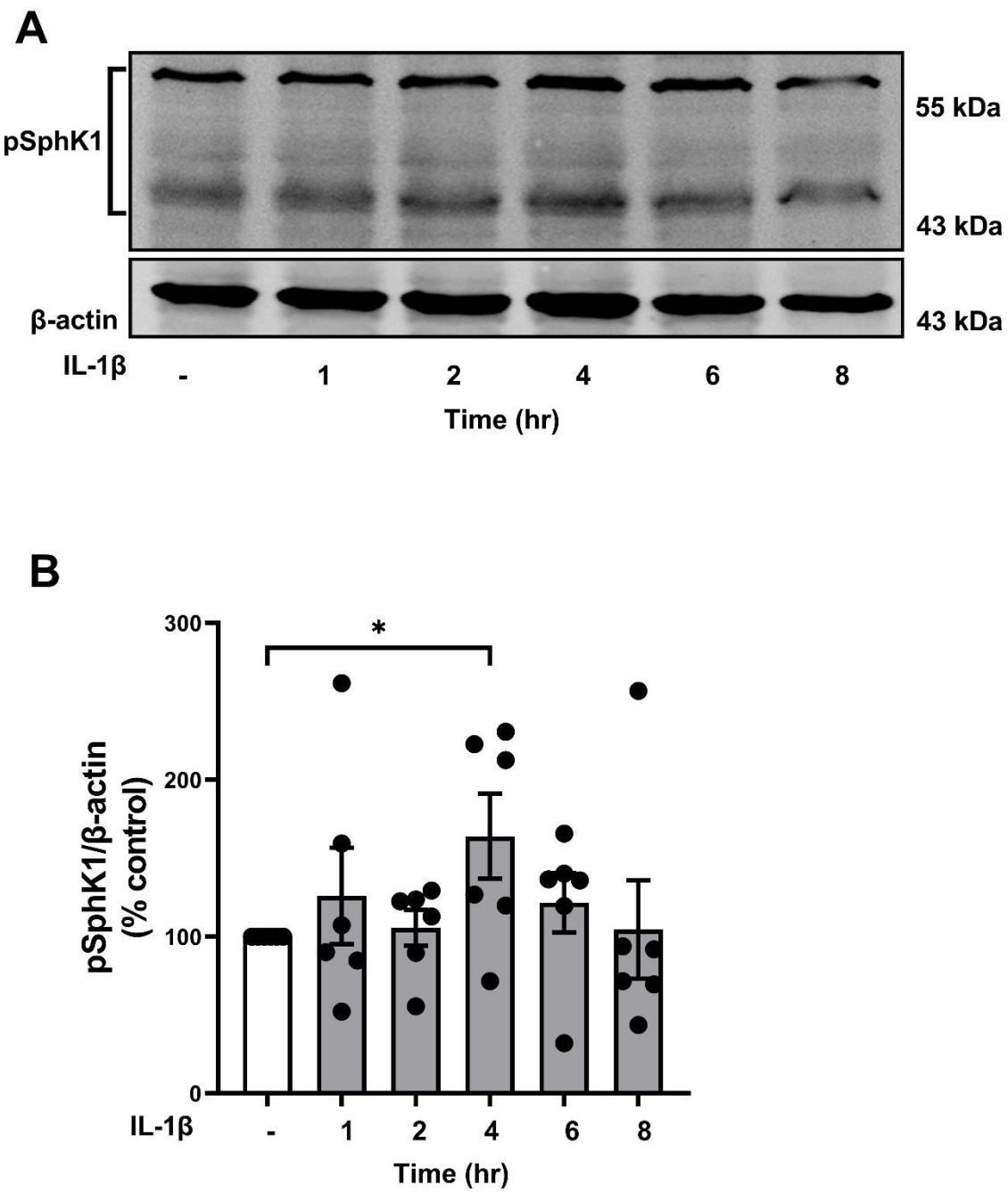

Figure 5-12 Effect of an inflammatory stimulus (IL-1β) on pSphK1 expression in PVAT of rat thoracic aorta.

Perivascular adipose tissue (PVAT) was stimulated with IL-1β (10 ng/ml) for various time points. PVAT lysates were prepared at indicated time points and resolved by SDS-PAGE with the appropriate antibodies. (A and B) representative western blotting images and graph for the change in SphK1 protein phosphorylation. Protein level of pSphK1 was normalised to level of β-actin. The data represent samples from six different experiments expressed as the mean ± SEM of the % fold change relative to control (untreated). Statistical analysis was carried out using one-way ANOVA. Asterisk indicates a p value of *p<0.05.

5.3.13 IL-1β upregulates SphK1 mRNA in rings with PVAT and Isolated PVAT

To establish if IL-1ß induces SphK1 gene expression in PVAT from thoracic aorta (TA), rings containing PVAT and isolated PVAT itself were stimulated with IL-1ß (10 ng/ml) for 4 h. RNA was isolated then quantified by qPCR. Stimulation of aortic rings containing PVAT with IL-1ß (Figure 5-13A), caused a significant (*<0.05) increase in SphK1 mRNA level, compared to control rings (untreated). Similarly, stimulation of isolated PVAT with IL-1ß displayed a tendency to increase SphK1 mRNA level although it did not reach significance due to the high degree of variability (Figure 5-13B).

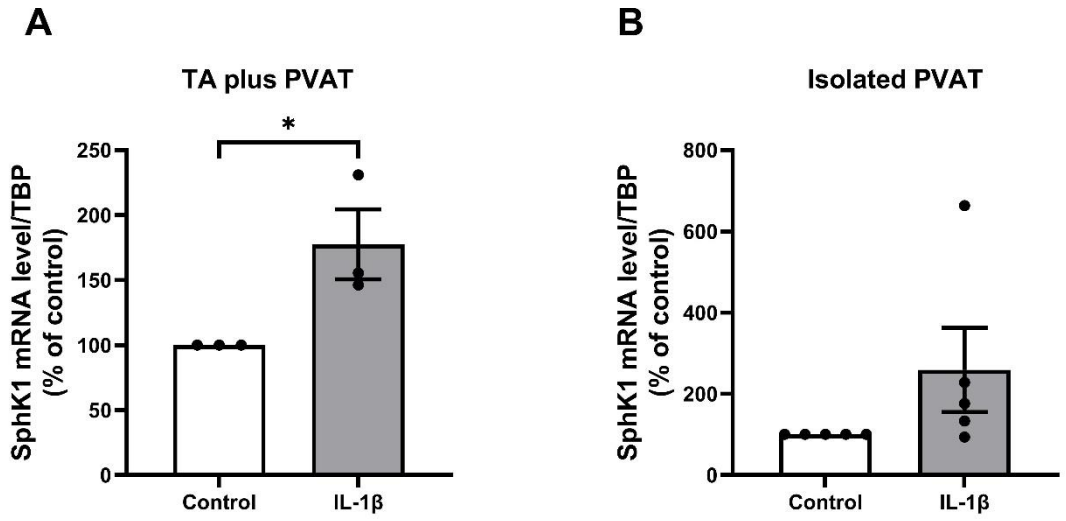

Figure 5-13 Effect of IL-1β on SphK1 mRNA expression in aortic rings containing PVAT and in PVAT itself.

Aortic rings with intact PVAT or isolated PVAT was stimulated with IL-1β (10 ng/ml) for 4 hours. RNA was isolated and quantified by qPCR. qPCR analysis showing the changes in mRNA levels of SphK1 following 4h of 10 ng/ml IL-1β in TA plus PVAT (A) and PVAT (B) relative to levels of TATA binding protein (TBP) mRNA. The data represent samples from at least three different experiments expressed as the mean± SEM of the % fold change relative to control (untreated). Statistical analysis was carried out using the unpaired T-test. Asterisk indicates a p value of *<0.05.

5.3.14 Role of SphK1/S1P on IL-1β-mediated hyporeactivity in rat aortic ring with PVAT

5.3.14.1 SphK1 inhibition does not reverse the hypo-reactivity induced by IL-1β

Since I have shown that IL-1ß increases SphK1 phosphorylation in rat aortic PVAT and also upregulates SphK1 mRNA level in aortic rings containing PVAT (Figure 5-12 and Figure 5-13), I now investigated whether SphK1 enzyme inhibition would affect IL-1ß-mediated hyporeactivity. Addition of U46619 ($1x10^{-9}$-$1x10^{-6}$ M) to endothelium-intact thoracic aorta with PVAT in the presence and absence of PF543 (100 nM) resulted in a concentration-dependent contraction under control and inflammatory (10 ng/ml IL-1ß) conditions. PF543 was added 30 min before treating vessels with (IL-1ß).

The contractile response in rat thoracic rings with PVAT to U46619 was similar in the presence (% of maximum KPSS-induced contraction 130.04.04 ± 15.41%) and absence (% of maximum KPSS-induced contraction 115.46 ± 28.5%) of PF543 under control conditions (Figure 5-14A). Similarly, the contractile response in rat thoracic rings with PVAT to U46619 was similar in the presence (% of maximum KPSS-induced contraction 78.03 ± 29.67%) and absence (% of maximum KPSS-induced contraction 83.39 ± 32.33%) of PF543 under inflammatory condition (IL-1ß) (Figure 5-14B).

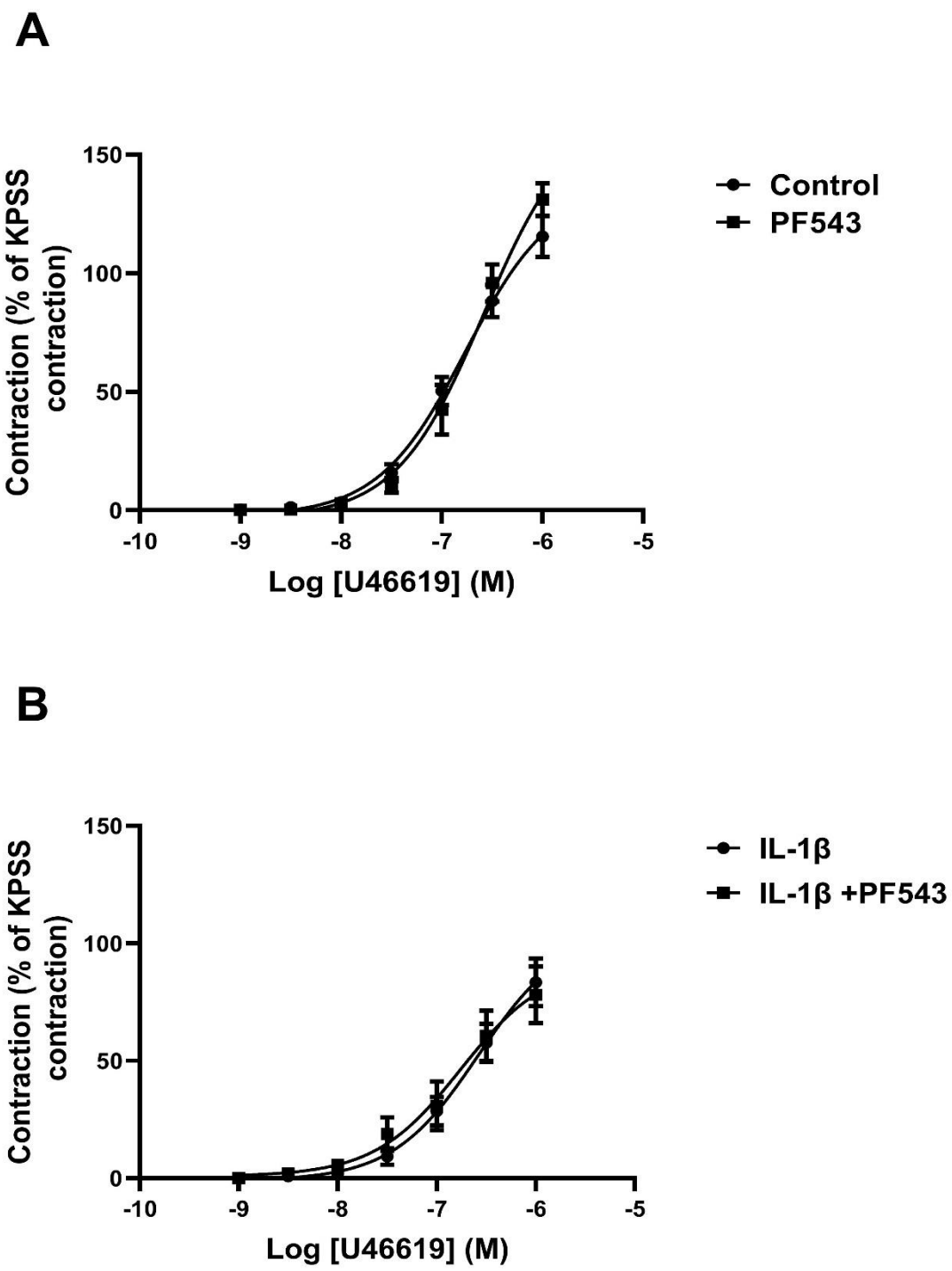

Figure 5-14 Contractile responses to U46619 in rat aorta with intact PVAT in the presence and absence of SphK1 inhibitor PF543 (100 nM) under control and inflammatory conditions (10 ng/ml IL-1β).

(A) Concentration response curves for the contractile effect of U46619 (1×10^{-9}-1×10^{-6} M) in endothelium-intact rat aorta with PVAT in presence (n=11) and absence (n=5) of PF543 under control conditions. (B) Concentration response curves for the contractile effect of U46619 (1×10^{-9}-1×10^{-6} M) in endothelium-intact rat aorta with PVAT in presence (n=10) and absence (n=6) of PF543 under inflammatory conditions (10 ng/ml IL-1ß). Data are expressed as a percentage of maximum KPSS contraction and shown as mean ± SEM for n arteries from different animals. Statistical analysis was carried out using two-way ANOVA (with Bonferroni's test).

5.3.14.2 S1PR2 inhibition does not reverse the hypo-reactivity induced by IL-1β

Since I established in the previous chapter that a $S1PR_2$ antagonist inhibits IL-1ß-mediated iNOS expression and NO production in adipocytes. I now investigated whether blocking this receptor would affect IL-1ß-mediated hyporeactivity in rat aortic vessels. Addition of U46619 ($1x10^{-9}$-$1x10^{-6}$ M) to intact thoracic aorta with PVAT in the presence and absence of the $S1P_2$ receptor antagonist JTE 013 (10 μM) resulted in a concentration-dependent contraction under control and inflammatory (10 ng/ml IL-1ß) conditions. JTE 013 was added 30 min before treating vessels with (IL-1ß).

JTE 013 significantly decreased the contractile response of rat thoracic rings with PVAT to U46619 (% of maximum KPSS-induced contraction 95.86 ± 32.88%), compared to untreated vessels (% of maximum KPSS-induced contraction 113.1 ± 28.90%) under normal conditions (Figure 5-15A). However, the contractile response in rat thoracic rings with PVAT to U46619 was similar in the presence (% of maximum KPSS-induced contraction 79.27 ± 19.08%) and absence (% of maximum KPSS-induced contraction 83.39 ± 32.33%) of JTE 013 under inflammatory conditions (Figure 5-15B).

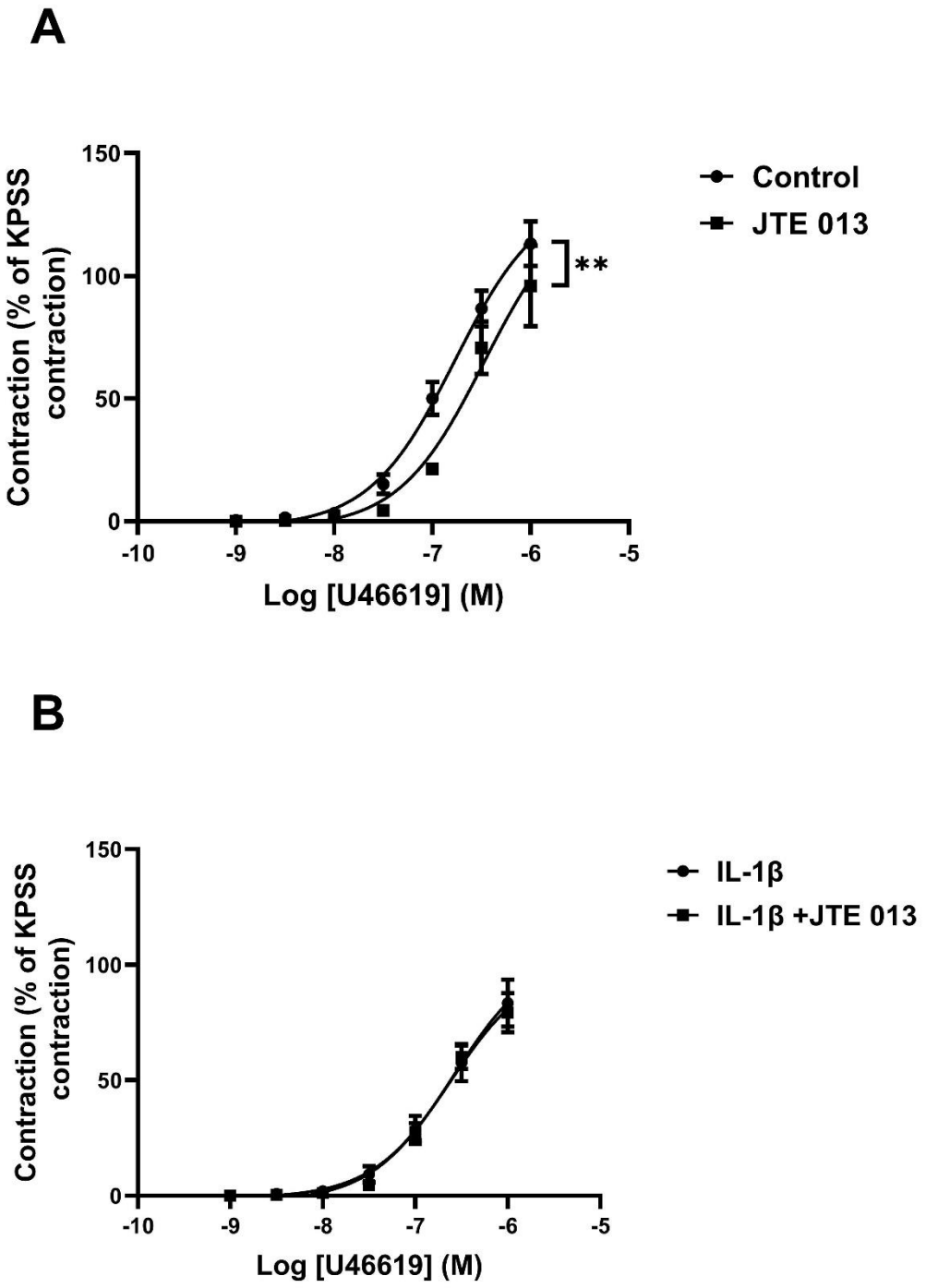

Figure 5-15 Contractile responses to U46619 in rat aorta with PVAT in presence and absence of S1PR$_2$ antagonist JTE 013 (10 μM) under control and inflammatory conditions (10 ng/ml IL-1β).

(A) Concentration response curves for the contractile effect of U46619 (1×10^{-9}-1×10^{-6} M) in endothelium-intact rat aorta with PVAT in presence (n=10) and absence (n=4) of JTE 013 under control conditions. (B) Concentration response curves for the contractile effect of U46619 (1×10^{-9}-1×10^{-6} M) in endothelium-intact rat aorta with PVAT in presence (n=10) and absence (n=5) of JTE 013 under inflammatory conditions (10 ng/ml IL-1β). Data are expressed as a percentage of maximum KPSS contraction and shown as mean ± SEM for n arteries from different animals. Statistical analysis was carried out using two-way ANOVA (with Bonferroni's test). Asterisks indicate a p value of **<0.01.

5.3.14.3 Exogenous S1P does not affect the hypo-reactivity induced by IL-1β

In a previous study, S1P has been shown to modulate vascular reactivity by causing a vasorelaxation effect on rat thoracic artery (Alganga et al, 2019) while in this thesis I have shown that IL-1ß upregulates SphK1 in adipocytes, and is involved in IL-1ß-mediated iNOS expression and NO production in adipocytes and Figure 5-12 and Figure 5-13 show that IL-1ß upregulates SphK1 in rat aortic PVAT. Hence, I now investigated whether exogenous S1P, the product of SphK1 would affect IL-1ß-mediated hyporeactivity in rat aortic vessels. Addition of U46619 ($1x10^{-9}$-$1x10^{-6}$ M) to intact thoracic aorta with PVAT in the presence and absence of S1P (10 μM) resulted in a concentration-dependent contraction under inflammatory (10 ng/ml IL-1ß) conditions. S1P was added at the same time as the Inflammatory stimulus. The contractile response in rat thoracic rings with PVAT to U46619 was similar in the presence (% of maximum KPSS-induced contraction 99.72 ± 13.03%) and absence (% of maximum KPSS-induced contraction 83.39 ± 32.33%) of S1P under inflammatory conditions (Figure 5-16).

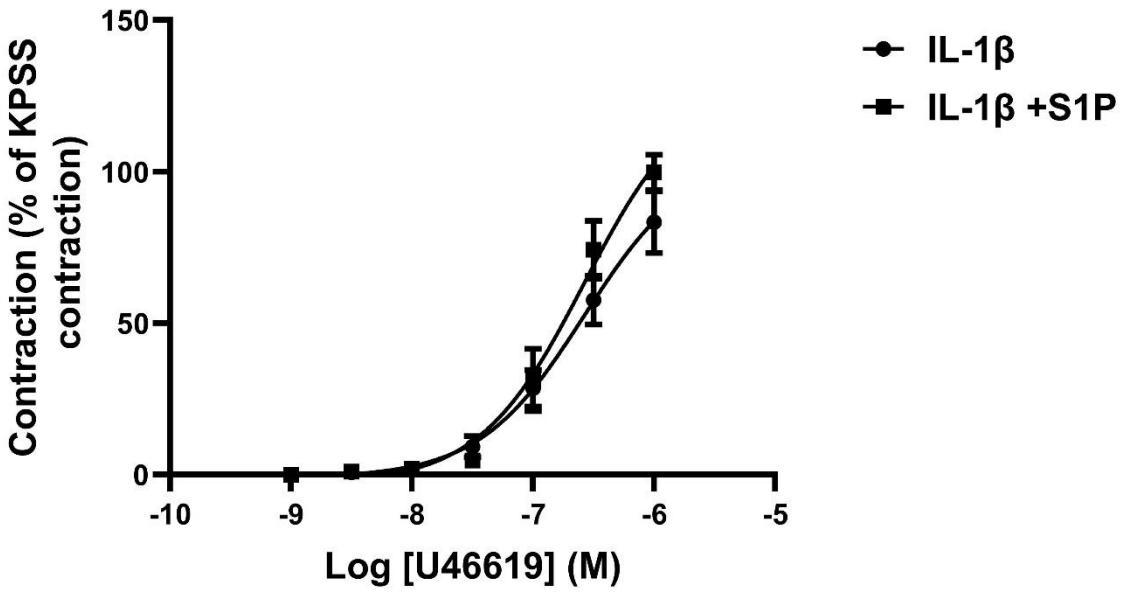

Figure 5-16 Contractile responses to U46619 in rat aorta with PVAT in presence and absence of S1P (10 μM) under inflammatory conditions (10 ng/ml IL-1β).

Concentration response curves for the contractile effect of U46619 ($1×10^{-9}$-$1×10^{-6}$ M) in endothelium-intact rat aorta with PVAT in presence (n=10) and absence (n=5) of S1P under inflammatory conditions (10 ng/ml IL-1β). Data are expressed as a percentage of maximum KPSS contraction and shown as mean ± SEM for n arteries from different animals. Statistical analysis was carried out using two-way ANOVA (with Bonferroni's test).

5.3.14.4 The effect of exogenous S1P on IL-1β mediated iNOS expression and NO production in PVAT

As I have shown that IL-1β influences SphK1 protein expression and mRNA levels in PVAT, I now investigated whether S1P, the sphingolipid product of the SphK1 enzyme, would affect iNOS expression and NO production in PVAT treated with IL-1β. Rat thoracic PVAT was stimulated with IL-1β (10 ng/ml) in the presence and absence of S1P (10 μM) for 4 hours. After treatment, lysate was prepared, and iNOS expression was assessed by western blotting while NO production was determined by nitrite/nitrate in the medium. RNA was isolated and quantified by qPCR.

Stimulation of PVAT with IL-1β in the absence of S1P caused a significant increase in iNOS expression (***$p<0.001$) and NO production (*$p<0.05$). In the presence of S1P, iNOS expression was decreased significantly (**$p<0.01$) compared to cells treated with IL-1β alone. However, the level of NO production, the product of iNOS was not altered by co-treatment with S1P compared with PVAT treated with IL-1β alone. S1P alone, in the absence of IL-1β, had no effect on iNOS expression or NO production by PVAT (Figure 5-17B and C).

Moreover, stimulation of PVAT with IL-1β in the absence of S1P caused a significant (***$p<0.001$) increase in iNOS mRNA expression. In the presence of S1P, there was a tendency towards a decrease in iNOS mRNA expression (Figure 5-17D) in IL-1β-stimulated PVAT, compared to the PVAT treated with IL-1β alone, although this did not reach statistical significance due to the high degree of variability.

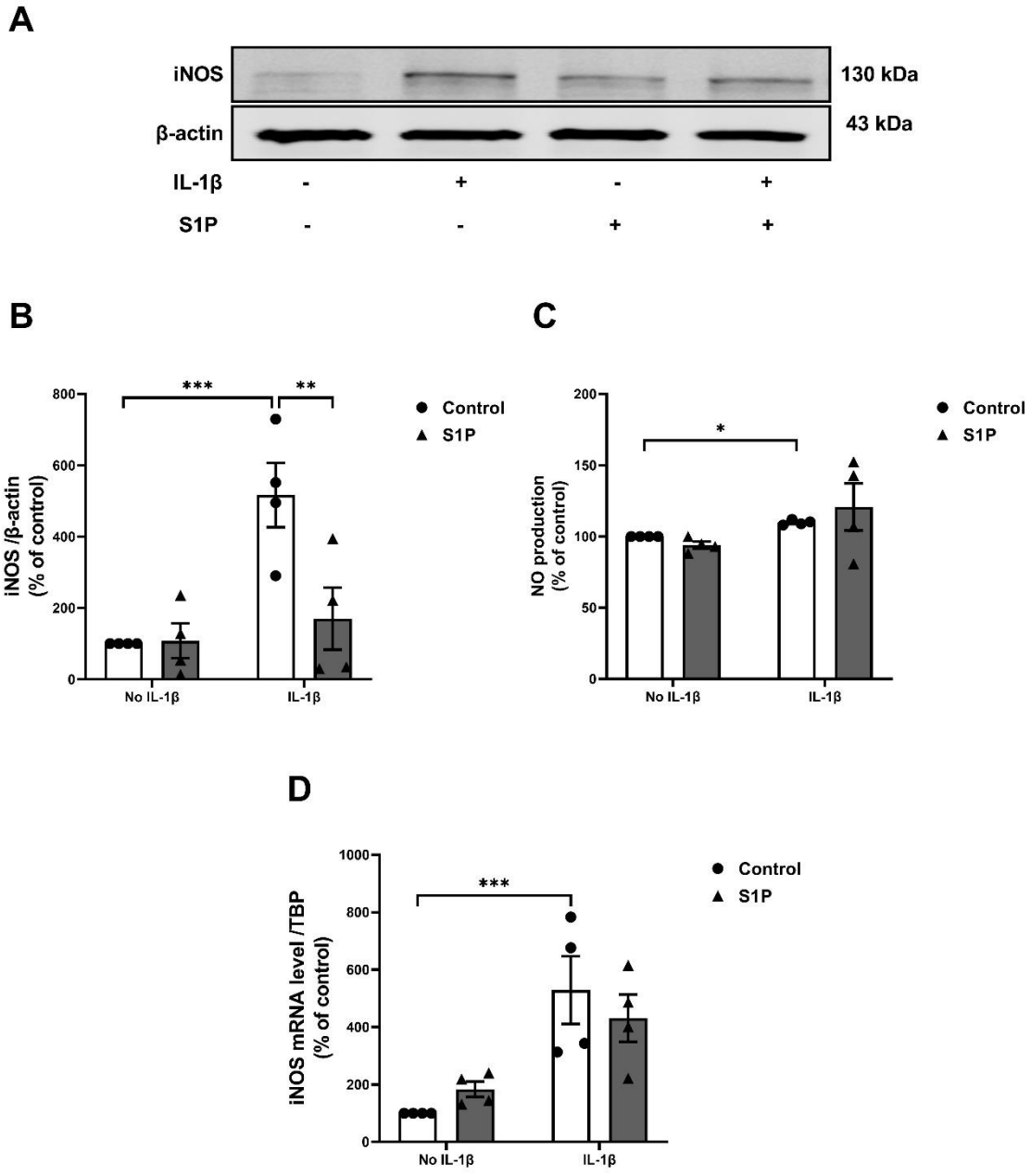

Figure 5-17 Effect of exogenous S1P on iNOS protein expression and NO production in perivascular adipose tissue (PVAT) stimulated with IL-1β.

PVAT lysates were prepared at indicated time points and resolved by SDS-PAGE with the appropriate antibodies. Media was collected and NO production was investigated by using a Sievers 280A NO Meter. RNA isolated and quantified by qPCR. (A and B) representative western blotting images and graph for the change in iNOS protein expression. Protein level of iNOS was normalised to level of β-actin. (C) IL-1β stimulated NO production in PVAT. (D) qPCR analysis showing the changes in iNOS mRNA levels following 4h of 10ng/ml IL-1β treatment of PVAT relative to levels of TATA binding protein (TBP) mRNA. The data represent samples from four different experiments expressed as the mean ± SEM of the % fold change relative to control. Statistical analysis was carried out using two-way ANOVA. Asterisks indicate a p value of (*p<0.05, **p<0.01, ***p<0.001).

5.4 Discussion

In chapters 3 and 4, I showed that IL-1ß induces iNOS expression and NO production in 3T3 adipocytes via the SphK1/S1P/S1PR$_2$ axis. However, this is a cell line and therefore it was important to test whether this effect is also seen in the more complex milieu of PVAT which contains a variety of cells. Additionally, this chapter sought to determine if the effect of IL-1ß on iNOS had functional effects on vasorelaxation and whether the sphingolipid system was involved. The experiments presented in this chapter were initially carried out using mouse aortic rings but it was apparent that IL-1ß did not elicit a noticeable effect on the PVAT-mediated anticontractile response to PE and the presence of S1P did not alter this. Additionally, S1P and selective S1P agonists failed to induce any observable relaxant effect, suggesting an absence of functional receptors on the mouse thoracic aorta. Consequently, the second part of this study was carried out on a rat model where we have previously demonstrated that S1P does induce a vasodilator effect (Alganga et al, 2019). In rat aortic rings it was shown that IL-1ß enhances the anti-contractile effect of PVAT, which is most likely mediated by iNOS upregulation, increased NO production, and subsequent potassium channel activation. Interestingly, although IL-1ß did upregulate SphK1 in rat aortic PVAT it seems that the IL-1ß-induced hyporeactive effect is independent of the sphingolipid axis pathway.

A series of experiments was carried out to investigate the effect of PVAT on PE-induced contraction in endothelium-intact mouse aortic rings. Many studies have reported that PVAT decreases contractile sensitivity to phenylephrine and serotonin in isolated mouse aortic rings (Nóbrega et al, 2019; Szasz et al, 2012). In the current study, it was shown that the presence of PVAT in endothelium-intact mouse aortic rings decreases the contractile sensitivity to PE compared with vessels without PVAT (Figure 5-1). These data support and confirm a plethora of evidence that PVAT has an anticontractile effect in human subcutaneous vessels (Greenstein et al, 2009), mouse gracilis artery (Saxton et al, 2022), and mouse thoracic aorta (Almabrouk et al, 2017). This effect is thought to be mediated by the release of various vasoactive substances from PVAT, such as adiponectin (Almabrouk et al, 2018), hydrogen peroxide (H_2O_2)(Gao et al, 2007), and nitric

oxide (NO)(Xia & Li, 2017), which act to inhibit vasoconstriction and promote vasorelaxation.

PVAT is considered as a highly active endocrine organ that releases a range of adipocytokines as well as other substances that have a paracrine effect on vascular tone under physiological and pathological conditions. Moreover, SphKs and its product-S1P, have been shown to regulate many physiological processes in adipose tissue and adipocytes (Fang et al, 2019). Importantly, it has been demonstrated that SphK1 expression and its product S1P are upregulated in inflamed adipose tissue in mice and humans (Guitton et al, 2020). This upregulation was seen in adipocytes and immune cells within the adipose tissue microenvironment; and linked to the modulation of various inflammatory signalling pathways, including the activation of pro-inflammatory cytokines and chemokines, recruitment of immune cells, and impairment of insulin signalling (Asano et al, 2023; Tous et al, 2014; Wang et al, 2014). Therefore, it might be possible that the S1P generated from PVAT is transported out of the cell to activate S1PRs on vascular beds to modulate vascular reactivity in a paracrine manner. Indeed, S1P itself causes a vasorelaxant effect in rat and mouse mesenteric arteries (Dantas et al, 2003; Igarashi & Michel, 2009), so could be one of a number of vasorelaxant substances generated by PVAT which contribute to an anticontractile effect. In terms of the receptors involved, it was shown that $S1PR_3$ and $S1PR_1$ activation cause a vasorelaxant effect in mouse thoracic aorta (Igarashi & Michel, 2009; Tölle et al, 2005). However, in the present study neither S1P agonist nor $S1PR_{1-3}$ selective agonists induced a noticeable vasorelaxant effect in mouse thoracic aorta in the presence or absence of PVAT (Figure 5-2). These findings contradict a few published studies. For example, a study carried out by Mitidieri et al, (2020) has shown that L-serine is involved in the de novo sphingolipid biosynthesis resulting in S1P production in mouse aorta rings. In this study, it was shown that blocking $S1PR_1$ using W146 decreased L-serine or L-cysteine relaxant effect in mouse thoracic aorta (Mitidieri et al, 2020); however, in this study they did not directly test the selective activation of specific S1PRs, which is different from our study design. Also, it has been shown that S1P (100 nM) causes a vasorelaxant effect in mouse mesenteric arteries precontracted with norepinephrine (Dantas et al, 2003), and it has been shown that the cumulative addition of S1P (1 nM to 5 μM) to mouse aorta precontracted with U46619 causes a vasorelaxant effect. The

explanation for these differences could be variation in the experimental conditions, such as differences in contractile agents and concentration, technique differences, and tissue regional differences. Receptor distribution of S1PRs could also play a role but the reason for the divergent results in this study need to be further explored.

It has been demonstrated that inflammatory stimulation causes a vasorelaxant effect in several arteries from different animals. For example, LPS induces a vasorelaxant effect in rat thoracic aorta (Vo et al, 2005) and in rat superior mesenteric artery via iNOS-dependent pathway (Hernanz et al, 2004). Moreover, it has been shown that IL-1β causes a hyporeactivity in isolated rat superior mesenteric arteries (Yuui et al, 2016), and in rat thoracic aorta (Soler et al, 2003). However, in these studies the vessels did not have PVAT intact and so the direct effect of IL-1β on PVAT-mediated hyporeactivity via the iNOS pathway is still poorly studied. In chapters 3 and 4, I confirmed that the SphK1/S1P/$S1PR_2$ axis pathway participates in IL-1β-mediated iNOS expression and NO production from adipocytes. Therefore, one aim of this chapter was to investigate the effect of IL-1β on the relaxant effect of PVAT in mouse thoracic aorta and test whether S1P participates in this effect. Initially, I used a mouse model to study the effect of IL-1β on the PVAT anticontractile effect. However, IL-1β did not significantly alter the contractile response to PE (Figure 5-3). To investigate whether S1P might unmask an effect of IL-1β and subsequently enhance the relaxing effect of PVAT, I incubated the thoracic vessels containing PVAT with a combination of IL-1β and S1P. However, addition of S1P did not alter the contractile response to PE under either normal or inflammatory conditions (Figure 5-3). It might be that the incubation time for IL-1β was not long enough to upregulate iNOS expression and subsequently NO production. No further experiments were done to investigate the direct effect of IL-1β on iNOS protein expression since S1P and S1P-selective agonists did not show any significant effect on vascular tone in the mouse aorta.

It has been confirmed in our lab that S1P causes a vasorelaxant effect in rat thoracic aorta (Alganga et al, 2019), and I was able to confirm that, as shown in Figure 5-4. Therefore, I decided to use rat aortic rings to investigate the involvement of the SphK1/S1P/$S1PR_2$ axis pathway in the IL-1β-mediated hyporeactivity effect and the role of PVAT. It is known from the literature that

the presence of PVAT reduces precontractile tone in several different rat vessels (Dubrovska et al, 2004; Löhn et al, 2002). In the current study, the presence of PVAT decreased the contractile response to U46619 in rat thoracic aorta as shown in Figure 5-5. To investigate whether IL-1β alters the relaxant effect of PVAT via iNOS upregulation, it was initially important to examine at what time point iNOS protein expression was upregulated. Here, I found that iNOS expression and NO production from rat thoracic PVAT significantly increased at 4 hours following IL-1β treatment (Figure 5-6). Thus, in all subsequent experiments characterising the effect of IL-1β on the PVAT pro-relaxant effect, the IL-1β incubation time was kept at 4 h. In the current study, it was shown that preincubation of endothelium-intact rat vessels with IL-1β in the presence and absence of PVAT decreased the contractile response to U46619 (Figure 5-7). It is worth noting that the effect of IL-1β is much stronger in vessels with PVAT compared to vessels without PVAT, emphasising the direct effect of IL-1β on PVAT. As would perhaps be anticipated, the effect of IL-1β was shown to diminish in denuded vessels with PVAT as illustrated in Figure 5-9, indicating that part of the effect of IL-1β is likely due to upregulation of iNOS in the endothelial cells. In line with this, the hypocontractile effect of IL-1β was lost in denuded vessels of rat superior mesenteric arteries (Yuui et al, 2016), and rat thoracic aorta (Lu & Fiscus, 1999). Further investigations are needed to validate this explanation by treating the PVAT with IL-1β and then transferring the conditioned media into the chamber to avoid the direct effect of IL-1β on the vessel and endothelial cells. However, it's worth noting that short-lived mediators such as NO may be lost during this process. Furthermore, the iNOS inhibitor (1400W) was used to determine whether the IL-1β-enhanced relaxant effect of PVAT is mediated by iNOS-derived NO production. It was observed that pre-treatment of rat aortic rings containing PVAT with 1400W abolished the hypocontractile effect of IL-1β (Figure 5-10). These results suggest that the enhanced relaxant effect of IL-1β on PVAT is attributed to iNOS protein synthesis, ultimately leading to NO generation by PVAT. This suggestion is supported by data which showed an increase in iNOS mRNA level and NO production in rings treated with IL-1β as illustrated in Figure 5-8. These data align with a number of studies investigating the anticontractile effect of PVAT via iNOS-derived NO production. LPS has been shown to cause vascular hyporeactivity in rat thoracic aorta with and without PVAT, and it was via iNOS pathway upregulation (Hai-Mei et al, 2013). Additionally, in a septic rat model, it was demonstrated that PVAT of thoracic

aorta causes hypocontractility to a vasoconstrictor which was reversed by 1400W (Awata et al, 2019). To my knowledge, the direct effect of an individual cytokine (IL-1β) on the vasorelaxant effect of rat aortic PVAT via iNOS-derived NO production has not been investigated prior to this study.

It has been demonstrated that potassium channels contribute to vasorelaxant effect induced by PVAT (Szasz et al, 2013). For example, NO is one of many endogenous substances that directly activate potassium channels in endothelium and vascular smooth muscle cells as part of the vasodilator effect. The NO released by PVAT can activate potassium channels in smooth muscle cells, leading to hyperpolarization, inhibition of calcium influx, and ultimately vasodilation (Stanek et al, 2021). Thus, I evaluated the role of potassium channels in hyporeactivity induced by IL-1β in rat thoracic aorta. As a general means of testing if potassium channels were involved, I used the non-selective inhibitor TEA which I found to diminish the hyporeactivity induced by IL-1β in rings containing PVAT (Figure 5-11). This implies that potassium channels play a role in the hyporeactivity response observed. These data support many studies investigating the involvement of potassium channels in the vasorelaxant effect of PVAT under inflammatory conditions. Recently, it was shown that a high-carbohydrate diet enhances the anticontractile effect of PVAT via iNOS-derived NO production and subsequently activates the voltage-gated potassium channels (Reis Costa et al, 2021). Similarly, it was observed that the augmented vasorelaxant response attributed to perivascular adipose tissue (PVAT) under hypoxic conditions was decreased upon administration of the non-selective potassium channel blocker, TEA (Maenhaut et al, 2010). It is known that potassium channels are expressed in adipose tissue and adipocytes and have been implicated in the anticontractile effect of PVAT (Gollasch, 2017; Ramírez-Ponce et al, 2002; Shi et al, 1999). Moreover, I have shown in Chapter 4 (Figure 4-11) that glibenclamide (an ATP-sensitive potassium (K_{ATP}) antagonist) attenuates IL-1β-mediated iNOS expression and NO production in adipocytes. Therefore, further studies are required to investigate which of the many types of potassium channel might directly affect IL-1β-mediated iNOS regulation in adipose tissue. Future experiments could test if glibenclamide has the same effect in IL-1β mediated iNOS expression and NO production from rat thoracic PVAT.

It's known that PVAT meditates relaxant effect either via endothelium dependent pathway or VSMC-dependent pathway. PVAT-derived factors such as adiponectin and H_2O_2 may activate NO production from endothelial cell which would diffuse into adjacent smooth muscle cells to activate soluble guanylyl cyclase (sGC) to promote vasodilation. On the other hand, PVAT-derived NO diffuses to adjacent VSMCs to exert vasodilation either by directly activating potassium channels or indirectly activating the sGC-cGMP pathway, promoting membrane hyperpolarization. Indeed, these results indicate that IL-1β enhances the production of NO from both PVAT and the endothelium. This combined NO production mediates vasorelaxation through the activation of potassium channels on VSMC. However, the direct effect of iNOS derived NO produced by PVAT and endothelial cells on the sGC pathway was not investigated in this study. It seems that NO produced by the endothelium is required, along with NO produced by PVAT to fully mediate this effect. Indeed, a previous study reported that eNOS activation is required for LPS-induced iNOS expression in endothelial cells of rat aortic rings (Vo et al, 2005). In addition there is evidence demonstrating that the NO itself can activate NF-KB activation, which is the prominent pathway regulating iNOS expression (Kröncke, 2003). These two studies suggest that endothelial cells expressing eNOS could be a significant player in the induction of iNOS expression within endothelial cells or even may affect iNOS expression within adipose tissue. In addition, under inflammatory condition, much of NO production by PVAT could react with superoxide (O_2^-) to generate the highly reactive molecule peroxynitrite ($ONOO^-$), which has a pro inflammatory effect (Beckman, 1996; Beckman & Koppenol, 1996). However, endothelium derived NO has been shown to have anti-inflammatory effect against peroxynitrite to maintain vascular haemostasis under inflammatory condition (Nguyen et al, 2016). Therefore, it is also possible that endothelial cells secrete more NO to counteract the proinflammatory effect of peroxynitrite overproduction, and also mediate a vasodilator effect.

In order to further explore the SphK1/S1P pathway as a potential mechanism for IL-1β-induced hyporeactivity in rat aortic rings containing PVAT, molecular and functional experiments were carried out. SphK1 activation was investigated in rat aortic PVAT treated with IL-1β. Initial studies were undertaken to assess whether IL-1β could induce SphK1 in rat aortic PVAT. IL-1β has been reported to upregulate SphK1 in several cell types including glioblastoma cells (Paugh et al, 2009) and

lung carcinoma cells (Billich et al, 2005). Moreover, in chapter 3, IL-1β has been shown to upregulate SphK1 in 3T3-L1 adipocytes (Figure 3-8). In this chapter, Figure 5-12 shows that IL-1β upregulated SphK1 phosphorylation in rat aortic PVAT. This observation is further supported by an increase in SphK1 mRNA in both rat aortic rings containing PVAT and PVAT itself (Figure 5-13). Given these findings, it was important to explore whether IL-1β-induced SphK1 is involved in regulation of vascular activity. It was found that pretreatment of endothelium-intact rat aortic rings containing PVAT with the SphK1 inhibitor PF543 (Figure 5-14) 30 min prior to incubation with IL-1β failed to inhibit IL-1β-induced hyporeactivity. Similarly, treatment of endothelium-intact rat aortic rings containing PVAT with S1P (Figure 5-16) and IL-1β did not alter the contractile response to U46619 under inflammatory condition. Therefore, these data imply that although IL-1β upregulates SphK1 in PVAT, the enhanced relaxant effect caused by the presence of PVAT is most likely not mediated by SphK1/S1P.

$S1PR_2$ has been implicated in regulation of many inflammatory processes in adipose tissue. It has been reported that HFD-induced macrophage polarization and recruitment to adipose tissue are ablated in mice lacking $S1PR_2$ (Kitada et al, 2016). In the same study, it was also shown that $S1PR_2$ regulates iNOX2 gene expression in epididymal adipocytes of HFD mice. It has also been confirmed in this study that inhibition of $S1PR_2$ by JTE 013 decreases IL-1β-mediated iNOS expression in adipocytes and regulates iNOS expression resulting from interaction between macrophages and adipocytes. Based on these findings, I hypothesised that $S1PR_2$ in PVAT of rat thoracic aorta could regulate iNOS expression in response to IL-1β and then contribute to the hyporeactivity induced by IL-1β. However, it was found that pretreatment of endothelium-intact rat aortic rings containing PVAT with JTE 013 (Figure 5-15B) 30 min prior to incubation with IL-1β did not reverse the hyporeactivity induced by IL-1β. Nevertheless, pretreatment of endothelium-intact rat aortic rings containing PVAT with JTE 013 did decrease the contractile response to U46619 under normal conditions (Figure 5-15A). This finding suggests that $S1PR_2$ inhibition by JTE 013 may have a direct effect on vascular contractility via affecting $S1PR_2$ in VSMCs. This effect could mask the direct effect of $S1PR_2$ inhibition in IL-1β mediated PVAT hyporeactivity via iNOS pathway. Similar to our result, a previous report demonstrated that JTE 013 decreases the contractile response to U46619 in mouse basilar artery (Salomone

et al, 2008). Although I did not measure the expression of iNOS protein in PVAT treated with IL-1ß and JTE 013, our observations suggest that $S1PR_2$ inhibition did not contribute to the IL-1ß-mediated hyporeactivity via iNOS-derived NO production.

The discrepancy in the findings from 3T3-L1 adipocytes and the ex vivo study in this chapter which investigated the role of SphK1/S1P/$S1PR_2$ axis pathway could be attributed to many factors. The complexity of PVAT could influence the signalling pathways activated in response to IL-1ß compared to 3T3-L1 adipocyte cell line. This is supported by findings in Figure 5-17B, indicating a significant downregulation in IL-1ß-induced iNOS expression in rat aortic PVAT by S1P. Furthermore, JTE 013 may directly impact vascular contractility by affecting $S1PR_2$ in VSMCs, as evidenced by the findings in Figure 5-15A, where it was shown that JTE 013 decreases the contractile response to U46619 under normal conditions. This suggests that $S1PR_2$ inhibition by JTE 013 may have broader effects on vascular cells along with PVAT and potentially masking its inhibition of iNOS-derived NO production from PVAT-induced by IL-1ß. Moreover, considering a high production of NO in response to IL-1ß, it's pertinent to consider the interaction between nitric oxide and sphingolipid metabolism as a contributing factor. A number of studies have shown that NO could interact indirectly with S1P via altering its metabolism. For example , NO has been observed to inhibit the action of sphingomyelinase, an enzyme that converts ceramide to sphingosine (Perrotta et al, 2008). It also was shown that NO decreases ceramide generation via sphingomyelinase inhibition (Clementi et al, 2003). Therefore, this might influence the role of sphingolipid system in IL-1ß-mediated iNOS regulation in PVAT. In future experiments, isolation of primary adipocytes from PVAT of rat thoracic aorta, with removal of other cell types, followed by culturing with IL-1ß and sphingolipid modulators could help to address this.

5.5 Conclusion

In this chapter, the investigations focused on assessing the effect of IL-1ß on PVAT-mediated anticontractile effect in both mouse and rat aortic rings, with a specific examination of the potential involvement of the sphingolipid system in this effect. Notably, S1P agonists in mouse experiments exhibited no discernible influence on

vascular tone. Additionally, IL-1β did not induce alterations in the anticontractile effect in the mouse thoracic aorta. Conversely, in the rat model, IL-1β was found to enhance the relaxant effect of PVAT through an iNOS-dependent pathway, subsequently activating potassium channels. Furthermore, IL-1β upregulated SphK1 in rat aortic PVAT, although this did not impact the hyporeactivity induced by IL-1β. Despite functional studies not revealing a significant role for the SphK1/S1P/$S1PR_2$ axis pathway in IL-1β-mediated hyporeactivity in the rat thoracic artery containing PVAT, the potential contribution of the sphingolipid system to IL-1β-mediated iNOS expression in PVAT cannot be ruled out and needs further experiments.

Chapter 6 - General discussion

6.1 Summary and General discussion

Perivascular adipose tissue (PVAT) surrounds blood vessels and has an anti-contractile effect. It also helps to maintain vascular homeostasis via release of a variety of bioactive molecules (Cheng et al, 2018). In obesity-induced inflammation, PVAT becomes dysfunctional and ultimately this leads to loss of the anticontractile effect of PVAT and impaired endothelial function (Szasz et al, 2013). However, a few published studies have demonstrated that inflamed PVAT can compensate or have an adaptive role to preserve endothelial function in obese mice and rat models; via upregulating iNOS protein and increasing NO production (Araujo et al, 2018; Nakladal et al, 2022; Reis Costa et al, 2021). A growing body of evidence supports the significant contribution of the sphingolipid system in adipose tissue inflammation under conditions of obesity. For example, levels of SphKs and S1P have been shown to be elevated in both obese humans and experimental murine models of obesity (Hashimoto et al, 2009; Ito et al, 2013; Nojiri et al, 2014; Wang et al, 2014). In published studies, inhibition of SphK1 and SphK2 in vitro and in vivo results in a decrease in the expression of proinflammatory markers in adipose tissue (Tous et al, 2014; Wang et al, 2014; Zhang et al, 2014). Further studies indicate that $S1PR_2$ promotes inflammation and cytokine release within the adipose tissue in animal models of obesity (Asano et al, 2023; Kitada et al, 2016). However, the role of SphKs/S1P in iNOS derived NO and how this modulates the effect of PVAT on vascular function under inflammatory conditions remains to be fully elucidated. This thesis investigated the involvement of SphKs/S1P pathway in IL-1ß-mediated iNOS upregulation in 3T3-L1 adipocytes and related proinflammatory signalling pathways. Furthermore, vascular function studies were carried out to investigate the role of this system in hyporeactivity of PVAT mediated by IL-1ß and whether this operates through a pathway dependent on NO derived from iNOS. The present study has shown for the first time that the sphingolipid system is required for IL-1ß to upregulate iNOS and NO production in 3T3-L1 adipocytes under inflammatory conditions. Although it was observed previously that sphingolipids promote iNOS regulation in a number of cells and tissues (Gong et al, 2020; Nayak et al, 2010; Vasconcelos et al, 2017; Wang et al, 2021; Zhang et al, 2021), this observation in 3T3-L1 adipocytes is novel. Furthermore, it was shown in this thesis that IL-1ß-augments PVAT-

mediated hyporeactivity in thoracic aorta of rat via the iNOS pathway but this effect was independent of the sphingolipid system.

The work in chapter 3 confirmed the expression of SphK1 in 3T3-L1 adipocytes over the period of adipogenesis and further characterised the impact of exogenous S1P in various inflammatory pathways. SphK1 expression increased gradually throughout the period of adipogenesis, consistent with previous studies (Hashimoto et al, 2009; Mastrandrea, 2013). This finding suggests that S1P may regulate multiple cellular processes in adipose tissue. The PI3K/Akt pathway (Kugo et al, 2021), MAPKs family pathway (Nepali et al, 2015), and NF-KB pathways (Yang et al, 2002) are proinflammatory pathways that have been implicated in many metabolic disorders in adipose tissue and are linked to many proinflammatory processes within adipose tissue such as iNOS regulation. In this study, S1P was shown to stimulate the MAPKs pathway, particularly ERK1/2 and JNK, and PI3K/Akt. In support of this finding, S1P was shown to activate ERK1/2 and JNK phosphorylation in 3T3-L1 differentiated adipocytes (Jun et al, 2006; Kitada et al, 2016). However, P38 which is a member of MAPKs family pathway was not activated in response to S1P treatment in 3T3-L1 adipocytes, which contradicts some published studies in rat white adipocytes (Jun et al, 2006) and bone marrow-derived monocyte/macrophages (Hou et al, 2021). Like P38, the NF-KB pathway was not activated in response to S1P in 3T3-L1 adipocytes, supporting a similar finding by Gurgui in primary cultured rat intestinal smooth muscle cells in response to S1P (Gurgui et al, 2010).

IL-1β is a proinflammatory cytokine highly expressed in adipose tissue under inflammatory conditions, and is linked to cardiovascular damage and multiple organ dysfunction (Engin, 2017; Ghanbari et al, 2021). Therefore, IL-1β was used in this study as a proinflammatory stimulus. IL-1β has been reported to activate SphK1 expression in a number of cell types, including isolated rat pancreatic islets (Mastrandrea et al, 2005) human glioblastoma U373-MG cells (Bryan et al, 2008) and astrocytes (Paugh et al, 2009). However, the effect of IL-1β activation on SphK1 expression in adipocytes had never been examined. In the current study, SphK1 levels were upregulated in response to IL-1β. The increase in SphK1 in response to IL-1β in 3T3-L1 adipocytes may contribute significantly to generation of more S1P which acts as a proinflammatory lipid mediator to regulate a number

of proinflammatory enzymes. However, no effect was observed on Sphk2 expression, suggesting that this is a SphK1-specific effect.

A number of studies have shown that IL-1β upregulates iNOS expression including in preadipocytes (Park et al, 2021). To explore the involvement of S1P in IL-1β-induced iNOS expression, IL-1β induced-iNOS expression and NO production was assessed in 3T3-L1 adipocytes in the presence and absence of S1P. In this study, S1P augmented iNOS expression and NO production induced by IL-1β, indicating that S1P produced by the upregulation of SphK1 by IL-1β may have an additive effect on IL-1β-mediated NO production. These data support similar observations reported in murine HAPI microglial cell line where S1P contributed to iNOS upregulation in response to LPS (Wang et al, 2021). However, this is the first study investigating the direct role of S1P in iNOS regulation in adipocytes. It is known that IL-1β regulates a wide range of inflammatory pathways including PI3K/Akt, MAPKs family kinases, and NF-KB, resulting in regulation of a number of proinflammatory mediators (Martin & Wesche, 2002). Moreover, iNOS expression in 3T3-L1 adipocytes was suggested to be regulated by these pathways (Nepali et al, 2015). In the current study, S1P was found to augment IL-1β-induced MAPKs pathways and PI3K/Akt pathway with no effect on NF-KB. These data support previous findings that S1P augments cytokine-induced MAPKs (Fernández-Pisonero et al, 2012; Ohama et al, 2008; Wang et al, 2021) and PI3K/Akt pathway activation (Osawa et al, 2001). Hence, it is conceivable that upregulation of SphK1 by IL-1β induces the production of S1P, potentially resulting in enhanced iNOS expression via MAPKs and PI3K/Akt signalling.

Chapter 4 investigated more fully how distinct SphKs isoforms and S1PRs modulate iNOS regulation in adipocytes stimulated with the cytokine IL-1β. SphK1 inhibition was found to decrease iNOS expression and NO production in stimulated 3T3-L1 adipocytes, implying that IL-1β required SphK1 to mediate iNOS regulation in adipocytes. These data support similar observations that SphK1 regulates iNOS expression in microglial cells (Nayak et al, 2010). Moreover, the proinflammatory effect of S1P in iNOS regulation was likely mediated through $S1PR_2$ as JTE 013, a selective $S1PR_2$ antagonist strongly attenuated iNOS expression and NO production stimulated by IL-1β in 3T3-L1 adipocytes. In support of this, activation of $S1PR_2$ with CYM 5478 increased iNOS expression and NO production in adipocytes

stimulated by IL-1ß. These data support similar recent data that $S1PR_2$ inhibition led to decreased iNOS expression in a rat glomerular mesangial cell line (Gong et al, 2020), and iNOS expression and NO production in placenta tissue of the preeclampsia rat (Zhang et al, 2021).

ABCA1 is widely implicated in transporting S1P out of many cells, including adipocytes. In the present study, inhibiting ABCA1 with glybenclamide, diminished the additive effect of S1P on iNOS expression and NO production in stimulated adipocytes, suggesting that SphK1 is activated in response to IL-1ß to catalyse S1P production from sphingosine, which is subsequently released through the ABCA1 transporter to eventually modulate its function via S1PRs. However, further experiments are required to obtain a complete picture by testing another transporter such as Spn2 and more importantly, measuring S1P concentration released by the adipocytes.

$S1PR_2$ has been reported to regulate various cellular signalling pathways, including PI3K/Akt, NF-KB and MAPK in a number of cells (Kluk & Hla, 2002; Wang et al, 2023; Yang et al, 2022). Moreover, it was discussed previously that these pathways are implicated in many inflammatory processes and linked to iNOS regulation within adipose tissue (Nepali et al, 2015), suggesting that the $S1PR_2$ is critical for IL-1ß induced iNOS expression and NO production in adipocytes. The present study investigated the effect of $S1PR_2$ with JTE 013 on IL-1ß-stimulated signal transduction pathways. Our findings demonstrated that JTE 013 has a strong inhibitory effect on IL-1ß-stimulated MAPK and PI3K/Akt signalling, suppressing phosphorylation of ERK1/2, P38, JNK and Akt whereas the NF-KB pathway was unaltered, leading to the suppression of subsequent proinflammatory iNOS expression and NO production. This is in accordance with previous studies where it has been demonstrated that JTE 013 suppresses MAPKs and PI3K/Akt pathway (Hou et al, 2021; Liu et al, 2015). Further investigations confirmed that the PI3K/Akt and MAPKs pathways, particularly ERK1/2 and JNK, accounts for the iNOS expression and NO production in stimulated adipocytes as iNOS expression and NO production were ablated by the inhibition of these pathways. Taken together, this study has shown for the first time in adipocytes that $S1PR_2$ inhibition suppresses IL-1ß stimulated phosphorylation of MAPKs and PI3K/Akt signalling pathway intermediates, and subsequent activation of proinflammatory iNOS enzyme. It

remains unclear how $S1PR_2$ regulates P38 signalling and its role in iNOS expression, since P38 inhibition resulted in augmented IL-1ß-induced iNOS expression and NO production in adipocytes. Further study is required to uncover the precise role of $S1PR_2$ in P38 pathway activation, particularly in iNOS regulation in adipocytes.

Macrophage recruitment and M1 activation is a key component of the proinflammatory environment within the adipose tissue under conditions of obesity, thereby contributing to iNOS upregulation (Weisberg et al, 2003). Moreover, SphK1-derived S1P is expressed in adipose tissue macrophages and in activated RAW 264.7 cells, suggesting a proinflammatory role in adipose tissue (Asano et al, 2023; Hammad et al, 2008; Kitada et al, 2016; Wang et al, 2014; Wu et al, 2004). In the current study, stimulation of RAW cells with LPS resulted in activation of SphK1, suggesting that inflammation increased S1P production from macrophages. Stimulation of 3T3-L1 adipocytes with activated macrophage conditioned media caused a significant increase in iNOS expression and NO production, which was decreased when activated macrophages were treated with SphK1 inhibitor, suggesting that S1P released from macrophages may act on S1P receptors on adjacent adipocytes to augment iNOS expression. To confirm this, $S1PR_2$ receptor inhibition on adipocytes resulted in inhibition of iNOS expression and reduced NO production in adipocytes stimulated with RAW CM. Moreover, $S1PR_2$ has been shown to promote immune cell infiltration in obese mice (Kitada et al, 2016), and induce cytokine production in mice treated with LPS (Skoura et al, 2011). Furthermore, in the current study, stimulation of 3T3-L1 adipocytes with activated macrophage conditioned media causes a significant increase in iNOS expression and NO production, which was decreased when activated macrophages were treated with $S1PR_2$ inhibitor. Taken together, this study suggests that targeting SphK1/S1P/$S1PR_2$ in adipocytes and macrophages may reduce the proinflammatory iNOS upregulation in adipose tissue which is associated with obesity and insulin resistance.

The expression of iNOS within the perivascular adipose tissue has been associated with augmented anti-contractile effect in inflammatory related disease such as obesity (Araujo et al, 2018; Reis Costa et al, 2021) atherosclerosis (Nakladal et al, 2022) and sepsis (Awata et al, 2019; Hai-Mei et al, 2013). Moreover, the significant role of S1P in mediating vascular tone is well recognised and S1P, therefore, may

play an important role in the anticontractile effect of PVAT induced by IL-1ß via iNOS regulation. An interesting finding from chapter 3 and 4 was that attenuation of SphK1/S1P/$S1PR_2$ resulted in diminished iNOS and NO production from adipocytes stimulated with IL-1ß. Extending our investigations to include PVAT of rat and mouse models will offer a more comprehensive understanding of the physiological relevance and translational implications of these findings; which was the focus of chapter 5. Here, these effects were initially investigated using isolated mouse thoracic aortic rings. However, PE-induced contraction was not altered in mouse aortic rings following exposure to IL-1ß compared with control. Furthermore, exogenous S1P and selective S1P agonists had no significant vasorelaxant effect in mouse rings and importantly, addition of S1P prior to IL-1ß incubation exerted no effect. On the other hand, thoracic aorta from the rat does vasodilate in response to S1P (Alganga et al, 2019), and since it was confirmed in this study that S1P induces vasodilation in rat aorta, the rat model was used for further experiments on vascular function. In the current study, it was initially confirmed that IL-1ß induced alterations in the anticontractile effect in the rat thoracic aorta through an iNOS-dependent pathway, subsequently activating potassium channels. These observations are in line with a number of studies where it was shown PVAT of rat thoracic aorta enhances relaxation via the iNOS pathway under inflammatory condition (Awata et al, 2019; Hai-Mei et al, 2013). SphK1 and its product S1P is well known to be activated in inflamed adipose tissue (Hashimoto et al, 2009; Wang et al, 2014). In this study, IL-1ß upregulated mRNA expression of Sphk1 and pSphK1 in PVAT isolated from rat thoracic aorta, suggesting that more S1P generated from PVAT could act as vasodilator alongside NO released from PVAT in response to IL-1ß. However, the data presented here in rat PVAT proposes that, unlike in 3T3-L1 adipocytes, the SphK1/S1P axis does not play a major role in IL-1ß-induced PVAT anticontractile effect via iNOS derived NO. Moreover, $S1PR_2$ has been found recently to regulate iNOS gene expression in epididymal adipose tissue of HFD-mice (Kitada et al, 2016), suggesting that the $S1PR_2$ is critical for IL-1ß derived NO from PVAT. However, I found that $S1PR_2$ is not required for IL-1ß- induced PVAT anticontractile effect via iNOS derived NO pathway. Collectively, these data indicate that SphK1/S1P/$S1PR_2$ axis pathway is not a significant player in the context of hyporeactivity induced by IL-1ß in the rat thoracic artery containing PVAT.

Although the results in this study imply that SphK1/S1P/$S1PR_2$ might participate in adipose tissue inflammation via iNOS regulation, the results do not support the pathway being involved in the anticontractile effect of PVAT. However, I can't definitively conclude that this system is not involved in iNOS regulation within adipocytes of PVAT since the microenvironment of PVAT which is composed of several cell types, including smooth muscle cells, endothelial cells and immune cells, present a complexity in iNOS regulation via sphingolipid system. For example, it was demonstrated that S1P inhibits iNOS expression and NO production in rat vascular smooth muscle cells stimulated with IL-1β (Machida et al, 2008). Another study has reported that S1P/$S1PR_1$ inhibits LPS-mediated expression of iNOS in macrophages (Hughes et al, 2008). These studies suggest that S1P might have opposing effects on endothelial cells, VSMC and other cells within adipose tissue; possibly masking the effect that S1P produced from adipocytes under inflammatory conditions. In addition, NO has been found to interact with sphingolipid system metabolism, causing an inhibition in sphingomyelinase, an enzyme that converts ceramide to sphingosine, leading to a low level of S1P production (Perrotta et al, 2008). Therefore, this could potentially counteract the involvement of the sphingolipid system in iNOS derived NO from adipocytes in PVAT in response to IL-1β.

Although the current study characterises the link between iNOS regulation and sphingolipids in PVAT, it is not yet known whether this link is implicated in other adipose tissue disorders such as insulin resistance and lipid metabolism. As discussed in section 1-4-3 and 1-4-4, iNOS was shown to promote lipid metabolism under inflammatory conditions and was linked to insulin resistance in adipocytes and adipose tissue. It was proven in a number of studies that the SphK1/$S1PR_2$ axis regulates inflammation within adipose tissue, contributing to insulin resistance and glucose intolerance (Kitada et al, 2016; Olefsky & Glass, 2010; Wang et al, 2014; Zhang et al, 2014). This indicates that this system may promote insulin resistance within adipocytes via iNOS regulation. Therefore, characterisation of the link between the sphingolipid system and iNOS regulation in the context of insulin resistance and T2D are critical in attaining a better, more comprehensive, understanding of this complex relationship. This could ultimately identify novel potential therapeutic targets, leading to the development of novel therapies for adipose tissue related diseases.

6.2 Limitation and future direction

Although these findings yield valuable insights into the intricate role of the sphingolipid system in iNOS regulation in 3T3-L1 adipocyte cell line, it is important to acknowledge that these cells have several limitations. Firstly, while 3T3-L1 adipocytes are the most common model used to study adipose tissue function and biology, it does not represent a specific adipose tissue depot and so does not fully recapitulate the complexity of adipose tissue. So, really, it would be important to repeat some of these experiments in isolated primary adipocytes from different depots, particularly PVAT. To do this, primary adipocytes can be isolated from PVAT through enzymatic digestion and subsequent purification to be cultured and exposed to IL-1ß in the presence and absence of sphingolipid modulators. Secondly, while the mouse 3T3-L1 adipocyte cell line provides valuable insights into adipocyte biology and related processes, including the regulation of iNOS expression, it is important to recognise that mouse species may not fully reflect the effect in human. To address this limitation, future studies could use human adipocytes such as Simpson-Golabi-Behmel syndrome (SGBS) cells and human preadipocyte cell lines to determine the clinical relevance of the current findings within a broader and more clinically translatable context.

Another limitation of the current study is that enzymatic activity of SphK1 and S1P concentration in response to IL-1ß in 3T3-L1 adipocytes and RAW 267.4 was not directly measured. To address this, a SphK1 enzymatic assay could be performed, which typically involves incubating the cell lysate with radiolabelled sphingosine substrate and ATP to allow SphK1 to phosphorylate sphingosine to S1P. The formation and production of S1P from 3T3-L1 adipocytes in response to IL-1ß could be measured using various methods such as mass spectrometry (MS), high-performance liquid chromatography (HPLC), or enzyme-linked immunosorbent assay (ELISA).

It is important to highlight unanswered questions related to mechanistic pathways regulating iNOS in adipocytes via $S1PR_2$. iNOS phosphorylation is regulated at the post-translation level via RhoA/ROCK pathway (Glotfelty et al, 2023), and $S1PR_2$ has also been shown to activate this pathway. Therefore, it would be interesting to address the relationship between iNOS regulation and $S1PR_2$ regulated

RhoA/ROCK pathway. This approach can be performed by treating the stimulated adipocytes with inhibitors of the Rho/ROCK pathway, such as Y-27632 or fasudil in the presence and absence of $S1PR_2$ agonists to assess whether $S1PR_2$-mediated iNOS activation is Rho/ROCK pathway dependent. Then, measuring iNOS expression levels and NO production using techniques such as western blotting and a Sievers 280A NO Meter. Another future direction that could help to understand the role of SphK1 and $S1PR_2$ in iNOS regulation in 3T3-L1 cell would be the generation of a 3T3-L1 knockout for the SphK1 or $S1PR_2$. It's important to acknowledge that there is a difficulty of knocking down protein function by molecular biology techniques such as siRNA, however, some studies have attempted and succeeded in generation of a 3T3-L1 adipocyte knockout of SphK1 and $S1PR_2$ by siRNA technique (Hashimoto et al, 2009; Jeong et al, 2015). Using adipocytes isolated from SphK1 or $S1PR_2$ knockout animals should be considered as another future direction.

It was found in this thesis that SphK1/$S1PR_2$ axis in RAW 264.7 cells might play a role in inducing iNOS expression in adipocytes. It is likely that S1P produced as a result of SphK1 activation in response to LPS, in turn, activates $S1PR_2$ in RAW 264.7 cells, subsequently inducing cytokine release. However, the impact of this axis on macrophage polarisation and the secretion of proinflammatory mediators from macrophages has not been confirmed in this study. This approach could be performed by measuring the levels of pro-inflammatory and anti-inflammatory cytokines released by RAW 264.7 cells upon LPS stimulation in the presence and absence of SphK1 inhibitor and $S1PR_2$ inhibitor, using techniques such as ELISA or multiplex cytokine analysis.

When incubating rat aortic rings with PVAT with IL-1β, it should be recognised that IL-1β exerts effects not only on PVAT but also on other cell types within the vascular environment, including smooth muscle cells and endothelial cells. Therefore, it may be challenging to attribute the observed hyporeactivity solely to iNOS-derived NO production in PVAT. To address this, an alternative approach involves the isolation of PVAT from the thoracic aorta followed by incubation with IL-1β to induce upregulation of iNOS protein, then transfer the PVAT to the myograph bath to conduct functional studies. This approach may mitigate the direct impact of IL-1β on vascular cells, allowing for a more focused investigation

into the role of PVAT-derived factors, including iNOS-mediated NO production, in vascular hyporeactivity.

One other limitation in chapter 5 of this study is the reliance on ex vivo models, using isolated PVAT from healthy animal models and incubating it with an individual cytokine (IL-1β). While these models provide valuable insights into the mechanisms underlying vascular function and are commonly used, they do not represent the complexity of in vivo study. Therefore, it would be interesting to study the involvement of the sphingolipid system in the PVAT-mediated anticontractile effect isolated from the rat obesity model and rat sepsis model, given previous findings have indicated the involvement of PVAT in the relaxant effect via an iNOS-dependent pathway in a HFD rat model (Araujo et al, 2018) and a cecal ligation and puncture (CLA) sepsis rat model (Awata et al, 2019). In addition, it would be worthwhile to use rat models of obesity, endotoxemia or CLA sepsis and to treat these animals in vivo with sphingolipid modulators. Such experiments can provide insights into the physiological relevance of the sphingolipid system in PVAT-mediated vascular regulation under inflammatory conditions.

Previously, broad investigations have identified a potential link between iNOS expression and insulin resistance in adipose tissue of HFD animal model and adipocyte (Fite et al, 2015; Tsuchiya et al, 2007; Vilela et al, 2022). The present study has shown that IL-1β induces iNOS regulation in 3T3-L1 adipocytes via SphK1/S1P/S1PR$_2$ dependent pathway. Since this study has only focused on testing the involvement of sphingolipid system in PVAT-mediated hyporeactivity via iNOS pathway, it would be interesting to determine the link between iNOS regulation and sphingolipid system with respect to insulin resistance associated with obesity. This could be accomplished by using animal models that develop insulin resistance such as HFD-induced obesity and targeting sphingolipid modulators either by pharmacological or genetical intervention. Measurements could include determining iNOS expression and activity, sphingolipid levels, insulin sensitivity, and markers of inflammation in adipose tissue in response to various treatments or genetic manipulations. It is also important to investigate the signalling pathway regulating iNOS expression in adipose tissue such as MAPKs pathway and NF-KB.

This approach will allow for examination the role of the sphingolipid system in iNOS regulation and hence its link to insulin resistance.

6.3 Conclusion

In summary, the current study has shown the significance of the sphingolipid system in modulating iNOS regulation in adipocytes and PVAT. This thesis has demonstrated for the first time that IL-1β induces iNOS regulation in 3T3-L1 adipocytes via SphK1/S1P/$S1PR_2$/MAPK (ERK1/2 and JNK pathway) and PI3K/Akt pathway. This thesis has also demonstrated the pivotal role that SphK1/S1P/$S1PR_2$ signalling plays in mediating the interaction between macrophages and adipocytes, thereby influencing the regulation of iNOS within the adipose tissue microenvironment. However, the functional studies on PVAT did not support a significant role for SphK1/S1P/$S1PR_2$ axis in IL-1β-mediated hyporeactivity via iNOS upregulation. Hence, although this work revealed an important role for S1P in the pro-inflammatory regulation of iNOS in adipocytes, future work is required to fully elucidate the patho-physiological importance of this signalling within the context of conditions associated with inflamed adipose tissue.

Chapter 7 References

Aaronson, P. I., Ward, J. P. & Connolly, M. J. (2020) *The cardiovascular system at a glance*John Wiley & Sons.

Aarthi, J., Darendeliler, M. & Pushparaj, P. (2011) Dissecting the role of the S1P/S1PR axis in health and disease. *Journal of dental research*, 90(7), 841-854.

Ahmad, B., Serpell, C. J., Fong, I. L. & Wong, E. H. (2020) Molecular mechanisms of adipogenesis: the anti-adipogenic role of AMP-activated protein kinase. *Frontiers in molecular biosciences*, 7, 76.

Ahmadian, M., Wang, Y. & Sul, H. S. (2010) Lipolysis in adipocytes. *The international journal of biochemistry & cell biology*, 42(5), 555-559.

Ahmed, A., Bibi, A., Valoti, M. & Fusi, F. (2023) Perivascular Adipose Tissue and Vascular Smooth Muscle Tone: Friends or Foes? *Cells*, 12(8), 1196.

Aktan, F. (2004) iNOS-mediated nitric oxide production and its regulation. *Life sciences*, 75(6), 639-653.

Alemany, R., van Koppen, C. J., Danneberg, K., Ter Braak, M. & Meyer zu Heringdorf, D. (2007) Regulation and functional roles of sphingosine kinases. *Naunyn-Schmiedeberg's archives of pharmacology*, 374, 413-428.

Alewijnse, A. E., Peters, S. L. & Michel, M. C. (2004) Cardiovascular effects of sphingosine-1-phosphate and other sphingomyelin metabolites. *British journal of pharmacology*, 143(6), 666-684.

Alganga, H., Almabrouk, T. A., Katwan, O. J., Daly, C. J., Pyne, S., Pyne, N. J. & Kennedy, S. (2019) Short periods of hypoxia upregulate sphingosine kinase 1 and increase vasodilation of arteries to sphingosine 1-phosphate (S1P) via S1P3. *Journal of Pharmacology and Experimental Therapeutics*, 371(1), 63-74.

Almabrouk, T., Ewart, M., Salt, I. & Kennedy, S. (2014) Perivascular fat, AMP-activated protein kinase and vascular diseases. *British Journal of Pharmacology*, 171(3), 595-617.

Almabrouk, T. A., Ugusman, A. B., Katwan, O. J., Salt, I. P. & Kennedy, S. (2017) Deletion of AMPKα1 attenuates the anticontractile effect of perivascular adipose tissue (PVAT) and reduces adiponectin release. *British Journal of Pharmacology*, 174(20), 3398-3410.

Almabrouk, T. A., White, A. D., Ugusman, A. B., Skiba, D. S., Katwan, O. J., Alganga, H., Guzik, T. J., Touyz, R. M., Salt, I. P. & Kennedy, S. (2018) High fat diet attenuates the anticontractile activity of aortic PVAT via a mechanism involving AMPK and reduced adiponectin secretion. *Frontiers in physiology*, 9, 51.

Alvarez, S. E., Harikumar, K. B., Hait, N. C., Allegood, J., Strub, G. M., Kim, E. Y., Maceyka, M., Jiang, H., Luo, C. & Kordula, T. (2010) Sphingosine-1-phosphate is a missing cofactor for the E3 ubiquitin ligase TRAF2. *Nature*, 465(7301), 1084-1088.

Anderson, A. K., Lambert, J. M., Montefusco, D. J., Tran, B. N., Roddy, P., Holland, W. L. & Cowart, L. A. (2020) Depletion of adipocyte sphingosine

kinase 1 leads to cell hypertrophy, impaired lipolysis, and nonalcoholic fatty liver disease. *Journal of Lipid Research*, 61(10), 1328-1340.

Andersson, K., Gaudiot, N., Ribiere, C., Elizalde, M., Giudicelli, Y. & Arner, P. (1999) A nitric oxide-mediated mechanism regulates lipolysis in human adipose tissue in vivo. *British journal of pharmacology*, 126(7), 1639-1645.

Anelli, V., Gault, C. R., Cheng, A. B. & Obeid, L. M. (2008) Sphingosine kinase 1 is up-regulated during hypoxia in U87MG glioma cells: role of hypoxia-inducible factors 1 and 2. *Journal of Biological Chemistry*, 283(6), 3365-3375.

Araki, S., DoBAsHI, K., KuBo, K., KAwAGoE, R., YAMAMoTo, Y. & Shirahata, A. (2007) N-acetylcysteine inhibits induction of nitric oxide synthase in 3T3-L1 adipocytes. *Journal of UOEH*, 29(4), 417-429.

Araujo, H. N., Victório, J. A., Valgas da Silva, C. P., Sponton, A. C., Vettorazzi, J. F., de Moraes, C., Davel, A. P., Zanesco, A. & Delbin, M. A. (2018) Anti-contractile effects of perivascular adipose tissue in thoracic aorta from rats fed a high-fat diet: role of aerobic exercise training. *Clinical and Experimental Pharmacology and Physiology*, 45(3), 293-302.

Asano, M., Kajita, K., Fuwa, M., Kajita, T., Mori, I., Akahoshi, N., Ishii, I. & Morita, H. (2023) Opposing Roles of Sphingosine 1-Phosphate Receptors 1 and 2 in Fat Deposition and Glucose Tolerance in Obese Male Mice. *Endocrinology*, 164(3), bqad019.

Awata, W. M., Gonzaga, N. A., Borges, V. F., Silva, C. B., Tanus-Santos, J. E., Cunha, F. Q. & Tirapelli, C. R. (2019) Perivascular adipose tissue contributes to lethal sepsis-induced vasoplegia in rats. *European Journal of Pharmacology*, 863, 172706.

Bavelloni, A., Santi, S., Sirri, A., Riccio, M., Faenza, I., Zini, N., Cecchi, S., Ferri, A., Auron, P. & Maraldi, N. M. (1999) Phosphatidylinositol 3-kinase translocation to the nucleus is induced by interleukin 1 and prevented by mutation of interleukin 1 receptor in human osteosarcoma Saos-2 cells. *Journal of cell science*, 112(5), 631-640.

Becerril, S., Rodriguez, A., Catalán, V., Méndez-Giménez, L., Ramírez, B., Sainz, N., Llorente, M., Unamuno, X., Gomez-Ambrosi, J. & Frühbeck, G. (2018) Targeted disruption of the iNOS gene improves adipose tissue inflammation and fibrosis in leptin-deficient ob/ob mice: role of tenascin C. *International Journal of Obesity*, 42(8), 1458-1470.

Beckman, J. S. (1996) Oxidative damage and tyrosine nitration from peroxynitrite. *Chemical research in toxicology*, 9(5), 836-844.

Beckman, J. S. & Koppenol, W. H. (1996) Nitric oxide, superoxide, and peroxynitrite: the good, the bad, and ugly. *American Journal of Physiology-cell physiology*, 271(5), C1424-C1437.

Bektas, M., Allende, M. L., Lee, B. G., Chen, W., Amar, M. J., Remaley, A. T., Saba, J. D. & Proia, R. L. (2010) Sphingosine 1-phosphate lyase deficiency disrupts lipid homeostasis in liver. *Journal of Biological Chemistry*, 285(14), 10880-10889.

Billich, A., Bornancin, F., Mechtcheriakova, D., Natt, F., Huesken, D. & Baumruker, T. (2005) Basal and induced sphingosine kinase 1 activity in A549 carcinoma cells: function in cell survival and IL-1β and TNF-α induced production of inflammatory mediators. *Cellular signalling*, 17(10), 1203-1217.

Bing, C. (2015) Is interleukin-1β a culprit in macrophage-adipocyte crosstalk in obesity? *Adipocyte*, 4(2), 149-152.

Birchwood, C. J., Saba, J. D., Dickson, R. C. & Cunningham, K. W. (2001) Calcium influx and signaling in yeast stimulated by intracellular sphingosine 1-phosphate accumulation. *Journal of Biological Chemistry*, 276(15), 11712-11718.

Bischoff, A., Czyborra, P., Fetscher, C., Meyer zu Heringdorf, D., Jakobs, K. H. & Michel, M. C. (2000) Sphingosine-1-phosphate and sphingosylphosphorylcholine constrict renal and mesenteric microvessels in vitro. *British journal of pharmacology*, 130(8), 1871-1877.

Blankenbach, K. V., Schwalm, S., Pfeilschifter, J. & Meyer zu Heringdorf, D. (2016) Sphingosine-1-phosphate receptor-2 antagonists: therapeutic potential and potential risks. *Frontiers in Pharmacology*, 7, 167.

Blüher, M. (2012) Clinical relevance of adipokines. *Diabetes & metabolism journal*, 36(5), 317-327.

Blüher, M. (2019) Obesity: global epidemiology and pathogenesis. *Nature Reviews Endocrinology*, 15(5), 288-298.

Bonica, J., Mao, C., Obeid, L. M. & Hannun, Y. A. (2020) Transcriptional regulation of sphingosine kinase 1. *Cells*, 9(11), 2437.

Boutari, C. & Mantzoros, C. S. (2022) A 2022 update on the epidemiology of obesity and a call to action: as its twin COVID-19 pandemic appears to be receding, the obesity and dysmetabolism pandemic continues to rage on. Elsevier.

Brinkmann, V., Billich, A., Baumruker, T., Heining, P., Schmouder, R., Francis, G., Aradhye, S. & Burtin, P. (2010) Fingolimod (FTY720): discovery and development of an oral drug to treat multiple sclerosis. *Nature reviews Drug discovery*, 9(11), 883-897.

Brizuela, L., Rábano, M., Gangoiti, P., Narbona, N., Macarulla, J. M., Trueba, M. & Gomez-Munoz, A. (2007) Sphingosine-1-phosphate stimulates aldosterone secretion through a mechanism involving the PI3K/PKB and MEK/ERK 1/2 pathways. *Journal of lipid research*, 48(10), 2264-2274.

Brouet, A., Sonveaux, P., Dessy, C., Balligand, J.-L. & Feron, O. (2001) Hsp90 ensures the transition from the early Ca2+-dependent to the late phosphorylation-dependent activation of the endothelial nitric-oxide synthase in vascular endothelial growth factor-exposed endothelial cells. *Journal of Biological Chemistry*, 276(35), 32663-32669.

Bruno, G., Cencetti, F., Bernacchioni, C., Donati, C., Blankenbach, K. V., Thomas, D., Zu Heringdorf, D. M. & Bruni, P. (2018) Bradykinin mediates myogenic differentiation in murine myoblasts through the involvement of SK1/Spns2/S1P2 axis. *Cellular Signalling*, 45, 110-121.

Bryan, A. M. & Del Poeta, M. (2018) Sphingosine-1-phosphate receptors and innate immunity. *Cellular microbiology*, 20(5), e12836.

Bryan, L., Paugh, B. S., Kapitonov, D., Wilczynska, K. M., Alvarez, S. M., Singh, S. K., Milstien, S., Spiegel, S. & Kordula, T. (2008) Sphingosine-1-phosphate and interleukin-1 independently regulate plasminogen activator inhibitor-1 and urokinase-type plasminogen activator receptor expression in glioblastoma cells: implications for invasiveness. *Molecular Cancer Research*, 6(9), 1469-1477.

Bu, Y., Wu, H., Deng, R. & Wang, Y. (2021) Therapeutic potential of SphK1 inhibitors based on abnormal expression of sphk1 in inflammatory immune related-diseases. *Frontiers in pharmacology*, 12, 733387.

Byun, H.-S., Pyne, S., MacRitchie, N., Pyne, N. J. & Bittman, R. (2013) Novel sphingosine-containing analogues selectively inhibit sphingosine kinase (SK) isozymes, induce SK1 proteasomal degradation and reduce DNA synthesis in human pulmonary arterial smooth muscle cells. *Medchemcomm*, 4(10), 1394-1399.

Cai, Z., Huang, Y. & He, B. (2022) New insights into adipose tissue macrophages in obesity and insulin resistance. *Cells*, 11(9), 1424.

Candi, E., Tesauro, M., Cardillo, C., Lena, A. M., Schinzari, F., Rodia, G., Sica, G., Gentileschi, P., Rovella, V. & Annicchiarico-Petruzzelli, M. (2018) Metabolic profiling of visceral adipose tissue from obese subjects with or without metabolic syndrome. *Biochemical Journal*, 475(5), 1019-1035.

Cannavo, A., Liccardo, D., Komici, K., Corbi, G., De Lucia, C., Femminella, G. D., Elia, A., Bencivenga, L., Ferrara, N. & Koch, W. J. (2017) Sphingosine kinases and sphingosine 1-phosphate receptors: signaling and actions in the cardiovascular system. *Frontiers in pharmacology*, 8, 556.

Cannon, B. & Nedergaard, J. (2004) Brown adipose tissue: function and physiological significance. *Physiological reviews*.

Cao, C., Dai, L., Mu, J., Wang, X., Hong, Y., Zhu, C., Jin, L. & Li, S. (2019) S1PR2 antagonist alleviates oxidative stress-enhanced brain endothelial permeability by attenuating p38 and Erk1/2-dependent cPLA2 phosphorylation. *Cellular Signalling*, 53, 151-161.

Catalan, V., Gomez-Ambrosi, J., Rodríguez, A., Ramírez, B., Rotellar, F., Valentí, V., Silva, C., Gil, M. J., Salvador, J. & Frühbeck, G. (2012) Increased tenascin C and Toll-like receptor 4 levels in visceral adipose tissue as a link between inflammation and extracellular matrix remodeling in obesity. *The Journal of Clinical Endocrinology & Metabolism*, 97(10), E1880-E1889.

Chait, A. & Den Hartigh, L. J. (2020) Adipose tissue distribution, inflammation and its metabolic consequences, including diabetes and cardiovascular disease. *Frontiers in cardiovascular medicine*, 7, 522637.

Chakrabarty, S., Bui, Q., Badeanlou, L., Hester, K., Chun, J., Ruf, W., Ciaraldi, T. P. & Samad, F. (2022) S1P/S1PR3 signalling axis protects against obesity-induced metabolic dysfunction. *Adipocyte*, 11(1), 69-83.

Chandru, H. & Boggaram, V. (2007) The role of sphingosine 1-phosphate in the TNF-α induction of IL-8 gene expression in lung epithelial cells. *Gene*, 391(1-2), 150-160.

Chang, M.-C., Lin, S.-I., Pan, Y.-H., Lin, L.-D., Wang, Y.-L., Yeung, S.-Y., Chang, H.-H. & Jeng, J.-H. (2019) IL-1ß-induced ICAM-1 and IL-8 expression/secretion of dental pulp cells is differentially regulated by IRAK and p38. *Journal of the Formosan Medical Association*, 118(8), 1247-1254.

Chaurasia, B., Kaddai, V. A., Lancaster, G. I., Henstridge, D. C., Sriram, S., Galam, D. L. A., Gopalan, V., Prakash, K. B., Velan, S. S. & Bulchand, S. (2016) Adipocyte ceramides regulate subcutaneous adipose browning, inflammation, and metabolism. *Cell metabolism*, 24(6), 820-834.

Chen, H., Ahmed, S., Zhao, H., Elghobashi-Meinhardt, N., Dai, Y., Kim, J. H., McDonald, J. G., Li, X. & Lee, C.-H. (2023a) Structural and functional insights into Spns2-mediated transport of sphingosine-1-phosphate. *Cell*, 186(12), 2644-2655. e16.

Chen, R., McVey, D. G., Shen, D., Huang, X. & Ye, S. (2023b) Phenotypic Switching of Vascular Smooth Muscle Cells in Atherosclerosis. *Journal of the American Heart Association*, 12(20), e031121.

Cheng, C. K., Bakar, H. A., Gollasch, M. & Huang, Y. (2018) Perivascular adipose tissue: the sixth man of the cardiovascular system. *Cardiovascular drugs and therapy*, 32, 481-502.

Chew, W. S., Wang, W. & Herr, D. R. (2016) To fingolimod and beyond: The rich pipeline of drug candidates that target S1P signaling. *Pharmacological research*, 113, 521-532.

Cinti, S. (2011) Between brown and white: novel aspects of adipocyte differentiation. *Annals of medicine*, 43(2), 104-115.

Clementi, E., Borgese, N. & Meldolesi, J. (2003) Interactions between nitric oxide and sphingolipids and the potential consequences in physiology and pathology. *Trends in pharmacological sciences*, 24(10), 518-523.

Contos, J. J., Ishii, I. & Chun, J. (2000) Lysophosphatidic acid receptors. *Molecular pharmacology*, 58(6), 1188-1196.

Coppack, S. W. (2001) Pro-inflammatory cytokines and adipose tissue. *Proceedings of the nutrition society*, 60(3), 349-356.

Cortese-Krott, M. M., Kulakov, L., Opländer, C., Kolb-Bachofen, V., Kröncke, K.-D. & Suschek, C. V. (2014) Zinc regulates iNOS-derived nitric oxide formation in endothelial cells. *Redox biology*, 2, 945-954.

Coussin, F., Scott, R. H., Wise, A. & Nixon, G. F. (2002) Comparison of sphingosine 1-phosphate–induced intracellular signaling pathways in vascular smooth muscles: differential role in vasoconstriction. *Circulation research*, 91(2), 151-157.

Cowart, L. A. (2016) Sphingosine-1-Phosphate Signaling in Non-Alcoholic Steatohepatitis. *The FASEB Journal*, 30, 870.6-870.6.

Coyle, P. K., Freedman, M. S., Cohen, B. A., Cree, B. A. & Markowitz, C. E. (2024) Sphingosine 1-phosphate receptor modulators in multiple sclerosis

treatment: A practical review. *Annals of Clinical and Translational Neurology*.

Dallaire, P., Bellmann, K., Laplante, M., Gélinas, S., Centeno-Baez, C., Penfornis, P., Peyot, M.-L., Latour, M. G., Lamontagne, J. & Trujillo, M. E. (2008) Obese mice lacking inducible nitric oxide synthase are sensitized to the metabolic actions of peroxisome proliferator–activated receptor-γ agonism. *Diabetes*, 57(8), 1999-2011.

Daly, C. J. (2019) Examining vascular structure and function using confocal microscopy and 3d imaging techniques. *Biomedical Visualisation: Volume 1*, 97-106.

Dantas, A. P. V., Igarashi, J. & Michel, T. (2003) Sphingosine 1-phosphate and control of vascular tone. *American Journal of Physiology-Heart and Circulatory Physiology*, 284(6), H2045-H2052.

Deanfield, J. E., Halcox, J. P. & Rabelink, T. J. (2007) Endothelial function and dysfunction: testing and clinical relevance. *Circulation*, 115(10), 1285-1295.

Deutschman, D. H., Carstens, J. S., Klepper, R. L., Smith, W. S., Page, M. T., Young, T. R., Gleason, L. A., Nakajima, N. & Sabbadini, R. A. (2003) Predicting obstructive coronary artery disease with serum sphingosine-1-phosphate. *American heart journal*, 146(1), 62-68.

di Villa Bianca, R. d. E., Sorrentino, R., Sorrentino, R., Imbimbo, C., Palmieri, A., Fusco, F., Maggi, M., De Palma, R., Cirino, G. & Mirone, V. (2006) Sphingosine 1-phosphate induces endothelial nitric-oxide synthase activation through phosphorylation in human corpus cavernosum. *Journal of Pharmacology and Experimental Therapeutics*, 316(2), 703-708.

Digby, G. J., Conn, P. J. & Lindsley, C. W. (2010) Orthosteric-and allosteric-induced ligand-directed trafficking at GPCRs. *Current opinion in drug discovery & development*, 13(5), 587.

Du, J., Zeng, C., Li, Q., Chen, B., Liu, H., Huang, X. & Huang, Q. (2012) LPS and TNF-α induce expression of sphingosine-1-phosphate receptor-2 in human microvascular endothelial cells. *Pathology-Research and Practice*, 208(2), 82-88.

Dubrovska, G., Verlohren, S., Luft, F. C. & Gollasch, M. (2004) Mechanisms of ADRF release from rat aortic adventitial adipose tissue. *American Journal of Physiology-Heart and Circulatory Physiology*, 286(3), H1107-H1113.

Edwards, M. & Mohiuddin, S. S. (2020) Biochemistry, Lipolysis.

El-Shewy, H. M., Parnham, S., Fedarovich, D., Bullesbach, E. & Luttrell, L. M. (2018) Sphingosine 1 Phosphate Regulates Store-Operated Calcium Entry through binding to STIM1. *The FASEB Journal*, 32, 815.10-815.10.

Engeli, S., Janke, J., Gorzelniak, K., Böhnke, J., Ghose, N., Lindschau, C., Luft, F. C. & Sharma, A. M. (2004) Regulation of the nitric oxide system in human adipose tissue. *Journal of lipid research*, 45(9), 1640-1648.

Engin, A. (2017) The pathogenesis of obesity-associated adipose tissue inflammation. *Obesity and lipotoxicity*, 221-245.

Fajas, L. (2003) Adipogenesis: a cross-talk between cell proliferation and cell differentiation. *Annals of medicine*, 35(2), 79-85.

Fang, L., Zhao, J., Chen, Y., Ma, T., Xu, G., Tang, C., Liu, X. & Geng, B. (2009) Hydrogen sulfide derived from periadventitial adipose tissue is a vasodilator. *Journal of hypertension*, 27(11), 2174-2185.

Fang, Z., Pyne, S. & Pyne, N. J. (2019) Ceramide and sphingosine 1-phosphate in adipose dysfunction. *Progress in lipid research*, 74, 145-159.

Fayyaz, S., Henkel, J., Japtok, L., Krämer, S., Damm, G., Seehofer, D., Püschel, G. P. & Kleuser, B. (2014) Involvement of sphingosine 1-phosphate in palmitate-induced insulin resistance of hepatocytes via the S1P 2 receptor subtype. *Diabetologia*, 57, 373-382.

Fedorenko, A., Lishko, P. V. & Kirichok, Y. (2012) Mechanism of fatty-acid-dependent UCP1 uncoupling in brown fat mitochondria. *Cell*, 151(2), 400-413.

Feistritzer, C. & Riewald, M. (2005) Endothelial barrier protection by activated protein C through PAR1-dependent sphingosine 1–phosphate receptor-1 crossactivation. *Blood*, 105(8), 3178-3184.

Fernández-Pisonero, I., Dueñas, A. I., Barreiro, O., Montero, O., Sánchez-Madrid, F. & García-Rodríguez, C. (2012) Lipopolysaccharide and sphingosine-1-phosphate cooperate to induce inflammatory molecules and leukocyte adhesion in endothelial cells. *The Journal of Immunology*, 189(11), 5402-5410.

Fields, J. K., Günther, S. & Sundberg, E. J. (2019) Structural basis of IL-1 family cytokine signaling. *Frontiers in immunology*, 10, 1412.

Fite, A., Abou-Samra, A. B. & Seyoum, B. (2015) Macrophages inhibit insulin signalling in adipocytes: role of inducible nitric oxide synthase and nitric oxide. *Canadian Journal of Diabetes*, 39(1), 36-43.

Fitzgibbons, T. P., Kogan, S., Aouadi, M., Hendricks, G. M., Straubhaar, J. & Czech, M. P. (2011) Similarity of mouse perivascular and brown adipose tissues and their resistance to diet-induced inflammation. *American Journal of Physiology-Heart and Circulatory Physiology*, 301(4), H1425-H1437.

Förstermann, U. & Sessa, W. C. (2012) Nitric oxide synthases: regulation and function. *European heart journal*, 33(7), 829-837.

French, K. J., Schrecengost, R. S., Lee, B. D., Zhuang, Y., Smith, S. N., Eberly, J. L., Yun, J. K. & Smith, C. D. (2003) Discovery and evaluation of inhibitors of human sphingosine kinase. *Cancer research*, 63(18), 5962-5969.

Fujimoto, M., Shimizu, N., Kunii, K., Martyn, J. J., Ueki, K. & Kaneki, M. (2005) A role for iNOS in fasting hyperglycemia and impaired insulin signaling in the liver of obese diabetic mice. *Diabetes*, 54(5), 1340-1348.

Fujita, T., Okada, T., Hayashi, S., Jahangeer, S., Miwa, N. & Nakamura, S.-i. (2004) δ-Catenin/NPRAP (neural plakophilin-related armadillo repeat protein) interacts with and activates sphingosine kinase 1. *Biochemical Journal*, 382(2), 717-723.

Fukuda, Y., Aoyama, Y., Wada, A. & Igarashi, Y. (2004) Identification of PECAM-1 association with sphingosine kinase 1 and its regulation by agonist-induced

phosphorylation. *Biochimica et Biophysica Acta (BBA)-Molecular and Cell Biology of Lipids*, 1636(1), 12-21.

Fukuhara, S., Simmons, S., Kawamura, S., Inoue, A., Orba, Y., Tokudome, T., Sunden, Y., Arai, Y., Moriwaki, K. & Ishida, J. (2012) The sphingosine-1-phosphate transporter Spns2 expressed on endothelial cells regulates lymphocyte trafficking in mice. *The Journal of clinical investigation*, 122(4), 1416-1426.

Funcke, J.-B. & Scherer, P. E. (2019) Beyond adiponectin and leptin: adipose tissue-derived mediators of inter-organ communication. *Journal of lipid research*, 60(10), 1648-1697.

Gabriel, T. L., Mirzaian, M., Hooibrink, B., Ottenhoff, R., van Roomen, C., Aerts, J. M. & van Eijk, M. (2017) Induction of Sphk1 activity in obese adipose tissue macrophages promotes survival. *PLoS One*, 12(7), e0182075.

Galvez-Prieto, B., Dubrovska, G., Cano, M., Delgado, M., Aranguez, I., Gonzalez, M. C., Ruiz-Gayo, M., Gollasch, M. & Fernandez-Alfonso, M. S. (2008) A reduction in the amount and anti-contractile effect of periadventitial mesenteric adipose tissue precedes hypertension development in spontaneously hypertensive rats. *Hypertension research*, 31(7), 1415-1423.

Gálvez-Prieto, B., Somoza, B., Gil-Ortega, M., García-Prieto, C. F., de Las Heras, A. I., González, M. C., Arribas, S., Aranguez, I., Bolbrinker, J. & Kreutz, R. (2012) Anticontractile effect of perivascular adipose tissue and leptin are reduced in hypertension. *Frontiers in pharmacology*, 3, 103.

Ganbaatar, B., Fukuda, D., Shinohara, M., Yagi, S., Kusunose, K., Yamada, H., Soeki, T., Hirata, K.-i. & Sata, M. (2021) Inhibition of S1P receptor 2 attenuates endothelial dysfunction and inhibits atherogenesis in apolipoprotein E-deficient mice. *Journal of Atherosclerosis and Thrombosis*, 28(6), 630-642.

Gandy, K. A. O. & Obeid, L. M. (2013) Targeting the sphingosine kinase/sphingosine 1-phosphate pathway in disease: review of sphingosine kinase inhibitors. *Biochimica et Biophysica Acta (BBA)-Molecular and Cell Biology of Lipids*, 1831(1), 157-166.

Gao, D., Madi, M., Ding, C., Fok, M., Steele, T., Ford, C., Hunter, L. & Bing, C. (2014) Interleukin-1β mediates macrophage-induced impairment of insulin signaling in human primary adipocytes. *American Journal of Physiology-Endocrinology and Metabolism*, 307(3), E289-E304.

Gao, Y. J., Lu, C., Su, L. Y., Sharma, A. & Lee, R. (2007) Modulation of vascular function by perivascular adipose tissue: the role of endothelium and hydrogen peroxide. *British journal of pharmacology*, 151(3), 323-331.

Ghanbari, M., Maragheh, S. M., Aghazadeh, A., Mehrjuyan, S. R., Hussen, B. M., Shadbad, M. A., Dastmalchi, N. & Safaralizadeh, R. (2021) Interleukin-1 in obesity-related low-grade inflammation: From molecular mechanisms to therapeutic strategies. *International immunopharmacology*, 96, 107765.

Gil-Ortega, M., Stucchi, P., Guzman-Ruiz, R., Cano, V., Arribas, S., Gonzalez, M. C., Ruiz-Gayo, M., Fernandez-Alfonso, M. S. & Somoza, B. (2010) Adaptative nitric oxide overproduction in perivascular adipose tissue during early diet-induced obesity. *Endocrinology*, 151(7), 3299-3306.

Glotfelty, E. J., Tovar-y-Romo, L. B., Hsueh, S.-C., Tweedie, D., Li, Y., Harvey, B. K., Hoffer, B. J., Karlsson, T. E., Olson, L. & Greig, N. H. (2023) The RhoA-ROCK1/ROCK2 Pathway Exacerbates Inflammatory Signaling in Immortalized and Primary Microglia. *Cells*, 12(10), 1367.

Goetzl, E. J., Wang, W., McGiffert, C., Huang, M. C. & Gräler, M. H. (2004) Sphingosine 1-phosphate and its G protein-coupled receptors constitute a multifunctional immunoregulatory system. *Journal of cellular biochemistry*, 92(6), 1104-1114.

Gollasch, M. (2017) Adipose-vascular coupling and potential therapeutics. *Annual review of pharmacology and toxicology*, 57, 417-436.

Gonda, K., OKAMOTO, H., TAKUWA, N., YATOMI, Y., OKAZAKI, H., SAKURAI, T., KIMURA, S., SILLARD, R., HARII, K. & TAKUWA, Y. (1999) The novel sphingosine 1-phosphate receptor AGR16 is coupled via pertussis toxin-sensitive and-insensitive G-proteins to multiple signalling pathways. *Biochemical Journal*, 337(1), 67-75.

Gong, W., Li, J., Chen, W., Feng, F. & Deng, Y. (2020) Resveratrol inhibits lipopolysaccharide-induced extracellular matrix accumulation and inflammation in rat glomerular mesangial cells by SphK1/S1P2/NF-κB pathway. *Diabetes, Metabolic Syndrome and Obesity*, 4495-4505.

Gosejacob, D., Jäger, P. S., Vom Dorp, K., Frejno, M., Carstensen, A. C., Köhnke, M., Degen, J., Dörmann, P. & Hoch, M. (2016) Ceramide synthase 5 is essential to maintain C16: 0-ceramide pools and contributes to the development of diet-induced obesity. *Journal of Biological Chemistry*, 291(13), 6989-7003.

Greenstein, A. S., Khavandi, K., Withers, S. B., Sonoyama, K., Clancy, O., Jeziorska, M., Laing, I., Yates, A. P., Pemberton, P. W. & Malik, R. A. (2009) Local inflammation and hypoxia abolish the protective anticontractile properties of perivascular fat in obese patients. *Circulation*, 119(12), 1661-1670.

Gregoire, F. M., Smas, C. M. & Sul, H. S. (1998) Understanding adipocyte differentiation. *Physiological reviews*, 78(3), 783-809.

Guitton, J., Bandet, C. L., Mariko, M. L., Tan-Chen, S., Bourron, O., Benomar, Y., Hajduch, E. & Le Stunff, H. (2020) Sphingosine-1-phosphate metabolism in the regulation of obesity/type 2 diabetes. *Cells*, 9(7), 1682.

Gurgui, M., Broere, R., Kalff, J. C. & van Echten-Deckert, G. (2010) Dual action of sphingosine 1-phosphate in eliciting proinflammatory responses in primary cultured rat intestinal smooth muscle cells. *Cellular signalling*, 22(11), 1727-1733.

Habibian, J. S., Jefic, M., Bagchi, R. A., Lane, R. H., McKnight, R. A., McKinsey, T. A., Morrison, R. F. & Ferguson, B. S. (2017) DUSP5 functions as a feedback regulator of TNFα-induced ERK1/2 dephosphorylation and inflammatory gene expression in adipocytes. *Scientific Reports*, 7(1), 12879.

Hai-Mei, L., Song-Yin, H., Run-Mei, L., Xiao-Huang, X., Le-Quan, Z., Xiao-Ping, L. & Jin-Wen, X. (2013) Andrographolide protects against lipopolysaccharide-induced vascular hyporeactivity by suppressing the expression of inducible

nitric oxide in periaortic adipose. *Journal of cardiovascular pharmacology*, 62(2), 154-159.

Hait, N. C., Bellamy, A., Milstien, S., Kordula, T. & Spiegel, S. (2007) Sphingosine kinase type 2 activation by ERK-mediated phosphorylation. *Journal of Biological Chemistry*, 282(16), 12058-12065.

Hait, N. C., Sarkar, S., Le Stunff, H., Mikami, A., Maceyka, M., Milstien, S. & Spiegel, S. (2005) Role of sphingosine kinase 2 in cell migration toward epidermal growth factor. *Journal of Biological Chemistry*, 280(33), 29462-29469.

Hammad, S. M., Crellin, H. G., Wu, B. X., Melton, J., Anelli, V. & Obeid, L. M. (2008) Dual and distinct roles for sphingosine kinase 1 and sphingosine 1 phosphate in the response to inflammatory stimuli in RAW macrophages. *Prostaglandins & other lipid mediators*, 85(3-4), 107-114.

Handa, M., Vanegas, S., Maddux, B. A., Mendoza, N., Zhu, S., Goldfine, I. D. & Mirza, A. M. (2013) XOMA 052, an anti-IL-1ß monoclonal antibody, prevents IL-1ß-mediated insulin resistance in 3T3-L1 adipocytes. *Obesity*, 21(2), 306-309.

Harms, M. & Seale, P. (2013) Brown and beige fat: development, function and therapeutic potential. *Nature medicine*, 19(10), 1252-1263.

Hashimoto, T., Igarashi, J. & Kosaka, H. (2009) Sphingosine kinase is induced in mouse 3T3-L1 cells and promotes adipogenesis [S]. *Journal of lipid research*, 50(4), 602-610.

Hazar-Rethinam, M., de Long, L. M., Gannon, O. M., Topkas, E., Boros, S., Vargas, A. C., Dzienis, M., Mukhopadhyay, P., Simpson, F. & Endo-Munoz, L. (2015) A novel E2F/sphingosine kinase 1 axis regulates anthracycline response in squamous cell carcinoma. *Clinical Cancer Research*, 21(2), 417-427.

Hemmings, D. G. (2006) Signal transduction underlying the vascular effects of sphingosine 1-phosphate and sphingosylphosphorylcholine. *Naunyn-Schmiedeberg's archives of pharmacology*, 373, 18-29.

Hemmings, D. G., Hudson, N. K., Halliday, D., O'Hara, M., Baker, P. N., Davidge, S. T. & Taggart, M. J. (2006) Sphingosine-1-phosphate acts via rho-associated kinase and nitric oxide to regulate human placental vascular tone. *Biology of reproduction*, 74(1), 88-94.

Hernanz, R., Alonso, M. J., Zibrandtsen, H., Alvarez, Y., Salaices, M. & Simonsen, U. (2004) Measurements of nitric oxide concentration and hyporeactivity in rat superior mesenteric artery exposed to endotoxin. *Cardiovascular research*, 62(1), 202-211.

Herr, D. R., Reolo, M. J., Peh, Y. X., Wang, W., Lee, C.-W., Rivera, R., Paterson, I. C. & Chun, J. (2016) Sphingosine 1-phosphate receptor 2 (S1P2) attenuates reactive oxygen species formation and inhibits cell death: implications for otoprotective therapy. *Scientific reports*, 6(1), 24541.

Hisano, Y., Kobayashi, N., Kawahara, A., Yamaguchi, A. & Nishi, T. (2011) The sphingosine 1-phosphate transporter, SPNS2, functions as a transporter of the phosphorylated form of the immunomodulating agent FTY720. *Journal of Biological Chemistry*, 286(3), 1758-1766.

Hisano, Y., Kobayashi, N., Yamaguchi, A. & Nishi, T. (2012) Mouse SPNS2 functions as a sphingosine-1-phosphate transporter in vascular endothelial cells. *PloS one*, 7(6), e38941.

Hla, T. & Maciag, T. (1990) An abundant transcript induced in differentiating human endothelial cells encodes a polypeptide with structural similarities to G-protein-coupled receptors. *Journal of Biological Chemistry*, 265(16), 9308-9313.

Hou, L., Zhang, Z., Yang, L., Chang, N., Zhao, X., Zhou, X., Yang, L. & Li, L. (2021) NLRP3 inflammasome priming and activation in cholestatic liver injury via the sphingosine 1-phosphate/S1P receptor 2/Gα (12/13)/MAPK signaling pathway. *Journal of Molecular Medicine*, 99, 273-288.

Hu, H., Garcia-Barrio, M., Jiang, Z.-s., Chen, Y. E. & Chang, L. (2021) Roles of perivascular adipose tissue in hypertension and atherosclerosis. *Antioxidants & Redox Signaling*, 34(9), 736-749.

Hu, S. L., Huang, C. C., Tseng, T. T., Liu, S. C., Tsai, C. H., Fong, Y. C. & Tang, C. H. (2020) S1P facilitates IL-1ß production in osteoblasts via the JAK and STAT3 signaling pathways. *Environmental toxicology*, 35(9), 991-997.

Hughes, J. E., Srinivasan, S., Lynch, K. R., Proia, R. L., Ferdek, P. & Hedrick, C. C. (2008) Sphingosine-1-phosphate induces an antiinflammatory phenotype in macrophages. *Circulation research*, 102(8), 950-958.

Igarashi, J. & Michel, T. (2009) Sphingosine-1-phosphate and modulation of vascular tone. *Cardiovascular research*, 82(2), 212-220.

Ikeda, Y., Tsuchiya, H., Hama, S., Kajimoto, K. & Kogure, K. (2014) Resistin regulates the expression of plasminogen activator inhibitor-1 in 3T3-L1 adipocytes. *Biochemical and biophysical research communications*, 448(2), 129-133.

Ishii, I., Friedman, B., Ye, X., Kawamura, S., McGiffert, C., Contos, J. J., Kingsbury, M. A., Zhang, G., Brown, J. H. & Chun, J. (2001) Selective loss of sphingosine 1-phosphate signaling with no obvious phenotypic abnormality in mice lacking its G protein-coupled receptor, LPB3/EDG-3. *Journal of Biological Chemistry*, 276(36), 33697-33704.

Ito, S., Iwaki, S., Koike, K., Yuda, Y., Nagasaki, A., Ohkawa, R., Yatomi, Y., Furumoto, T., Tsutsui, H. & Sobel, B. E. (2013) Increased plasma sphingosine-1-phosphate in obese individuals and its capacity to increase the expression of plasminogen activator inhibitor-1 in adipocytes. *Coronary artery disease*, 24(8), 642-650.

Jager, J., Grémeaux, T., Cormont, M., Le Marchand-Brustel, Y. & Tanti, J.-F. (2007) Interleukin-1ß-induced insulin resistance in adipocytes through down-regulation of insulin receptor substrate-1 expression. *Endocrinology*, 148(1), 241-251.

Jang, B.-C., Paik, J.-H., Kim, S.-P., Bae, J.-H., Mun, K.-C., Song, D.-K., Cho, C.-H., Shin, D.-H., Kwon, T. K. & Park, J.-W. (2004) Catalase induces the expression of inducible nitric oxide synthase through activation of NF-κB and PI3K signaling pathway in Raw 264.7 cells. *Biochemical pharmacology*, 68(11), 2167-2176.

Jang, J. E., Ko, M. S., Yun, J.-Y., Kim, M.-O., Kim, J. H., Park, H. S., Kim, A.-R., Kim, H.-J., Kim, B. J. & Ahn, Y. E. (2016) Nitric oxide produced by macrophages inhibits adipocyte differentiation and promotes profibrogenic responses in preadipocytes to induce adipose tissue fibrosis. *Diabetes*, 65(9), 2516-2528.

Japtok, L., Schmitz, E. I., Fayyaz, S., Krämer, S., Hsu, L. J. & Kleuser, B. (2015) Sphingosine 1-phosphate counteracts insulin signaling in pancreatic ß-cells via the sphingosine 1-phosphate receptor subtype 2. *The FASEB journal*, 29(8), 3357-3369.

Jarman, K. E., Moretti, P. A., Zebol, J. R. & Pitson, S. M. (2010) Translocation of sphingosine kinase 1 to the plasma membrane is mediated by calcium-and integrin-binding protein 1. *Journal of Biological Chemistry*, 285(1), 483-492.

Jayarathne, S., Stull, A. J., Miranda, A., Scoggin, S., Claycombe-Larson, K., Kim, J. H. & Moustaid-Moussa, N. (2018) Tart cherry reduces inflammation in adipose tissue of zucker fatty rats and cultured 3T3-L1 adipocytes. *Nutrients*, 10(11), 1576.

Jeon, M. J., Leem, J., Ko, M. S., Jang, J. E., Park, H.-S., Kim, H. S., Kim, M., Kim, E. H., Yoo, H. J. & Lee, C.-H. (2012) Mitochondrial dysfunction and activation of iNOS are responsible for the palmitate-induced decrease in adiponectin synthesis in 3T3L1 adipocytes. *Experimental & molecular medicine*, 44(9), 562-570.

Jeong, J. K., Moon, M. H. & Park, S. Y. (2015) Modulation of the expression of sphingosine 1-phosphate 2 receptors regulates the differentiation of pre-adipocytes. *Molecular medicine reports*, 12(5), 7496-7502.

Jo, E., Bhhatarai, B., Repetto, E., Guerrero, M., Riley, S., Brown, S. J., Kohno, Y., Roberts, E., Schürer, S. C. & Rosen, H. (2012) Novel selective allosteric and bitopic ligands for the S1P3 receptor. *ACS chemical biology*, 7(12), 1975-1983.

Jozefczuk, E., Guzik, T. & Siedlinski, M. (2020) Significance of sphingosine-1-phosphate in cardiovascular physiology and pathology. *Pharmacological research*, 156, 104793.

Jun, D.-J., Lee, J.-H., Choi, B.-H., Koh, T.-K., Ha, D.-C., Jeong, M.-W. & Kim, K.-T. (2006) Sphingosine-1-phosphate modulates both lipolysis and leptin production in differentiated rat white adipocytes. *Endocrinology*, 147(12), 5835-5844.

Kaneko, N., Kurata, M., Yamamoto, T., Morikawa, S. & Masumoto, J. (2019) The role of interleukin-1 in general pathology. *Inflammation and regeneration*, 39, 1-16.

Kang, S.-C., Kim, B.-R., Lee, S.-Y. & Park, T.-S. (2013) Sphingolipid metabolism and obesity-induced inflammation. *Frontiers in endocrinology*, 4, 67.

Kapur, S., Marcotte, B. & Marette, A. (1999) Mechanism of adipose tissue iNOS induction in endotoxemia. *American Journal of Physiology-Endocrinology and Metabolism*, 276(4), E635-E641.

Karuppuchamy, T., Behrens, E., González-Cabrera, P., Sarkisyan, G., Gima, L., Boyer, J. D., Bamias, G., Jedlicka, P., Veny, M. & Clark, D. (2017)

Sphingosine-1-phosphate receptor-1 (S1P1) is expressed by lymphocytes, dendritic cells, and endothelium and modulated during inflammatory bowel disease. *Mucosal immunology*, 10(1), 162-171.

Kawahara, A., Nishi, T., Hisano, Y., Fukui, H., Yamaguchi, A. & Mochizuki, N. (2009) The sphingolipid transporter spns2 functions in migration of zebrafish myocardial precursors. *Science*, 323(5913), 524-527.

Kawai, T., Autieri, M. V. & Scalia, R. (2021) Adipose tissue inflammation and metabolic dysfunction in obesity. *American Journal of Physiology-Cell Physiology*, 320(3), C375-C391.

Keul, P., Polzin, A., Kaiser, K., Gräler, M., Dannenberg, L., Daum, G., Heusch, G. & Levkau, B. (2019) Potent anti-inflammatory properties of HDL in vascular smooth muscle cells mediated by HDL-S1P and their impairment in coronary artery disease due to lower HDL-S1P: a new aspect of HDL dysfunction and its therapy. *The FASEB Journal*, 33(1), 1482-1495.

Kim, H. L., Ha, A. W. & Kim, W. K. (2020) Effect of saccharin on inflammation in 3T3-L1 adipocytes and the related mechanism. *Nutrition Research and Practice*, 14(2), 109-116.

Kim, V. N., Han, J. & Siomi, M. C. (2009) Biogenesis of small RNAs in animals. *Nature reviews Molecular cell biology*, 10(2), 126-139.

Kitada, Y., Kajita, K., Taguchi, K., Mori, I., Yamauchi, M., Ikeda, T., Kawashima, M., Asano, M., Kajita, T. & Ishizuka, T. (2016) Blockade of sphingosine 1-phosphate receptor 2 signaling attenuates high-fat diet-induced adipocyte hypertrophy and systemic glucose intolerance in mice. *Endocrinology*, 157(5), 1839-1851.

Kleinert, H., Art, J. & Pautz, A. (2010) Regulation of the expression of inducible nitric oxide synthase. *Nitric Oxide*, 211-267.

Kleinert, H., Pautz, A., Linker, K. & Schwarz, P. M. (2004) Regulation of the expression of inducible nitric oxide synthase. *European journal of pharmacology*, 500(1-3), 255-266.

Kluk, M. J. & Hla, T. (2002) Signaling of sphingosine-1-phosphate via the S1P/EDG-family of G-protein-coupled receptors. *Biochimica et Biophysica Acta (BBA)-Molecular and Cell Biology of Lipids*, 1582(1-3), 72-80.

Kobayashi, N., Nishi, T., Hirata, T., Kihara, A., Sano, T., Igarashi, Y. & Yamaguchi, A. (2006) Sphingosine 1-phosphate is released from the cytosol of rat platelets in a carrier-mediated manner. *Journal of lipid research*, 47(3), 614-621.

Kolak, M., Westerbacka, J., Velagapudi, V. R., Wagsater, D., Yetukuri, L., Makkonen, J., Rissanen, A., Hakkinen, A.-M., Lindell, M. & Bergholm, R. (2007) Adipose tissue inflammation and increased ceramide content characterize subjects with high liver fat content independent of obesity. *Diabetes*, 56(8), 1960-1968.

Kröncke, K.-D. (2003) Nitrosative stress and transcription.

Krüger-Genge, A., Blocki, A., Franke, R.-P. & Jung, F. (2019) Vascular endothelial cell biology: an update. *International journal of molecular sciences*, 20(18), 4411.

Kugo, H., Sukketsiri, W., Iwamoto, K., Suihara, S., Moriyama, T. & Zaima, N. (2021) Low glucose and serum levels cause an increased inflammatory factor in 3T3-L1 cell through Akt, MAPKs and NF-κB activation. *Adipocyte*, 10(1), 232-241.

Kyriakis, J. M. & Avruch, J. (2012) Mammalian MAPK signal transduction pathways activated by stress and inflammation: a 10-year update. *Physiological reviews*, 92(2), 689-737.

Lacaná, E., Maceyka, M., Milstien, S. & Spiegel, S. (2002) Cloning and characterization of a protein kinase A anchoring protein (AKAP)-related protein that interacts with and regulates sphingosine kinase 1 activity. *Journal of Biological Chemistry*, 277(36), 32947-32953.

Lagathu, C., Yvan-Charvet, L., Bastard, J.-P., Maachi, M., Quignard-Boulange, A., Capeau, J. & Caron, M. (2006) Long-term treatment with interleukin-1β induces insulin resistance in murine and human adipocytes. *Diabetologia*, 49, 2162-2173.

Lahti, A., Kankaanranta, H. & Moilanen, E. (2002) P38 mitogen-activated protein kinase inhibitor SB203580 has a bi-directional effect on iNOS expression and NO production. *European journal of pharmacology*, 454(2-3), 115-123.

Lai, W.-Q., Irwan, A. W., Goh, H. H., Melendez, A. J., McInnes, I. B. & Leung, B. P. (2009) Distinct roles of sphingosine kinase 1 and 2 in murine collagen-induced arthritis. *The Journal of Immunology*, 183(3), 2097-2103.

Lee, C.-F., Dang, A., Hernandez, E., Pong, R.-C., Chen, B., Sonavane, R., Raj, G., Kapur, P., Lin, H.-Y. & Wu, S.-R. (2019) Activation of sphingosine kinase by lipopolysaccharide promotes prostate cancer cell invasion and metastasis via SphK1/S1PR4/matriptase. *Oncogene*, 38(28), 5580-5598.

Lee, M.-H., Hammad, S. M., Semler, A. J., Luttrell, L. M., Lopes-Virella, M. F. & Klein, R. L. (2010) HDL3, but not HDL2, stimulates plasminogen activator inhibitor-1 release from adipocytes: the role of sphingosine-1-phosphate. *Journal of lipid research*, 51(9), 2619-2628.

Lee, S.-Y., Lee, H.-Y., Song, J.-H., Kim, G.-T., Jeon, S., Song, Y.-J., Lee, J. S., Hur, J.-H., Oh, H. H. & Park, S.-Y. (2017) Adipocyte-specific deficiency of de novo sphingolipid biosynthesis leads to lipodystrophy and insulin resistance. *Diabetes*, 66(10), 2596-2609.

Lee, Y.-M., Venkataraman, K., Hwang, S.-I., Han, D. K. & Hla, T. (2007) A novel method to quantify sphingosine 1-phosphate by immobilized metal affinity chromatography (IMAC). *Prostaglandins & other lipid mediators*, 84(3-4), 154-162.

Li, Q., Li, Y., Lei, C., Tan, Y. & Yi, G. (2021) Sphingosine-1-phosphate receptor 3 signaling. *Clinica Chimica Acta*, 519, 32-39.

Li, Q., Qian, J., Li, Y., Huang, P., Liang, H., Sun, H., Liu, C., Peng, J., Lin, X. & Chen, X. (2020) Generation of sphingosine-1-phosphate by sphingosine kinase 1 protects nonalcoholic fatty liver from ischemia/reperfusion injury through alleviating reactive oxygen species production in hepatocytes. *Free Radical Biology and Medicine*, 159, 136-149.

Li, W., Xu, H. & Testai, F. D. (2016) Mechanism of action and clinical potential of fingolimod for the treatment of stroke. *Frontiers in neurology*, 7, 139.

Lim, K. G., Sun, C., Bittman, R., Pyne, N. J. & Pyne, S. (2011) (R)-FTY720 methyl ether is a specific sphingosine kinase 2 inhibitor: Effect on sphingosine kinase 2 expression in HEK 293 cells and actin rearrangement and survival of MCF-7 breast cancer cells. *Cellular signalling*, 23(10), 1590-1595.

Liu, H., Li, L., Chen, Z., Song, Y., Liu, W., Gao, G., Li, L., Jiang, J., Xu, C. & Yan, G. (2021) S1PR2 inhibition attenuates allergic asthma possibly by regulating autophagy. *Frontiers in pharmacology*, 11, 598007.

Liu, R., Li, X., Qiang, X., Luo, L., Hylemon, P. B., Jiang, Z., Zhang, L. & Zhou, H. (2015) Taurocholate induces cyclooxygenase-2 expression via the sphingosine 1-phosphate receptor 2 in a human cholangiocarcinoma cell line. *Journal of Biological Chemistry*, 290(52), 30988-31002.

Liu, X., Ren, K., Suo, R., Xiong, S.-L., Zhang, Q.-H., Mo, Z.-C., Tang, Z.-L., Jiang, Y., Peng, X.-S. & Yi, G.-H. (2016) ApoA-I induces S1P release from endothelial cells through ABCA1 and SR-BI in a positive feedback manner. *Journal of physiology and biochemistry*, 72, 657-667.

Liu, X., Wu, J., Zhu, C., Liu, J., Chen, X., Zhuang, T., Kuang, Y., Wang, Y., Hu, H. & Yu, P. (2020) Endothelial S1pr1 regulates pressure overload-induced cardiac remodelling through AKT-eNOS pathway. *Journal of cellular and molecular medicine*, 24(2), 2013-2026.

Löhn, M., Dubrovska, G., Lauterbach, B., Luft, F. C., Gollasch, M. & Sharma, A. M. (2002) Periadventitial fat releases a vascular relaxing factor. *The FASEB Journal*, 16(9), 1057-1063.

Long, J. Z., Svensson, K. J., Tsai, L., Zeng, X., Roh, H. C., Kong, X., Rao, R. R., Lou, J., Lokurkar, I. & Baur, W. (2014) A smooth muscle-like origin for beige adipocytes. *Cell metabolism*, 19(5), 810-820.

Lowe, G. D. (2001) The relationship between infection, inflammation, and cardiovascular disease: an overview. *Annals of periodontology*, 6(1), 1-8.

Lu, L. F. & Fiscus, R. R. (1999) Interleukin-1ß causes different levels of nitric oxide-mediated depression of contractility in different positions of rat thoracic aorta. *Life sciences*, 64(16), 1373-1381.

Lu, Z., Zhang, W., Gao, S., Jiang, Q., Xiao, Z., Ye, L. & Zhang, X. (2015) MiR-506 suppresses liver cancer angiogenesis through targeting sphingosine kinase 1 (SPHK1) mRNA. *Biochemical and biophysical research communications*, 468(1-2), 8-13.

Lynch, F. M., Withers, S. B., Yao, Z., Werner, M. E., Edwards, G., Weston, A. H. & Heagerty, A. M. (2013) Perivascular adipose tissue-derived adiponectin activates BKCa channels to induce anticontractile responses. *American Journal of Physiology-Heart and Circulatory Physiology*, 304(6), H786-H795.

Maceyka, M., Alvarez, S. E., Milstien, S. & Spiegel, S. (2008) Filamin A links sphingosine kinase 1 and sphingosine-1-phosphate receptor 1 at lamellipodia to orchestrate cell migration. *Molecular and cellular biology*, 28(18), 5687-5697.

Machida, T., Hamaya, Y., Izumi, S., Hamaya, Y., Iizuka, K., Igarashi, Y., Minami, M., Levi, R. & Hirafuji, M. (2008) Sphingosine 1-phosphate inhibits nitric

oxide production induced by interleukin-1β in rat vascular smooth muscle cells. *Journal of Pharmacology and Experimental Therapeutics*, 325(1), 200-209.

Maenhaut, N., Boydens, C. & Van de Voorde, J. (2010) Hypoxia enhances the relaxing influence of perivascular adipose tissue in isolated mice aorta. *European journal of pharmacology*, 641(2-3), 207-212.

Mair, K., Robinson, E., Kane, K., Pyne, S., Brett, R., Pyne, N. & Kennedy, S. (2010) Interaction between anandamide and sphingosine-1-phosphate in mediating vasorelaxation in rat coronary artery. *British journal of pharmacology*, 161(1), 176-192.

Martin, M. U. & Wesche, H. (2002) Summary and comparison of the signaling mechanisms of the Toll/interleukin-1 receptor family. *Biochimica et Biophysica Acta (BBA)-Molecular Cell Research*, 1592(3), 265-280.

Martinez, N., Cheng, C. Y., Ketheesan, N., Cullen, A., Tang, Y., Lum, J., West, K., Poidinger, M., Guertin, D. A. & Singhal, A. (2019) mTORC2/Akt activation in adipocytes is required for adipose tissue inflammation in tuberculosis. *EBioMedicine*, 45, 314-327.

Mastrandrea, L. D. (2013) Role of sphingosine kinases and sphingosine 1-phosphate in mediating adipogenesis. *Journal of Diabetes Mellitus*, 3(02), 52-61.

Mastrandrea, L. D., Sessanna, S. M. & Laychock, S. G. (2005) Sphingosine kinase activity and sphingosine-1 phosphate production in rat pancreatic islets and INS-1 cells: response to cytokines. *Diabetes*, 54(5), 1429-1436.

Matrone, G., Meng, S., Gu, Q., Lv, J., Fang, L., Chen, K. & Cooke, J. P. (2017) Lmo2 (LIM-domain-only 2) modulates Sphk1 (sphingosine kinase) and promotes endothelial cell migration. *Arteriosclerosis, thrombosis, and vascular biology*, 37(10), 1860-1868.

Matsuzaki, E., Hiratsuka, S., Hamachi, T., Takahashi-Yanaga, F., Hashimoto, Y., Higashi, K., Kobayashi, M., Hirofuji, T., Hirata, M. & Maeda, K. (2013) Sphingosine-1-phosphate promotes the nuclear translocation of β-catenin and thereby induces osteoprotegerin gene expression in osteoblast-like cell lines. *Bone*, 55(2), 315-324.

Meijer, R. I., Bakker, W., Alta, C.-L. A., Sipkema, P., Yudkin, J. S., Viollet, B., Richter, E. A., Smulders, Y. M., van Hinsbergh, V. W. & Serné, E. H. (2013) Perivascular adipose tissue control of insulin-induced vasoreactivity in muscle is impaired in db/db mice. *Diabetes*, 62(2), 590-598.

Melton, E. & Qiu, H. (2021) Interleukin-1β in multifactorial hypertension: inflammation, vascular smooth muscle cell and extracellular matrix remodeling, and non-coding RNA regulation. *International Journal of Molecular Sciences*, 22(16), 8639.

Mendelson, K., Evans, T. & Hla, T. (2014) Sphingosine 1-phosphate signalling. *Development*, 141(1), 5-9.

Michaud, J., Im, D.-S. & Hla, T. (2010) Inhibitory role of sphingosine 1-phosphate receptor 2 in macrophage recruitment during inflammation. *The journal of immunology*, 184(3), 1475-1483.

Michel, M. C., Mulders, A. C., Jongsma, M., Alewijnse, A. E. & Peters, S. L. (2007) Vascular effects of sphingolipids. *Acta Paediatrica*, 96, 44-48.

Mitidieri, E., Gurgone, D., Caiazzo, E., Tramontano, T., Cicala, C., Sorrentino, R. & d'Emmanuele di Villa Bianca, R. (2020) L-cysteine/cystathionine-ß-synthase-induced relaxation in mouse aorta involves a L-serine/sphingosine-1-phosphate/NO pathway. *British Journal of Pharmacology*, 177(4), 734-744.

Mitra, P., Oskeritzian, C. A., Payne, S. G., Beaven, M. A., Milstien, S. & Spiegel, S. (2006) Role of ABCC1 in export of sphingosine-1-phosphate from mast cells. *Proceedings of the national academy of sciences*, 103(44), 16394-16399.

Moon, M.-H., Jeong, J.-K., Lee, Y.-J., Seol, J.-W. & Park, S.-Y. (2014) Sphingosine-1-phosphate inhibits the adipogenic differentiation of 3T3-L1 preadipocytes. *International journal of molecular medicine*, 34(4), 1153-1158.

Moon, M. H., Jeong, J. K. & Park, S. Y. (2015) Activation of S1P2 receptor, a possible mechanism of inhibition of adipogenic differentiation by sphingosine 1-phosphate. *Molecular medicine reports*, 11(2), 1031-1036.

Morishige, J.-i., Yoshioka, K., Nakata, H., Ishimaru, K., Nagata, N., Tanaka, T., Takuwa, Y. & Ando, H. (2023) Sphingosine kinase 1 is involved in triglyceride breakdown by maintaining lysosomal integrity in brown adipocytes. *Journal of Lipid Research*, 64(11).

Morris, B. J., Markus, A. M., Glenn, C. L., Adams, D. J., Colagiuri, S. & Wang, X. (2002) Association of a functional inducible nitric oxide synthase promoter variant with complications in type 2 diabetes. *Journal of molecular medicine*, 80, 96-104.

Moschen, A. R., Molnar, C., Enrich, B., Geiger, S., Ebenbichler, C. F. & Tilg, H. (2011) Adipose and liver expression of interleukin (IL)-1 family members in morbid obesity and effects of weight loss. *Molecular medicine*, 17, 840-845.

Müller, J., von Bernstorff, W., Heidecke, C.-D. & Schulze, T. (2017) Differential S1P receptor profiles on M1-and M2-polarized macrophages affect macrophage cytokine production and migration. *BioMed research international*, 2017.

Muniyappa, H. & Das, K. C. (2008) Activation of c-Jun N-terminal kinase (JNK) by widely used specific p38 MAPK inhibitors SB202190 and SB203580: a MLK-3-MKK7-dependent mechanism. *Cellular signalling*, 20(4), 675-683.

Murakami, M., Ichihara, M., Sobue, S., Kikuchi, R., Ito, H., Kimura, A., Iwasaki, T., Takagi, A., Kojima, T. & Takahashi, M. (2007) RET signaling-induced SPHK1 gene expression plays a role in both GDNF-induced differentiation and MEN2-type oncogenesis. *Journal of neurochemistry*, 102(5), 1585-1594.

Muslin, A. J. (2008) MAPK signalling in cardiovascular health and disease: molecular mechanisms and therapeutic targets. *Clinical science*, 115(7), 203-218.

Nagahashi, M., Kim, E. Y., Yamada, A., Ramachandran, S., Allegood, J. C., Hait, N. C., Maceyka, M., Milstien, S., Takabe, K. & Spiegel, S. (2013) Spns2, a transporter of phosphorylated sphingoid bases, regulates their blood and lymph levels, and the lymphatic network. *The FASEB Journal*, 27(3), 1001.

Nakladal, D., Sijbesma, J., Visser, L., Tietge, U., Slart, R., Deelman, L., Henning, R., Hillebrands, J. & Buikema, H. (2022) Perivascular adipose tissue-derived nitric oxide compensates endothelial dysfunction in aged pre-atherosclerotic apolipoprotein E-deficient rats. *Vascular pharmacology*, 142, 106945.

Nayak, D., Huo, Y., Kwang, W., Pushparaj, P., Kumar, S., Ling, E.-A. & Dheen, S. (2010) Sphingosine kinase 1 regulates the expression of proinflammatory cytokines and nitric oxide in activated microglia. *Neuroscience*, 166(1), 132-144.

Nepali, S., Son, J.-S., Poudel, B., Lee, J.-H., Lee, Y.-M. & Kim, D.-K. (2015) Luteolin is a bioflavonoid that attenuates adipocyte-derived inflammatory responses via suppression of nuclear factor-κB/mitogen-activated protein kinases pathway. *Pharmacognosy Magazine*, 11(43), 627.

Neubauer, H. A. & Pitson, S. M. (2013) Roles, regulation and inhibitors of sphingosine kinase 2. *The FEBS journal*, 280(21), 5317-5336.

Neumann, D., Lienenklaus, S., Rosati, O. & Martin, M. U. (2002) IL-1β-induced phosphorylation of PKB/Akt depends on the presence of IRAK-1. *European journal of immunology*, 32(12), 3689-3698.

Nguyen, M. C., Park, J. T., Jeon, Y. G., Jeon, B. H., Hoe, K. L., Kim, Y. M., Lim, H. K. & Ryoo, S. (2016) Arginase inhibition restores peroxynitrite-induced endothelial dysfunction via L-arginine-dependent endothelial nitric oxide synthase phosphorylation. *Yonsei Medical Journal*, 57(6), 1329.

Nijnik, A., Clare, S., Hale, C., Chen, J., Raisen, C., Mottram, L., Lucas, M., Estabel, J., Ryder, E. & Adissu, H. (2012) The role of sphingosine-1-phosphate transporter Spns2 in immune system function. *The Journal of Immunology*, 189(1), 102-111.

Nisar, M. A., Zheng, Q., Saleem, M. Z., Ahmmed, B., Ramzan, M. N., Ud Din, S. R., Tahir, N., Liu, S. & Yan, Q. (2021) IL-1β promotes vasculogenic mimicry of breast cancer cells through p38/MAPK and PI3K/Akt signaling pathways. *Frontiers in Oncology*, 11, 618839.

Nóbrega, N., Araújo, N. F., Reis, D., Facine, L. M., Miranda, C. A. S., Mota, G. C., Aires, R. D., Capettini, L. d. S. A., dos Santos Cruz, J. & Bonaventura, D. (2019) Hydrogen peroxide and nitric oxide induce anticontractile effect of perivascular adipose tissue via renin angiotensin system activation. *Nitric Oxide*, 84, 50-59.

Nojiri, T., Kurano, M., Tokuhara, Y., Ohkubo, S., Hara, M., Ikeda, H., Tsukamoto, K. & Yatomi, Y. (2014) Modulation of sphingosine-1-phosphate and apolipoprotein M levels in the plasma, liver and kidneys in streptozotocin-induced diabetic mice. *Journal of Diabetes Investigation*, 5(6), 639-648.

Nosalski, R. & Guzik, T. J. (2017) Perivascular adipose tissue inflammation in vascular disease. *British journal of pharmacology*, 174(20), 3496-3513.

O'Sullivan, C. & Dev, K. K. (2013) The structure and function of the S1P1 receptor. *Trends in pharmacological sciences*, 34(7), 401-412.

Ohama, T., Okada, M., Murata, T., Brautigan, D. L., Hori, M. & Ozaki, H. (2008) Sphingosine-1-phosphate enhances IL-1ß-induced COX-2 expression in mouse intestinal subepithelial myofibroblasts. *American Journal of Physiology-Gastrointestinal and Liver Physiology*, 295(4), G766-G775.

Okamoto, H., Takuwa, N., Gonda, K., Okazaki, H., Chang, K., Yatomi, Y., Shigematsu, H. & Takuwa, Y. (1998) EDG1 is a functional sphingosine-1-phosphate receptor that is linked via a Gi/o to multiple signaling pathways, including phospholipase C activation, Ca2+ mobilization, Ras-mitogen-activated protein kinase activation, and adenylate cyclase inhibition. *Journal of Biological Chemistry*, 273(42), 27104-27110.

Okazaki, H., Ishizaka, N., Sakurai, T., Kurokawa, K., Goto, K., Kumada, M. & Takuwa, Y. (1993) Molecular cloning of a novel putative G protein-coupled receptor expressed in the cardiovascular system. *Biochemical and biophysical research communications*, 190(3), 1104-1109.

Olefsky, J. M. & Glass, C. K. (2010) Macrophages, inflammation, and insulin resistance. *Annual review of physiology*, 72, 219-246.

Olivera, A. & Spiegel, S. (1993) Sphingosine-1-phosphate as second messenger in cell proliferation induced by PDGF and FCS mitogens. *Nature*, 365(6446), 557-560.

Organization, W. H. (2000) Obesity: preventing and managing the global epidemic: report of a WHO consultation.

Osada, M., Yatomi, Y., Ohmori, T., Ikeda, H. & Ozaki, Y. (2002) Enhancement of sphingosine 1-phosphate-induced migration of vascular endothelial cells and smooth muscle cells by an EDG-5 antagonist. *Biochemical and biophysical research communications*, 299(3), 483-487.

Osawa, Y., Banno, Y., Nagaki, M., Brenner, D. A., Naiki, T., Nozawa, Y., Nakashima, S. & Moriwaki, H. (2001) TNF-α-induced sphingosine 1-phosphate inhibits apoptosis through a phosphatidylinositol 3-kinase/Akt pathway in human hepatocytes. *The Journal of Immunology*, 167(1), 173-180.

Osawa, Y., Seki, E., Kodama, Y., Suetsugu, A., Miura, K., Adachi, M., Ito, H., Shiratori, Y., Banno, Y. & Olefsky, J. M. (2011) Acid sphingomyelinase regulates glucose and lipid metabolism in hepatocytes through AKT activation and AMP-activated protein kinase suppression. *The FASEB Journal*, 25(4), 1133.

Osborn, O. & Olefsky, J. M. (2012) The cellular and signaling networks linking the immune system and metabolism in disease. *Nature medicine*, 18(3), 363-374.

Otto, T. C. & Lane, M. D. (2005) Adipose development: from stem cell to adipocyte. *Critical reviews in biochemistry and molecular biology*, 40(4), 229-242.

Ouyang, J., Shu, Z., Chen, S., Xiang, H. & Lu, H. (2020) The role of sphingosine 1-phosphate and its receptors in cardiovascular diseases. *Journal of cellular and molecular medicine*, 24(18), 10290-10301.

Pan, S., Mi, Y., Pally, C., Beerli, C., Chen, A., Guerini, D., Hinterding, K., Nuesslein-Hildesheim, B., Tuntland, T. & Lefebvre, S. (2006) A monoselective sphingosine-1-phosphate receptor-1 agonist prevents allograft rejection in a stringent rat heart transplantation model. *Chemistry & biology*, 13(11), 1227-1234.

Parham, K. A., Zebol, J. R., Tooley, K. L., Sun, W. Y., Moldenhauer, L. M., Cockshell, M. P., Gliddon, B. L., Moretti, P. A., Tigyi, G. & Pitson, S. M. (2015) Sphingosine 1-phosphate is a ligand for peroxisome proliferator-activated receptor-γ that regulates neoangiogenesis. *The FASEB Journal*, 29(9), 3638.

Park, Y.-K., Wang, S. & Jang, B.-C. (2021) Interleukin 1ß Up-Regulates mRNA Expression of Inducible Nitric Oxide Synthase in 3T3-L1 Preadipocytes: Role of JAKs/STATs, PKCs, and Src. *Keimyung Medical Journal*, 40(1), 1-8.

Parrill, A. L., Sardar, V. M. & Yuan, H. (2004) Sphingosine 1-phosphate and lysophosphatidic acid receptors: agonist and antagonist binding and progress toward development of receptor-specific ligands, *Seminars in cell & developmental biology*. Elsevier.

Paugh, B. S., Bryan, L., Paugh, S. W., Wilczynska, K. M., Alvarez, S. M., Singh, S. K., Kapitonov, D., Rokita, H., Wright, S. & Griswold-Prenner, I. (2009) Interleukin-1 regulates the expression of sphingosine kinase 1 in glioblastoma cells. *Journal of Biological Chemistry*, 284(6), 3408-3417.

Peek, V., Neumann, E., Inoue, T., Roth, J. & Rummel, C. (2020) Age-dependent changes of adipokine and cytokine secretion from rat adipose tissue by endogenous and exogenous toll-like receptor agonists. *Frontiers in Immunology*, 11, 549901.

Penfornis, P. & Marette, A. (2005) Inducible nitric oxide synthase modulates lipolysis in adipocytes. *Journal of lipid research*, 46(1), 135-142.

Perreault, M. & Marette, A. (2001) Targeted disruption of inducible nitric oxide synthase protects against obesity-linked insulin resistance in muscle. *Nature medicine*, 7(10), 1138-1143.

Perrotta, C., De Palma, C. & Clementi, E. (2008) Nitric oxide and sphingolipids: mechanisms of interaction and role in cellular pathophysiology.

Pitman, M. R. & Pitson, S. M. (2010) Inhibitors of the sphingosine kinase pathway as potential therapeutics. *Current cancer drug targets*, 10(4), 354-367.

Pitson, S. M., Moretti, P. A., Zebol, J. R., Lynn, H. E., Xia, P., Vadas, M. A. & Wattenberg, B. W. (2003) Activation of sphingosine kinase 1 by ERK1/2-mediated phosphorylation. *The EMBO journal*, 22(20), 5491-5500.

Plotnikov, A., Zehorai, E., Procaccia, S. & Seger, R. (2011) The MAPK cascades: signaling components, nuclear roles and mechanisms of nuclear translocation. *Biochimica et Biophysica Acta (BBA)-Molecular Cell Research*, 1813(9), 1619-1633.

Polzin, A., Piayda, K., Keul, P., Dannenberg, L., Mohring, A., Gräler, M., Zeus, T., Kelm, M. & Levkau, B. (2017) Plasma sphingosine-1-phosphate concentrations are associated with systolic heart failure in patients with ischemic heart disease. *Journal of Molecular and Cellular Cardiology*, 110, 35-37.

Powell-Wiley, T. M., Poirier, P., Burke, L. E., Després, J.-P., Gordon-Larsen, P., Lavie, C. J., Lear, S. A., Ndumele, C. E., Neeland, I. J. & Sanders, P. (2021) Obesity and cardiovascular disease: a scientific statement from the American Heart Association. *Circulation*, 143(21), e984-e1010.

Pulkoski-Gross, M. J., Donaldson, J. C. & Obeid, L. M. (2015) Sphingosine-1-phosphate metabolism: A structural perspective. *Critical reviews in biochemistry and molecular biology*, 50(4), 298-313.

Puneet, P., Yap, C. T., Wong, L., Yulin, L., Koh, D. R., Moochhala, S., Pfeilschifter, J., Huwiler, A. & Melendez, A. J. (2010) SphK1 regulates proinflammatory responses associated with endotoxin and polymicrobial sepsis. *Science*, 328(5983), 1290-1294.

Pyne, S., Adams, D. R. & Pyne, N. J. (2020) Sphingosine kinases as druggable targets. *Lipid Signaling in Human Diseases*, 49-76.

Pyne, S. & Pyne, N. J. (2000) Sphingosine 1-phosphate signalling in mammalian cells. *Biochemical Journal*, 349(2), 385-402.

Qi, Y., Wang, W., Song, Z., Aji, G., Liu, X. T. & Xia, P. (2021) Role of sphingosine kinase in Type 2 diabetes mellitus. *Frontiers in Endocrinology*, 11, 627076.

Quesada, I., Cejas, J., García, R., Cannizzo, B., Redondo, A. & Castro, C. (2018) Vascular dysfunction elicited by a cross talk between periaortic adipose tissue and the vascular wall is reversed by pioglitazone. *Cardiovascular therapeutics*, 36(3), e12322.

Radeff-Huang, J., Seasholtz, T. M., Chang, J. W., Smith, J. M., Walsh, C. T. & Brown, J. H. (2007) Tumor necrosis factor-α-stimulated cell proliferation is mediated through sphingosine kinase-dependent Akt activation and cyclin D expression. *Journal of Biological Chemistry*, 282(2), 863-870.

Ramírez-Ponce, M., Mateos, J. & Bellido, J. (2002) Insulin increases the density of potassium channels in white adipocytes: possible role in adipogenesis. *Journal of endocrinology*, 174(2), 299-308.

Rao, X., Huang, X., Zhou, Z. & Lin, X. (2013) An improvement of the 2ˆ (-delta delta CT) method for quantitative real-time polymerase chain reaction data analysis. *Biostatistics, bioinformatics and biomathematics*, 3(3), 71.

Ravichandran, S., Finlin, B. S., Kern, P. A. & Özcan, S. (2019) Sphk2−/− mice are protected from obesity and insulin resistance. *Biochimica et Biophysica Acta (BBA)-Molecular Basis of Disease*, 1865(3), 570-576.

Reilly, S. M. & Saltiel, A. R. (2017) Adapting to obesity with adipose tissue inflammation. *Nature Reviews Endocrinology*, 13(11), 633-643.

Reis Costa, D. E. F. d., Silveira, A. L. M., Campos, G. P., Nóbrega, N. R. C., De Araújo, N. F., de Figueiredo Borges, L., dos Santos Aggum Capettini, L., Ferreira, A. V. M. & Bonaventura, D. (2021) High-carbohydrate diet enhanced the anticontractile effect of perivascular adipose tissue through activation of renin-angiotensin system. *Frontiers in physiology*, 11, 628101.

Renovato-Martins, M., Moreira-Nunes, C., Atella, G. C., Barja-Fidalgo, C. & Moraes, J. A. d. (2020) Obese adipose tissue secretion induces

inflammation in preadipocytes: Role of Toll-like receptor-4. *Nutrients*, 12(9), 2828.

Robinson, S. (2021) Cardiovascular disease, *Priorities for Health Promotion and Public Health*Routledge, 355-393.

Ropelle, E. R., Pauli, J. R., Cintra, D. E., Da Silva, A. S., De Souza, C. T., Guadagnini, D., Carvalho, B. M., Caricilli, A. M., Katashima, C. K. & Carvalho-Filho, M. A. (2013) Targeted disruption of inducible nitric oxide synthase protects against aging, S-nitrosation, and insulin resistance in muscle of male mice. *Diabetes*, 62(2), 466-470.

Rose, B. A., Force, T. & Wang, Y. (2010) Mitogen-activated protein kinase signaling in the heart: angels versus demons in a heart-breaking tale. *Physiological reviews*, 90(4), 1507-1546.

Roviezzo, F., Bucci, M., Delisle, C., Brancaleone, V., Lorenzo, A. D., Mayo, I. P., Fiorucci, S., Fontana, A., Gratton, J. P. & Cirino, G. (2006) Expression of Concern: Essential requirement for sphingosine kinase activity in eNOS-dependent NO release and vasorelaxation. *The FASEB journal*, 20(2), 340-342.

Saberi, M., Woods, N.-B., de Luca, C., Schenk, S., Lu, J. C., Bandyopadhyay, G., Verma, I. M. & Olefsky, J. M. (2009) Hematopoietic cell-specific deletion of toll-like receptor 4 ameliorates hepatic and adipose tissue insulin resistance in high-fat-fed mice. *Cell metabolism*, 10(5), 419-429.

Sakers, A., De Siqueira, M. K., Seale, P. & Villanueva, C. J. (2022) Adipose-tissue plasticity in health and disease. *Cell*, 185(3), 419-446.

Salomone, S., Potts, E., Tyndall, S., Ip, P., Chun, J., Brinkmann, V. & Waeber, C. (2008) Analysis of sphingosine 1-phosphate receptors involved in constriction of isolated cerebral arteries with receptor null mice and pharmacological tools. *British journal of pharmacology*, 153(1), 140-147.

Salomone, S. & Waeber, C. (2011) Selectivity and specificity of sphingosine-1-phosphate receptor ligands: caveats and critical thinking in characterizing receptor-mediated effects. *Frontiers in pharmacology*, 2, 9.

Samad, F., Hester, K. D., Yang, G., Hannun, Y. A. & Bielawski, J. (2006) Altered adipose and plasma sphingolipid metabolism in obesity: a potential mechanism for cardiovascular and metabolic risk. *Diabetes*, 55(9), 2579-2587.

Sanna, M. G., Wang, S.-K., Gonzalez-Cabrera, P. J., Don, A., Marsolais, D., Matheu, M. P., Wei, S. H., Parker, I., Jo, E. & Cheng, W.-C. (2006) Enhancement of capillary leakage and restoration of lymphocyte egress by a chiral S1P1 antagonist in vivo. *Nature chemical biology*, 2(8), 434-441.

Sato, K., Malchinkhuu, E., Horiuchi, Y., Mogi, C., Tomura, H., Tosaka, M., Yoshimoto, Y., Kuwabara, A. & Okajima, F. (2007) Critical role of ABCA1 transporter in sphingosine 1-phosphate release from astrocytes. *Journal of neurochemistry*, 103(6), 2610-2619.

Satsu, H., Schaeffer, M.-T., Guerrero, M., Saldana, A., Eberhart, C., Hodder, P., Cayanan, C., Schürer, S., Bhhatarai, B. & Roberts, E. (2013) A sphingosine 1-phosphate receptor 2 selective allosteric agonist. *Bioorganic & medicinal chemistry*, 21(17), 5373-5382.

Sattler, K. J., Elbasan, Ş., Keul, P., Elter-Schulz, M., Bode, C., Gräler, M. H., Bröcker-Preuss, M., Budde, T., Erbel, R. & Heusch, G. (2010) Sphingosine 1-phosphate levels in plasma and HDL are altered in coronary artery disease. *Basic research in cardiology*, 105, 821-832.

Saxton, S. N., Withers, S. B. & Heagerty, A. M. (2022) Perivascular Adipose Tissue Anticontractile Function Is Mediated by Both Endothelial and Neuronal Nitric Oxide Synthase Isoforms. *Journal of Vascular Research*, 59(5), 288-302.

Schaffler, A., Muller-Ladner, U., Scholmerich, J. & Buchler, C. (2006) Role of adipose tissue as an inflammatory organ in human diseases. *Endocrine reviews*, 27(5), 449-467.

Schnute, M. E., McReynolds, M. D., Kasten, T., Yates, M., Jerome, G., Rains, J. W., Hall, T., Chrencik, J., Kraus, M. & Cronin, C. N. (2012) Modulation of cellular S1P levels with a novel, potent and specific inhibitor of sphingosine kinase-1. *Biochemical Journal*, 444(1), 79-88.

Shah, A. M. (2000) Inducible nitric oxide synthase and cardiovascular disease. *Cardiovascular research*, 45(1), 148-155.

Shi, H., Moustaid-Moussa, N., Wilkison, W. & Zemel, M. B. (1999) Role of the sulfonylurea receptor in regulating human adipocyte metabolism. *The FASEB journal*, 13(13), 1833-1838.

Siehler, S. & Manning, D. R. (2002) Pathways of transduction engaged by sphingosine 1-phosphate through G protein-coupled receptors. *Biochimica et Biophysica Acta (BBA)-Molecular and Cell Biology of Lipids*, 1582(1-3), 94-99.

Siehler, S., Wang, Y., Fan, X., Windh, R. T. & Manning, D. R. (2001) Sphingosine 1-phosphate activates nuclear factor-κB through Edg receptors: activation through Edg-3 and Edg-5, but not Edg-1, in human embryonic kidney 293 cells. *Journal of Biological Chemistry*, 276(52), 48733-48739.

Silvani, A., Bastianini, S., Berteotti, C., Franzini, C., Lenzi, P., Lo Martire, V. & Zoccoli, G. (2009) Sleep modulates hypertension in leptin-deficient obese mice. *Hypertension*, 53(2), 251-255.

Singleton, P. A., Dudek, S. M., Chiang, E. T. & Garcia, J. G. (2005) Regulation of sphingosine 1-phosphate-induced endothelial cytoskeletal rearrangement and barrier enhancement by S1P1 receptor, PI3 kinase, Tiam1/Rac1, and α-actinin. *The FASEB Journal*, 19(12), 1646-1656.

Skoura, A. & Hla, T. (2009) Regulation of vascular physiology and pathology by the S1P2 receptor subtype. *Cardiovascular research*, 82(2), 221-228.

Skoura, A., Michaud, J., Im, D.-S., Thangada, S., Xiong, Y., Smith, J. D. & Hla, T. (2011) Sphingosine-1-phosphate receptor-2 function in myeloid cells regulates vascular inflammation and atherosclerosis. *Arteriosclerosis, thrombosis, and vascular biology*, 31(1), 81-85.

Skoura, A., Sanchez, T., Claffey, K., Mandala, S. M., Proia, R. L. & Hla, T. (2007) Essential role of sphingosine 1–phosphate receptor 2 in pathological angiogenesis of the mouse retina. *The Journal of clinical investigation*, 117(9), 2506-2516.

Sobue, S., Hagiwara, K., Banno, Y., Tamiya-Koizumi, K., Suzuki, M., Takagi, A., Kojima, T., Asano, H., Nozawa, Y. & Murate, T. (2005) Transcription factor specificity protein 1 (Sp1) is the main regulator of nerve growth factor-induced sphingosine kinase 1 gene expression of the rat pheochromocytoma cell line, PC12. *Journal of neurochemistry*, 95(4), 940-949.

Soler, M., Camacho, M. & Vila, L. (2003) Imidazolineoxyl N-oxide prevents the impairment of vascular contraction caused by interleukin-1ß through several mechanisms. *The Journal of infectious diseases*, 188(6), 927-937.

Soltis, E. E. & Cassis, L. A. (1991) Influence of perivascular adipose tissue on rat aortic smooth muscle responsiveness. *Clinical and Experimental Hypertension. Part A: Theory and Practice*, 13(2), 277-296.

Soskić, S. S., Dobutović, B. D., Sudar, E. M., Obradović, M. M., Nikolić, D. M., Djordjevic, J. D., Radak, D. J., Mikhailidis, D. P. & Isenović, E. R. (2011) Regulation of inducible nitric oxide synthase (iNOS) and its potential role in insulin resistance, diabetes and heart failure. *The open cardiovascular medicine journal*, 5, 153.

Sowka, A. & Dobrzyn, P. (2021) Role of perivascular adipose tissue-derived adiponectin in vascular homeostasis. *Cells*, 10(6), 1485.

Spiegel, S. & Milstien, S. (2003) Sphingosine-1-phosphate: an enigmatic signalling lipid. *Nature reviews Molecular cell biology*, 4(5), 397-407.

Spranger, J., Kroke, A., Mohlig, M., Hoffmann, K., Bergmann, M. M., Ristow, M., Boeing, H. & Pfeiffer, A. F. (2003) Inflammatory cytokines and the risk to develop type 2 diabetes: results of the prospective population-based European Prospective Investigation into Cancer and Nutrition (EPIC)-Potsdam Study. *Diabetes*, 52(3), 812-817.

Stanek, A., Brożyna-Tkaczyk, K. & Myśliński, W. (2021) The role of obesity-induced perivascular adipose tissue (PVAT) dysfunction in vascular homeostasis. *Nutrients*, 13(11), 3843.

Stradner, M., Hermann, J., Angerer, H., Setznagl, D., Sunk, I.-G., Windhager, R. & Graninger, W. (2008) Spingosine-1-phosphate stimulates proliferation and counteracts interleukin-1 induced nitric oxide formation in articular chondrocytes. *Osteoarthritis and cartilage*, 16(3), 305-311.

Strub, G. M., Paillard, M., Liang, J., Gomez, L., Allegood, J. C., Hait, N. C., Maceyka, M., Price, M. M., Chen, Q. & Simpson, D. C. (2011) Sphingosine-1-phosphate produced by sphingosine kinase 2 in mitochondria interacts with prohibitin 2 to regulate complex IV assembly and respiration. *The FASEB Journal*, 25(2), 600.

Sun, J., Yan, G., Ren, A., You, B. & Liao, J. K. (2006) FHL2/SLIM3 decreases cardiomyocyte survival by inhibitory interaction with sphingosine kinase-1. *Circulation research*, 99(5), 468-476.

Suomalainen, L., Pentikäinen, V. & Dunkel, L. (2005) Sphingosine-1-phosphate inhibits nuclear factor κB activation and germ cell apoptosis in the human testis independently of its receptors. *The American journal of pathology*, 166(3), 773-781.

Szasz, T., Bomfim, G. F. & Webb, R. C. (2013) The influence of perivascular adipose tissue on vascular homeostasis. *Vascular health and risk management*, 105-116.

Szasz, T., Carrillo-Sepulveda, M. A. & Webb, R. C. (2012) Aging Decreases the Anticontractile Effect of Perivascular Adipose Tissue in the Mouse Aorta. Am Heart Assoc.

Szekely, Y. & Arbel, Y. (2018) A review of interleukin-1 in heart disease: where do we stand today? *Cardiology and therapy*, 7, 25-44.

ter Braak, M., Danneberg, K., Lichte, K., Liphardt, K., Ktistakis, N. T., Pitson, S. M., Hla, T., Jakobs, K. H. & zu Heringdorf, D. M. (2009) Gαq-mediated plasma membrane translocation of sphingosine kinase-1 and cross-activation of S1P receptors. *Biochimica et Biophysica Acta (BBA)-Molecular and Cell Biology of Lipids*, 1791(5), 357-370.

Terlizzi, M., Colarusso, C., Somma, P., De Rosa, I., Panico, L., Pinto, A. & Sorrentino, R. (2022) S1P-induced TNF-α and IL-6 release from PBMCs exacerbates lung cancer-associated inflammation. *Cells*, 11(16), 2524.

Theodoulou, F. L. & Kerr, I. D. (2015) ABC transporter research: going strong 40 years on. *Biochemical Society Transactions*, 43(5), 1033-1040.

Thuy, A. V., Reimann, C.-M., Hemdan, N. Y. & Gräler, M. H. (2014) Sphingosine 1-phosphate in blood: function, metabolism, and fate. *Cellular Physiology and Biochemistry*, 34(1), 158-171.

Tölle, M., Levkau, B., Keul, P., Brinkmann, V., Giebing, G. n., Schönfelder, G., Schäfers, M., Lipinski, K. v. W., Jankowski, J. & Jankowski, V. (2005) Immunomodulator FTY720 Induces eNOS-dependent arterial vasodilatation via the lysophospholipid receptor S1P3. *Circulation research*, 96(8), 913-920.

Tous, M., Ferrer-Lorente, R. & Badimon, L. (2014) Selective inhibition of sphingosine kinase-1 protects adipose tissue against LPS-induced inflammatory response in Zucker diabetic fatty rats. *American Journal of Physiology-Endocrinology and Metabolism*, 307(5), E437-E446.

Tsao, C. W., Aday, A. W., Almarzooq, Z. I., Anderson, C. A., Arora, P., Avery, C. L., Baker-Smith, C. M., Beaton, A. Z., Boehme, A. K. & Buxton, A. E. (2023) Heart disease and stroke statistics—2023 update: a report from the American Heart Association. *Circulation*, 147(8), e93-e621.

Tsuchiya, K., Sakai, H., Suzuki, N., Iwashima, F., Yoshimoto, T., Shichiri, M. & Hirata, Y. (2007) Chronic blockade of nitric oxide synthesis reduces adiposity and improves insulin resistance in high fat-induced obese mice. *Endocrinology*, 148(10), 4548-4556.

Turner, N., Kowalski, G., Leslie, S. J., Risis, S., Yang, C., Lee-Young, R. S., Babb, J. R., Meikle, P. J., Lancaster, G. I. & Henstridge, D. C. (2013) Distinct patterns of tissue-specific lipid accumulation during the induction of insulin resistance in mice by high-fat feeding. *Diabetologia*, 56, 1638-1648.

Turpin, S. M., Nicholls, H. T., Willmes, D. M., Mourier, A., Brodesser, S., Wunderlich, C. M., Mauer, J., Xu, E., Hammerschmidt, P. & Brönneke, H. S. (2014) Obesity-induced CerS6-dependent C16: 0 ceramide production

promotes weight gain and glucose intolerance. *Cell metabolism*, 20(4), 678-686.

Um, J.-Y., Chung, H.-S., Song, M.-Y., Shin, H.-D. & Kim, H.-M. (2004) Association of interleukin-1ß gene polymorphism with body mass index in women. *Clinical chemistry*, 50(3), 647-650.

Urwyler, S. A., Ebrahimi, F., Burkard, T., Schuetz, P., Poglitsch, M., Mueller, B., Donath, M. Y. & Christ-Crain, M. (2020) IL (interleukin)-1 receptor antagonist increases ang (angiotensin [1–7]) and decreases blood pressure in obese individuals. *Hypertension*, 75(6), 1455-1463.

Ussar, S., Lee, K. Y., Dankel, S. N., Boucher, J., Haering, M.-F., Kleinridders, A., Thomou, T., Xue, R., Macotela, Y. & Cypess, A. M. (2014) ASC-1, PAT2, and P2RX5 are cell surface markers for white, beige, and brown adipocytes. *Science translational medicine*, 6(247), 247ra103-247ra103.

Vasconcelos, J. F., Meira, C. S., Silva, D. N., Nonaka, C. K. V., Daltro, P. S., Macambira, S. G., Domizi, P. D., Borges, V. M., Ribeiro-dos-Santos, R. & de Freitas Souza, B. S. (2017) Therapeutic effects of sphingosine kinase inhibitor N, N-dimethylsphingosine (DMS) in experimental chronic Chagas disease cardiomyopathy. *Scientific Reports*, 7(1), 6171.

Venkataraman, K., Lee, Y.-M., Michaud, J., Thangada, S., Ai, Y., Bonkovsky, H. L., Parikh, N. S., Habrukowich, C. & Hla, T. (2008) Vascular endothelium as a contributor of plasma sphingosine 1-phosphate. *Circulation research*, 102(6), 669-676.

Venkataraman, K., Thangada, S., Michaud, J., Oo, M. L., Ai, Y., Lee, Y.-M., Wu, M., Parikh, N. S., Khan, F. & Proia, R. L. (2006) Extracellular export of sphingosine kinase-1a contributes to the vascular S1P gradient. *Biochemical Journal*, 397(3), 461-471.

Verlohren, S., Dubrovska, G., Tsang, S.-Y., Essin, K., Luft, F. C., Huang, Y. & Gollasch, M. (2004) Visceral periadventitial adipose tissue regulates arterial tone of mesenteric arteries. *Hypertension*, 44(3), 271-276.

Vilela, V. R., Samson, N., Nachbar, R., Perazza, L. R., Lachance, G., Rokatoarivelo, V., Centano-Baez, C., Zancan, P., Sola-Penna, M. & Bellmann, K. (2022) Adipocyte-specific Nos2 deletion improves insulin resistance and dyslipidemia through brown fat activation in diet-induced obese mice. *Molecular metabolism*, 57, 101437.

Villarroya, F., Cereijo, R., Gavaldà-Navarro, A., Villarroya, J. & Giralt, M. (2018) Inflammation of brown/beige adipose tissues in obesity and metabolic disease. *Journal of internal medicine*, 284(5), 492-504.

Vo, P. A., Lad, B., Tomlinson, J. A., Francis, S. & Ahluwalia, A. (2005) Autoregulatory role of endothelium-derived nitric oxide (NO) on lipopolysaccharide-induced vascular inducible NO synthase expression and function. *Journal of Biological Chemistry*, 280(8), 7236-7243.

Wacker, B. K., Park, T. S. & Gidday, J. M. (2009) Hypoxic preconditioning-induced cerebral ischemic tolerance: role of microvascular sphingosine kinase 2. *Stroke*, 40(10), 3342-3348.

Walford, G. & Loscalzo, J. (2003) Nitric oxide in vascular biology. *Journal of Thrombosis and Haemostasis*, 1(10), 2112-2118.

Wang, C.-Q., Lin, C.-Y., Huang, Y.-L., Wang, S.-W., Wang, Y., Huang, B.-F., Lai, Y.-W., Weng, S.-L., Fong, Y.-C. & Tang, C.-H. (2019) Sphingosine-1-phosphate promotes PDGF-dependent endothelial progenitor cell angiogenesis in human chondrosarcoma cells. *Aging (Albany NY)*, 11(23), 11040.

Wang, C., Xu, T., Lachance, B. B., Zhong, X., Shen, G., Xu, T., Tang, C. & Jia, X. (2021) Critical roles of sphingosine kinase 1 in the regulation of neuroinflammation and neuronal injury after spinal cord injury. *Journal of Neuroinflammation*, 18, 1-19.

Wang, J., Badeanlou, L., Bielawski, J., Ciaraldi, T. P. & Samad, F. (2014) Sphingosine kinase 1 regulates adipose proinflammatory responses and insulin resistance. *American Journal of Physiology-Endocrinology and Metabolism*, 306(7), E756-E768.

Wang, N., Li, J.-Y., Zeng, B. & Chen, G.-L. (2023) Sphingosine-1-Phosphate Signaling in Cardiovascular Diseases. *Biomolecules*, 13(5), 818.

Watson, D. G., Tonelli, F., Alossaimi, M., Williamson, L., Chan, E., Gorshkova, I., Berdyshev, E., Bittman, R., Pyne, N. J. & Pyne, S. (2013) The roles of sphingosine kinases 1 and 2 in regulating the Warburg effect in prostate cancer cells. *Cellular signalling*, 25(4), 1011-1017.

Wattenberg, B. W., Pitson, S. M. & Raben, D. M. (2006) The sphingosine and diacylglycerol kinase superfamily of signaling kinases: localization as a key to signaling function. *Journal of lipid research*, 47(6), 1128-1139.

Weber, A., Wasiliew, P. & Kracht, M. (2010) Interleukin-1 (IL-1) pathway. *Science signaling*, 3(105), cm1-cm1.

Weigel, C., Bellaci, J. & Spiegel, S. (2023) Sphingosine-1-phosphate and its receptors in vascular endothelial and lymphatic barrier function. *Journal of Biological Chemistry*, 299(6).

Weigert, A., von Knethen, A., Thomas, D., Faria, I., Namgaladze, D., Zezina, E., Fuhrmann, D., Petcherski, A., Zu Heringdorf, D. M. & Radeke, H. H. (2019) Sphingosine kinase 2 is a negative regulator of inflammatory macrophage activation. *Biochimica et Biophysica Acta (BBA)-Molecular and Cell Biology of Lipids*, 1864(9), 1235-1246.

Weisberg, S. P., McCann, D., Desai, M., Rosenbaum, M., Leibel, R. L. & Ferrante, A. W. (2003) Obesity is associated with macrophage accumulation in adipose tissue. *The Journal of clinical investigation*, 112(12), 1796-1808.

Whitmarsh, A. & Davis, R. (1996) Transcription factor AP-1 regulation by mitogen-activated protein kinase signal transduction pathways. *Journal of molecular medicine*, 74, 589-607.

Wilson, D. P. (2011) Vascular smooth muscle structure and function. *Mechanisms of Vascular*, 459.

Winters, B., Mo, Z., Brooks-Asplund, E., Kim, S., Shoukas, A., Li, D., Nyhan, D. & Berkowitz, D. E. (2000) Reduction of obesity, as induced by leptin, reverses endothelial dysfunction in obese (Lepob) mice. *Journal of Applied Physiology*, 89(6), 2382-2390.

Wollny, T., Wątek, M., Durnaś, B., Niemirowicz, K., Piktel, E., Żendzian-Piotrowska, M., Góźdź, S. & Bucki, R. (2017) Sphingosine-1-phosphate

metabolism and its role in the development of inflammatory bowel disease. *International Journal of Molecular Sciences*, 18(4), 741.

Wu, W., Mosteller, R. D. & Broek, D. (2004) Sphingosine kinase protects lipopolysaccharide-activated macrophages from apoptosis. *Molecular and cellular biology*, 24(17), 7359-7369.

Xia, N., Horke, S., Habermeier, A., Closs, E. I., Reifenberg, G., Gericke, A., Mikhed, Y., Münzel, T., Daiber, A. & Förstermann, U. (2016) Uncoupling of endothelial nitric oxide synthase in perivascular adipose tissue of diet-induced obese mice. *Arteriosclerosis, thrombosis, and vascular biology*, 36(1), 78-85.

Xia, N. & Li, H. (2017) The role of perivascular adipose tissue in obesity-induced vascular dysfunction. *British journal of pharmacology*, 174(20), 3425-3442.

Xia, P., Wang, L., Moretti, P. A., Albanese, N., Chai, F., Pitson, S. M., D'Andrea, R. J., Gamble, J. R. & Vadas, M. A. (2002) Sphingosine kinase interacts with TRAF2 and dissects tumor necrosis factor-α signaling. *Journal of Biological Chemistry*, 277(10), 7996-8003.

Xin, C., Ren, S., Kleuser, B., Shabahang, S., Eberhardt, W., Radeke, H., Schäfer-Korting, M., Pfeilschifter, J. & Huwiler, A. (2004) Sphingosine 1-phosphate cross-activates the Smad signaling cascade and mimics transforming growth factor-ß-induced cell responses. *Journal of Biological Chemistry*, 279(34), 35255-35262.

Xu, H., Barnes, G. T., Yang, Q., Tan, G., Yang, D., Chou, C. J., Sole, J., Nichols, A., Ross, J. S. & Tartaglia, L. A. (2003) Chronic inflammation in fat plays a crucial role in the development of obesity-related insulin resistance. *The Journal of clinical investigation*, 112(12), 1821-1830.

Xu, Z., Liu, Y., Yang, D., Yuan, F., Ding, J., Wang, L., Qu, M., Yang, G. & Tian, H. (2017) Glibenclamide–sulfonylurea receptor 1 antagonist alleviates LPS-induced BV2 cell activation through the p38/MAPK pathway. *RSC advances*, 7(44), 27206-27213.

Xue, G., Chen, J.-p., Li, Y., Zhang, Z.-q., Zhu, J.-l. & Dong, W. (2021) MicroRNA-6862 inhibition elevates sphingosine kinase 1 and protects neuronal cells from MPP+-induced apoptosis. *Aging (Albany NY)*, 13(1), 1369.

Yaghobian, D., Don, A. S., Yaghobian, S., Chen, X., Pollock, C. A. & Saad, S. (2016) Increased sphingosine 1-phosphate mediates inflammation and fibrosis in tubular injury in diabetic nephropathy. *Clinical and Experimental Pharmacology and Physiology*, 43(1), 56-66.

Yamawaki, H., Tsubaki, N., Mukohda, M., Okada, M. & Hara, Y. (2010) Omentin, a novel adipokine, induces vasodilation in rat isolated blood vessels. *Biochemical and biophysical research communications*, 393(4), 668-672.

Yamazaki, K., Gohda, J., Kanayama, A., Miyamoto, Y., Sakurai, H., Yamamoto, M., Akira, S., Hayashi, H., Su, B. & Inoue, J.-i. (2009) Two mechanistically and temporally distinct NF-κB activation pathways in IL-1 signaling. *Science Signaling*, 2(93), ra66-ra66.

Yang, G., Badeanlou, L., Bielawski, J., Roberts, A. J., Hannun, Y. A. & Samad, F. (2009) Central role of ceramide biosynthesis in body weight regulation, energy metabolism, and the metabolic syndrome. *American Journal of Physiology-Endocrinology and Metabolism*, 297(1), E211-E224.

Yang, G., Gu, M., Chen, W., Liu, W., Xiao, Y., Wang, H., Lai, W., Xian, G., Zhang, Z. & Li, Z. (2018) SPHK-2 promotes the particle-induced inflammation of RAW264. 7 by maintaining consistent expression of TNF-α and IL-6. *Inflammation*, 41, 1498-1507.

Yang, J.-Y., Koo, B.-S., Kang, M.-K., Rho, H.-W., Sohn, H.-S., Jhee, E.-C. & Park, J.-W. (2002) Retinoic acid inhibits inducible nitric oxide synthase expression in 3T3-L1 adipocytes. *Experimental & Molecular Medicine*, 34(5), 353-360.

Yang, J., Tang, X., Li, B. & Shi, J. (2022) Sphingosine 1-phosphate receptor 2 mediated early stages of pancreatic and systemic inflammatory responses via NF-kappa B activation in acute pancreatitis. *Cell Communication and Signaling*, 20(1), 157.

Yang, N.-C., Lu, L.-H., Kao, Y.-H. & Chau, L.-Y. (2004) Heme oxygenase-1 attenuates interleukin-1ß-induced nitric oxide synthase expression in vascular smooth muscle cells. *Journal of Biomedical Science*, 11(6), 799-809.

Yao, C., Ruan, J.-W., Zhu, Y.-R., Liu, F., Wu, H.-m., Zhang, Y. & Jiang, Q. (2020) The therapeutic value of the SphK1-targeting microRNA-3677 in human osteosarcoma cells. *Aging (Albany NY)*, 12(6), 5399.

Yatomi, Y., Ruan, F., Hakomori, S.-i. & Igarashi, Y. (1995) Sphingosine-1-phosphate: a platelet-activating sphingolipid released from agonist-stimulated human platelets. *Blood*, 86(1), 193-202.

Yi, X., Tang, X., Li, T., Chen, L., He, H., Wu, X., Xiang, C., Cao, M., Wang, Z. & Wang, Y. (2023) Therapeutic potential of the sphingosine kinase 1 inhibitor, PF-543. *Biomedicine & Pharmacotherapy*, 163, 114401.

Yoh, T., Noriko, T. & Naotoshi, S. (2002) The Edg Family G Protein-Coupled Receptors for Lysophospholipids: Their Signaling Properties and Biological Activities. *The Journal of Biochemistry*, 131(6), 767-771.

Yu, H. (2021) Targeting S1PRs as a Therapeutic Strategy for Inflammatory Bone Loss Diseases—Beyond Regulating S1P Signaling. *International Journal of Molecular Sciences*, 22(9), 4411.

Yuui, K., Kudo, R., Kasuda, S. & Hatake, K. (2016) Ethanol attenuates vasorelaxation via inhibition of inducible nitric oxide synthase in rat artery exposed to interleukin-1 ß. *Human & Experimental Toxicology*, 35(9), 938-945.

Zaborska, K. E., Wareing, M., Edwards, G. & Austin, C. (2016) Loss of anti-contractile effect of perivascular adipose tissue in offspring of obese rats. *International Journal of Obesity*, 40(8), 1205-1214.

Zamora, R., Vodovotz, Y. & Billiar, T. R. (2000) Inducible nitric oxide synthase and inflammatory diseases. *Molecular medicine*, 6(5), 347-373.

Zatterale, F., Longo, M., Naderi, J., Raciti, G. A., Desiderio, A., Miele, C. & Beguinot, F. (2020) Chronic adipose tissue inflammation linking obesity to insulin resistance and type 2 diabetes. *Frontiers in physiology*, 10, 1607.

Zeyda, M. & Stulnig, T. M. (2007) Adipose tissue macrophages. *Immunology letters*, 112(2), 61-67.

Zhang, F., Xia, Y., Yan, W., Zhang, H., Zhou, F., Zhao, S., Wang, W., Zhu, D., Xin, C. & Lee, Y. (2016) Sphingosine 1-phosphate signaling contributes to cardiac inflammation, dysfunction, and remodeling following myocardial infarction. *American Journal of Physiology-Heart and Circulatory Physiology*, 310(2), H250-H261.

Zhang, H., Desai, N. N., Olivera, A., Seki, T., Brooker, G. & Spiegel, S. (1991) Sphingosine-1-phosphate, a novel lipid, involved in cellular proliferation. *The Journal of cell biology*, 114(1), 155-167.

Zhang, H., Wang, Q., Zhao, Q. & Di, W. (2013) MiR-124 inhibits the migration and invasion of ovarian cancer cells by targeting SphK1. *Journal of ovarian research*, 6(1), 1-9.

Zhang, T., Guo, D., Zheng, W. & Dai, Q. (2021) Effects of S1PR2 antagonist on blood pressure and angiogenesis imbalance in preeclampsia rats. *Molecular Medicine Reports*, 23(6), 1-8.

Zhang, W., Mottillo, E. P., Zhao, J., Gartung, A., VanHecke, G. C., Lee, J.-F., Maddipati, K. R., Xu, H., Ahn, Y.-H. & Proia, R. L. (2014) Adipocyte lipolysis-stimulated interleukin-6 production requires sphingosine kinase 1 activity. *Journal of Biological Chemistry*, 289(46), 32178-32185.

Zhao, J. & Lee, M.-J. (2023) Sphingosine Kinase 2 Knockout Mice Resist HFD-Induced Obesity Through Increasing Energy Expenditure. *International Journal of Endocrinology and Metabolism*, 21(3).

Zhu, L., Wang, Z., Lin, Y., Chen, Z., Liu, H., Chen, Y., Wang, N. & Song, X. (2015) Sphingosine kinase 1 enhances the invasion and migration of non-small cell lung cancer cells via the AKT pathway. *Oncology Reports*, 33(3), 1257-1263.

Zwick, R. K., Guerrero-Juarez, C. F., Horsley, V. & Plikus, M. V. (2018) Anatomical, physiological, and functional diversity of adipose tissue. *Cell metabolism*, 27(1), 68-83.